UNITED STATES DEPARTMENT OF COMMERCE
HARRY L. HOPKINS, Secretary
NATIONAL BUREAU OF STANDARDS
Lyman J. Briggs, Director

✦

Journal of Research

of the

National Bureau of Standards

✦

Volume 22, Number 5
May 1939

[Published with approval of the Director of the Budget]

UNITED STATES
GOVERNMENT PRINTING OFFICE
WASHINGTON : 1939

For sale by the Superintendent of Documents, Washington, D. C. - - - - - - Price 30 cents
$3.50 per year on subscription

The prices of the separate Research Papers appearing in this JOURNAL are given on the front cover page. If 100 or more copies of any separate are ordered, a discount of 25 percent is allowed. Those who desire copies of separate Research Papers should send their orders and remittances without delay to the Superintendent of Documents, U. S. Government Printing Office, Washington, D. C. This will aid him to determine the number of copies to be printed for sale. Research Papers are not printed from electrotypes, and usually no more reprints can be had when the first and only printing is exhausted.

U. S. DEPARTMENT OF COMMERCE NATIONAL BUREAU OF STANDARDS

RESEARCH PAPER RP1200

Part of Journal of Research of the National Bureau of Standards, Volume 22, May 1939

AN ABSOLUTE DETERMINATION OF THE AMPERE, USING IMPROVED COILS

By Harvey L. Curtis, Roger W. Curtis, and Charles L. Critchfield

ABSTRACT

The absolute value of a current has been measured by the current balance, using improved coils. The previous work had shown that improvements in the coils were required in order to make them fulfill more nearly the conditions assumed in developing the equations for computing the absolute value of a current from the force measured by the current balance. These new coils consisted of one moving coil made in the form of a short solenoid and one moving coil and one pair of fixed coils wound from anodized aluminum ribbon in the form of a flat spiral.

The results obtained with various combinations of these new coils and one pair of the old fixed coils are consistent among themselves, and their weighted average can be expressed as

1 NBS international ampere=0.999 86 absolute ampere.

This result differs appreciably from that obtained in the preceding work, but it is felt that this new value is more reliable because of the improved coils which were used and the greater consistency of the results.

CONTENTS

	Page
I. Introduction	486
II. Modifications of the current balance	487
1. The weights for the balance	487
2. The improved coils	487
(a) Solenoidal moving coil	487
(b) Moving coil of aluminum ribbon	489
(c) Fixed coils of aluminum ribbon	490
III. Measurement of the dimensions of the coils	492
1. Diameters of the coils	492
2. Axial widths of the windings	493
3. Radial depths of the windings	494
IV. Electric circuit of the current balance	496
1. Adjustment of the current	496
2. The storage battery	497
3. Reversal of the current in the fixed coils of aluminum ribbon	497
4. Insulation resistance	497
V. Computation of the maximum force for unit current	499
1. Maximum force between circular filaments	499
2. Maximum force between coaxial coils	499
VI. Ratio of the radii of the coils	500
1. Temperature and load coefficients of the coils	501
2. Length of the magnet	502
3. Effect of the cross-sectional dimensions of the coils	502
4. Results	503

Page
VII. Experimental determination of the maximum force between the coils. 504
1. Sources of error and corrections 504
(a) Acceleration of gravity 505
(b) Temperature of the coils 505
(c) Electrical load on the coils 505
(d) Effect of errors in the measurement of the cross sections of the coils 506
(e) Summary of estimated accidental errors in determining the absolute value of the current 506
VIII. Value of a current in NBS international amperes and in absolute amperes 507
IX. Discussion of results 508
X. Comparison with results recently obtained in other laboratories 511
XI. Appendix I. An addition to the derivation of the force formula to include some terms of the sixth degree in the coil dimensions (by Chester Snow) 512
XII. Appendix II. Correction to the force caused by an axial displacement of some of the turns in the coils made from aluminum ribbon (by Chester Snow) 516

I. INTRODUCTION

An investigation to determine the absolute value of the international ampere has been in progress at the National Bureau of Standards for more than a decade. This paper reports the progress that has been made, since the previous publication,[1] by the use of improved coils in the Rayleigh current balance. A description is given of the improvements in apparatus and methods that have been made, and the results obtained by using these developments are recorded. An effort has been made to have this paper so complete that the reader can understand the purpose of all the changes in apparatus and methods that have been used in the recent measurements. However, he will need to consult the previous paper for a description of many of the details of the apparatus which have not been changed.

The method consisted in determining the ratio of the value of a current in absolute amperes to that of the same current in NBS international amperes. The value in NBS international amperes was determined by comparing the electromotive force of a standard cell with a drop in potential produced by the current in a known resistance. The value in absolute amperes was determined in the current balance from the electromagnetic force between parts of a circuit which carried the current. The electromagnetic force was exerted between the current in a moving coil and that in a pair of fixed coils. The coils were coaxial and their planes horizontal, and the moving coil was midway between the two fixed coils. The moving coil was hung from the arm of a balance and the electromagnetic force compared directly with the gravitational force on a known mass. The vertical distance between the moving coil and each fixed coil was adjusted until the electromagnetic force for a constant current was a maximum. In this position, the current in absolute amperes can be computed from the measured force, the number of turns in each coil, and the ratios of the radius of the moving coil to that of each fixed coil. The formula for this computation includes some correction terms which depend on the ratios of the dimensions of the cross section of each coil to its radius.

[1] Curtis and Curtis, *An absolute determination of the ampere*, BS J. Research **12**, 665 (1934) RP685. Throughout the present paper statements regarding "the previous paper," "the previous publication," etc., relate to this reference. This previous work was based on the work of Rosa, Dorsey, and Miller, Bul. BS **8**, 269 (1911) S171, which will be referred to as the older or earlier work.

In the previous publication the statement is made that "the most obvious improvement in the current balance is the construction of new coils, the cross sections of which can be more accurately measured and the windings of which conform more nearly to the conditions assumed in deriving the equation for the force." The present paper describes such coils as were then projected. Two new moving coils were first made and were used in the current balance with the two pairs of fixed coils previously described.[2] Two new fixed coils were then made for use with each of the new moving coils. In the present paper all of these new moving and fixed coils are described, the modifications required by their use are discussed, and the results obtained with them are given.

II. MODIFICATIONS OF THE CURRENT BALANCE

The principal modification of the current balance [3] consisted in the use of new coils of improved construction. Also, arrangements were made to keep the humidity continuously below 40 percent in summer, both in the weighing room and in the observation room.

1. THE WEIGHTS FOR THE BALANCE

New calibrated weights and new counterweights were used. A separate cylindrical weight of platinum-iridium was made and calibrated for measuring each of the different electromagnetic forces, so that for each combination of coils as many weights were required as the number of different currents used with that combination of coils. Also, new counterweights were prepared for each of the new moving coils. Each of these counterweights had the same density as the coil with which it was used, so that the buoyancy of the air was the same for the counterweights as for the moving coil. Hence, changes in barometric pressure did not change the rest point of the balance.

2. THE IMPROVED COILS

One of the improved moving coils was wound with round copper wire in the form of a single-layer solenoid. The other moving coil and both of the improved fixed coils were wound with aluminum ribbon in the form of a flat, compact spiral. The dimensions of each of these coils could be measured with sufficient accuracy so that errors from this source would in no case introduce into the absolute value of the current an uncertainty of more than a few parts in a million. All of the materials used in these coils were tested magnetically to insure that no error was introduced by their magnetic susceptibility. As the construction of these coils involved several new features, a careful description of the methods used will be given.

(a) SOLENOIDAL MOVING COIL

The solenoidal moving coil (designated P1) was constructed by winding copper wire in a helical groove ground in the outer surface of

[2] The results obtained with these coils are given in a report to the International Committee on Weights and Measures. See *Rapport supplémentaire sur la détermination absolue de l'ampére par MM. Harvey L. Curtis, Roger W. Curtis, et Charles L. Critchfield.* Procès-Verbaux des Séances du Comité International des Poids et Mesures [2] **18**, 149 (1937). The values there reported are, for the same coils, slightly different in some cases from those which are given in this report. The differences are largely the result of an improved determination of the temperature coefficient of expansion of one of the coils.

[3] In the previous publication are shown a drawing (fig. 1) and a photograph (fig. 2) of the current balance.

a short glass cylinder. This coil, mounted in the current balance with fixed coils L3 and L4, is shown in figure 1. The thread was ground and lapped in the form by the method developed by Moon.[4] The pitch of the thread was 0.65 mm. The profile of the finished thread is shown in figure 2 as a sinusoidal line between the white and black areas. Disks of various diameters were placed on this profile, as shown in the figure, to determine the size of wire which should be used in winding the solenoid. The wire chosen, corresponding to the disk at the left, had a diameter of 0.51 mm, which was large enough to insure that the wire rested on the sides of the groove and could not touch the bottom, yet was small enough so that adjacent turns could not touch one another. Commercial wire having a diameter of 0.57 mm was drawn through two dies to reduce it to 0.51 mm. For the second drawing, the wire passed from the die directly to the glass form, with the result that the tension on the wire when wound on the coil was equal to the force (about 3 kg) required to draw the wire through the die. The constants of the coil are given in table 1.

In order to test the uniformity of the windings and to provide polished spots for use in measuring the pitch, a fine, flat oilstone was rubbed axially against the outer surface of the completed winding at eight equally spaced azimuths. This produced eight small elliptical spots on each turn of the wire. The uniformity of the spots showed that the variation in the outside diameter from one wire to the next did not exceed a few tenths of a mircon (μ).

On each spot were ruled [5] two lines parallel to the axis of the wire. These lines were used in measuring the axial length from which the pitch of the winding was obtained.

TABLE 1.—*Constants of the solenoidal moving coil,* P1, *at 22° C*

Quantity	Measured value	Quantity	Measured value
Average outside diameter	24.5121 cm.	Conicality—difference between diameters at bottom and top	0.0001 cm.
Diameter of wire	0.0512 cm.	Ellipticity—difference between maximum and minimum diameters	0.0016 cm.
Mean diameter	24.4609 cm.	Temperature coefficient of expansion of outside diameter of completed coil	4.1×10^{-6}/° C.
Number of turns	41.		
Axial width of winding	2.6650 cm.		
Thickness of form	1.1 cm.		
Length of form	3.6 cm.		
Weight of completed coil	700 g.		
Resistance of winding	2.75 ohms.		

The ends of the winding were held by hooks which extended through radial holes near the ends of the form and which were drawn against the wire by nuts on their shanks. The mechanical fastening at each end was several centimeters beyond the places at which the electrical leads were attached.

The electrical leads were attached to the last turn at each end. This method of attachment is shown in figure 3 and is described in the legend of this figure. The leads which connected the winding of the coil to the twisted leads were called the permanent leads of the coil. The permanent leads were at right angles to the windings of the coil itself, so that no vertical force was exerted on these leads by the windings of the fixed coils. The exceedingly small force between

[4] See Curtis, Moon, and Sparks, *A determination of the absolute ohm, using an improved self inductor,* J. Research NBS 21, 375 (1938) RP1137. The method is described on p. 378.

[5] The method of ruling these lines is described on p. 381 of the reference given in footnote 4.

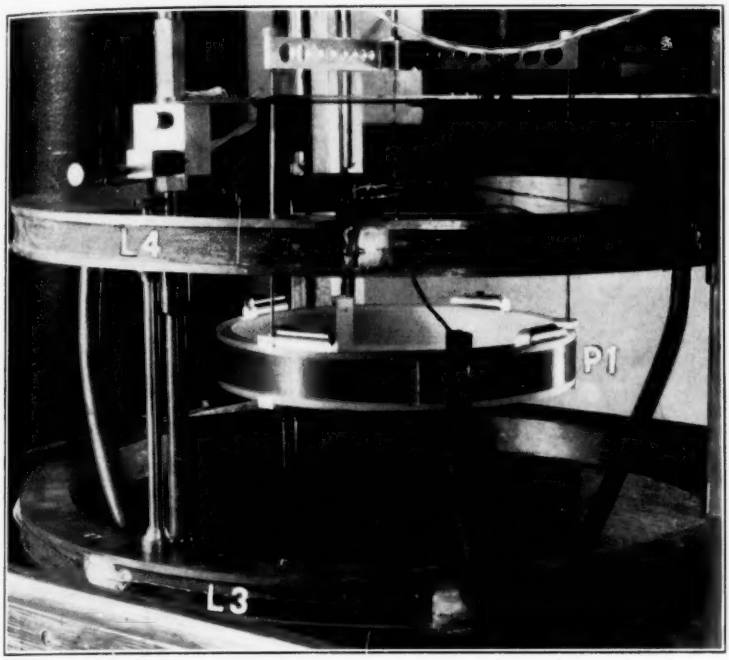

FIGURE 1.—*Solenoidal moving coil,* P1, *mounted in the current balance between the fixed coils,* L3 *and* L4.

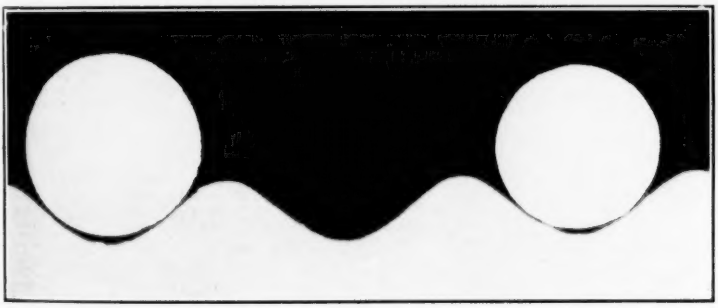

FIGURE 2.—*Profile of the form of the solenoidal coils with disks placed in the threads to represent the cross sections of wires.*

The disk at the left represents the size of wire actually used; the disk at the right represents a wire that was too small. The criterion for size was that the wire should make contact with the sides of the groove and should not touch the bottom, and that there be a space of more than 0.1 mm between adjacent turns. Magnification ×50.

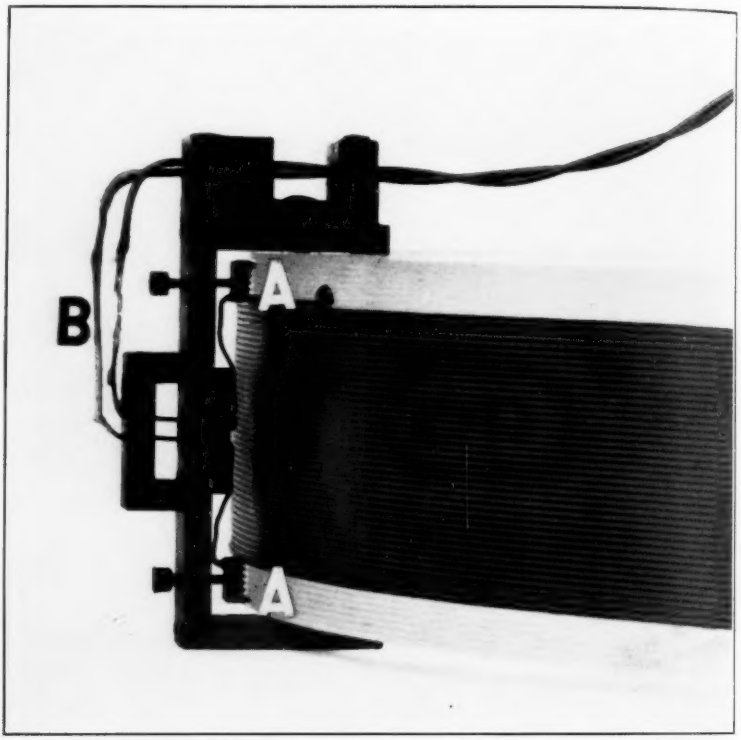

FIGURE 3.—*The terminal of the solenoidal moving coil.*

The brass contact pieces, *A*, were threaded with the same pitch as the glass form. Each touched only the outside wire of the winding and was pressed against the wire by the screw through the hard-rubber bushing in the brass clamp that surrounded the glass form. The permanent leads were soldered to the brass blocks and extended through the middle of the clamp. When making the lead correction, the lead nearer the coil was unsoldered from its permanent lead at the point *B* and the outer end connected to the other lead by a drop of solder. Magnification ×1.5.

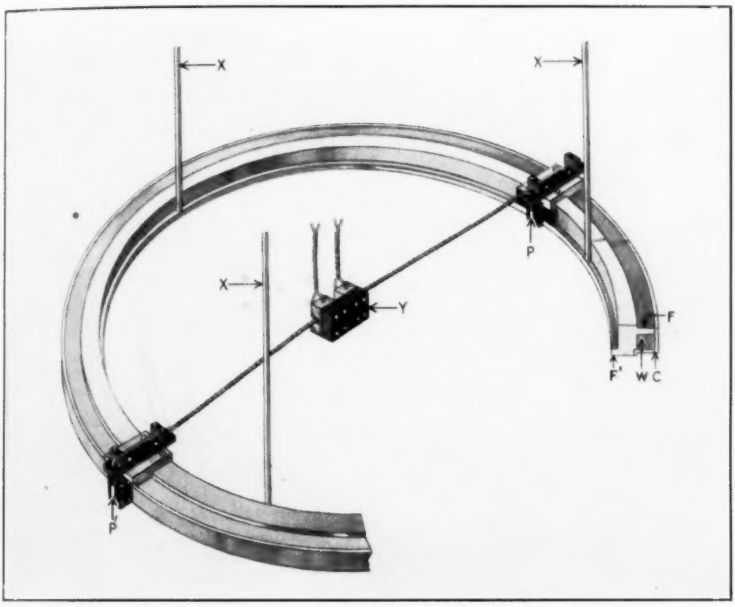

FIGURE 4.—*Schematic drawing of the moving coil of aluminum ribbon,* A1.

The coil was suspended from one pan of the balance by the rods, *X*. The cross section is shown at the right, where the winding, *W*, consisting of two separate ribbons, presses against the flange, *F*, and is protected by the cover, *C*. The internal flange is shown at *F'*. The attachment of the aluminum ribbon at the beginning of one winding to the wire of the permanent leads is shown at *P* and at the end of the other winding at *P'*. Of the two pairs of twisted leads at the center of the coil, one pair, the current leads, was for conducting the current to the coil; the other pair, the potential leads, was used in measuring the temperature of the coil. The commutator, *Y*, was used when measuring the insulation resistance between windings.

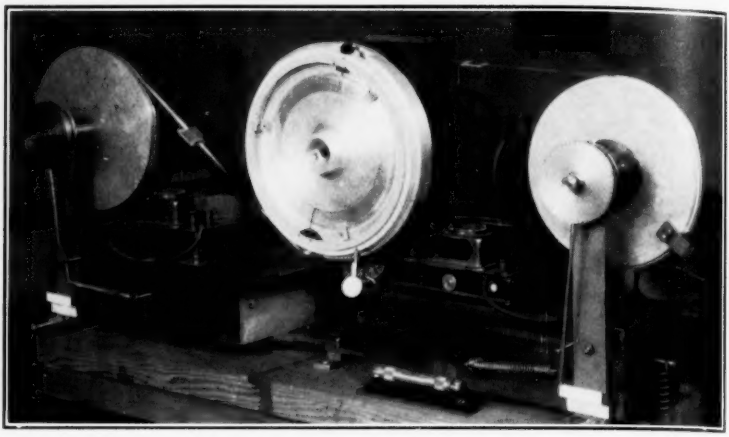

FIGURE 5.—*Photograph taken at the completion of the winding of the moving coil of aluminum ribbon, coil* A1.

The coil form in the center of the photograph was attached to an aluminum disk that was fastened to the spindle of a lathe which could be driven at a speed of 1 revolution in 4 minutes. The two spools which held the ribbons are at the right and left. A definite force on each ribbon was maintained by the friction clutch seen on the axle in the foreground of each spool. The force could be regulated by a nut on the axis of the clutch, and its value determined from the reading on a scale of the position of the pointer attached to the clutch. The electric circuits were so arranged that a short-circuit between turns or between either turn and the form produced a deflection on a voltmeter. Chamois-skin wipers are attached to each ribbon between its spool and the form and held in position manually during the winding.

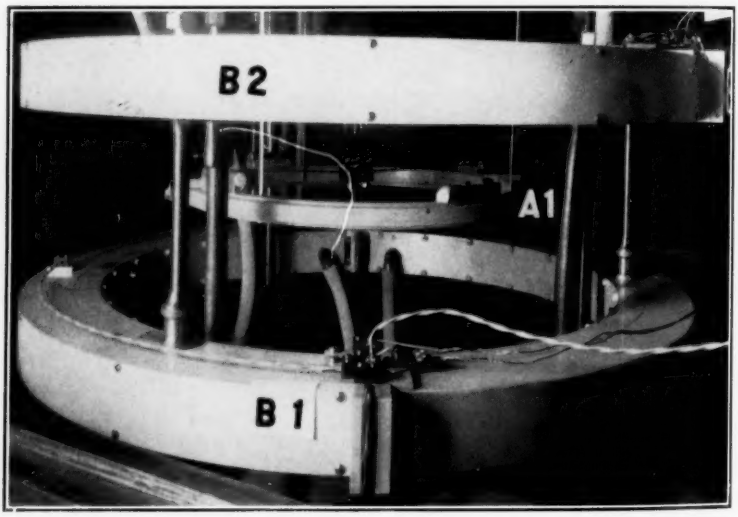

FIGURE 6.—*The moving coil of aluminum ribbon,* A1, *mounted in the current balance between the fixed coils,* B1 *and* B2, *also of aluminum ribbon.*

the permanent leads of the fixed coils and the moving coils was minimized by placing them with their azimuths approximately 90° from each other. In order to obtain the correction for all the leads, except those that are permanent, auxiliary measurements were made in which one of the wires in the twisted pair was unsoldered from its permanent lead and connected by a drop of solder to the other wire of the twisted pair, thus making a minimum change in the position of the leads.

(b) MOVING COIL OF ALUMINUM RIBBON

The moving coil of aluminum ribbon, designated as A1, was made by winding two anodized aluminum ribbons in a compact spiral on an aluminum form. A diagram showing the cross section of the form and winding and also the method of attaching the terminals is given in figure 4. The important constants of the coil are given in table 2. The form was made from a thick sheet of aluminum alloy and was anodized before the ribbon was wound on it. The anodizing produced a layer of aluminum oxide which served to insulate the turns from each other and from the form. A layer of condenser paper was placed on the face of the form before the winding was started to improve the insulation.

The form was designed to be light and was made rigid with respect to the radial compressive forces produced by the winding by means of an internal and an external flange (see fig. 4). The external flange also served as a guide in winding the ribbon.

TABLE 2.—*Constants of the moving coil of aluminum ribbon,* A1, *at 22° C*

Quantity	Measured value	Quantity	Measured value
Average outside diameter	25.8043 cm.	Insulation resistance between frame and winding A	0 ohm.
Width of ribbon over oxide layer	0.6372 cm.	Ellipticity—difference between maximum and minimum outside diameters	0.0039 cm.
Thickness of ribbon over oxide layer	.0072 cm.	Compression of form during winding	.0005 cm.
Thickness of oxide film	.0004 cm.	Temperature coefficient of expansion of the outside diameter of the completed coil	21×10^{-6}/° C.
Number of turns of each ribbon	45.		
Radial depth	0.6521 cm.		
Mean diameter	25.1522 cm.		
Weight of completed coil	473 g.		
Resistance of each winding {A	2.91 ohms.		
Resistance of each winding {B	2.83 ohms.		
Insulation resistance between windings at 40 percent humidity	18 megohms.		

Each ribbon was anodized by slowly passing it through a solution of chromic acid (3 to 10 percent maintained at 40° C) while it was connected to the positive terminal of a source of electric power which maintained a constant potential difference of 40 volts between the ribbon and the long iron tank containing the acid. An arrangement of reduction gearing and pulleys was devised so that the ribbon was pulled through the anodizing bath, washed, dried, and spooled in one continuous process. Each part of the strip was in the anodizing bath about an hour. About 24 hours was required to anodize one ribbon.

The two ribbons were simultaneously wound on the form, one ribbon starting from one end of a diameter, the other ribbon from the opposite end of the same diameter. A photograph taken at the completion of the winding of this coil is reproduced in figure 5. An im-

portant feature of the set-up was the two chamois-skin wipers which cleaned the ribbon just before it reached the coil. Other features are described in the legend to the figure.

In order to make a secure mechanical fastening and to attach the electrical terminals, the ends of each ribbon were extended a short distance in a radial direction. At the inside end each ribbon passed through a slot in the form. Each slot was lined with sheets of hard rubber to insure good insulation between the ribbon and form at this point. At the outside end each ribbon was held by a clamp attached to the external flange of the form. The electrical terminals were close to the mechanical fastenings. The arrangement of fastenings and terminals is shown in figure 4.

Electrical contact with the ribbon was made by clamping it between two sheets of platinum. The aluminum oxide, which is very hard, was removed by a "diamond file" which was made by charging a strip of copper with diamond dust. To insure good contact, filings of a hard platinum-iridium alloy were sprinkled between the aluminum ribbon and the platinum sheets. The contact resistance between the ribbon and the platinum was less than 0.004 ohm, when the coil was constructed. A wire was soldered to the platinum sheets at each end of each winding. These wires were held in a definite position by a hard-rubber frame attached to the coil form. The free ends of the two wires attached to the winding were brought close together at a point near the inside edge of the form. At this point the twisted leads were attached. The portion of the leads between these twisted leads and the winding proper was called the permanent leads of the winding. When this coil was mounted in the balance, the twisted leads attached to each winding were brought to a terminal block at the center of the coil where the windings were connected, either in series or in parallel, to the twisted pair leading to the pan of the balance. This arrangement of leads can be seen in figure 6, which is a photograph of coil A1 mounted in the current balance between the new fixed coils, B1 and B2. An equivalent arrangement was used in measuring the ratio of the radii. When making the auxiliary measurements for determining the lead correction, one wire of a twisted pair was unsoldered from its permanent lead and then soldered to the other wire of the twisted pair with as little change in position as possible.

(c) FIXED COILS OF ALUMINUM RIBBON

The fixed coils of aluminum ribbon, designated as B1 and B2, were similar to the moving coil of that material. They were made of wider and thicker ribbon and the number of turns was larger. Also, they were arranged for water cooling. Figure 6 shows these coils in the current balance. A diagram showing the cross section of the form and winding and indicating the method of attaching terminals is given in figure 7. The important constants of the coils are given in table 3.

Each form consisted of a base ring, two flanges, and covers for the coil and water channel. These parts were made from a thick sheet of aluminum alloy. On the inside surface of the base ring a channel was

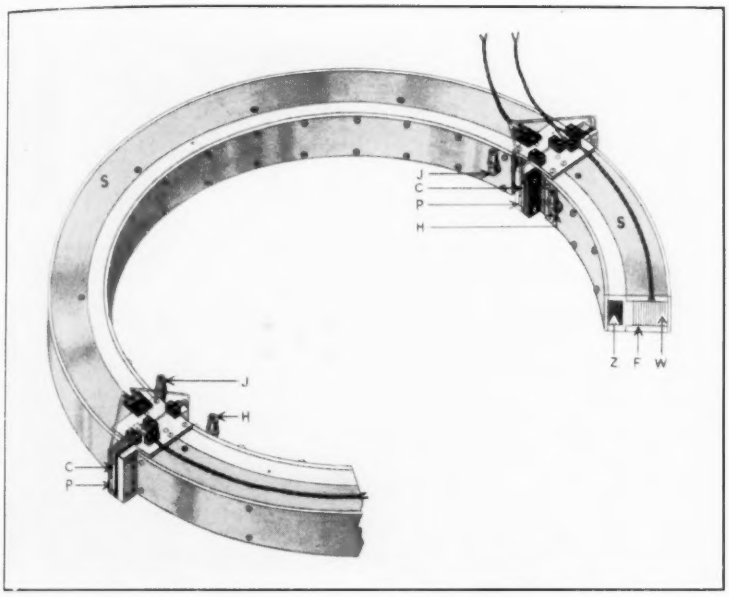

FIGURE 7.—*Schematic drawing of a fixed coil of aluminum ribbon.*

A fixed coil of aluminum ribbon, equivalent to either B1 or B2, is shown with its cover attached. The cross section is shown at the right. The winding, *W*, consisting of two interleaved and insulated ribbons, presses against the circular flange, *F*, which was attached before starting the winding. The two semicircular flanges, *S*, were attached after the winding was completed. The water channel, *Z*, had connections at *H*—*H*, and the connections to the water channel for the opposite side of the coil were at *J*—*J*. The connections of the aluminum ribbon to the potential leads are shown at *P*—*P*. The connections to the current leads are at *C*—*C*. The permanent current leads in the foreground are shown as connected to a twisted pair of wires which extend along the upper flange to the opposite side of the coil where they are shown as connected in parallel with the second winding and joined to a twisted pair that forms part of the external circuit. The potential drop for determining the temperature was normally measured over only one of the windings.

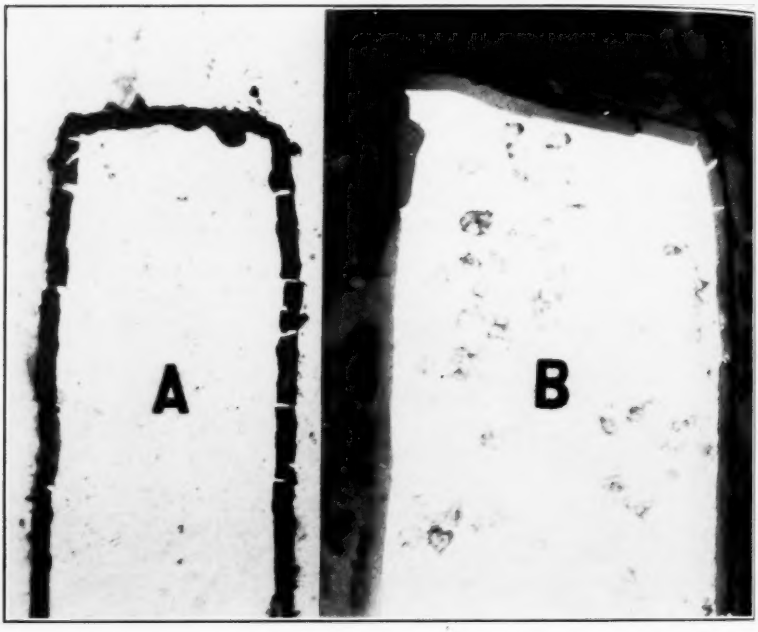

FIGURE 8.—*Photomicrographs of the aluminum-oxide coating on the aluminum ribbon after it was anodized.*

The ribbons were imbedded in a matrix so that a cross section could be cut and polished. Sample *A*, from coil A1, was imbedded in metal matrix; sample *B*, from coil B1, was imbedded in a Bakelite matrix. Both samples were subjected to heavy pressure in applying the matrix which probably accounts for the breaks in the oxide coating. Magnification ×500

TABLE 3.—*Constants of the fixed coils of aluminum ribbon,* B1 *and* B2, *at 22° C*

Quantity	Measured values	
	B1	B2
Average diameter of form	42.7050 cm	42.7064 cm
Width of ribbon over oxide layer	2.5410 cm	2.5409 cm
Thickness of ribbon over oxide layer	0.0104 cm	0.0104 cm
Thickness of oxide film	.0006 cm	.0006 cm
Number of turns of each ribbon	125	125
Radial depth	2.624 cm	2.637 cm
Mean diameter	45.329 cm	45.344 cm
Resistance of each winding {A	2.176 ohms	2.150 ohms
Resistance of each winding {B	2.146 ohms	2.182 ohms
Insulation resistance between windings at 40 percent humidity	0.1 megohm	* 0.1 megohm
Insulation resistance between frame and windings	2500 megohms	5000 megohms
Ellipticity of form—difference between maximum and minimum diameters	0.0052 cm	0.0032 cm
Temperature coefficient of expansion of the outside diameter of the completed coil	21.1×10^{-6}/°C	20.7×10^{-6}/°C

* A short-circuit between windings occurred just as measurements were completed. (See footnote 8.)

cut, except for 10° at each end of a diameter. The portions in which the channel was not cut were utilized for bringing out the inside leads of the two ribbons. The two portions of the channel were fitted with watertight covers, and each had a water connection at each end. The outside cover of the coil was merely to protect it against accident. The forms were anodized before the coils were wound, and the oxide coating gave sufficient insulation, so that no paper was used, as was the case with the moving coil.

The ribbons were anodized by the same process that was used for anodizing the ribbons for the moving coil. The same tank was used, but the ribbon was so long that about 6 days of continuous operation were needed for anodizing a single ribbon. This required a few modifications in the procedure. It was necessary to add chromic acid from time to time to maintain its concentration. A spray of tap water was used to wash the ribbon after it left the anodizing bath and before it was washed with distilled water.

In order to determine the thickness of the oxide coating, samples of ribbon were mounted in a matrix, and a cross section was cut and polished. Photomicrographs were made showing the thickness of the oxide layer, which could be readily measured. Two of these photomicrographs are reproduced in figure 8, one from the moving coil, A1, and one from fixed coil, B1. They show that the coating is quite uniform, even at the corners.

The first coils that were wound were not satisfactory. The ribbon was longer at the edges than in the center, apparently as a result of being cut by dull shears. As a result, there was a slight ruffling at each edge, which was barely noticeable when a short length of the ribbon was held straight. When wound in a coil, the ribbon did not lie flat but was curved with its concave side away from the center of the coil. When about 250 turns had been wound, this concavity amounted to more than 1 mm. This winding was removed and the forms were rewound with new ribbon. The thickness of the new ribbon was twice that of the first ribbon (0.1 mm vs. 0.05 mm), and

the new ribbon was hard-rolled aluminum, whereas the first was soft or annealed aluminum. The new ribbon, which was cut in a different factory, did not show any ruffles, but the edges had been slightly turned by the shearing. The ribbon, before anodizing, was passed between rollers which flattened the edges, but did not otherwise change its form. The second winding produced coils which were satisfactory.

The terminals were attached to these coils in nearly the same manner as those of the moving coil of aluminum ribbon. A slight modification was made in the method of attaching the potential leads which were used in measuring the resistance of the coil. In the moving coil of aluminum ribbon, the potential leads were attached to the current leads at the point where the two windings were connected in parallel, so that the measured resistance included the contact resistances between the platinum sheets and the aluminum ribbon. In the fixed coils, separate platinum sheets were provided for the potential terminals. There was no difference in accuracy between the two methods.

III. MEASUREMENT OF THE DIMENSIONS OF THE COILS

The new coils were so constructed that their mechanical dimensions could be measured with greater accuracy than could those of the older coils. The dimensions were required in order to compute the corrections for the cross sections of the coils.

1. DIAMETERS OF THE COILS

The diameters of the coils were measured by a motor-operated micrometer [6] mounted in a frame, or ring, of invar. The micrometer head was graduated to read directly in microns. The divisions were about a millimeter apart, so that readings could be made with an accuracy of 0.1 or 0.2μ. The micrometer would, under favorable conditions, repeat readings as accurately as it could be read.

The micrometer was used merely to obtain the difference between the diameter of a coil and the length of an end standard. The end standard never differed in length by more than a few tenths of a millimeter from the diameter to be measured. For this difference in length, the calibration error of the micrometer did not introduce an error as great as 0.1μ. The end standard either consisted of a number of calibrated gage blocks which had been wrung together or was a rod with spherical ends which had been compared by the micrometer with such gage blocks. The largest source of error was the uncertainty in the uniformity of the temperature throughout the measuring chamber.

The outside diameter of the solenoidal moving coil, P1, was measured in 10 axial planes and at 3 altitudes in each plane.

The diameter of the form of the moving coil of aluminum ribbon was measured before winding, and the diameter over the outside turn of ribbon was measured after winding. The method was the same as for the solenoidal coil, except that only one altitude was used in determining the mean diameter. These measurements were used in determining the radial depth of the coil and will be discussed under that heading. A ledge below the winding space was measured before

[6] Moon, BS J. of Research **10**, 249 (1933) RP528.

and after winding, in order to obtain an estimate of the compression caused by the winding.

2. AXIAL WIDTHS OF THE WINDINGS

The axial width of the solenoidal coil was equal to the pitch times the number of turns. The pitch was determined by measuring, with a traveling microscope, the distance between the centers of wires on the two outside turns and dividing this distance by one less than the total number of turns. In order to be able to set the microscope on the center of the wire, lines were ruled on the elliptical spots that had been polished on the wires for determining the uniformity of diameter of the coil. Two lines were ruled [7] on each spot, using opposite sides of the wire as a guide for the ruling device. The intersection of the cross hairs in the traveling microscope was set midway between the two lines on one outside wire and the reading of the micrometer recorded. The microscope was then moved by the micrometer screw until it was set on the corresponding position on the other outside wire. The difference between readings, when corrected for the calibration errors of the micrometer screw, gave the distance between the outside turns. The calibration was made by making readings with the traveling microscope on two graduations of a standard scale. Also, readings were made on the middle wire to determine the uniformity of pitch. The values obtained are given in table 4.

TABLE 4.—*Axial width of solenoidal coil in four azimuths at 24° C*

Azimuth	Difference in micrometer readings			
	Wires 1 to 21	Wires 21 to 41	Wires 1 to 41	Lines 1 to 27 on standard scale
Degrees	*mm*	*mm*	*mm*	*mm*
0	12.998	13.001	25.999	26.001
90	13.000	13.000	26.000	26.001
180	13.002	12.999	26.001	
270	13.001	12.999	26.000	26.001
Average	13.000	13.000	26.000	26.001

NOTE.—The length between lines 1 and 27 of the standard scale as furnished by the Interferometry Section of this Bureau was 26.001 mm at 24° C. As this length agrees exactly with the reading of the micrometer microscope, there was no calibration correction.
The pitch was 0.650 00 mm and the axial width was 26.650 mm.

The diameter of the wire on the solenoidal moving coil was measured with a special micrometer caliper which could be read to tenths of a micron. The variation in diameter with different azimuths was less than 1μ. The average diameter of two samples, one from the beginning and one from the end of the winding, was 0.5123 mm for each sample.

The axial widths of the winding of the ribbon coils were determined from the width of the ribbon, since the effect of the axial displacement of the ribbons relative to the mean position is negligible as shown later. The width of the ribbon was measured by comparing it with a gage block by means of a hand micrometer. To prevent the ribbon from deforming, it was held in a clamp, the parallel faces of which had

[7] A photomicrograph showing spots with lines ruled on them is given in figure 4, p. 380, of the paper by Curtis, Moon, and Sparks. The method of ruling the lines is also described in that paper. (See reference in footnote 4.)

such dimensions that the ribbon extended a few tenths of a millimeter on each side of them. The micrometer reading could be estimated to 1 μ. A series of values obtained from samples of the ribbon used on each of the ribbon coils is given in table 5. These results indicate that the average width of the ribbon on any coil is not in error by as much as 10 μ.

The average axial displacement of the turns from the mean position was estimated from measurements at a few places where the displacement appeared to be largest. Since the winding was guided by a flange, there was no cumulative error. However, in winding, the operators could not keep the ribbon against the flange at every instant and even when this was accomplished, a turn sometimes slipped away from the flange as a result of the pressure of outside turns. To measure the displacement of one turn relative to an adjacent one, a microscope with an objective having a focal length of 5 mm was placed with its axis perpendicular to the plane of the coil, so that the edges of the two strips were both in the field of the microscope. The microscope was focused first on one, then on the other of the edges, and the motion of the microscope tube was measured.

TABLE 5.—*Width of the aluminum ribbon on the different coils*

[Measurements made on the anodized ribbon]

Winding	Position	Coil A1			Coil B1			Coil B2		
		Number of observed positions	Width	Average deviation from mean of group	Number of observed positions	Width	Average deviation from mean of group	Number of observed positions	Width	Average deviation from mean of group
			mm	μ		*mm*	μ		*mm*	μ
A	Beginning				52	25.398	±5	53	25.436	±9
	End	34	6.374	±8	27	25.417	7	23	25.401	7
		34	6.370	10						
B	Beginning				40	25.408	7	38	25.394	8
	End	34	6.365	8	23	25.416	8	18	25.404	10
		34	6.379	9						
Average			6.372			25.410			25.409	
Twice thickness of oxide film			0.008			0.012			0.012	
Width of aluminum			6.364			25.398			25.397	
Average deviation of the mean of each group from the average of all the groups			±0.004			±0.007			±0.014	

Readings could be repeated to 0.01 mm. Measurements made at four positions on coil B1, where the displacement seemed to be the largest, gave differences between adjacent turns of 0.46, 0.43, 0.30, and 0.28 mm. It was estimated that the average value was less than 0.1 mm. A computation by the formula given in appendix II showed that the effect of such a displacement on the absolute value of the current was less than 1 part in a million. Hence, an extensive survey was not undertaken.

3. RADIAL DEPTHS OF THE WINDINGS

Since the solenoidal coil had only a single layer, no measurements of the radial depth, other than the diameter of the wire, were made.

The radial depth of moving coil A1 was obtained from measurements, with a micrometer, of the diameter of the form before winding and of the diameter over the winding after completion of the coil. Corrections were introduced for the compression of the form and for a layer of paper, 15 μ thick, which was placed over the form before the winding was started. The compression was determined by measuring the ledge outside the winding both before and after winding. These measurements showed that the diameter which extended from one terminal to the other was not compressed, while a diameter at right angles to this one was compressed 12 μ. The average compression was 5 μ.

The diameter over the winding was measured with a micrometer having flat measuring faces that extended the full width of the ribbon. Since the ribbon was slightly concave outwards, the micrometer faces made contact with the two outside edges of the ribbon, but the measuring force of 300 g compressed these edges by a measurable amount. The assumption was made that the reading obtained with this pressure gave the average outside diameter, by means of which the average radial depth was determined. Since the maximum difference between the radial depth at the edge of the ribbons and that at their centers was only 100 μ, as determined by comparison with a template having a known radius of curvature, a measurement at either place with zero pressure would give a result that differed from the average value by about 50 μ. With the pressure used it seems improbable that there was an error of more than 20 μ in the radial depth. (See table 12.)

The diameter was measured at 10 positions before winding and at the same 10 positions after winding. However, because of the compression and change in shape resulting from the winding, the difference between the readings at any one place made before and after winding does not give twice the radial depth at that place. The average radial depth was obtained from the *average* diameter before winding, the *average* diameter after winding, the *average* compression of the form, and the thickness of the paper layer over the form. The radial depth obtained by this method was, by two independent sets of data,

0.6520 cm at 20° C
and 0.6523 cm at 30° C.

The difference of 3 μ between the values at the two temperatures is about twice that which would arise from the thermal expansion of the aluminum. The value used in the computations was

0.6521 cm at 22° C.

As already explained, this may be in error by as much as 20 μ because of an uncertainty in the amount of compression produced by the measuring force. The readings of the micrometer at any point could always be reproduced within 1 or 2 μ, generally within a few tenths of a micron.

The radial depths of fixed coils B1 and B2 were measured by a traveling microscope. In this arrangement settings were made on the first few turns at the inside edge of the coil, a few in the middle of the coil,

and a few at the outside edge. This was done for six different equally spaced radial positions. The setting of the micrometer screw moving the microscope could be estimated to 1 μ.

TABLE 6.—*Radial depth of the fixed coils of aluminum ribbon*

[Measurements were made on the exposed edge of the winding before attaching the semicircular flanges]

Azimuth	B1	B2
Degrees	*cm*	*cm*
0	2.6266	2.6479
60	302	450
120	208	378
180	246	420
240	265	395
300	213	385
Average radial depth at edge	2.6250	2.6418
Concavity correction	−0.0013	−0.0045
Mean radial depth	2.6237	2.6373
Average deviation from mean	±0.0028	±0.0032

The values of the radial depth given for the different azimuths in table 6 are for an edge of the coil. Since the ribbon was, throughout the winding, slightly concave outwards with the largest concavity at the outside turn, the mean value of the radial depth was less than that obtained by measurements on the edge of the coil. In order to obtain the necessary correction to the measured depth, a large number of observations were made on the concavity of the outside turn. While in some azimuths the depth of the concavity was as much as 0.02 cm, yet the average depth gave a correction for concavity of only 0.0013 cm for B1 and 0.0045 cm for B2.

IV. ELECTRIC CIRCUIT OF THE CURRENT BALANCE

The same electric circuit used in the previous work was employed for a part of the present work. In this circuit the fixed and moving coils were connected in series. A modification in which the moving coil was connected in parallel with the two fixed coils was, however, used for some of the observations. A diagram of the electric circuit with the coils in series is given in figure 5 of the previous publication. A diagram of the electric circuit with the coils in parallel is given in figure 9 of this paper. All of the conditions which are necessary for an accurate measurement of the current, as enumerated in the previous paper, are as well fulfilled by the parallel connection as by the series connection.

1. ADJUSTMENT OF THE CURRENT

In the series connection of the coils, any variation in the current from the selected value was indicated by the deflection of a galvanometer, and this value was maintained by the adjustment of a single resistor. In the parallel connection, two different currents had to be maintained constant. When the series connection was used, a single observer maintained the current and read the deflections of the bal-

ance. When the parallel connection was used, two observers were generally employed, one to maintain the two currents and the other to read the balance. In either case, the variations in the currents were less than 1 part in a million of their nominal values.

2. THE STORAGE BATTERY

The current was supplied by a lead storage battery. In order that the current might be maintained sufficiently constant by adjusting the resistance once or twice a minute, a battery of large capacity was required. For the series connection where the maximum current was 1 ampere, a 100-volt, 400-ampere-hour battery was satisfactory. For

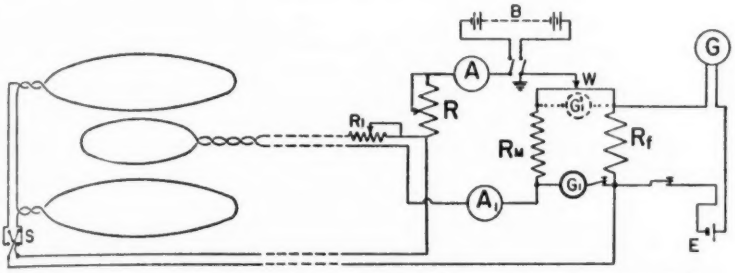

FIGURE 9.—*Electric circuit of the current balance with coils in parallel.*

The total current and the current through the moving coil were adjusted by the resistances, R and R_1, to their desired values. The approximate values were determined from the readings of the ammeters A and A_1; the precise values by determining the drop in potential over the resistances, R_M and R_f. For the precise adjustment, the deflection of the galvanometer, G_1', was made zero by adjusting the slide wire W, which consisted of a clamp on a heavy copper wire. Then R_1 was adjusted until there was no deflection of G_1. Finally, R was adjusted until there was no deflection of the galvanometer, G, which was in the circuit with the standard cell, E. During the operation of the balance, W, was adjusted only occasionally, but R and R_1 were adjusted almost continuously to keep the deflections of G and G_1 at zero.

the parallel connection, the maximum current used was 6 amperes, and a 20-volt, 2,000-ampere-hour battery was employed.

3. REVERSAL OF THE CURRENT IN THE FIXED COILS OF ALUMINUM RIBBON

The reversal of the current in the fixed coils of aluminum ribbon was given some study because of the large capacitance between the two windings. When the two windings were connected in series, there was a storage of electricity on the surfaces of the ribbons because of the potential difference between adjacent surfaces. Oscillograms showed that the rise in potential across the coil, when the circuit was opened, was less when the windings were in series than when they were in parallel. Also, it was shown that the rise in voltage was much greater when opening the circuit with 0.7 ampere in the coils than when decreasing the current from 4 to 2.5 amperes. Hence, the step-by-step reversing switch which was used (S in figure 9) was so designed that the first step made a large change in current and the last step a relatively small change.

4. INSULATION RESISTANCE

The insulation resistance between the frame and each winding of the fixed coils of aluminum strips B1 and B2 was more than 10^9 ohms.

As the potential difference between the windings and frame during an observation was never more than 10 volts, the leakage current to the grounded frame was always negligible. The insulation resistance between the two windings was, for each fixed coil,[8] about 10^5 ohms, when measured after a potential of 1.5 volts had been applied for 1 minute. When the windings were connected in parallel, the potential difference between windings was never more than 0.04 volt, so that the leakage current between them was less than 10^{-6} ampere and hence negligible. However, when the windings were connected in series, the potential difference between turns, though never more than 2.5 volts, produced a leakage current which was not quite negligible, and a small correction was required. In this case the insulation resistance had to be measured with the same time interval after applying the potential as elapsed in making the other observations. An example to show that this correction can be made with precision is given in table 7, which lists data taken in connection with a measurement of the ratio of the radii. The uncertainty in the absolute value of a current, caused by the leakage current between the windings of the fixed coils when connected in series, was less than 2 parts in a million.

TABLE 7.—*Example to show the precision that can be attained by applying the correction for the insulation resistance when the windings of a fixed coil are connected in series*

[Different elapsed times after reversal of the current were used in measuring the ratio of the radii, and the same time intervals were used between reversals of the potential when measuring the insulation resistance. Each result given, both for the ratio of the radii and for the insulation resistance, is the average of four observations.]

Time between reversals	Results—mean of four sets		Correction computed from insulation resistance	Corrected ratio of radii, A1:B1
	Apparent ratio of radii	Apparent insulation resistance		
Minutes		*Megohms*	*ppm*	
1	0.554 5311	0.10	10	0.554 5308
2	21	.13	8	65
3	38	.16	6	71
Mean				0.554 5367

In the moving coil of aluminum strip, one winding was accidentally and permanently connected to the frame during manufacture. This grounding caused no leakage to earth, since in the balance the frame and pan of the balance were insulated from earth by the agate planes

[8] Near the end of the observations a short-circuit developed between the two windings of coil B2. Before continuing observations with this coil after the short-circuit was observed, measurements were made to insure that the coil could be used with its windings in parallel in such a way that there could be no current through the short-circuit. By connecting a galvanometer to one winding and sending a current through the other winding, it was first established that there was only a single short-circuit between the windings. Since there was no deflection of the galvanometer, there could have been only one short-circuit. By connecting a battery from a terminal of one ribbon to a terminal of the other, and measuring the potential difference between the two other terminals, the resistance of the short-circuit was found to be 0.0008 ohm.

To make certain that, when the two windings were used in parallel, the potential difference between windings at the point where they were in contact was zero, a resistance equal to that of about a half a turn of ribbon was added to the inside end of one winding and the outside end of the other winding. By measuring the resistances of the different parts of the windings, the amount and location of the required resistance could be accurately determined. The results obtained with this arrangement after the short-circuit occurred differed from those obtained before the short-circuit occurred by 1 part in a million, which is within experimental error. (See footnote to table 10.)

of the balance, and in measuring the ratio of the radii the frame was mounted on an insulated support. The insulation resistance between windings was 18 megohms or more, depending on the humidity of the surrounding air. Since the windings were always connected in parallel, the potential difference between windings was only a small fraction of a volt, and the leakage current was negligible.

There was no possibility of measuring insulation resistance with the solenoidal moving coil, as it was a single winding on a glass form. However, it seems certain that leakage currents were not sufficiently large to introduce an error of 1 part in a million in the final results. Static charges might have collected on the glass form, but the electrostatic forces produced by them were eliminated by the reversal of the current in the fixed coils.

V. COMPUTATION OF THE MAXIMUM FORCE FOR UNIT CURRENT

The computation of the maximum force per unit current in the coils of a current balance was divided into two parts: First, the force for filaments at the centers of the windings, and second, the corrections for the finite cross sections of the coils.

1. MAXIMUM FORCE BETWEEN CIRCULAR FILAMENTS

The maximum force between circular filaments was computed by Maxwell's elliptic-integral formula which was given in the previous paper. The variation formulas there given were also applicable to the present work. However, a more accurate empirical formula has been devised for determining the axial distance at which the force per unit current between two filaments in the form of coaxial circles is a maximum. This formula is

$$y_m = 0.5 - 0.45\alpha^2 - 0.0633\alpha^4 \qquad \text{if } 0 < \alpha < 0.65, \tag{1}$$

where

y_m = ratio of the axial distance for maximum force to the radius of the larger filament,

α = ratio of the radii of the filaments.

This formula differs from the one given in the previous publication only in the coefficient of the last term, which was there given as 0.0625. The range of the present formula is less than the one formerly given, but in its range the maximum numerical difference between the values of y_m obtained by it and those given in Grover's table [9] is only 50 parts per million, which is about one-tenth of the difference obtained with the previous formula. As the error in the computed force is a function of the square of the error in the value of y_m, the improved formula gives a value of y_m which will not introduce an error of as much as 1 part in a hundred million in the computed force.

2. MAXIMUM FORCE BETWEEN COAXIAL COILS

The maximum force between coaxial coils differs, for two reasons, from that which would be obtained if the current in each coil were concentrated in a filament at the geometric center of its cross section.

[9] This is table 4, page 372, of Grover's paper on the maximum force between two coaxial circular currents. Bul. BS 12, 317 (1915) S255.

In the first place, the force between coils is different from that between filaments, because at any point the magnetic field of a coil is, in general, different in both magnitude and direction from that of a central filament with an equivalent current. The correction term to the force for this difference in magnetic fields is given in eq 4 of appendix I.

In the second place, the distance for maximum force is not the same for coils as for filaments. The correction terms to the force between the coils, when both these effects are considered, are given in eq 10 of appendix I. This equation is an extension of eq 7 of the previous paper. The additional terms were required only when moving coil P1 was being used.

Before the derivation of the equations in the appendix, a method was developed for computing the current from the measured distance between the coils when the force per unit current was a maximum. This treatment was necessary when using moving coil P1 and fixed coils S1 and S2 since in this case the axial distance for maximum force was so much greater for the coils than for the filaments at their centers that the correction for this difference as given in the previous paper was not sufficiently precise. Hence, after the distance between the fixed coils had been adjusted by trial until the force per unit current on the moving coil was the maximum that could be obtained, the distance between the fixed coils was measured by a micrometer. The distance, z, between the plane of either and that of the moving coil was determined from this distance and the dimensions of the coils. Then the force per unit current was computed by eq 6 of Snow's paper.[10] This equation applies even if z is not the distance for maximum force between filaments. However, in evaluating the Δ's it is necessary to know λ_1, which is zero only when z has the value required to make the force between the filaments a maximum. The formula for λ_1, which has not been previously given except as a derivative, is [11]

$$\lambda_1 = 1 - \frac{y^2k^2}{2\alpha(1-k^2)}\left[2 - k^2 + \frac{3yk^2}{\sqrt{\alpha}F}\left(\frac{M}{\sqrt{a_1a_2}}\right)\right]$$

$$= 1 - \frac{y^2k^2}{2\alpha(1-k^2)}[2 - k^2 + 3k^2\phi/\psi] \qquad (2)$$

where $\alpha = a_2/a_1$, $y = z/a_1$, $k^2 = 4a_1a_2/[(a_1+a_2)^2+y^2]$, and M and F are, respectively, the mutual inductance and the force per unit current between the filaments at the centers of the windings.[11] The complete formulas for λ_2, λ_3, and λ_4, when $\lambda_1 \neq 0$, are given in Snow's paper (see footnote 10). The computed value of the force per unit current by this method differed by less than 2 parts per million from that obtained by the complete formula, as given in appendix I.

VI. RATIO OF THE RADII OF THE COILS

The ratio of the radius of each moving coil to that of each fixed coil was determined by an electromagnetic method. A fixed and a moving coil were mounted with their centers coincident and their planes vertical and in the magnetic meridian. Currents were then sent through the coils in opposite directions, so that their magnetic fields had opposite directions at the common center. With a fixed current in one coil, the current in the second coil was adjusted until a reversal of both currents did not produce a steady deflection of a magnet placed at the common center of the coils. Then the magnetic fields at the center of the coils were equal and opposite, and the ratio of the radii of the coils was equal to the product of the ratio of

[10] BS J. Research **11**, 681 (1933) RP615.

[11] The functions $\phi = M/\sqrt{a_1a_2}$ and $\psi = F\sqrt{\alpha}/y = F\sqrt{a_1a_2}/z$ are tabulated with k^2 as argument by Nagaoka and Sakurai, table 2, Sci. Pap. of the Institute of Physical and Chemical Research, Tokyo, 1927.

the number of turns of wire on the coils and the ratio of the currents in the coils. Small corrections were made for the length of the magnet, the temperature and load coefficients of the coils, the leads, and the sectional dimensions of the coils. All of these corrections were made in the manner described in the previous paper, but the formula for the correction for the sectional dimensions, which is in the form of a power series, was extended to make it sufficiently accurate for use with the solenoidal coil.

Only one variation in procedure has been introduced since the method was described in the previous publication. The effect of this variation is discussed in the following section, but for all other details of procedure in measuring the ratio of the radii the reader is referred to the previous publication. Measurements with the two windings in series were made only with the fixed coils of aluminum ribbon and in this case required a correction because of the relatively low insulation resistance between the windings. This correction has been discussed in section IV–4, and an illustrative example is given in table 7.

1. TEMPERATURE AND LOAD COEFFICIENTS OF THE COILS

The temperature and load coefficients of expansion of the coils are given in table 8. The temperature coefficient of each of the fixed coils was determined in connection with measurements of the ratio of its radius to that of one of the moving coils. The data for a given coil were obtained by keeping the temperature of the room constant and changing the temperature of the water circulating through the fixed coil. In this way the temperature of the moving coil remained approximately constant, so the change in ratio resulted principally from the change in temperature of the fixed coil. From these data, the temperature coefficient of the fixed coil was computed.

TABLE 8.—*Temperature and load coefficients of expansion of the coils*

Designation of coil	Kind of coil	Material of winding	Material of form	Coefficients of expansion	
				Temperature	Load
				ppm/°C	*ppm/watt*
P1	Moving	Copper wire	Pyrex glass	4.1	1.0
A1	do	Aluminum ribbon	Aluminum alloy	21.0	0.0
B1	Fixed	do	do	21.1	.11
B2	do	do	do	20.7	.08
S1	do	Copper wire	Brass	17.0	.35
S2	do	do	do	17.4	.50
L3	do	do	do	17.6	.30
L4	do	do	do	18.9	.61

The temperature coefficient of each moving coil was determined directly by measuring with a micrometer a diameter at two different temperatures, usually 20° and 30° C. The glass coil, P1, was measured with the micrometer as used to determine its diameter, so that the measuring force was 300 g. However, for the coil of aluminum strip, A1, the micrometer was modified by using spherical surfaces for its measuring faces and by reducing the measuring force to less than 20 g.

The temperature coefficients of the moving coils were also determined by the same method as used for the fixed coils. In this case the temperature of the moving coil was changed by changing the temperature of the room, and the temperature of the fixed coil was kept approximately constant by means of the water circulating through it. The values by the two methods agreed within experimental error, but those obtained by direct measurement were the more accurate.

The load coefficients of the moving coils are not important, since in them the same load was used in the current balance as in the measurement of the ratio of radii. The load coefficients of B1 and B2, the new fixed coils of aluminum strip, were less than one-third of that of the older fixed coils. This decrease resulted from the improved thermal contact between the form and the current-carrying parts of the coil.

2. LENGTH OF THE MAGNET

In all the measurements of the ratio of the radii, the over-all length of the magnet was 1.41 mm and the distance between poles was 1.13 mm. The corrections were computed by eq 46 of the previous paper. The values were between 9 and 12 parts per million.

3. EFFECT OF THE CROSS-SECTIONAL DIMENSIONS OF THE COILS

The cross-sectional dimensions of a coil introduce a correction term in computing the ratio of its radius to that of another coil. This correction is required, because the magnetic field at the center of the coil is dependent on its cross-sectional dimensions as well as on its mean radius. As shown in appendix I, the magnetic field at the center of a coil of radius a and of rectangular cross section with the axial dimension $2b$ and radial dimension $2c$ is, to an accuracy of 1 part in a million for all coils used in this investigation, represented by the equation

$$H=\frac{2\pi nI}{a}\left(1-\frac{b^2}{2a^2}+\frac{c^2}{3a^2}+\frac{3b^4}{8a^4}+\frac{c^4}{5a^4}-\frac{b^2c^2}{a^4}-\frac{5b^6}{16a^6}+\cdots\right)=\frac{2\pi nI}{a}(1-\Delta). \quad (3)$$

This equation differs from the similar equation given in the previous publication (eq 48, page 707) by the addition of the sixth-degree term in the series. For the solenoidal moving coil, this new term had a value of 0.5×10^{-6}. For all the other coils, it was entirely negligible. Values of Δ are given in table 9.

TABLE 9.—*Dimensions of coils and the corrections for cross-sectional dimensions in measuring the ratio of radii*

[The correction to a coil is required in order to determine its mean radius from the number of turns in it and from the magnetic field produced at its center by unit current in its winding]

Designation of coil	Number of windings	Number of turns in each winding	Radius=a	Axial width=$2b$	Radial depth=$2c$	Correction for cross-sectional dimensions=Δ
			cm	*cm*	*cm*	*ppm*
P1	1	41	12.2304	2.6650	0.0512	5881
A1	2	45	12.5761	0.6364	.6521	96
B1	2	125	22.664	2.5398	2.6236	458
B2	2	125	22.672	2.5397	2.6373	445
S1	2	392	19.97	1.580	1.528	295
S2	2	392	19.96	1.579	1.522	298
L3	2	647	25.00	1.969	1.943	273
L4	2	647	25.00	1.965	1.925	279

With the new coils the correction for cross-sectional dimensions is, except for A1, larger than for the older coils. However, the cross sections of the new coils were measured with so much greater accuracy that the error on this account was much less than for the older coils.

4. RESULTS

The results of the measurements on the ratio of radii are given in table 10. The average deviation of a single observation from the mean of its group is in every case small, the maximum for all the groups being 4 parts per million. The adjusted values of the ratio of the radii, which were obtained as explained in the heading of the table, were used in computing the absolute value of the current.

As a further test of the reliability of the values of the ratio of radii, the ratio of the radii of the two moving coils has been computed, using each of the fixed coils as intermediary. The results are given in table 11. The average variation from the mean is 5 parts per million. However, this agreement does not of necessity indicate that each ratio is known with the indicated accuracy. If an error had been made in the measurement of the cross-sectional dimensions of a moving coil, or even in the computation of the correction factor from its dimensions, this would not affect the value of the ratio A1:P1.

TABLE 10.—*Ratio of radii of the various coil combinations*

[The observed values of the ratio of the radii were those obtained by the electromagnetic method, when they were corrected to 22° C and no load. From each pair of values which involve the same fixed coil, a value can be obtained for the ratio of radii A1:P1 as given in table 11. The adjusted values, given in the last column, were obtained from each pair of observed values that involved a single fixed coil. The same amount was added to one observed value as was subtracted from the other, in order that the ratio of A1:P1 as obtained from these adjusted values would be the same as the average value of A1:P1 as obtained from the observed values using all the fixed coils. In the case of fixed coil L3, the data for A1:L3 were less reliable than the data for P1:L3, so that the ratio A1:L3 was given twice as large an adjustment as was given to P1:L3.]

Moving coil	Fixed coil	Number of observations	Observed ratio of radii	Deviation from mean	Adjusted ratio of radii
				ppm	
P1	B1	7	0.539 3497	±1	0.539 3505
	B2 [a]	13	.539 0832	2	.539 0814
	S1	5	.612 5251	2	.612 5231
	S2	9	.612 8091	2	.612 8099
	L3	7	.489 4701	1	.489 4714
	L4	4	.489 3822	1	.489 3820
A1	B1 [b]	19	.554 5363	3	.554 5354
	B2	9	.554 2569	2	.554 2587
	S1	11	.629 7661	3	.629 7681
	S2	8	.630 0638	3	.630 0629
	L3	7	.503 2552	4	.503 2520
	L4	4	.503 1601	2	.503 1601

[a] These measurements include 7 runs which were made with the 2 windings of B1 connected in series. These series results were corrected for the leakage caused by the insulation resistance between turns (see table 7). The mean of the series results, taken separately, differed by less than 1 part in a million from the mean of the results taken with the usual parallel connection of the windings.

[b] 6 measurements taken before the short-circuit occurred gave an average value of 0.539 0829, and 7 measurements taken after the compensating resistors had been installed (see footnote 8) gave an average value of 0.539 0835. Measurements after the short-circuit had been discovered and before the compensating resistors had been installed gave values 42 parts per million lower than the average.

TABLE 11.—*Computed ratio of the radii of the moving coils, using each fixed coil as intermediary*

Intermediary fixed coil	Ratio of radii A1:P1	Deviation from mean
B1	1.028 157	+3
B2	147	−7
S1	147	−7
S2	157	+3
L3	163	+9
L4	154	0
Average	1.028 154	±5

VII. EXPERIMENTAL DETERMINATION OF THE MAXIMUM FORCE BETWEEN THE COILS

The procedure for determining the maximum force was essentially the same as described in the previous paper. The moving coil was suspended from one arm of a sensitive balance. Two fixed coils having diameters about double that of the moving coil were mounted one above, the other below the moving coil. The planes of the three coils were made horizontal by means of sensitive levels, and their coaxiality was checked by electrical measurements with the balance itself. The distance between the fixed coils was that at which the force per unit current on the moving coil was the maximum that could be obtained with this set of coils. In this position there were measured both the sum of the forces of the two fixed coils on the moving coil and their difference. When the moving coil was connected in series with the fixed coils, the procedure in making the measurements of force and in adjusting the coils was the same as described in the previous paper. When the moving coil was in parallel with the fixed coils, as shown in figure 9, the procedure for making a measurement required not only the reading of the swings of the balance but also the frequent adjustment of the two resistors by which the currents in the fixed and the moving coils were maintained constant.

The measurement of the force and the adjustment of the coils was carried out in the same manner as previously described. Also, the difference of the forces was regularly measured to make the necessary corrections for lack of perfect adjustment of the coils. This measured difference of the forces was compared with the computed difference of the forces as a check on the computations. As the check was satisfactory in every case, detailed values are not given.

1. SOURCES OF ERROR AND CORRECTIONS

Thirteen different sources of error were discussed in the previous publication. Only five of them will be discussed here, since for eight of them—the adjustment of the coils, the sensitivity of the balance, the weights and buoyancy correction, the lead correction, the changes in rest point, convection currents in the air, the presence of magnetic bodies, and the effect of external magnetic fields—the same considerations hold now as formerly. The sum of the maximum uncertainties which were assigned to these eight sources was between 7 and 12 parts per million in the current. As all of these which may have produced an appreciable effect were accidental errors, the average result from

a number of observations would probably not be influenced by any of them.

In addition to the 13 sources of error previously considered, there is the question, already discussed, of the insulation resistance when the windings of the fixed coils of aluminum ribbon were connected in series and the possibility that, in the coils of aluminum ribbon, the current distribution was affected by the magnetic field. Such a change in distribution would be produced by the Hall effect. However, a mathematical analysis [12] showed that the effect on the force was much less than 1 part in a million and might be zero.

The only other variation from uniform current distribution was the absence of current in the insulation between the turns. Although this insulation in the aluminum-ribbon coils was only 4 to 6 μ in thickness, the insulation occupied about 10 percent of the cross section. However, this lack of uniformity produced a negligible effect on the computed current, since the magnetic intensity produced by a current in a ribbon at a point which is farther from the center of the ribbon than its width is, to a high degree of approximation, independent of the thickness of the ribbon.

(a) ACCELERATION OF GRAVITY

The value of gravity has been taken as 980.095 cm/sec ^{2}, the same as in the previous work. This was based on the value of 981.274 cm/sec ^{2} at Potsdam. However, absolute determinations [13] made at the National Bureau of Standards and the National Physical Laboratory, since the previous publication, gave values 20 parts per million and 13 parts per million, respectively, lower than the one derived from the Potsdam value. While this must be considered in arriving at a value of the ampere which will be used to fix the electrical units, yet comparisons with previous determinations and those of other laboratories are facilitated by using for the present the old value of gravity.

(b) TEMPERATURE OF THE COILS

The temperature of the coils introduced a larger correction with some of the new coils than with those formerly used. The reason is that the correction involves the difference of the temperature coefficients as well as the differences in temperatures of the two coils from the standard temperature (22° C). As the temperature coefficients of the new coils were carefully determined, and the temperatures were obtained during every observation by measuring the resistance of the winding, the error of a single observation resulting from the temperature correction was about the same as formerly; namely, 2 parts per million.

(c) ELECTRICAL LOAD ON THE COILS

The effect of the electrical load was much less for the new coils than for the older ones. With the moving coils, the same load was used in the current balance as in measuring the ratio of the radii. Hence, no correction for load was required for these coils. For the fixed coils of aluminum ribbon, the load coefficients were so small that the maximum correction on this account was only 3 parts per million. The

[12] This analysis was carried out by C. Snow.

[13] Heyl and Cook, *The value of gravity at Washington*, J. Research NBS **17**, 805 (1936) RP946; Clark, *An absolute determination of the acceleration due to gravity*. Roy. Soc. Phil. Trans. (London) **238A**, 65 (1939).

error in applying this correction was probably less than 1 part in a million for the new coils, whereas it may have been as large as 3 parts in a million for the older fixed coils.

(d) EFFECT OF ERRORS IN THE MEASUREMENT OF THE CROSS SECTIONS OF THE COILS

The effect on the measured force of errors in the measured cross sections of the coils was computed by eq 57 of the previous paper. The results are given in table 12, which, for convenience of comparison, includes data on the coils used in the previous investigation. The estimated uncertainty of 20μ for the half-sectional dimension of each of the old coils is twice that given in the previous paper, since a re-examination of the original data shows that this is a more probable estimate. For the new coils, the corresponding estimated uncertainty in the measured dimensions is one-half the average deviation of each group of observations from the mean of all the groups. Since the sign of each computed error cannot be known, the maximum error resulting from these estimated uncertainties is the sum of the individual errors, but the square root of the sum of the squares is a more useful method of comparing results as it is proportional to the probable error.

TABLE 12.—*Effect of estimated uncertainties in the measured dimensions of the cross sections of the coils on the computed force*

Fixed coil	Estimated uncertainty[a] in cross-sectional dimensions		Moving coil	Estimated uncertainty[a] in cross-sectional dimensions		Computed[b] error in F from estimated uncertainties					
	Axial δb_1	Radial δc_1		Axial δb_2	Radial δc_2	b_1	c_1	b_2	c_2	Maximum for coil combination	Square root of sum of squares
	μ	μ		μ	μ	*ppm*	*ppm*	*ppm*	*ppm*	*ppm*	*ppm*
S1 or S2	20	20	M2	20	20	4.8	4.8	30	30	±69	±43
L3 or L4	20	20	M2	20	20	2.0	2.0	21	21	46	30
S1 or S2	20	20	M3	20	20	2.4	2.4	33	33	71	47
L3 or L4	20	20	M3	20	20	2.2	1.2	26	26	54	37
B1 or B2	5	15	P1	0.5	0.5	1.0	3.0	1.5	0	5.5	3
S1 or S2	20	20	P1	0.5	0.5	5.0	5.0	2.0	0	12.0	7
L3 or L4	20	20	P1	0.5	0.5	1.5	1.5	1.5	0	4.5	3
B1 or B2	5	15	A1	2.5	10	1.0	3.0	2.0	8	14.0	9
S1 or S2	20	20	A1	2.5	10	5.0	5.0	2.5	10	22.5	12
L3 or L4	20	20	A1	2.5	10	1.0	1.0	2.0	7	11.0	7

[a] Values given in these columns are one-half the estimated uncertainty of the cross-sectional dimensions in order that they may be used directly in the equation for computing the error in F.
[b] This error was computed by eq 57, page 724, of the previous publication.

(e) SUMMARY OF ESTIMATED ACCIDENTAL ERRORS IN DETERMINING THE ABSOLUTE VALUE OF THE CURRENT

A summary giving the effect on the absolute value of the current of the estimated uncertainty from each of the sources of error to which a value of the average deviation can be assigned is given in table 13. Of these sources, the acceleration of gravity is common to all the observations. The finite cross section of the coils was the largest source of error for most observations, but the changes in rest point gave, with some sets of coils, as large an error when the force was very small.

The resultant effect of the errors is different for each of the different combinations of coils. The resultant uncertainty for each combination of the coils lies between 4 and 24 parts per million.

In the observations with a given current and set of coils, the differences between individual runs were the result of only four of the sources of error listed in table 13; namely, adjustment of coils, sensitivity of balance, temperature of coils, and changes in rest point. Using the values given in the table, the probable uncertainty of an individual value from the mean of the set is 5 parts per million. This estimated value is in good agreement with the observed values given in the last column of table 14, which are the average deviations of a single observation from the mean of the group. The observed values include not only the uncertainties in the absolute value of the current, but also those connected with the measurement of the current in NBS international amperes. These latter uncertainties were estimated to be less than 2 parts in a million, since they involved only standard cells, standard resistors, and a very simple measuring circuit.

TABLE 13.—*Summary of sources of error in the absolute measurement of current and estimates of their maximum magnitudes*

Sources of error	Effect on value of current of probable uncertainties
	ppm
Adjustment of coils	3
Sensitivity of balance	<1
Weights and buoyancy correction	<1
Acceleration of gravity [a]	2
Ratio of radii	4
Temperature of the coils	2
Electrical load coefficient of the coils [b] moving coils	<1
Electrical load coefficient of the coils [b] old fixed coils	5
Electrical load coefficient of the coils [b] new fixed coils	1
Lead correction	2
Changes in rest point	2 to 7
Convection currents in the air	<1
Magnetic bodies	<1
External magnetic fields	<1
Finite cross section of coils [b]	[c] 4.5 to 22
Hall effect	<1
Insulation resistance when windings of B1 and B2 are in series	2

[a] The value used was the same as in the previous work, namely, 980.005 cm/sec² at the beam of the balance. The error given is concerned only with the transfer from Potsdam to Washington.
[b] Value given is different from that in previous paper.
[c] See table 12.

In addition to accidental errors, there are systematic errors which can be estimated only by comparing the results with the different sets of coils. This comparison will be made when discussing the results of all the measurements.

VIII. VALUE OF A CURRENT IN NBS INTERNATIONAL AMPERES AND IN ABSOLUTE AMPERES

The value, in absolute amperes, of a current having a value of 1 NBS international ampere has been obtained for six combinations of coils. The results, expressed in the form $(I_{NBS}-I_a)/I_a$, are given in table 14 for all of these combinations, where I_{NBS} is the value of the current in NBS international amperes and I_a is the value of the current in absolute amperes. In the table are also given the nominal values of the measured force and of the currents in the coils.

TABLE 14.—*Summary of the results on the absolute determination of the ampere*

Date	Moving coil	Fixed coils	Approximate force in grams	Approximate current: Moving coil	Approximate current: Fixed coil	No. of observations in group	$\frac{I_{NBS}-I_a}{I_a}$	Average deviation from mean of group
				Amperes	*Amperes*		*ppm*	*ppm*
May 1935	P1	S1, S2	6.26	1.02		11	101	
June 1935	P1	S1, S2	2.78	.68		3	102	±1
Dec. 1936	A1	S1, S2	7.60	1.02		5	79	3
May and June 1937	A1	S1, S2	3.38	.68		9	80	2
Average with coils S1 and S2							90	
Average deviation of the mean of each group from the mean of all the groups in which coils S1 and S2 were used							±11	
Feb. and Mar. 1936	P1	L3, L4	5.67	1.02		19	123	±4
Do	P1	L3, L4	2.52	.68		24	118	3
May and June 1936	A1	L3, L4	6.71	1.02		11	108	4
Do	A1	L3, L4	2.98	.68		9	118	11
Average with coils L3 and L4							117	
Average deviation of the mean of each group from the mean of all the groups in which coils L3 and L4 were used							±4	
June 1938	A1	B1, B2	*3.35	1.02		9	147	±1
Do	A1	B1, B2	1.07	1.02		6	147	3
Aug. and Sep. 1938	P1	B1, B2	*2.81	1.02		6	148	3
Sept. 1938	P1	B1, B2	1.40	1.02		11	151	6
Sept. and Oct. 1938	P1	B1, B2	7.03	1.02	5.09	9	148	2
Oct. 1938	P1	B1, B2	2.81	.4	5.09	4	149	2
Average with coils B1 and B2							148	
Average deviation of the mean of each group from mean of all the groups in which coils B1 and B2 were used							±1	

* The windings of the fixed coils were connected in series which doubled the number of turns and therefore the heating effects and the force. A correction of 3 parts in a million was made for leakage currents.

IX. DISCUSSION OF RESULTS

The discussion of results is for the purpose of indicating the uncertainty that may exist in the result when any coil or combination of coils was used. A summary of all the results obtained in this and the previous investigation is given in table 15. In analyzing the sources of error in a previous section, it was shown that the uncertainty in a result was largely caused either by uncertainties in the cross-sectional dimensions of the coils that were used or by systematic errors that can be detected only when comparing the results from different sets of coils. Hence, this discussion will be mainly concerned with these questions, since the result with any set of coils could be repeated within a few parts in a million (see table 14).

The construction of the older coils is such that the cross sections cannot be remeasured, so that it is necessary to depend on the values obtained when they were constructed some 30 years ago. The coils made for the present investigation were so designed and constructed that the cross-sectional dimensions could be accurately measured and can be remeasured whenever necessary.

Each of the fixed coils, S1 and S2, had 28 layers of wire, and the wires were brought up from one layer to the next on the same diameter, so that, as stated in the earlier work, "the winding became elliptical with the long axis along this diameter." This ellipticity was important mainly because it affected the cross section. As a result, the correction for cross section was quite uncertain. This uncertainty was confirmed by the variability in the results with this pair of fixed coils (column 1 of table 15) when used with different moving coils. For these reasons all the results when using the fixed coils, S1 and S2, have been given zero weight.

TABLE 15.—*Summary of all the results obtained in this and the previous investigation*

Moving coils ↓	Pairs of fixed coils →	Values of $(I_{NBS}-I_a)/I_a$		
		S1, S2	L3, L4	B1, B2
M2		10×10^{-6}	94×10^{-6}	
M3		53	81	
A1		80	113	147×10^{-6}
P1		102	120	149

The uncertainties in the cross sections of the moving coils, M2 and M3, produced, as shown in table 12, a large uncertainty in the results obtained with these coils. The experimental results obtained with these coils (first and second rows of table 15) and only two of the sets of fixed coils show differences such as might be expected from large uncertainties in the cross-sectional dimensions. Moreover, the construction of these coils was similar to that of S1 and S2, so that the same kinds of systematic errors were undoubtedly present as have been deemed sufficient to give all results obtained with S1 and S2 a weight of zero. Hence these three lines of evidence indicate that the results using the moving coils, M2 and M3, should be given very little weight. They have not been used in determining the weighted mean.

Fixed coils L3 and L4, while wound with 36 layers of wire, were made so as to avoid the ellipticity that occurred in S1, S2, M2, and M3. The method of winding was described in the earlier publication as follows: "The wire was brought up from one layer to the next at a point one thirty-sixth of a revolution short of the point at which it was brought up the layer before. Thus the coil is kept circular and each winding has one turn less than by the old method." Although this method of winding increased the uniformity of radial depth, it introduced an uncertainty concerning the current distribution, since a part of a turn was lacking in every layer. However, these coils were 50 cm in diameter, whereas S1 and S2 were only 40 cm, and the increase in diameter made a knowledge of the cross section less important. These conclusions concerning the reliability of coils L3 and L4 are substantiated by the results which were obtained when using them with different moving coils (2d column of table 15). Hence, those results obtained with L3 and L4 and the moving coils, P1 and A1, have been retained.

The moving coils, P1 and A1, had quite different cross-sectional shapes, yet both met the requirements imposed in deriving the formula for computing the absolute value of the current. Because of the difference in shape, there seems to be little chance of a common source

of systematic errors. While the results for A1 (3d row of table 15) are, for corresponding pairs of fixed coils, somewhat lower than those for P1 (4th row), yet these differences are probably all the result either of uncertainties in the fixed coils or of experimental errors. No sufficient reason has been found for weighting the results obtained with one coil differently from those obtained with the other coil.

Fixed coils B1 and B2 more nearly conformed to the theoretical requirements than did the coils L3 and L4. Only in two respects was there a measurable deviation from the cross section postulated in deriving the theory. The edges of the ribbon did not all lie in a plane perpendicular to the axis of the coil, but formed a series of steps. The effect of this was shown to be negligible. Also, the ribbon was slightly longer at the edges than at the center, so that the outside layers of the coil were concave outwards. This necessitated taking an average radial depth, but the uncertainty in this did not introduce an uncertainty of more than 1 or 2 parts in a million in the result. After considering the facts, the authors have arbitrarily given the results with B1 and B2 (last column of table 15) twice the weight of those with L3 and L4.

The computation of the weighted mean of the results is given in table 16. Those that have been given zero weight are not included

TABLE 16.—*Evaluation of the weighted mean of all the results which have not been discarded*

Fixed coils	Moving coil	$\frac{I_{NBS}-I_a}{I_a}$	Ratio of the value of a current in absolute amperes to the value in NBS international amperes	Weight	Deviation from weighted mean
		ppm			
L3, L4	A1	113	0.999 887	1	$+25\times10^{-6}$
	P1	120	880	1	+18
B1, B2	A1	147	853	2	−9
	P1	149	851	2	−11
Weighted mean			0.999 862		$\pm14\times10^{-6}$

in this table. The weighted mean of this and the previous investigation is

1 NBS international ampere=0.999 86 absolute ampere.

However, the weighting had little effect on the result. If the results from both sets of fixed coils, which are given in table 16, had been given equal weight, the weighted mean would have been decreased by only 5 parts in a million, but if coils B1 and B2 had been given a weight of 5, the increase would have been 5 parts per million.

The difference between this result and that previously published is 68 parts in a million. This difference now appears to be largely, if not entirely, the result of systematic errors in the previous investigation. There is no indication that there has been any drift in the NBS units of resistance or electromotive force on which the NBS international ampere is based. The systematic error resulted because the actual coils used in the previous investigation did not sufficiently

well conform to the requirements imposed in developing the theoretical formulas. In the present investigation the probability of a systematic error affecting the results was greatly reduced by using two different types of moving coils and two different types of fixed coils. The authors are convinced that the accidental errors of the present investigation have not introduced an error of as much as 20 parts per million in the final result.

From the results of the international comparison of standard resistors and standard cells at the International Bureau of Weights and Measures in 1937, the result here given can be expressed in mean international amperes. In order to indicate the difference between the two international amperes, it is necessary to carry results to six significant figures. Then

$$1 \text{ mean international ampere} \begin{cases} = 1.000\,006 \text{ NBS international ampere.} \\ = 0.999\,868 \text{ absolute ampere.} \end{cases}$$

The above values are based on the value of gravity as determined at Potsdam. Using the value of gravity recently obtained at the National Bureau of Standards,

1 mean international ampere = 0.999 858 absolute ampere.

X. COMPARISON WITH RESULTS RECENTLY OBTAINED IN OTHER LABORATORIES

Since the publication of the previous report, the results of three investigations in other laboratories have been published. The results, including the one from this paper, are given in table 17.

TABLE 17.—*Recent results on the absolute value of the ampere*

Date	Laboratory	Type of current balance	Published value of 1 national ampere in absolute amperes	Converted [1] value: 1 mean international ampere in absolute amperes	Published estimate of uncertainty in result
1935	LCE (France) [2]	Cotton	0.999 8	1.000 0	Several parts in 10 thousand.
1936	NPL (England) [3]	Ayrton-Jones	.999 86	.999 85	20 ppm.
1937	ETL (Japan) [4]	Rayleigh	.999 94	.999 93	No estimate. [5]
1939	NBS (United States)	do	.999 862	.999 868	20 ppm.

[1] The published values in terms of national amperes were converted to mean international amperes by means of the values for the different national units as obtained by the International Bureau of Weights and Measures. The French conversion factor was obtained from the Procès-Verbaux for 1935; the conversion factor for the other nations from the Procès-Verbaux for 1937.

[2] Dupouy and Jouaust, *Sur la measure absolue des champs magnétique et la detérmination de l'ampère en valeur absolue*, J. phys. radium [7] **6**, 123 (1935).

[3] Vigoureux, *An absolute determination of the ampere*, Roy. Soc. Phil. Trans. (London) **236A**, 133 (1936); Nat. Phys. Lab. Collected Researches **24**, 173 (1938).

[4] Yoneda and Ishibashi, *Détérmination absolue du courant*, Procès-Verbaux des Séances du Comité International des Poids et Mesures [2] **18**, 185 (1937).

[5] The average deviation of the experimental result with each set of coils from the mean of all the sets is $\pm 37 \times 10^{-6}$.

The authors acknowledge help from many of their associates at the National Bureau of Standards, only a few of whom have been mentioned in this paper.

WASHINGTON, February 14, 1939.

XI. APPENDIX I

An Addition to the Derivation of the Force Formula to Include Some Terms of the Sixth Degree in the Coil Dimensions

By Chester Snow

The force between two coaxial circles carrying unit current is denoted by $F(x,\alpha)$, where x and α are two dimensionless independent variables, α being the ratio of the radii $a_2/a_1 (a_2<a_1)$ and x being $z/\sqrt{a_1^2+a_2^2}$, where z is the distance between their planes. The force between actual coils of rectangular cross section carrying in each turn currents I_1 and I_2, respectively, is denoted by $\mathfrak{F}(x, \alpha)$, which depends on the current and number of turns in each coil and is proportional to F (x, a), where a_1 and a_2 are the mean radii of the coils and z is the distance between their mean planes. However, $\mathfrak{F}(x, a)$ also includes a factor which is only slightly different from unity and which is a function of the dimensionless ratios b/a and c/a for each of the two coils, where $2b$ is the axial breadth and $2c$ is the radial depth of the rectangular cross section of a coil of mean radius a.

In a previous paper [14] $\mathfrak{F}(x,a)$ was evaluated by assuming that the current was uniformly distributed over the cross section of the coil. In section V of that paper this assumption was shown to be a matter of convenience in reckoning only, provided that the effective ratio of the coils was measured by comparison of the magnetic fields at their centers, and also on the assumption that each wire was at the center of a square of such dimensions that the coil section was completely filled by these squares. With these assumptions the formula for the force may be put in the general form

$$\mathfrak{F}(x,\alpha)=n_1n_2I_1I_2\mathrm{F}(x,\alpha)\{1+\Delta_2(x,\alpha)+\Delta_4(x,\alpha)+\Delta_6(x,\alpha)\}. \quad (4)$$

where n_1 and n_2 are the number of turns in the coils, I_1 and I_2 are the currents in the coils, and Δ_2, Δ_4, and Δ_6 are algebraic terms involving the four small ratios b_1/a_1, c_1/a_1, b_2/a_2, and c_2/a_2 to the degrees two, four, and six, respectively. Terms of odd degree do not appear in the formula, because the centroid of each coil section is, for convenience, taken as the origin of reference, about which the force is expanded by Taylor's theorem in four variables.

In the measurements reported in the previous paper by Curtis and Curtis, the four small ratios given above were all of the same order of magnitude and so small that terms of sixth degree were less than 1 part in a million. For this reason the term Δ_6 has not previously been evaluated.

In the present paper there is described a new moving coil, P1, with a single layer whose axial width, $2b_2$, is so much larger than any previous coil (2.7 cm as compared with 1 cm) that the evaluation of a small number of the many terms of sixth degree was required. The number was not excessive because of the small radial depth, $2c$, which was only 0.1 that of the other coils.

[14] Snow, BS J. Research **11**, 681 (1933) RP615.

By the same methods used in obtaining Δ_2 and Δ_4, it is found that all terms of importance in Δ_6 are given by

$$\Delta_6=\frac{b_2^2}{6!}\left\{\left[\frac{b_2^4}{7}+b_1^2b_2^2+b_1^4\right]\frac{D_x^6F}{F}+c_1^2\left[b_2^2+\frac{10b_1^2}{3}\right]\frac{D_{a_1}^2D_x^4F}{F}+c_1^4\frac{D_{a_1}^4D_x^2F}{F}\right\} \tag{5}$$

Using the partial differential equation for F, these partial derivatives may all be expressed in terms of ordinary x-derivatives, as in the original derivation. The latter may then be expressed, as before, in terms of

$$\lambda_n(x)=\frac{(-1)^{n+1}x^nF^{(n)}_{(x)}}{F},$$

so that in addition to the λ_1, λ_2, λ_3, and λ_4 (defined in eq 12 of the paper listed in footnote 14) there are the two new ones

$$\lambda_5=\frac{x^2[-75x^2\lambda_1+213x^2\lambda_2-(117x^2+40)\lambda_3+20(x^2+1)\lambda_4]}{x^4+2x^2+\beta^2} \tag{6}$$

$$\lambda_6=\frac{x^2[-288x^2\lambda_2+447x^2\lambda_3-(177x^2+60)\lambda_4+24(x^2+1)\lambda_5]}{x^4+2x^2+\beta^2} \tag{7}$$

In computing the λ's by these formulas, $\lambda_1=0$ for the position of maximum force. Equation 5 becomes

$$\Delta_3=\frac{-b_2^2}{x^6A^46!}\left\{\left(\frac{b_1^4+b_1^2b_2^2+\frac{b_2^4}{7}}{A^2}\right)\lambda_6+\frac{c_1^2}{6a_1^2}(3b_2^2+10b_1^2)(x^2\lambda_4-48\beta\lambda_1)\right.$$

$$+\frac{c_1^2}{6a_1^2}(3b_2^2+10b_1^2-6c_1^2)[-(1+\beta)\lambda_6+(x^2-\beta)\lambda_5-5(x^2+\beta)\lambda_4$$

$$\left.-4\beta(5\lambda_3+15\lambda_2+18\lambda_1-30)]\right\}, \tag{8}$$

where

$$A^2=a_1^2+a_2^2,$$

$$\beta=(1-\alpha^2)/(1+\alpha^2),$$

and all the other quantities have been previously defined. The expressions for λ_1, λ_2, λ_3, and λ_4 are given in Snow's paper [15] and were reproduced for the case of maximum force in the previous paper [16] by Curtis and Curtis.

If this expression for Δ_6, together with those previously obtained for Δ_2 and Δ_4, be used in eq 4, this gives the force $\mathfrak{F}(x, a)$ for any axial separation of the coils. However, in practice this separation was adjusted to give the maximum force, denoted by $\mathfrak{F}_m=\mathfrak{F}(x_m, \alpha)$, where $x_m=z_m/A$ and z_m the separation which gives maximum force, $\mathfrak{F}_m$, between the actual coils, while $x_0=z_0/A$, where z_0 is the separation which gives maximum force, F_m, between two filaments. The relation between x_m and x_0 is $x_m=x_0+\delta x_0$, where δx_0 is obtained by substituting

[15] Reference in footnote 14.
[16] Reference in footnote 1.

in eq 16 of Snow's paper, expanding in powers of δx_0 and taking account of the fact that $F'(x_0,\alpha)=0$. It is thus found that

$$\frac{\delta x_0}{x_0}=\frac{x_0\Delta_2'}{\lambda_2}\left\{1-\Delta_2+\frac{\lambda_3}{2\lambda_2}\left(\frac{x_0\Delta_2'}{\lambda_2}\right)+\frac{x_0^2\Delta_2''}{\lambda_2}+\frac{\Delta_4}{\Delta_2'}\right\}_{x=x_0}, \tag{9}$$

where primes designate derivatives with respect to x. In the original application contemplated, where the degree of the term was the same as its order of magnitude, a precision of the fourth order in the maximum force was obtained by taking $\delta x_0/x_0=x_0\Delta_2'/\lambda_2$, which is the second degree. The additional terms in the bracket of eq 9 are now necessary, because the contributions of terms involving b_2 are larger. The order of magnitude of $\delta x_0/x_0$ is the same as before.

Applying a Taylor's expansion to the force, $\mathfrak{F}$, as a function of x, about the point x_0, and making use of eq 9, the formula is obtained by which the maximum force is computed

$$\mathfrak{F}_m=n_1n_2I_1I_2F(x_0,\alpha)\left\{1+\Delta_2+\Delta_4+\frac{(x_0\Delta_2')^2}{2\lambda_2}\right.$$
$$\left.+\left[\Delta_6+x_0\Delta_4\left(\frac{x_0\Delta_2'}{\lambda_2}\right)+\frac{1}{2}(x_0^2\Delta_2''-\lambda_2\Delta_2)\left(\frac{x_0\Delta_2'}{\lambda_2}\right)^2+\frac{\lambda_3}{6}\left(\frac{x_0\Delta_2'}{\lambda_2}\right)^3\right]\right\} \tag{10}$$

Formulas have been given (either in this or in the previous paper on the ampere) for computing all the above quantities except Δ_2''. This is

$$x_0^2\Delta_2''=-\frac{1}{12x_0^2}\left\{\frac{2(b_1^2-c_1^2+b_2^2-c_2^2)}{A^2}\lambda_4+\left[\left(\frac{c_1^2}{a_1^2}+\frac{c_2^2}{a_2^2}\right)x_0^2-\left(\frac{c_1^2}{a_1^2}-\frac{c_2^2}{a_2^2}\right)\beta\right]\lambda_3\right.$$
$$-2\left[\left(\frac{c_1^2}{a_1^2}+\frac{c_2^2}{a_2^2}\right)x_0^2+\left(\frac{c_1^2}{a_1^2}-\frac{c_2^2}{a_2^2}\right)\beta-\frac{(b_1^2-c_1^2+b_2^2-c_2^2)\lambda_2}{A^2}\right]\lambda_2$$
$$\left.+6\left(\frac{c_1^2}{a_1^2}-\frac{c_2^2}{a_2^2}\right)\right\} \tag{11}$$

The bracket of eq 10 which is added to the original formula for the force, contains only terms of sixth degree—and only those which are infinitesimals of the fourth order (considering b_1/a_1 and c_1/a_1 as infinitesimals of the first order.)

The value of α can be obtained more accurately by electrical measurements, than by mechanical measurements. For the electrical measurement of the ratio of the radii, the coils are mounted concentric and coplanar. Currents I_1' and I_2' in the coils are adjusted until the magnetic fields, H_1 and H_2 at the common center are equal and opposite. If $\tau=n_2I_2'/n_1I_1'$, when $H_1+H_2=0$, it is necessary to determine the relation between τ and α.

For the fixed coil of rectangular section, the magnetic field, H_1, at its center is given by eq 24 of Snow's previous paper,[17] when terms of sixth degree are negligible, as was the case with coils previously used and also in the present case.
This is

$$H_1=\frac{2\pi n_1I_1'}{a_1}\left[1+\frac{J_1}{a_1^2}+\frac{G_1}{a_1^4}\right] \tag{12}$$

[17] Reference in footnote 14.

For the solenoidal moving coil, the magnetic field, H_2, at its center is given with an accuracy of 1 part in a million, provided terms of sixth degree are now retained, which gives

$$H_2=\frac{2\pi n_2 I_2'}{a_2}\left[1+\frac{J_2}{a_2^2}+\frac{G_2}{a_2^4}+\frac{K_2}{a_2^6}\right] \tag{13}$$

In eq 12 and 13

$$J_i=\frac{c_i^2}{3}-\frac{b_i^2}{2},\ G_i=\frac{c_i^4}{5}-b_i^2c_i^2+\frac{3b_i^4}{8},\text{ and } K_i=-\frac{5b_i^6}{16}, \tag{14}$$

where the subscript i may be either 1 or 2, according as H has a subscript 1 or 2. Equating the values of H_1 and H_2, solving, and inserting the value of τ

$$\alpha\equiv\frac{a_2}{a_1}=\tau\left\{1-\frac{1}{a_1^2}\left(J_1-\frac{J_2}{\tau^2}\right)+\frac{1}{a_1^4}\left[J_1^2-G_1+\frac{J_1J_2}{\tau^2}+\frac{G_2-2J_2^2}{\tau^4}\right]\right.$$
$$\left.+\frac{1}{a_1^6}\left[\frac{K_2}{\tau^6}+\frac{4J_2}{\tau^2}\left(J_1-\frac{J_2}{\tau^2}\right)^2\right]\right\} \tag{15}$$

This equation gives the ratio of the radii of the centroids of the coils as a function of the ratio, τ (which is measured electrically), and of the ratios of the cross-sectional dimensions of both coils to the radius of the larger coil (which are determined from mechanical measurements).

In practice it has been found more convenient to compute a correction for each coil than to employ eq 15. Since for any coil the formula [18] for the magnetic field at its center may be written as

$$H=\frac{2\pi nI}{a}(1-\Delta), \tag{16}$$

it follows that, for any two coaxial and concentric coils in which there are currents I_1' and I_2' such that $H_1+H_2=0$ and in which the subscript 1 is used for all the constants of the larger coil and 2 for the smaller coil.

$$\alpha\equiv\frac{a_2}{a_1}=\frac{n_2I_2'(1-\Delta_2)}{n_1I_1'(1-\Delta_1)}, \tag{17}$$

where for each coil

$$1-\Delta=1-\frac{b^2}{2a^2}+\frac{c^2}{3a^2}+\frac{3b^4}{8a^4}-\frac{b^2c^2}{a^4}+\frac{c^4}{5a^4}-\frac{5b^6}{16a^6}+\ \ldots \tag{18}$$

The last term of the series was required only for the solenoidal moving coil. Since Δ is a function of the dimensions of the coil, it is a constant that, when once computed, can be applied to any combination for measuring the ratio of the radii in which it is used.

[18] See p. 707 of previous paper. Reference in footnote 1.

XII. APPENDIX II

Correction to the Force Caused by an Axial Displacement of Some of the Turns in the Coils Made from Aluminum Ribbon

By Chester Snow

The width, w, of the conducting ribbon with which the coil was wound was practically constant. The successive layers did not lie exactly one above the other, so that the axial width, $2b$, of the coil was not the same as the width of the ribbon, and the cross section of the winding was not exactly a rectangle of the axial width, $2b$, and the radial depth, $2c$ (area $S=2cw$), but was like that of a pack of cards which had been given a shear (nonuniform). The area, S, and the radial depth, $2c$, remain unaltered.

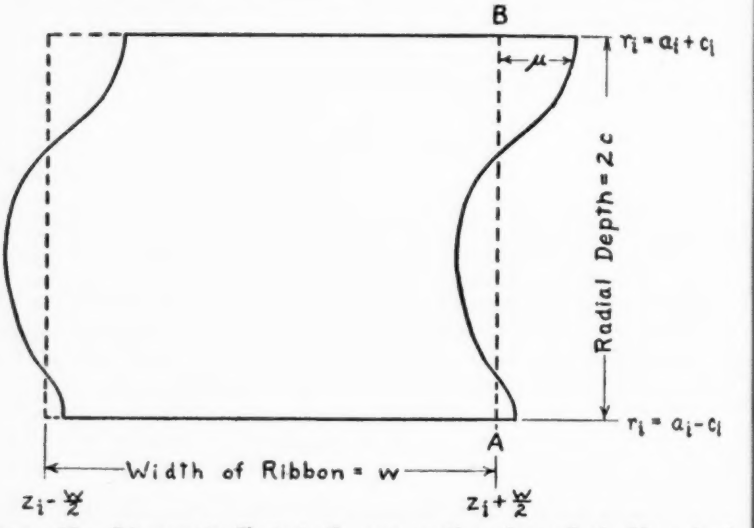

FIGURE 10.—*Diagram to illustrate the cross section of a coil of ribbon when the individual turns are displaced with respect to the average position.*

Let μ (which is a function of r) represent the amount by which the tape at radius r is displaced in the positive z-direction from the position it would have if the section were rectangular. The sides, in the radial direction, of this ideal rectangle are shown as dotted lines in figure 10. The true section is shown in the figure as bounded in the radial direction by two parallel curves. The two sections have the same center of gravity ($\Sigma\mu=0$) but do not have the same moments and products of inertia ($\Sigma\mu^2\neq 0$ and $\Sigma\mu_p\mu_q\neq 0$, where μ_p and μ_q are the displacements at any two positions, p and q).

The modification of the original formula for the force between coaxial coils to allow for the axial displacements of the ribbons was obtained by following through the unpublished details used in the original derivation. The following notation is the same as used in the original derivation [19], where the subscript i (=1 or 2) may refer to either of the two coils.

[19] C. Snow, BS J. Research 11, 681 (1933) RP615.

The centroid of each coil section is taken as the reference point both for the calculation of maximum force $\mathfrak{F}_m$ between the coils and for the determination of the ratio α of their effective radii, so that terms of odd degree in μ do not appear in the formula. The displacement, μ, is for each layer small relative to w, the width of the strip.

A reexamination of all the terms of the original expansion [20] for determining the force between coils shows that the only modification to be made in this equation is that b_i^2 must be replaced [21] by $\frac{w^2}{4}+\frac{3}{2}\bar{\mu}_i^2$, where $\bar{\mu}_i^2$ is the average of μ_i^2 with respect to r; that is,

$$\bar{\mu}_i^2=\frac{1}{2c_i}\int_{a_i-c_i}^{a_i+c_i}\mu^2(r_i)dr_i \qquad i=1, 2. \tag{19}$$

This correction comes from an integral representing the moment of inertia of the section. Two integrals of the same order of magnitude also appear. They represent products of intertia of the form

$$\frac{1}{S_i}\int\int(r_i-a_i)(z_i'-z_i)dS_i$$

but are multiplied by $D_{a_i}FD_{a_i}F$, and D_zF is zero for the maximum force, so the products of inertia are unimportant.

If $b_i-w_i/2=\delta b_i$, then from the above relationship

$$\frac{\delta b_i}{b_i}=\frac{3\bar{\mu}_i^2}{4b_i^2} \tag{20}$$

The complete effect of this error in b_1 and b_2 cannot be found until an examination is made of the effect of these μ-displacements on the magnetic field as it is related to the magnetic determination of the ratio, α, of the radii.

On repeating the derivation of eq 24 of the previous paper for this field, H, no products of inertia appear, and the same change in b is required as was found in the case of the formula for the force $\mathfrak{F}_m$.

This error in b_1 and b_2 causes an error, $\delta\mathfrak{F}_m$, in the final evaluation of the maximum force, $\mathfrak{F}_m$, in two ways: first, in the force formula; second, in the ratio, α, of the radii.

Both of these effects are taken into account in the variation formula of the previous paper.[22] If the value of $\delta b_i/b_i$ from eq 20 is inserted in this formula, then

$$\frac{\delta\mathfrak{F}_m}{\mathfrak{F}_m}=\frac{-3}{8x_0^2}\left\{\left[\left(\frac{1+\beta}{3}\right)\lambda_2-\beta\right]\frac{\bar{\mu}_1^2}{a_1^2}+\left[\left(\frac{1-\beta}{3}\right)\lambda_2+\beta\right]\frac{\bar{\mu}_2^2}{a_2^2}\right\}, \tag{21}$$

where $\bar{\mu}_i^2=\frac{1}{N_i}\sum_{n=1}^{N_i}\mu_i^2$, in which μ_i is the displacement of the nth turn. It is measured in the axial direction from the line AB so chosen that $\sum_{n=1}^{N_i}\mu_n=0$, where N_i is the number of turns.

[20] See eq 7 of the paper referred to in footnote 19.

[21] An equivalent formula is given, without derivation by Rosa, Dorsey, and Miller, Bul. BS 8, 269 (1911) S171. The formula is given on p. 316.

[22] See eq 27 of the paper referred to in footnote 19.

U. S. Department of Commerce National Bureau of Standards

RESEARCH PAPER RP1201

Part of Journal of Research of the National Bureau of Standards, Volume 22, May 1939

EFFICIENCY OF A ROTARY DISTILLATION COLUMN [1] [2]

By Beveridge J. Mair and Charles B. Willingham [3]

ABSTRACT

Determinations of the height equivalent to a theoretical plate (H.E.T.P.), hold-up, and through-put were made on a rotary distillation column of the Pegram-Urey-Huffman type having a rectifying section 56 cm long and 5.08 cm in diameter. Using as rotating members (1) baskets with fine holes, (2) flat plates, and (3) cones, tests of separating efficiency were made at speeds of rotation ranging from 250 to 1,500 rpm and through-puts ranging from 1 to 10 ml of liquid per minute. The binary system methylcyclohexane–*n*-heptane was used as the test mixture. The lowest H.E T.P. was obtained with the conical rotating members spaced 0.64 cm apart, with which the following average results were obtained: H.E.T.P., 1.04 cm; hold-up, 1.3 to 1.6 ml of liquid per theoretical plate; maximum through-put, 10 ml of liquid per minute. Within the reproducibility of these experiments, there was no variation in H.E.T.P. for values of through-put from 2 to 10 ml of liquid per minute and speeds of rotation from 250 to 1,500 rpm.

CONTENTS

	Page
I. Introduction	519
II. Column assembly	520
1. Baskets	522
2. Flat plates	522
3. Cones	522
III. Experiments	523
IV. Results	523
V. Conclusion	526
VI. References	527

I. INTRODUCTION

Though many improvements have been made in packed and bubble-cap laboratory distillation columns in the past few years, columns of still greater efficiency are needed for separating hydrocarbons of eight or more carbon atoms per molecule from the gasoline and kerosene fractions of petroleum. Of the major characteristics which describe a distillation column, namely, the height equivalent to a theoretical plate (H.E.T.P.), the hold-up, and the through-put, the through-put is of least importance when the greatest possible separation is desired.

Fenske and coworkers [1, 2, 3, 4] [4] have made a comprehensive

[1] Financial assistance has been received from the research fund of the American Petroleum Institute. This work is part of Project 6, The Separation, Identification, and Determination of the Constituents of Petroleum.

[2] Presented before the Division of Petroleum Chemistry at the ninety-seventh meeting of the American Chemical Society in Baltimore, Md., April 3 to 7, 1939.

[3] Research Associates at the National Bureau of Standards, representing the American Petroleum Institute.

[4] Figures in brackets indicate the literature references at the end of this paper.

study of the efficiency of packed columns. They found that for a given type of packing in columns from 5.4 cm to 2 cm in diameter, decreasing the diameter of the column decreased the H.E.T.P. [1]. The most efficient column described by these authors [3] had an H.E.T.P. of about 2.5 cm, an inside diameter of 2 cm, and was packed with single-turn helices (0.24 cm in diameter) made of No. 30 AWG stainless-steel wire. Bruun and coworkers [5, 6, 7, 8] have designed and tested a number of bubble-cap columns. The latest design of this type [7] has an H.E.T.P. of about 2.5 cm and a hold-up of about 1 ml per theoretical plate. Since so much work has been done on the improvement of packed and of bubble-cap columns, it seems unlikely that a substantial reduction in H.E.T.P. can be made in these columns.

Few data are available on rotary columns of the type designed by Pegram, Urey, and Huffman [9]. Their original column had a diameter of 15.2 cm and a hold-up of 10 to 20 ml per theoretical plate. Tested by Huffman and Urey [10] with a mixture of ordinary water and deuterium oxide, this column had an H.E.T.P. of about 1.6 cm. However, Huffman and Urey [10] have implied that a considerably better H.E.T.P. might be obtained with a hydrocarbon test mixture.

This paper describes tests with respect to H.E.T.P., hold-up, and through-put made with a hydrocarbon mixture in a rotary column of smaller dimensions than that of Pegram, Urey, and Huffman. These tests were made with different types of plates, different speeds of rotation, and different through-puts.

II. COLUMN ASSEMBLY

In all of the experiments, the same column and still assembly were used, but with three types of rotating members: (1) baskets with small holes, (2) flat plates, and (3) cones. The stationary members were in all cases sections of a cone and were held in position with spacers on the inner wall. The complete still assembly with rotating cones is shown schematically in figure 1. This assembly differs from the Pegram-Urey-Huffman column only in minor mechanical details and in the dimensions and spacings of its parts. The fractionating column consists of the cylinder, G, and the rotating shaft, A, which is located in the axis of the cylinder and which bears the rotating members, J (baskets, plates, or cones). The shaft, A, extends through the condenser, B, to the motor and is held in position by three bearings. Reflux from the condenser, B, flows from the stationary cone to the top of the rotating member, from which it is forced by centrifugal action to the next lower stationary cone. At the lower end of the condenser there is an inner seal, C, so that liquid returning from the condenser to the column flows first through the U-tube, D, from which samples may be withdrawn as desired. The still pot contains a charging tube into which fits a siphon which extends to a small well in the bottom of the still pot. To the charging tube there is also fitted a manometer, L, which contains butyl phthalate. The entire assembly was made of brass, with the exception of the glass sampling tube, D, and the manometer tube, L. These tubes were attached through standard taper Pyrex-to-brass joints sealed with soft solder.

The length of the cylinder, G, was 56 cm, its inside diameter 5.08 cm and outside diameter 5.4 cm. The diameter of the shaft was 0.95 cm. The spacers which held both the rotating and stationary members had a wall thickness of 0.16 cm. They were made from brass tubing and

had a sliding fit over the shaft and inside the cylinder. Other dimensions may be obtained from figure 1.

The column was electrically heated in two sections. Asbestos rope (0.64 cm diameter) was hung vertically down the outside of the

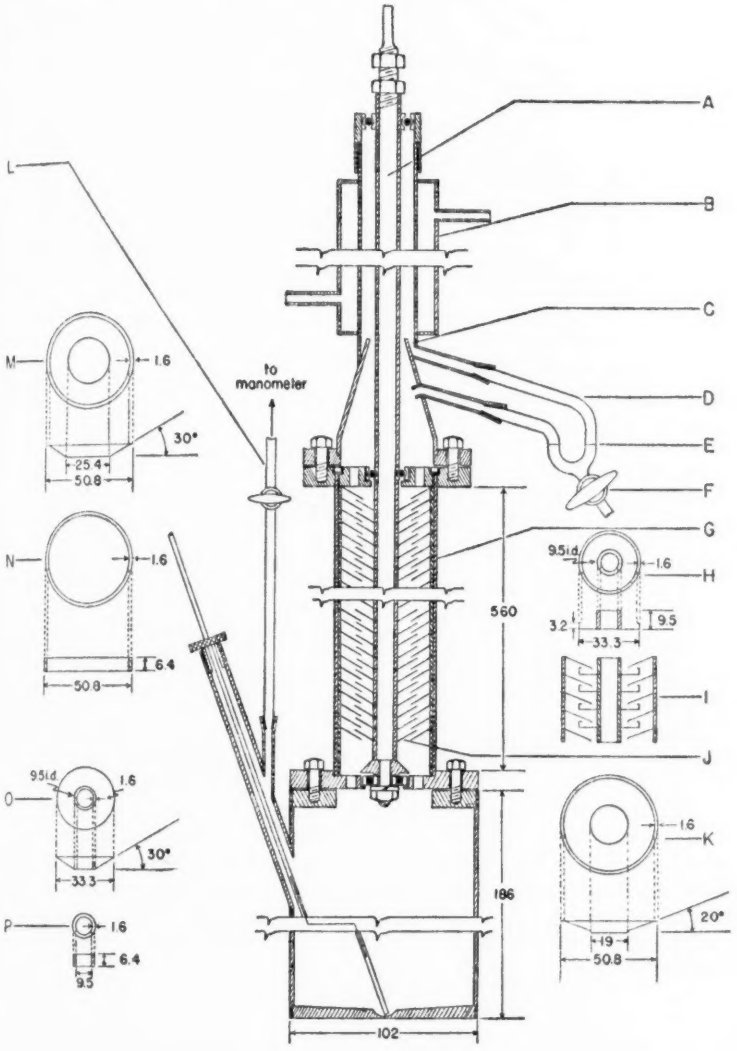

ALL DIMENSIONS IN MM

FIGURE 1.—*Schematic diagram of distillation column.*

column and around this was wound the asbestos-insulated heating wire. The heating wire was covered with a 2.5-cm layer of magnesia-asbestos. Weston bimetallic laboratory thermometers with dial faces were used to read the temperature of the column. The stems of these

instruments fitted through the magnesia-asbestos lagging and extended into brass tubes soldered to the outside of the column.

1. BASKETS [4]

The greatest separation would appear to be attained in a column in which a fog of colloidally small particles of reflux is traversed by a very slow stream of vapor. Such a column is not practicable, since only an infinitely slow vapor velocity would prevent such a fog from being carried along by the vapor stream. However, in the Pegram-Urey-Huffman column there may be an approximation to these conditions. In this column there is between the cylinder walls and the periphery of the rotating cones a gap of 1 cm in which a spray of fine globules of reflux is traversed by vapor, and it may be that a considerable portion of the efficiency of this column is attributable to the contact between spray and vapor rather than to the contact between the film of liquid on the metal surfaces and the vapor. This idea prompted the experiments with rotating baskets with holes in the outer edge, which it was thought might produce a better spray.

Preliminary experiments were made with baskets of this type and with flat plates in a short section of a 5-cm glass tube. Kerosene was allowed to flow down the tube and air up the tube to simulate the conditions in a column. For visual examination of the inside of the column, the metal spacers which held the stationary cones had strips cut out of the centers. Visual examination gave no information about the size of the globules, but did indicate that the spray produced by the baskets was distributed over a wider area than that from the plates.

A short section of the experimental column with baskets is shown in figure 1 (*I*). The baskets were 3.33 cm in diameter, the sides 0.32 cm high, and the lip 0.16 cm wide. In the sides of these baskets were 50 holes (each with a diameter of 0.045 cm) arranged in two rows. The stationary cones had an angle of 20°, and the diameter of the hole in the small end of the cone was 1.9 cm. The spacers for both baskets and stationary cones were 0.95 cm in height. Both the stationary cones and the rotating baskets had a wall thickness of 0.04 cm. The 56-cm section contained 55 baskets and 56 stationary cones.

2. FLAT PLATES

After the experiments with the baskets had been completed, the latter were replaced with flat plates of the same diameter (3.33 cm). No other part of the column was changed, in order that the effect on the H. E. T. P. of substituting flat plates for baskets would be directly determinable.

3. CONES

In the experiments with cones, the spacers were reduced to a height of 0.64 cm. This spacing is about the smallest practicable because any closer spacing is likely to cause flooding at very low through-puts. The angle on both sets of cones (*M* and *O*, fig. 1) was 30°. The diameter of the upper edge of the rotating cones was 3.33 cm, the same as that of the baskets and plates previously used. However, the diameter of the hole at the bottom of the stationary cones was

[4] Spraying devices similar to these baskets are used in the Maclaurin scrubber [11] to secure intimate contact between gases and liquids.

2.5 cm compared with 1.9 cm for the stationary cones used previously. In the direction parallel to their surfaces, the stationary and rotating cones overlapped only about 0.48 cm. It was thought that this small overlap might reduce any tendency to flood caused by the close spacing. The 56-cm section contained 77 rotating cones and 78 stationary cones.

III. EXPERIMENTS

The *n*-heptane and methylcyclohexane used in the test mixture were purified by filtration through silica gel and then by distillation in helix-packed columns having a separating efficiency corresponding to about 100 theoretical plates. The data obtained by Bromiley and Quiggle [12] for the analysis of this mixture by refractive index were used. The number of theoretical plates was computed with the aid of the equation derived by Fenske [13], using for the relative volatility, α, the value 1.07 given by Beatty and Calingaert [14].

The rotary column is not more difficult to operate than packed or bubble-cap columns and may be left to run unattended. The tests were made under total reflux, small samples of 1 to 2 ml being withdrawn from the still head and still pot at intervals of about 4 hours. When the refractive indices of successive head samples and pot samples were substantially constant (usually within ± 0.0003), equilibrium was considered to have been established.

To determine the through-put, the stopcock, *F*, was adjusted so that the liquid level in the U-tube fell to *E* and the rate of flow of condensate just balanced that of the liquid dripping through the stopcock. The volume dripping through the stopcock in unit time was then obtained. It will be noticed from figure 1 that the ring for collecting the condensate was very close to the condenser and considerable condensation probably occurred below this ring. Therefore, the values of through-put recorded are minimum and are not precise to better than ± 1 ml per minute.

Hold-up was determined by the method of Tongberg, Quiggle, and Fenske [2]. This method consists in introducing into the dry still pot a mixture of known composition of a volatile and a nonvolatile liquid. After the column is operating as desired, a sample is removed from the still pot and the relative concentrations of the volatile and nonvolatile substances are determined. From the change in composition, the hold-up can be computed. Benzene and Marcol (an aromatic-free fraction of petroleum having an initial boiling point of about 230° C at 56 mm Hg) were the liquids used. The sample was siphoned from the still pot into a trap chilled with solid carbon dioxide, so that no benzene was lost. The volume of liquid contained in the annular ring and sampling U-tube at the head of the still (4 ml) was deducted from the observed values of the hold-up. The hold-up values recorded are, therefore, for the rectifying section and still pot.

IV. RESULTS

The results of these experiments are tabulated in table 1 in the order in which they were obtained. The lowest H.E.T.P., 0.87 to 1.35 cm, was obtained with the cones which were spaced 0.64 cm apart (experiments 7 to 27). This is to be compared with an H.E.T.P. of 1.46 to 1.82 cm for the baskets (experiments 1 to 4) and 1.88 cm

for the plates (experiments 4 to 6) with a 0.95-cm spacing. The plate efficiency, that is, the ratio of the number of theoretical to the number of actual plates, varies from 0.56 to 0.70 for the baskets, is 0.54 for the plates, and varies from 0.54 to 0.84 for the cones. Although the plate efficiency of the baskets does not differ appreciably from that of the cones, it is evident that, since it is not possible to pack together the baskets as closely as the cones, the baskets can not be expected to produce as low an H.E.T.P. Moreover, the baskets are expensive to construct.

TABLE 1.—*Results of experiment on rotary column*

Experiment number	Rotating members [a]	Stationary members	Spacing of like members	Speed	Through-put [b]	Pressure drop from pot to head [c]	Composition of mixture mole percent *n*-heptane		Number of theoretical plates	Ratio: Theor. plates / Actual plates	H.E.T.P.
							Pot	Head			
			cm	*rpm*	*ml/min (liq.)*	*mm Hg*					*cm*
1	Baskets	Cone, angle 20°	0.95	500	7.6	1.38	20.5	69.0	30.8	0.56	1.82
2	do	do	.95	300		0.69	25.9	77.4	32.6	.59	1.72
3	do	do	.95	1,500	9.6		23.7	79.6	36.4	.65	1.54
4	do	do	.95	1,500	3.5		23.5	81.5	38.3	.70	1.46
5	Plates	do	.95	500	(10)	1.00	18.7	64.8	29.7	.54	1.88
6	do	do	.95	1,500	11	1.38	14.9	58.5	29.8	.54	1.88
7	Cone, angle 30°	Cone, angle 30°	.64	500	7	1.53	24.3	85.1	41.5	.54	1.35
8	do	do	.64	1,500	6.3	1.30	19.0	87.7	49.8	.65	1.12
9	do	do	.64	1,500	5.8	1.15	27.0	94.6	55.8	.72	1.00
10	do	do	.64	1,500	9.4	1.69	16.6	86.0	49.5	.64	1.13
11	do	do	.64	1,500	(6)	1.30	10.8	80.2	50.7	.66	1.10
12	do	do	.64	1,500		0.77	20.5	85.1	44.8	.58	1.25
13	do	do	.64	1,500	0.8	1.00	14.1	83.8	50.0	.65	1.12
14	do	do	.64	1,500	(2)	1.07	6.8	66.0	47.5	.62	1.18
15	do	do	.64	500	6.7	1.46	21.8	92.4	54.7	.71	1.02
16	do	do	.64	500	2.8	1.07	22.4	90.8	51.2	.67	1.09
17	do	do	.64	500	5.2	1.23	27.0	95.8	59.7	.78	0.94
18	do	do	.64	500	8.5	1.61	25.3	91.2	49.6	.64	1.13
19	do	do	.64	500	4.8	1.15	21.9	94.6	60.2	.78	0.93
20	do	do	.64	500	4.8	1.15	16.4	92.4	60.0	.78	.93
21	do	do	.64	1,500	4.7	1.30	14.8	90.8	58.7	.76	.95
22	do	do	.64	1,500	7	1.53	12.6	85.2	53.7	.70	1.04
23	do	do	.64	1,500	1.8	1.15	21.1	95.8	64.7	.84	0.87
24	do	do	.64	250	3.4	0.84	19.2	93.4	59.3	.77	.94
25	do	do	.64	250	3.7	.84	20.8	88.0	48.1	.62	1.16
26	do	do	.64	250	1.0	.61	17.4	88.9	52.7	.68	1.06
27	do	do	.64	250	5.6	.92	17.1	83.1	45.4	.59	1.23

[a] There were 55 rotating and 56 stationary members for experiments 1 to 6 and 77 rotating and 78 stationary members for experiments 7 to 27.

[b] For the basket-shaped rotating members, 0.95 cm apart, the flooding through-put is 25 to 30 ml of liquid per minute; for the flat-plate rotating members about the same; and for the conical rotating members, about 10 to 12 ml of liquid per minute. The values in brackets in this column were estimated from the pressure drop.

[c] The values recorded in this column were obtained by conversion of the readings of butyl phthalate

It is evident from figure 2 that the speed of rotation has no significant influence on the H.E.T.P. Huffman and Urey [10] found this true for their larger column with mixtures of ordinary water and deuterium oxide.

Within the reproducibility of these measurements, there appears also to be little if any variation in H.E.T.P. with through-puts varying from 1 to 10 ml per minute. With experiment 12 (not plotted in fig. 2) a lower efficiency was obtained. The through-put for this experiment was not determined, but, judging from the pressure drop, it

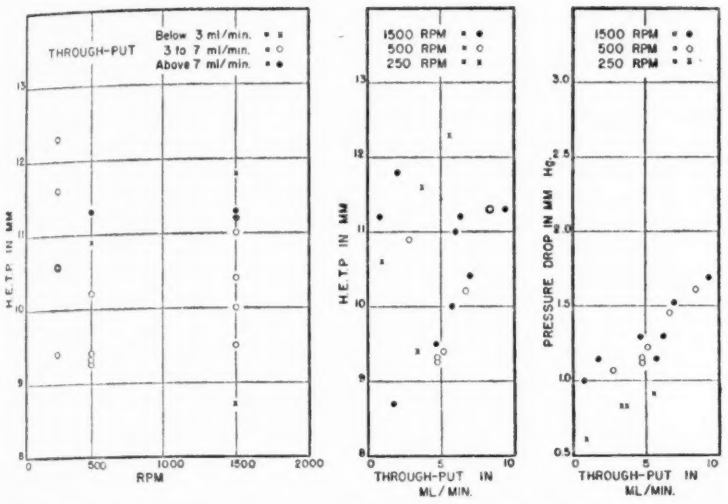

FIGURE 2.—*Chart showing for the column with conical rotating members: (a) H.E.T.P. with respect to revolutions per minute; (b) H.E.T.P. with respect to through-put; and (c) pressure drop with respect to through-put.*

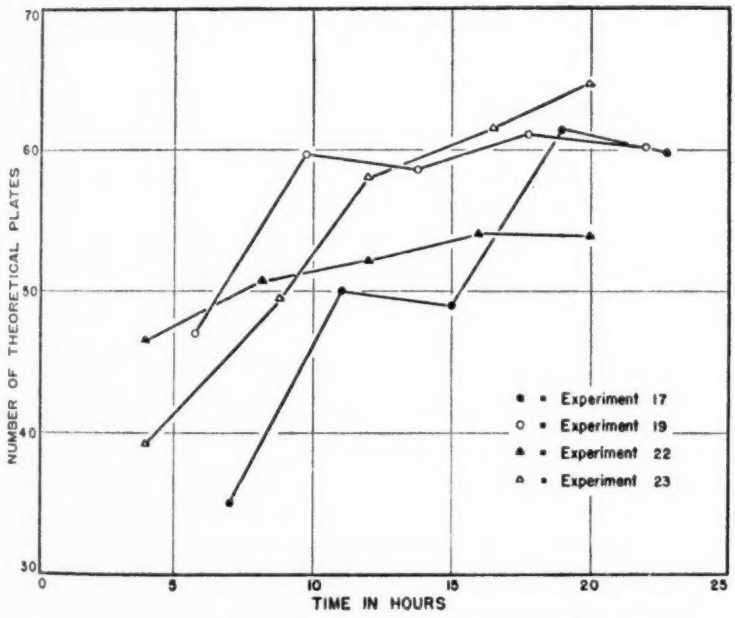

FIGURE 3.—*Chart showing variation in number of theoretical plates with respect to time.*

must have been very small, and it is questionable whether sufficient liquid was present to wet adequately the metal surfaces.

As is to be expected, the pressure drop in the column is greater, the greater the through-put. The pressure drop depends to some extent on the speed of rotation. At least it is less for a given through-put at 250 rpm than at 500 or 1,500 rpm.

The variation in the number of theoretical plates with time is shown for a few typical experiments in figure 3. After about 10 to 12 hours equilibrium is substantially established. Although sometimes a decrease and sometimes an increase in theoretical plates occurs after 12 hours, this variation is apparently normal for the column.

The variation in hold-up for various through-puts at rotation speeds of 500 and 1,500 rpm is shown in figure 4. The hold-up varies from about 70 to 86 ml with through-puts varying from 2 to 10 ml and does not depend appreciably on the speed of rotation, although at lower through-puts there appears to be a slightly lower hold-up at higher speeds.

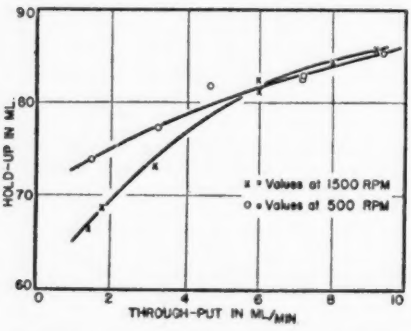

FIGURE 4.—*Chart showing the relationship between hold-up and through-put for two speeds of rotation.*

V. CONCLUSION

Disregarding experiment 7, since it was the first of a series, and experiment 12, for reasons already mentioned, the average value of the number of theoretical plates, using closely spaced cones, is 54, which corresponds to an H.E.T.P. of 1.04 cm. This may be compared with an H.E.T.P. of 2.5 cm for the best bubble-cap [7] or packed columns [3].

The hold-up of the rotary column though small, 1.3 to 1.6 ml per theoretical plate, is somewhat greater than the 1 ml per theoretical plate reported for the bubble-cap column by Bruun and Faulconer [7]. Tongberg, Lawroski, and Fenske [3] have not reported the hold-up for their helix-packed column of 2-cm diameter. However, the great advantage in H.E.T.P. makes the rotary column valuable despite its slightly greater hold-up.

The maximum through-put of the column is about 10 ml of liquid per minute. This compares with slightly over 20 ml per minute reported by Tongberg, Lawroski, and Fenske [3] for the 2-cm packed column and to 30 ml per minute of liquid benzene reported by Bruun and Faulconer [7] for the 2.5-cm bubble-cap column. This smaller through-put is of secondary importance in the last stages of the isolation of hydrocarbons from petroleum, where the time saved by effective distillation greatly outweighs the time involved in the distillation itself.

Judging from these tests, it appears possible to install in a room of ordinary height a laboratory rectifying column having a separating efficiency of from 200 to 250 theoretical plates.

The authors express their gratitude for the advice and encouragement of F. D. Rossini.

VI. REFERENCES

[1] M. R. Fenske, C. O. Tongberg, and D. Quiggle, Ind. Eng. Chem. **26,** 1169 (1934).
[2] C. O. Tongberg, D. Quiggle, and M. R. Fenske, Ind. Eng. Chem. **26,** 1213 (1934).
[3] C. O. Tongberg, S. Lawroski, and M. R. Fenske, Ind. Eng. Chem. **29,** 957 (1937).
[4] M. R. Fenske, S. Lawroski, and C. O. Tongberg, Ind. Eng. Chem. **30,** 297 (1938).
[5] J. H. Bruun, Ind. Eng. Chem., Anal. Ed. **1,** 212 (1929).
[6] J. H. Bruun, Ind. Eng. Chem., Anal. Ed. **8,** 224 (1936).
[7] J. H. Bruun and W. B. M. Faulconer, Ind. Eng. Chem., Anal. Ed. **9,** 192 (1937).
[8] J. H. Bruun and S. D. West, Ind. Eng. Chem., Anal. Ed. **9,** 247 (1937).
[9] G. B. Pegram, H. C. Urey, and J. R. Huffman, Phys. Rev. **49,** 883 (1936); J. Chem. Phys. **4,** 623 (1936).
[10] J. R. Huffman and H. C. Urey, Ind. Eng. Chem. **29,** 531 (1937).
[11] Walker, Lewis, and McAdams, Principles of Chemical Engineering, 2d ed., p. 474 (McGraw Hill Book Co., New York, N. Y., 1927).
[12] E. Bromiley and D. Quiggle, Ind. Eng. Chem. **25,** 1136 (1933).
[13] M. R. Fenske, Ind. Eng. Chem. **24,** 482 (1932).
[14] H. A. Beatty and G. Calingaert, Ind. Eng. Chem. **26,** 504 (1934).

WASHINGTON, February 10, 1939.

U. S. Department of Commerce National Bureau of Standards

RESEARCH PAPER RP1202

Part of Journal of Research of the National Bureau of Standards, Volume 22, May 1939

BEHAVIOR OF RUBBER HYDROCARBON IN A MOLECULAR STILL

By W. Harold Smith and Henry J. Wing [1]

ABSTRACT

The values of the molecular weight of rubber reported in the literature vary from 600 to 350,000 and higher. If the vapor pressure were sufficiently increased, and maintained below the decomposition point of rubber, it seemed possible that the molecules, if small, might distil. To determine this, three distillations were attempted at 160° C for different periods, and with different temperatures at the condensing surface. In one experiment, which was conducted for about 100 hours, the condensing surface was chilled by liquid air. A thin transparent deposit, consisting of about 2 mg, appeared on the condensing surface. It was feebly extensible and did not recover completely when deformed. Its physical properties more nearly resembled rubber than those of other distillates. In a second experiment lasting 250 hours, solid carbon dioxide and acetone were used in the condenser, and in a third one, which was continuous during 140 days, the condensing medium was tap water at about 10° C. It was difficult to remove oxygen from the specimens of rubber which were used. Consequently, the distillates in these experiments were oxidized, at least in part. The distillation products, one of which amounted to about 20 mg, were hard, transparent, and insoluble in ordinary solvents of rubber. In the third experiment the distillate amounted to about 20 mg and showed an iodine number of 328 as compared with 370 for the original purified rubber, indicating that oxidation or cyclization or both may have taken place.

CONTENTS

	Page
I. Introduction	529
II. Apparatus	530
III. Experimental results	531
IV. References	533

I. INTRODUCTION

Some investigators believe that rubber consists of associated molecules, and others accept Staudinger's view that long-chain molecules are formed by polymerization. Pummerer, Andriessen, and Gündel [1] [2] have obtained a molecular weight as low as 600. Meyer and Mark [2] believe that it is approximately 5,000, although they calculated on the basis of osmotic pressures, values as high as 350,000.

They, as well as Pummerer, consider that rubber is an associated colloid and that high molecular weights are caused by aggregates, sometimes called micelles. Staudinger [3], however, considers that the long-chain rubber molecule itself has a molecular weight of 200,000 or even 350,000, and that products with lower values, which may be formed in rubber, result from degradation.

If the molecules are small it might be possible to distil them, if their vapor pressure could be sufficiently increased, but none would distil without decomposition if the molecules are very large. Because the vapor pressure of rubber below its decomposition temperature is low, it appeared of interest to attempt to distil the material in a

[1] Present address, Milltown, N. J.

[2] Figures in brackets indicate literature references at the end of this paper.

molecular still. Paraffin wax and sugar, both substances of relatively high molecular weight, have been successfully distilled in this type of apparatus [4].

Subsequent to the work described in this paper, the molecular weight of sol rubber prepared at this Bureau was determined by E. O. Kraemer and J. D. Lansing [5] of E. I. du Pont de Nemours & Co., Inc. They used the Svedberg method of sedimentation equilibrium in an ultracentrifuge with ethereal solutions of sol rubber. The temperature of the solutions during determinations was approximately 10° C, and an average value of 460,000 was obtained. There was evidence of a mixture of molecular species.

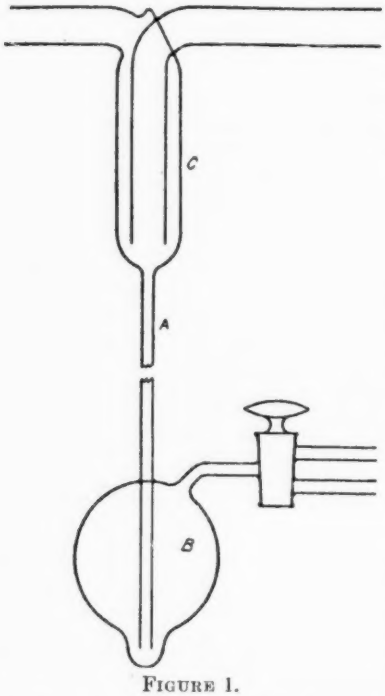

FIGURE 1.

II. APPARATUS

The stills, used in the attempt to distil rubber, consisted essentially of Pyrex Dewar flasks to which side-tubes were sealed that connected the flask to a mercury pump and its auxiliary equipment. The distance between the distilling and condensing glass surfaces was about 7 mm, and the area of the distilling surface was approximately 60 cm². The still was connected to a pumping system, equipped with a suitable trap to condense mercury vapor, and the apparatus was thoroughly evacuated before a distillation was attempted. When distillation extended over many weeks continuously, an automatic control was necessary, and between the still and the trap there was a device to isolate the high-vacuum system when the mercury pump or its condenser ceased to function. When either event occurred, a column of mercury automatically rose, effectively sealed the still, and maintained the low pressure within it. Simultaneously, a bell began to ring as a warning of trouble.

The equipment is illustrated in figures 1 to 4. The mercury cutoff is shown in figure 1. The length of the tube must be properly adjusted so that the mercury in *B* will rise to close the inner tube in *C* when it responds to atmospheric pressure. In figure 2, tube *B* is an extension of its union with the mercury well of the cutoff. A Pyrex rod was welded to the stopper of stopcock *C*. In the closed position, the stopper was supported by a string over the pins, as shown in the diagram. The string ended in a loop which was held at *D* by the catch at *C*. The catch, which resembles that on a common type of mousetrap, was opened when a current flowed through the electromagnet. The latter was operated by dry cells. When the catch was opened, the string was free to move, and was drawn away by a 200-g weight. The capillary shown at *A* in figure 2 prevented any surging of the mercury. At *E*

are shown the contact points of a relay which closed when the heater current to the pump was interrupted.

Figure 3 is a diagram of a switch, operated by water flowing to the condenser. The circuit to the electric heater of the pump was completed through tungsten contacts and mercury. The pressure of water passing through the tube, *AB*, to the condenser of the pump caused the mercury to rise and make contact. Two screw clamps at *A* and *B* regulated the speed and the head of the flow of water. In operation, the pressure head was so adjusted that the mercury stood well above the upper contact with water flowing, and well below when the flow of water stopped entirely. The position of the upper surface of the mercury was so adjusted that small fluctuations of the waterhead in the mains did not open the contact.

A wiring diagram is shown in figure 4. The resistance, *R*, was sufficient to keep the relay, *E*, open, when the heater current was

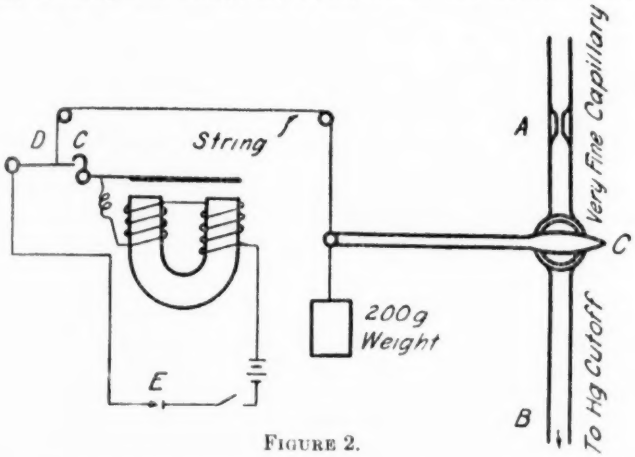

FIGURE 2.

flowing. For a heater drawing about 2 amperes at 110 volts, 5 or 6 inches of No. 26 Nichrome wire was used. Since the relay contacts at *E* were open when current was flowing through the relay magnet, any interruption of the current caused them to close, and completed the circuit to the trip of the mercury cutoff. If the heater current was stopped, the relay current also stopped, and in this case also the trip of the mercury cutoff responded.

III. EXPERIMENTAL RESULTS

Pure sol rubber hydrocarbon, prepared as described in a previous publication [6], was used in all of the experiments. Since the sol fraction is more mobile than the gel, it seemed probable that its molecules would become detached with greater ease. A solution of the rubber hydrocarbon in ether, saturated with nitrogen, was introduced and carefully spread over the distilling surface. The ether was removed at low pressure. The pressure maintained during distillation was too low to be measured by a McLeod gage, since the so-called "click" vacuum was obtained. Experiments with temperatures between 100° and 150° C around the distilling surface produced no distillate. At 160°, after a few days, a faint deposit was observed

on the condenser by using a suitable lens, and in subsequent experiments this temperature was maintained by a heating coil.

Three distillations were performed for different periods and with different temperatures in the condenser. During the first experiment the condensing surface was chilled by liquid air. Distillation was conducted each day for about 8 hours for a total period of 100 hours.

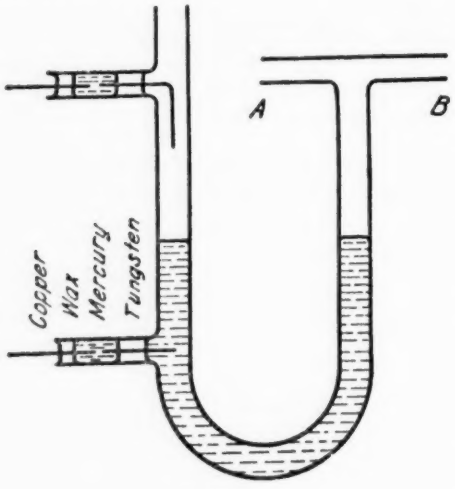

FIGURE 3.

The outer wall of the still was removed, and the condensing surface was washed with acetone. By using a hand lens, a very thin layer of transparent material, estimated to be not more than 2 mg, was visible on the condensing surface. A little was removed on the end of a glass rod and momentarily heated. There was a characteristic odor of burning rubber. The deposit was feebly extensible but did not recover completely when deformed. Its physical properties were more like those of the rubber from which it had been distilled than the properties of distillates obtained in any later experiments. Rubber of low molecular weight may have been distilled in this instance.

An earlier note [7] stated that this Bureau had succeeded in distilling purified rubber without decomposition by heating it in a high vacuum to the temperature of boiling water. This statement was based on the results of this experiment. However, the temperature of distillation was not that of boiling water, but 160° C. On the basis of this

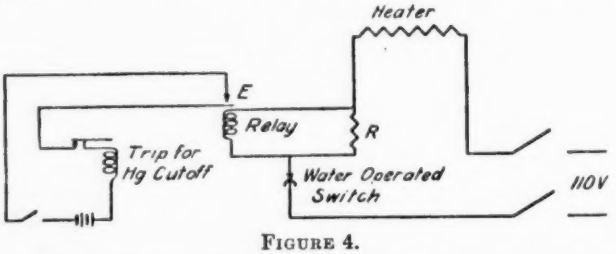

FIGURE 4.

statement, Lens [8] attempted a similar distillation with crude rubber. His experiments failed entirely, however, and probably the temperature of distillation was 100° C and consequently too low.

For the second experiment, solid carbon dioxide and acetone were used in the condenser, which was maintained at approximately −78° C. Distillation was conducted only during the day for a total operating period of about 250 hours. When the still was opened there was an odor of levulinic aldehyde, and when a portion of the undistilled rubber was placed in a hot solution of ammonium acetate,

the vapors of the latter gave a positive pyrrol test with a pine shaving which had been moistened with hydrochloric acid. [9] Levulinic aldehyde is an oxidation product of rubber that responds to the pyrrol test. The thin layer of distillate was transparent, hard, and insoluble in carbon disulfide. There was about 5 mg of distillate.

A third experiment was conducted with tap water in the condenser. The distillation was continuous over 140 days, and during most of the period the temperature of the tap water varied from 8° to 10° C. At the end of the experiment, the residue of undistilled rubber was clear, almost colorless, and recovered slowly when deformed. The material deposited on the condenser, amounting to not more than 20 mg, was visible without a lens. It had collected in droplets, was transparent, and was hard, and not extensible or plastic. There was a marked odor of levulinic aldehyde in the distillate and in the undistilled residue. The distillate was insoluble in ether, benzene, chloroform, ethyl acetate, alcohol, and acetone. Enough of it was scraped from the condenser for a determination of its iodine number by the Kemp-Wijs method [10], but with a dilute solution of iodine. Although the material was insoluble in carbon disulfide, it swelled sufficiently to permit penetration by the iodine solution. The end point was definite. A value of 328 was obtained. The iodine number of purified rubber, determined by the same procedure, was 370. The degree of unsaturation of a cyclic rubber, which was made by incorporating sulfonic acids and heating to 140° C, has been reported as 55 to 65 percent of that of the rubber hydrocarbon [11].

Marked oxidation had undoubtedly occurred during the second and third experiments. The original ethereal solution, though saturated with nitrogen before it was introduced into the still, was exposed to air during the process. It was hoped that any oxygen dissolved in the rubber as a result of this exposure would be removed at the low pressure used, but apparently some was retained. Furthermore, cyclic rubber may have slowly formed at 160° C, and may have distilled. In the second and third experiments, the marked difference in the physical characteristics of the distillate which had been maintained at 10° C, and that of the undistilled rubber which had been heated to 160° C, suggests this possibility. Rubber has a marked tendency to form cyclic compounds, and Kirchhof has shown that they are produced at 200° C.

IV. REFERENCES

[1] R. Pummerer, A. Andriessen, and W. Gündel, Ber. deut. chem. Ges. **62,** 2628 (1929).
[2] K. H. Meyer and H. Mark, Ber. deut. chem. Ges. **61,** 1945 (1928).
[3] H. Staudinger, Die hochmolecularen organischen Verbindungen (J. Springer, Berlin, 1932); H. Staudinger and E. O. Leupold, Ber. deut. chem. Ges. **67,** 304 (1934).
[4] E. W. Washburn, BS J. Research **2,** 476 (1929) RP45.
[5] E. O. Kraemer and J. D. Lansing, Rubber Age **37,** 25 (1935).
[6] W. Harold Smith, Charles Proffer Saylor, and Henry J. Wing, BS J. Research **10,** 479 (1933) RP544.
[7] BS Tech. News Bul. 161, p. 85 (Sept. 1930).
[8] J. Lens, Rec. Trav. Chim. **51,** 972 (1932).
[9] G. Bruni and C. Pelizzola, India Rubber J. **63,** 415 (1922).
[10] A. R. Kemp, Ind. Eng. Chem. **19,** 531 (1927).
[11] H. L. Fisher and E. M. McColm, Ind. Eng. Chem. **19,** 1329 (1927).

WASHINGTON, January 30, 1939.

U. S. DEPARTMENT OF COMMERCE NATIONAL BUREAU OF STANDARDS

RESEARCH PAPER RP1203

Part of Journal of Research of the National Bureau of Standards, Volume 22, May 1939

BASE-COMBINING CAPACITY OF WOOL

By Milton Harris and Henry A. Rutherford [1]

ABSTRACT

It is shown that the failure of wool to reach equilibrium with alkaline solutions under the conditions of titration experiments is due to the reaction of base with the disulfide groups of the cystine. The results indicate that the extent of this reaction can be determined. The data also afford confirmation of the earlier observation that the alkali degradation of the cystine in wool involves the loss of only one sulfur atom from each cystine residue.

The apparent base-combining capacity increases with increasing duration of contact of wool with alkali and with increasing temperature, but the intrinsic base-combining capacity, obtained by making corrections for the dissolved protein and for the base bound by the sulfhydryl groups, becomes constant after approximately 2 hours. The most consistent data are obtained at a low temperature, where, it appears, secondary reactions are greatly inhibited.

Determination of the amount of base absorbed from solutions of various concentrations indicates that a limiting amount of about 0.7 millimole per gram of wool is reached above concentrations of about 0.2 *N* sodium hydroxide. Because of discrepancies in the data obtained at concentrations greater than 0.3 *N*, it is suggested that this value be considered for the present as tentative.

CONTENTS

	Page
I. Introduction	535
II. Experimental procedure	536
1. Materials	536
2. Methods	537
III. Results and discussion	538
1. Effect of sodium hydroxide on the cystine in wool	538
2. Absorption of alkali as a function of time	538
3. Absorption of base from solutions of various concentrations	540
IV. Conclusions	541
V. References	542

I. INTRODUCTION

Many properties of wool are intimately related to the number of acidic and basic groups which it contains. Because of the stability of wool in acid solutions, few difficulties are encountered in determining the acid-combining capacity, which apparently reaches a maximum of about 0.80 millimole per gram of wool at about pH 1 [1].[2] In the alkaline region, however, there has been no indication of a maximum base-combining capacity or of a stoichiometric end point, and as a result, very little knowledge concerning the number of acidic groups in wool can be deduced from published titration data.

The results of recent investigations by Crowder and Harris [2] on the nature of the degradation of wool protein in alkaline solutions

[1] Research Associates at the National Bureau of Standards, representing the Textile Foundation.
[2] Figures in brackets indicate the literature references at the end of this paper.

suggested that the chief difficulty in determining the base-combining capacity arises from the fact that the alkali reacts not only with the free acidic groups, but also with the disulfide groups of the cystine in the protein. It appears that the primary process in the cleavage by alkali of the disulfide linkage consists in a hydrolytic rupture with the formation of a sulfhydryl compound and a sulfenic acid. The latter is unstable in alkaline solution and immediately loses hydrogen sulfide. The general scheme is given in the equations

$$RCH_2-S-S-CH_2R+2NaOH \rightarrow RCH_2SNa+RCH_2SONa+H_2O \quad (1)$$

$$RCH_2SONa \rightarrow RCHO+NaHS \quad (2)$$

The sulfhydryl and the sulfenic compounds, formed according to eq 1, are both acidic, and accordingly, 2 moles of base are taken up in the cleavage of each disulfide group. However, 1 mole is liberated in the breakdown of the sulfenic acid, as shown in eq 2. If the above mechanism is correct, the amount of inorganic sulfide sulfur (NaHS) formed during treatment of wool with a basic solution should be a measure not only of the number of disulfide groups hydrolyzed but also of the amount of base taken up by the sulfhydryl group formed in the wool.

The purpose of the present investigation was to study the absorption of base by wool from the viewpoint of the above hypothesis. It was intended that these studies form a background for the investigation of the basic portion of the complete titration curves.

II. EXPERIMENTAL PROCEDURE

1. MATERIALS

It has been demonstrated in this laboratory and elsewhere [3] that the disulfide group of the cystine in wool is readily attacked by light. Since it was necessary to know the number of disulfide groups which were split during the alkali treatment of the wool, considerable care was exercised in choosing suitable samples for these measurements. Obviously, it was particularly desirable to have the bulk of the sulfur in the form of intact disulfide groups.

Two types of materials were used in these experiments, namely, raw-wool fibers and a specially prepared wool yarn. The former were divided into three approximately equal sections, which were designated as the root, middle, and tip portions of the fiber. Each portion was purified by extraction with alcohol and ether and finally washed with distilled water. The analyses given in table 1 show that both the sulfur and cystine contents decrease from the root to the tip of the fiber, but that only in the tip portion has an appreciable amount of the cystine been destroyed.

The yarn was prepared from raw wool which had been extracted with Stoddard solvent and washed with water. It was further purified as described above. Determination of the total sulfur and cystine contents showed that 97 percent of the former could be accounted for as cystine sulfur, thus indicating that very little photochemical deterioration had occurred. The data reported in this work were obtained on root wool or yarn.

TABLE 1.—*Sulfur and cystine contents of the root, middle, and tip portions of wool fibers*

Sample	Total sulphur	Cystine		Total sulfur as cystine sulfur
		Found	Calculated[1]	
	%	%	%	%
Root	3.46	12.6	12.9	97
Middle	3.32	11.8	11.9	95
Tip	3.12	9.9	10.4	85

[1] Calculated from total sulfur, assuming that the destruction of each molecule of cystine involves the loss of only 1 atom of sulfur.

2. METHODS

The complete experimental procedure was as follows. Samples of wool weighing approximately 1 g were dried in an oven at 105° C. After each sample was dried and weighed it was treated with 50 ml of a sodium-hydroxide solution at 0° to 2° C (air bath) or 22° C. At the end of a given time, the supernatant liquor was poured off. A 5-ml aliquot was taken for nitrogen analysis, a 20-ml aliquot for inorganic sulfide sulfur analysis, and a 20-ml aliquot for volumetric titration with hydrochloric acid, using methyl red as the indicator. In some of the experiments, an excess of a cold solution of 0.1 *N* hydrochloric acid was immediately added to the residual wool to prevent further degradation of the fibers. The fibers were allowed to remain in the acid for 1 day and were then washed for 4 days in running distilled water. Finally, the cystine content of each sample was determined.

Nitrogen was determined by the micro-Kjeldahl method, total sulfur by the oxygen-bomb [4], and cystine by the Sullivan method [5]. In the latter determination, the wool was hydrolyzed with a hydrochloric-formic acid mixture, as described by Miller and du Vigneaud [6], and the color measured by the method described by Harris and Smith [7].

The inorganic sulfide sulfur was determined by the following procedure. An excess of bromine was immediately added[3] to the solution. The mixture was allowed to stand for several minutes, then acidified with hydrochloric acid, and finally warmed on a steam bath until free from bromine. The sulfate was precipitated as the barium salt and determined in the usual manner.

The apparent base-combining capacity is the value obtained directly from the measurement of the total amount of sodium hydroxide removed from the solution by the wool. The intrinsic base-combining capacity is the amount of base bound by the free acidic groups of the nondegraded wool. To obtain this, two corrections must be introduced. One of these is small, but the other will be shown to be very important.

The first correction, which is the less important, results from the conversion of a portion of the original wool into a soluble form during the treatment with alkali. Since methyl red was used as the indicator, the base bound by the dissolved material is neutralized during the titration. In order to correct for this effect and to obtain only the absorption by the insoluble portion of wool, it is necessary to sub-

[3] Sulfur in wool or in cystine is not oxidized to sulfate under these conditions.

tract the weight of the soluble fraction from the original weight of untreated material. The former is readily calculated from the nitrogen in the solution, since it has previously been shown [8] that the loss of nitrogen from wool during alkaline treatment is proportional to the loss in weight of the wool.

The second correction is for the base bound by sulfhydryl groups formed in the degradation of the disulfide groups of the cystine according to eq 1 and 2. The amount of base taken up as a result of these reactions is calculated from the inorganic sulfide sulfur which has gone into solution.

III. RESULTS AND DISCUSSION

1. EFFECT OF SODIUM HYDROXIDE ON THE CYSTINE IN WOOL

The mechanism suggested [2] for the alkali degradation of the cystine in wool involves the loss of only one sulfur atom for each disulfide group. In order to further test this hypothesis, a series of wool samples was treated with a 0.1 *N* solution of sodium hydroxide for different lengths of time at 0° to 2° C and at 22° C, the solutions and wool being handled as previously described. The effect of the treatment on the cystine is shown in table 2. Good agreement was obtained between the experimentally determined cystine values and those calculated from the loss in sulfur. Appreciable discrepancies occurred only in the experiments in which the wool was severely degraded by prolonged contact with the alkali.

2. ABSORPTION OF ALKALI AS A FUNCTION OF TIME

The time necessary to attain equilibrium was determined by measuring the absorption of base from 0.1 *N* solutions of sodium hydroxide. The data given in tables 3 and 4 were obtained at 0° to 2° C and at 22° C, respectively.

TABLE 2.—*Degradation of cystine in wool by 0.1 N solutions of sodium hydroxide at 0° to 2° C and at 22° C as a function of time*

Time	0° to 2° C			22° C		
	Inorganic sulfide sulfur in solution	Cystine		Inorganic sulfide sulfur in solution	Cystine	
		Calc.[1]	Expt.		Calc.[1]	Expt.
hr.	*mg/gm of wool*	%	%	*mg/gm of wool*	%	%
0			12.1			12.3
0.5	0.44	11.8	11.8	1.10	11.5	11.9
1.0	.46	11.8	11.9	1.49	11.2	11.3
1.5	.50	11.7	11.5	2.21	10.6	10.9
2	.62	11.6	11.6	2.70	10.2	9.9
3.25	.71	11.6	11.5	3.80	9.4	9.1
5	.82	11.5	11.4	5.02	8.5	8.9
6.5	.98	11.4	11.2			
8	1.14	11.2	11.3	6.18	7.7	7.7
20	2.27	10.4	10.2	9.34	5.3	6.1
48	3.85	9.2	9.0	12.12	3.2	5.0
90	6.02	7.6	8.1	14.00	1.8	4.2
240	9.36	5.1	6.3			

[1] These values were calculated on the basis that each atom of inorganic sulfide sulfur found in solution represented the destruction of a molecule of cystine.

TABLE 3.—*Absorption of base from 0.1 N solutions of sodium hydroxide at 0° to 2° C as a function of time*

Time	1 Nitrogen in solution	2 Inorganic sulfide sulfur in solution	3 Apparent base-combining capacity	4 Base-combining capacity corrected for dissolved protein	5 Base bound by sulfhydryl groups formed according to eq 1 and 2	6 Intrinsic base-combining capacity (4—5)
hr.	*mg/gm* [1]	*mg/gm*	*Millimoles/gm*	*Millimoles/gm*	*Millimoles/gm*	*Millimoles/gm*
0.50	0.52	0.44	0.50	0.50	0.014	0.49
.75	.54	.40	.56	.56	.013	.55
1.00	.71	.46	.57	.57	.014	.56
1.5	.93	.50	.58	.58	.016	.56
2	.92	.62	.58	.58	.019	.56
3.25	1.20	.71	.59	.59	.022	.57
5	1.42	.82	.60	.61	.026	.58
6.5	1.56	.98	.60	.61	.031	.58
8	1.94	1.14	.61	.62	.036	.58
20	2.61	2.27	.63	.64	.071	.57
48	3.70	3.85	.68	.70	.120	.58
90	4.57	6.02	.72	.74	.188	.55
240	5.47	9.36	.85	.88	.293	.59

[1] All values in this table are in terms of grams of dry wool.

TABLE 4.—*Absorption of base by wool from 0.1 N solutions of sodium hydroxide at 22° C as a function of time*

Time	1 Nitrogen in solution	2 Inorganic sulfide sulfur in solution	3 Apparent base-combining capacity	4 Base-combining capacity corrected for dissolved protein	5 Base bound by sulfhydryl groups formed according to eq 1 and 2	6 Intrinsic base-combining capacity (4—5)
hr.	*mg/gm* [1]	*mg/gm*	*Millimoles/gm*	*Millimoles/gm*	*Millimoles/gm*	*Millimoles/gm*
0.5	1.05	1.10	0.54	0.54	0.034	0.51
1.0	1.86	1.49	.61	.62	.047	.57
1.5	2.31	2.21	.59	.60	.069	.53
2.0	2.91	2.70	.61	.62	.084	.54
3.25	3.66	3.80	.63	.65	.119	.53
5	4.18	5.02	.64	.66	.157	.50
8	4.73	6.18	.70	.72	.193	.53
20	6.43	9.34	.74	.77	.293	.48
48	7.00	12.12	.80	.84	.378	.46
90	10.5	14.00	.94	1.00	.438	.56

[1] All values in this table are in terms of grams of dry wool.

Figure 1 shows that at 0° to 2° C the apparent base-combining capacity increased with increasing time of treatment, whereas the intrinsic base-combining capacity became constant after about 2 hours. The former arose, as shown in column 5 of table 3, from the combination of the base with sulfhydryl groups which were continuously formed in the degradation of the cystine. The amount of base which reacted in this manner increased with increasing time of treatment. After 240 hours, the correction amounted to 35 percent of the apparent value. On the other hand, the correction for the dissolved protein was negligible up to 5 hours and amounted to only 0.03 millimole per gram of wool after 240 hours. The constancy of the corrected values is shown in column 6 and indicates the absence of appreciable secondary reactions.

The intrinsic base-combining capacities obtained at 22° C, as shown in table 4, appear to be somewhat lower and considerably more erratic than those obtained at 0° to 2° C. This may be attributed to several factors. The rate of degradation as indicated by the amount of dissolved nitrogen (column 1, tables 3 and 4) was much greater at the higher temperature; for example, approximately the same amount of degradation occurred in 3¼ hours at 22° C as occurred in 48 hours at 0° to 2° C. It was also noticed that the reproducibility of the titrations decreased as the amount of degradation increased. The chief difficulty appeared to result from the effect of the dissolved protein on the sharpness of the end point. Finally, an error was intro-

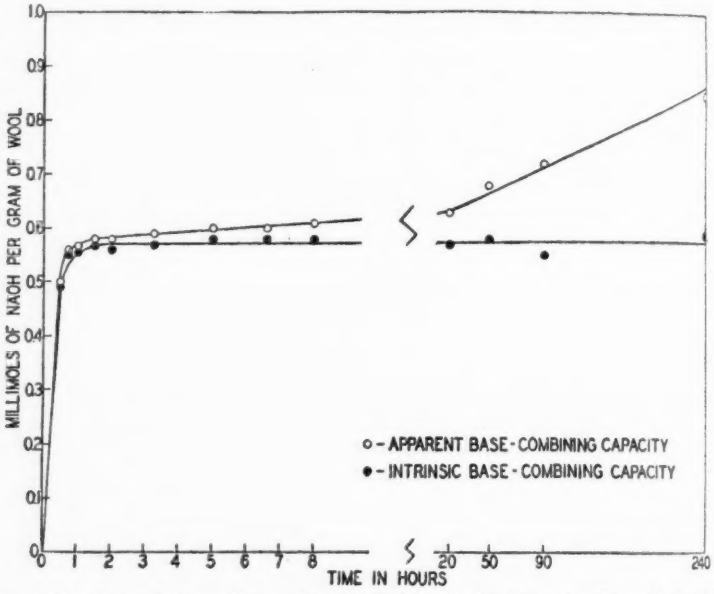

FIGURE 1.—*Rate of absorption of base from 0.1 N solutions of sodium hydroxide at 0° to 2° C.*

duced, since some sulfhydryl groups were probably present in the dissolved protein. The base bound by these groups was neutralized on addition of acid, and since the data in column 5 were calculated on the assumption that all of the sulfhydryl groups formed according to eq 1 and 2 bind base, these values may be too large. In the case of the low-temperature experiments, and especially for the shorter periods of time, this error is shown to be negligible (table 3). However, at 22° C the amount of protein which goes into solution may contain a sufficient number of sulfhydryl groups to account for a large portion of the discrepancy between the values obtained at this temperature and those obtained at 0° to 2° C.

3. ABSORPTION OF BASE FROM SOLUTIONS OF VARIOUS CONCENTRATIONS

The effect of varying the concentration of base is shown in figure 2. The absorptions were measured at 0° to 2° C, 2 hours being allowed to attain equilibrium. That equilibrium was reached under these

conditions in the most dilute and most concentrated solutions used was indicated by measurements made after 2 and 20 hours.

Each point represents the average of four determinations. Good agreement between the individual determinations for each concentration of alkali up to about 0.3 *N* was obtained. Above that concentration, there was considerable variation, as indicated by the dotted lines perpendicular to the lower curve, which show the spread of the values obtained. The discrepancies may have resulted from secondary reactions which occurred in the strongly alkaline solutions, or from the small temperature variations in the air bath used in this work.

The amount of base combined changes very little when the concentration of base exceeds 0.2 *N* and appears to approach a limiting value of about 0.70 millimole of base per gram of wool.

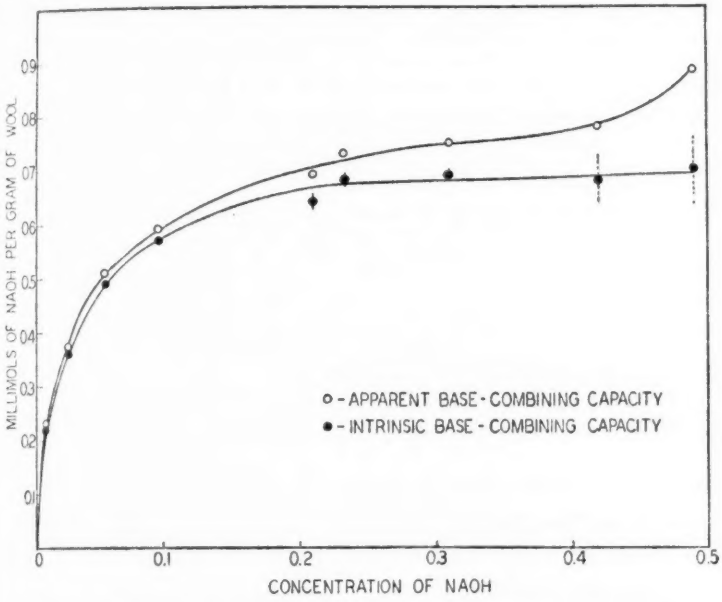

FIGURE 2.—*Absorption of base from solutions of various concentrations.*

The broken vertical lines indicate the maximum variations in the values obtained.

IV. CONCLUSIONS

The results of the present study show that the failure of wool [4] to reach equilibrium with alkaline solutions under the conditions of titration experiments is due to the reaction of base with disulfide groups of the cystine. It is demonstrated that the extent of this reaction can be determined.

The data afford confirmation of the earlier observation [2] that the alkali degradation of the cystine in wool involves the loss of only one sulfur atom from each cystine molecule. The remaining sulfur is apparently present in the form of sulfhydryl groups. On the basis

[4] This demonstrably applies to other cystine-containing proteins.

of this mechanism, it is possible to calculate the amount of base taken up in the degradation of the disulfide groups.

The apparent base-combining capacity increases with increasing duration of the contact of wool with alkali and with increasing temperature of the alkaline solutions, but the intrinsic base-combining capacity, obtained by making corrections for the dissolved protein and for the base bound by the sulfhydryl groups, becomes constant after approximately 2 hours. The results show that the more consistent data are obtained at the lower temperature where, it appears, secondary reactions are greatly inhibited.

Determination of the amount of base absorbed from solutions of various concentrations indicates that a limiting amount of about 0.7 millimole per gram of wool is reached above concentrations of about 0.2 *N* sodium hydroxide. Since some discrepancies occur in the data obtained at high concentrations of alkali, and since the possible influence of the naturally occurring ash has not been considered, it is suggested that this value be considered for the present as tentative.[4]

V. REFERENCES

[1] A. L. Smith and M. Harris, J. Research NBS **19,** 81 (1937) RP1012; J. B. Speakman, J. Soc. Dyers Colourists **40,** 408 (1924); E. Elod, Ber. dent. chem. Ges. **53,** 2164 (1920); Porai-Koschitz, J. prakt. Chem. **137,** 179 (1933).
[2] J. A. Crowder and M. Harris, J. Research NBS **16,** 479 (1936) RP885.
[3] A. L. Smith and M. Harris, J. Research NBS **17,** 97 (1936) RP904; P. R. McMahon and J. B. Speakman, Trans. Faraday Soc. **33,** 844 (1937); M. Harris and A. L. Smith, J. Research NBS **20,** 563 (1938) RP1091.
[4] R. T. Mease, J. Research NBS **13,** 617 (1934) RP721.
[5] M. X. Sullivan, Public Health Reports **86,** (1930).
[6] G. Miller and V. du Vigneaud, J. Biol. Chem. **118,** 101 (1937).
[7] M. Harris and A. L. Smith, J. Research NBS **18,** 623 (1937) RP998.
[8] M. Harris, J. Research NBS **15,** 63 (1935) RP810.

WASHINGTON, December 27, 1938.

[4] Further work, in which experiments are being made in a water thermostat which can be regulated to 0.02° C, is now in progress. The effect of the ash is also being studied. For these reasons, a discussion of the stoichiometry of the reaction of base with the free acidic groups in wool is not presented at this time.

U. S. DEPARTMENT OF COMMERCE NATIONAL BUREAU OF STANDARDS

RESEARCH PAPER RP1204

Part of Journal of Research of the National Bureau of Standards, Volume 22, May 1939

TOGGLE CLAMP FOR RUBBER TENSILE SPECIMENS

By William L. Holt and Archibald T. McPherson

ABSTRACT

The new toggle clamp is an adaptation of the familiar wedge grips used for metal specimens, and consists essentially of parallel blocks, each carried on two short links in such a way that a rubber specimen placed between the blocks is gripped more tightly the greater the pull. The clamp was designed primarily for tubular specimens of electrical insulation, but is equally applicable to specimens in the form of strips or dumbbells. Insulation from No. 14 Performite wire tested with the new clamp showed values of the tensile strength approximately 20 percent higher and ultimate elongation 10 percent higher than with the roll clamp. Insulation from ignition cable having a wall 0.1 inch in thickness showed a tensile strength 50 percent higher and an ultimate elongation 18 percent higher with the toggle than with a roll clamp. Tubular or strip specimens tested with the toggle clamp gave values of the tensile strength of the order of only 5 percent lower than obtained with dumbbells of the same composition. Specimens breaking in the clamps, whether roll or toggle, gave a symmetrical distribution of values about the mode, while those breaking between the clamps showed a skew distribution. The coefficient of variation did not vary significantly with the type of clamp or shape of specimen, the numerical values ranging from 0.043 to 0.060 for tensile strength and from 0.017 to 0.035 for ultimate elongation.

CONTENTS

	Page
I. Introduction	543
II. Description of clamp	544
III. Results of tests	544
1. Tests of No. 14 Performite insulation	545
2. Tests of insulation from ignition cable	547
3. Tests of flat sheets	548
IV. Interpretation of results	549
1. Comparison of roll and toggle clamps for tubular specimens	549
2. Comparison of strip and tube, with dumbbell specimens	550
3. Significance of the position of break	551
4. Coefficient of variation	552
V. Summary and conclusion	552

I. INTRODUCTION

One of the major problems in the tensile testing of rubber has to do with the application of uniform stress to the cross section of the specimen. While the definition of tensile strength stipulates that the stress shall be uniform, this condition is never fully realized in practice on account of localized stresses set up in attaching the specimens to the testing machine. Two general means are used to minimize these local stresses and secure a reasonably uniform tensile stress in the portion of the specimen under observation. One is by the use of test pieces having enlarged ends, such as the familiar dumbbell specimen, and the other is by the employment of clamps which distribute the clamping stresses over an area of the test piece which is relatively large in comparison to the cross section.

The lack of uniform stress distribution in the case of the dumbbell is shown by the fact that such specimens break most frequently in the curved portion just outside the gage marks, where the cross section is somewhat greater than in the central constricted portion.[1] This concentration of stresses in the fillet is readily demonstrated by photoelastic observations on transparent specimens.

When specimens of uniform cross section, such as insulation or tubing, are tested with the usual clamp of the roll type, failure occurs most frequently in the "bite," and the values obtained for the tensile strength and the ultimate elongation may be considerably lower than those found from dumbbell specimens of the same composition.

In order to obtain more satisfactory results with tubular specimens, the Simplex Wire and Cable Co. has developed a clamp[2] similar to the familiar wedge grips for metal specimens. As shown in figure 1, it consists of wedges which slide against surfaces inclined at such an angle that the faces of the wedges are parallel. The test piece is, therefore, gripped so as to distribute the clamping stresses over a relatively large area.

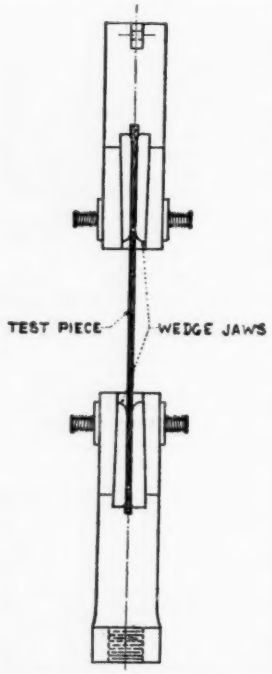

FIGURE 1.—*Simplex wedge clamps.*

II. DESCRIPTION OF CLAMP

The present clamp, which is shown in figure 2, was developed from the Simplex clamp, and differs from it essentially in that each of the two blocks which grip the specimen is carried on two short links or toggle levers. These links, which are 2 inches long, are bronze castings and are mounted by means of one-half inch pins on a $\frac{5}{16}$-inch steel base plate. The faces of the clamping blocks are $\frac{3}{4}$ inch wide and $1\frac{1}{2}$ inches long, with top and bottom edges rounded. Guides in the back of the blocks keep them in the proper juxtaposition at all times. Light springs tend to keep the clamps in the closed position.

Advantages of this clamp over the Simplex clamp are its adaptability to a greater range of sizes of specimens, and the facility with which specimens can be inserted and removed.

III. RESULTS OF TESTS

Since the clamps were intended primarily for rubber insulation, they were tried out with specimens from about a dozen different sizes and types of wire and cable. The clamps appeared to be equally satisfactory for sizes ranging from No. 18 to No. 6, American Wire Gage, and for compositions from "latex" rubber to "30-percent" and

[1] Report of Physical Testing Committee, Ind. Eng. Chem. 17, 535 (1925).
[2] Private communication to the author.

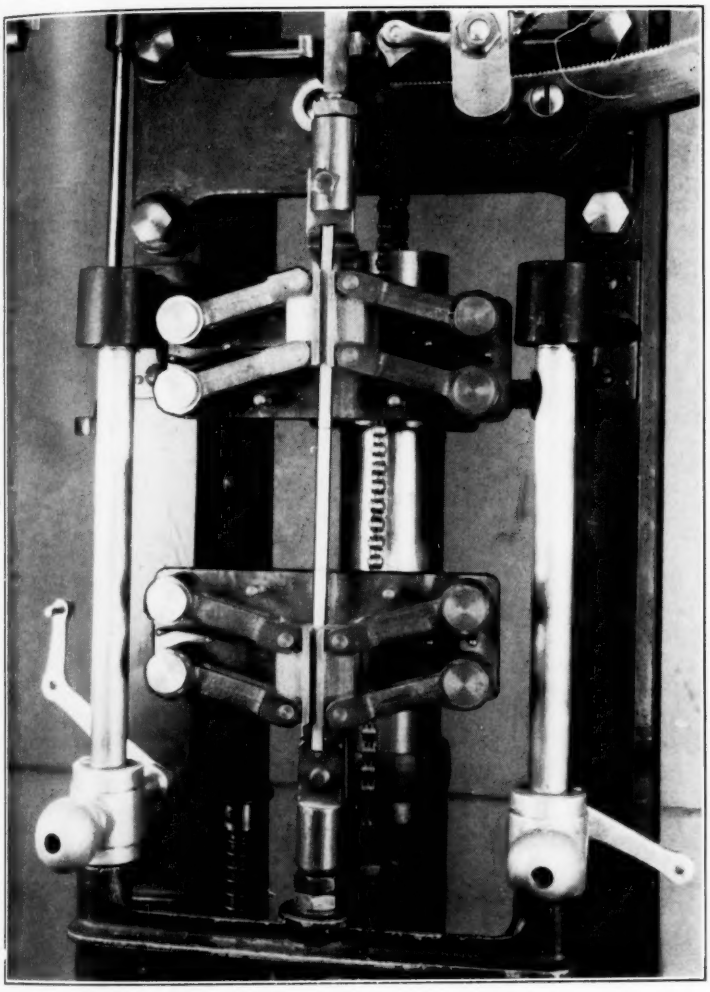

FIGURE 2.—*Toggle clamps mounted in tensile-test machine.*

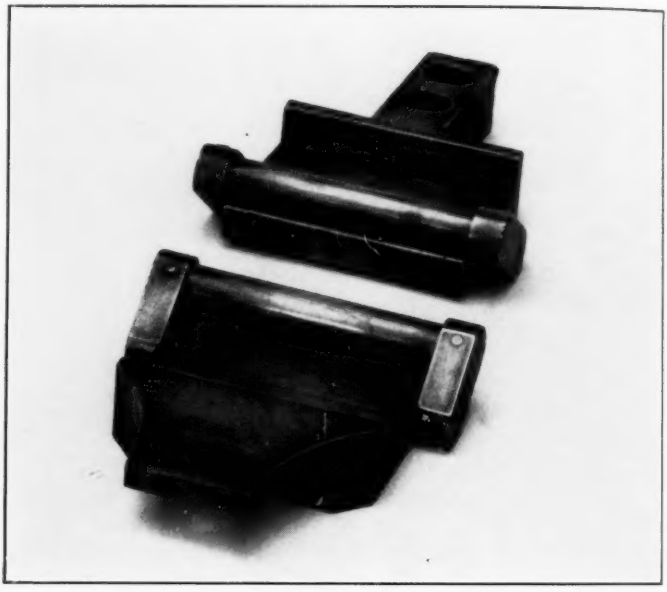

FIGURE 3.—*Roll clamps.*

"code" compounds. The breaking loads observed ranged from about 5 to 125 pounds.

Difficulty was encountered only in the case of specimens having a wax finish. These specimens sometimes slipped through the clamps. This difficulty could, in most cases, be remedied by wiping the specimens with a cloth moistened with acetone or simply by scrubbing them with pumice soap and water.

More extensive tests were also made on two samples of insulation for the purpose of comparing the new clamp with the usual clamp of the roll type. The satisfactory character of the results obtained with tubular specimens of insulation suggested the possibility of extending the use of the new clamps to specimens in the form of strips. Accordingly, tests were made on strip specimens cut from sheet material, comparison being made with dumbbell specimens cut from the same material.

In computing the results of tests, the standard deviation was found for all sets of determinations. The standard deviation is defined as "the square root of the mean of the squares of the deviations of all the observations," the deviation being "the difference between an observation and the mean of all the observations." [3]

1. TESTS OF NO. 14 PERFORMITE INSULATION

A number of tests were conducted on insulation from No. 14 AWG Performite wire for the purpose of making a statistical comparison of the performance of the new clamp with that of a conventional roll clamp. The latter was of the design shown in figure 3, and was provided with a roll ⅜ inch in diameter. Approximately 120 tubular test pieces, each 6 inches long, were prepared from one continuous length of wire. Alternate specimens were taken for tests with the respective clamps in order to eliminate the effect of any variation along the length of the sample. The wall thickness of the insulation was nominally 3/64 inch. The cross-sectional area of specimens was found from measurements of the diameter of the conductor and the external circumference of the insulated wire. The tensile measurements were made in the usual way by means of a Scott testing machine for rubber.

The results are summarized in table 1 and are shown in the form of histograms in figure 4. Two salient differences between the results obtained with the respective clamps are evident from the histograms. In the first place, the values for the tensile strength and the ultimate elongation obtained with the toggle clamp are significantly higher than those obtained with the roll clamp. In the second place, the values obtained with the roll clamp are symmetrically distributed about the mode (the value of most frequent occurrence), while those obtained with the toggle clamp give rise to a skew-shaped distribution curve with a larger range of values below the mode than beyond it.

All of the specimens tested with the roll clamp broke in the "bite" between the roll and the base plate. In the case of the toggle clamp however, 9 specimens broke in the clamp and 50 in the "clear." Of the latter, 35 breaks were between the gage marks and 15 were in the

[3] E. S. Pearson, The Application of Statistical Methods to Industrial Standardization and Quality Control, p. 109, British Standards Institution, London (1935).

lengths between the gage marks and the clamps. The results were classified according to the position of break and analyzed as shown in table 2. The differences between the three groups are not large

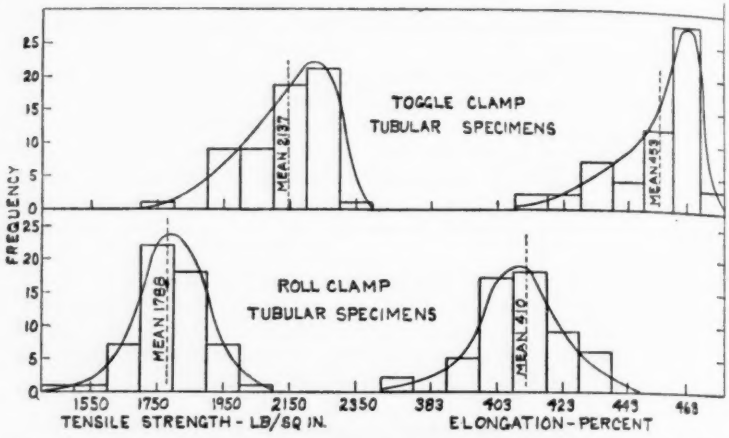

FIGURE 4.—*Histograms of tensile properties of insulation from No. 14 Performite wire.*

enough to be significant. The matter will be discussed subsequently in connection with comparable observations on other samples.

TABLE 1.—*Comparative tests of No. 14 Performite insulation with toggle and with roll clamp*

Measurement	Tensile Strength		Ultimate Elongation	
	Toggle clamp	Roll clamp	Toggle clamp	Roll clamp
	*lb/in.*²	*lb/in.*²	%	%
Range	1,790 to 2,300	1,460 to 2,010	415 to 470	375 to 440
Mean	2,137	1,788	453	410
Standard deviation	117	95	14	14

TABLE 2.—*Relation between position of break and tensile properties of No. 14 Performite insulation tested as tubular specimens with toggle clamp*

	Position of break		
	In clamps	Within gage marks	Between clamps and gage marks
Number of specimens	9	35	15
Tensile strength (lb/in.²):			
Range	1,900 to 2,300	2,190 to 2,290	1,920 to 2,270
Mean	2,130	2,152	2,107
Standard deviation	120	110	123
Ultimate elongation (%):			
Range	423 to 465	415 to 470	420 to 470
Mean	451	455	449
Standard deviation	15	13	15

2. TESTS OF INSULATION FROM IGNITION CABLE

Another series of comparative tests was made on samples of an ignition cable in which the ratio of wall thickness of insulation to conductor diameter was relatively large, the thickness of the wall being approximately 0.1 inch and the diameter of the conductor 0.035 inch. These dimensions were such that it was possible to prepare small dumbbell specimens having a constricted portion ⅛ inch in width.

Four different lengths of the ignition cable were used, and were regarded as different samples. They were taken from different shipments furnished by the same manufacturer under Navy Department Specification M–216b. Three lots of test pieces were prepared from each sample—one lot of dumbbell specimens and two lots of tubular specimens, one for each of the two types of clamps. The tensile determinations were made in the usual way. A Scott testing machine was employed for the tubular specimens, but it was necessary to use a spring-balance machine of lower range for the dumbbell specimens, since the latter had a relatively small cross section. Roll clamps were used for the dumbbell specimens, but the type of clamp was not a matter of consequence in this case, since none of the dumbbells broke in the clamp.

TABLE 3.—*Effect of type of clamp and test piece on tensile properties of the insulation of 4 samples of ignition cable*

TENSILE STRENGTH

Shape of specimen	Clamp	Measurement	Sample 1	Sample 2	Sample 3	Sample 4	Average of four samples
			lb/in.[2]	*lb/in.*[2]	*lb/in.*[2]	*lb/in.*[2]	*lb/in.*[2]
Dumbbell	Roll [1]	Range [2]	2,830 to 3,310	3,220 to 3,750	2,960 to 3,530	3,090 to 3,730	-------
Tubular	Toggle	do	2,860 to 3,430	3,070 to 3,300	2,430 to 3,260	3,100 to 3,390	-------
Do	Roll	do	2,000 to 2,460	2,050 to 2,650	1,480 to 2,105	1,515 to 2,320	-------
Dumbbell	Roll [1]	Mean	3,130	3,572	3,224	3,458	3,344
Tubular	Toggle	do	3,220	3,195	2,880	3,258	3,138
Do	Roll	do	2,227	2,395	1,845	1,900	2,091
Dumbbell	Roll [1]	Standard deviation.	141	137	136	186	150
Tubular	Toggle	do	135	74	244	72	131
Do	Roll	do	138	154	184	237	178

ULTIMATE ELONGATION

			%	%	%	%	%
Dumbbell	Roll [1]	Range [2]	580 to 620	575 to 610	560 to 610	560 to 620	-------
Tubular	Toggle	do	590 to 640	605 to 620	550 to 620	605 to 635	-------
Do	Roll	do	510 to 565	510 to 560	465 to 535	455 to 535	-------
Dumbbell	Roll [1]	Mean	604	602	586	596	597
Tubular	Toggle	do	621	612	593	620	612
Do	Roll	do	537	545	501	496	520
Dumbbell	Roll [1]	Standard deviation.	10	10	10	10	10
Tubular	Toggle	do	12	5	21	9	12
Do	Roll	do	16	13	20	23	21

[1] The type of clamp used with the dumbbell specimens is not significant since none of the specimens broke in the clamp.

[2] There were from 13 to 20 specimens in each group of which the range is given.

The results of tests on the four samples of ignition cable are shown in table 3. Values for the tensile strength and the ultimate elongation obtained from tubular specimens tested with the toggle clamp are of the same order of magnitude as those obtained with dumbbell specimens, while values obtained with the tubular specimens in the roll clamp are much lower.

In the case of sample 1, the tensile strength obtained with dumbbell specimens was a little lower than that obtained with tubular specimens in the toggle clamp, while in the other three cases it was a little higher. The elongation, however, was slightly higher for all samples when tested in the tubular form with the toggle clamp than when tested as dumbbells.

3. TESTS OF FLAT SHEETS

Further information regarding the relation between dumbbell and straight specimens was obtained by a series of tests in which a comparison was made between strips and dumbbells cut from the same

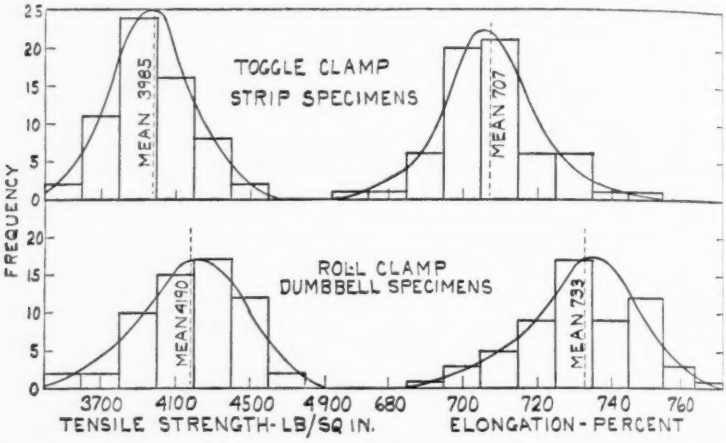

FIGURE 5.—*Histograms of tensile properties of strip and dumbbell specimens cut from sheets of a carbon-black compound.*

press-cured sheets. The rubber compound used for this work was made according to the following formula:

Ingredient	*Parts by weight*
Smoked sheet rubber	100
Sulfur	3
Zinc oxide	5
Stearic acid	4
Carbon black ("soft")	40
Mercaptobenzothiazole	1
Phenyl-beta-naphthylamine	1
	154

Sheets 0.060 to 0.080 inch in thickness were cured for 35 minutes at 259° F. The strips were 6 inches long and 1/4 inch wide, while the dumbbells were the same length and 1/4 inch wide in the constricted portion and 1 inch wide at the ends. Sixty test pieces of each type were prepared, being cut in approximately equal numbers from each test sheet so as to minimize the effect of any variation from one sheet to another.

The results of tensile tests are summarized in table 4, and are shown in histograms in figure 5. Both the tensile strength and the ultimate

elongation obtained with the dumbbell specimens were slightly higher than with the strip specimens, the difference being 5 percent in tensile strength and 3 percent in percentage of the ultimate elongation.

TABLE 4.—*Comparative tests of strip and dumbbell specimens from flat sheets*

Measurement	Tensile strength		Ultimate elongation	
	Dumbbell specimen	Strip specimen (with toggle clamp)	Dumbbell specimen	Strip specimen (with toggle clamp)
	lb/in.[2]	*lb/in.*[2]	%	%
Range	3,520 to 4,660	3,460 to 4,460	690 to 780	670 to 750
Mean	4,190	3,985	733	707
Standard deviation	253	213	18	15

The tests with each type of specimen were classified according to the position of break, as shown in table 5. In the case of the dumbbell specimens, 19 broke between the gage marks and 42 in the fillet just outside the gage marks. Of the strip specimens, 25 broke between the clamps and 38 in the clamps.

TABLE 5.—*Relation between position of break and tensile properties of strip and dumbbell specimens*

	Position of break			
	Dumbbell specimens		Strip specimens	
	Between gage marks	In fillet	Outside clamps	In clamps
Number of specimens	19	42	25	38
Tensile strength (lb/in.²):				
Range	3,830 to 4,600	3,520 to 4,660	3,800 to 4,370	3,460 to 4,460
Mean	4,178	4,196	4,055	3,939
Standard deviation	227	265	163	244
Ultimate elongation (%):				
Range	700 to 760	690 to 780	680 to 740	670 to 750
Mean	733	733	711	704
Standard deviation	15	19	14	15

IV. INTERPRETATION OF RESULTS

1. COMPARISON OF ROLL AND TOGGLE CLAMPS FOR TUBULAR SPECIMENS

The results of the tests of rubber insulation show that the toggle clamps give significantly higher values for the tensile strength and ultimate elongation than the usual roll clamps. The comparisons made in tables 1, 2, and 4 are shown on a percentage basis in table 6. In the case of the insulation from the No. 14 Performite wire, the toggle clamps gave a 20 percent higher value for the tensile strength and a 10 percent higher value for the ultimate elongation than did the roll clamp. The thicker insulation from the ignition cable showed a 50 percent greater tensile strength and an 18 percent greater elongation when tested with the toggle clamp than with the

roll clamp. The discrepancy between the two clamps, therefore, is not constant but appears to increase with the thickness of the specimen.

In the case of the roll clamp, the concentration of stresses in the clamp has a great deal to do with the rupture of the test specimen, as evidenced by the fact that all specimens tested broke in the clamp. Two factors contribute to this effect (1) compressional forces between the roll and the base plate, and (2) the greater elongation to which the outer circumference of the specimen is subjected when it is bent over the roll. The latter circumstance would be expected to result in a decrease in tensile strength with increase in the thickness of the specimen.

TABLE 6.—*Effect of type of clamp and shape of specimen on tensile properties and coefficient of variation*

Sample	Clamp	Shape of specimen	Relative tensile strength	Relative ultimate elongation	Coefficient of variation	
					Tensile strength	Ultimate elongation
Insulation from No. 14 Performite wire.	Roll	Tubular	100	100	0.053	0.034
	Toggle	do	119.5	110.5	.054	.031
Insulation from ignition cables.	Roll	do	100	100	.088	.035
	Toggle	do	150	118	.043	.029
	Roll [1]	Small dumbbell	160	115	.048	.017
Sheet of carbon black compound.	Toggle	Strip	100	100	.054	.021
	Roll [1]	Standard dumbbell	105	103.5	.060	.025

[1] The type of clamp used with the dumbbell specimens is not significant, since none of the specimens broke in the clamp.

The variations among the results of tests on four different samples of ignition cable indicate that, even when the size and type of specimen are kept the same, the ratio between tests with the two types of clamps is by no means constant. For example, when the tensile strength, as determined by the roll clamp is taken as 100, the values obtained by means of the toggle clamp were found to range from 139 to 170, with an average value of 150, as shown in table 6; similarly, taking the ultimate elongation with the roll clamp as 100, the elongations given by the toggle-clamp range from 111 to 125, with an average value of 118.

2. COMPARISON OF STRIP AND TUBE, WITH DUMBBELL SPECIMENS

The results summarized in table 6 indicate that the tensile strength shown by a dumbbell specimen is slightly higher than that given by a tubular or strip specimen of the same composition. This difference amounts to about 7 percent, on the average, for the four samples of ignition cable, and to about 5 percent for the sheet sample of the compound containing "soft" carbon. It would be expected that this difference in tensile strength would be accompanied by a corresponding difference in the ultimate elongation. In the case of the dumbbells and strips cut from the sheet material, the dumbbells gave the greater elongation, by about 4 percent of the total elongation. In the case of the ignition cable, however, the reverse was observed, the ulti-

mate elongation of the tubular specimens being about 2.5 percent greater than that of the dumbbells.

The present results do not warrant any precise statement as to the relation between results obtained with dumbbells and with strip or tubular specimens. For many practical purposes, however, it appears that the latter specimens can be satisfactorily employed when it is not practical to obtain dumbbells.

3. SIGNIFICANCE OF THE POSITION OF BREAK

The rupture of a specimen in a tensile test is likely to start at some point where the stresses are concentrated on account of the shape of the specimen or the means used for clamping it. If rupture does not occur at one of these points of concentrated stresses, it will start at some flaw or inhomogeneity in the rubber. In the latter case, higher values of the tensile strength and ultimate elongation are usually obtained than in the former case, and it is observed that the distribution of values is altered from a symmetrical distribution about the mode to a skew-shaped distribution with a larger range of values below the mode than above it. Such a skew-shaped distribution curve is consistent with the usual explanation that the presence of inhomogeneities alters the observed values of tensile strength and ultimate elongation in such a way as to give rise to a preponderance of lower values, as compared with the symmetrical curve of random distribution.

The fact that all the straight and tubular specimens tested with the roll clamp broke in the "bite" indicates that in this case the concentration of stresses in the clamps is a predominating factor. Consequently a symmetrical distribution of values about the mode would be expected and such is clearly shown by figure 4.

With the toggle clamp the test piece is gripped over a relatively large area so that the clamping stresses are correspondingly low. Consequently a proportionately larger number of the breaks are initiated by inhomogeneities in the rubber and hence occur outside the clamps. In the case of Performite insulation, which contained a relatively coarse filler, only 9 of the 59 breaks occurred in the clamps. With strip specimens made from a carbon-black compound, the relation was reversed and 38 out of 63 specimens broke in the clamps.

The curves which represent the distribution of values of tensile strength and ultimate elongation of Performite insulation, as determined with the toggle clamp, are markedly skewed, as shown by figure 4. On the other hand, the corresponding curves for the strip specimens of the carbon-black compound, as shown in figure 5, are not significantly skewed. This difference in the distribution of values for the two samples is consistent with the differences in the positions at which the respective specimens broke, but the number of observations is not sufficient to warrant a close analysis.

In the case of dumbbell specimens the majority of breaks occurred, as would be expected, in the fillet just outside the gage marks. The results shown in table 5 indicate that there is no large practical difference in tensile properties associated with the position of break, and consequently no reason for discarding the results of all determinations in which specimens break outside the gage marks, as is sometimes done.

The specimens of Performite insulation which broke outside the clamps were divided into two groups, depending on whether the break was inside or outside the 2-inch gage length that was employed for measurement of the elongation. As shown in table 2, the average values for these groups do not differ greatly from each other or from the average values of determinations in which the specimens broke in the clamps.

The position of break was observed to have a significant effect on the tensile properties only in the case of the strip specimens of the carbon-black compound shown in table 5. The specimens which broke in the "clear" showed on the average a 3-percent higher tensile strength than those which broke in the clamps. The ultimate elongation of specimens which broke outside the clamps was also slightly greater than that of specimens breaking within the clamps.

4. COEFFICIENT OF VARIATION

In order to determine whether the new clamp gave a spread of values different from that obtained with other clamps, the coefficient of variation (ratio of the standard deviation to the mean) was computed for the determinations given in tables 1, 2, 3, and 4. The results which are shown in table 6 indicate that except for one set of tests the coefficient of variation was not significantly influenced by either the type of clamp or the shape of the specimen. The coefficient for tensile-strength tests lies between 0.043 and 0.060, except for the test of tubular specimens of ignition cable in the roll clamp, when it is 0.088. A coefficient of about 0.05 is usual for tensile-strength measurements on rubber. The coefficient of variation for the measurements of ultimate elongation lies between 0.017 and 0.035, this range being of usual magnitude. The tests of ignition cable which showed the greatest spread in tensile-strength determinations, also showed the greatest spread in ultimate elongation, though in the latter case the coefficient of variation is not significantly out of line.

V. SUMMARY AND CONCLUSION

The toggle clamp described in this paper is adapted to use with a wide range of sizes and types of specimens for the tensile testing of rubber. Tubular and strip specimens, when tested with the new clamp, give values for the tensile strength that are only a little lower than those obtainable with dumbbell specimens of the same composition. The values are considerably higher, however, than those obtained with the roll clamp commonly used. The new clamp, therefore, is particularly suitable for the testing of rubber insulation and other products of such a shape that dumbbells cannot readily be prepared from them.

Acknowledgment is made to E. E. Creitz, who suggested a preliminary design of the toggle clamp.

WASHINGTON, February 23, 1939.

U. S. DEPARTMENT OF COMMERCE NATIONAL BUREAU OF STANDARDS

RESEARCH PAPER RP1205

Part of Journal of Research of the National Bureau of Standards, Volume 22, May 1939

DETERMINATION OF THE pH VALUE OF PAPERS

By Herbert F. Launer

ABSTRACT

A simple and rapid procedure for the determination of the pH value of papers is described. The paper is mixed with water, and after letting it stand for 1 hour in the cold, the pH is determined in the unfiltered mixture, using a glass electrode. The values so obtained are in good correlation with the amounts of alum used in the manufacture of the papers and are useful in predicting the chemical stability of the papers. The relationship between the percentages of alum and the pH obtained with the method described and with the method in general use employing hot extraction, was studied in detail for a large number of experimental papers produced in the paper mill at the National Bureau of Standards. The experiments showed that the increase in acidity upon heating, observed by previous workers, is usually three to four times the hydrogen-ion concentration of the cold paper-water mixtures. No advantage of using hot water for the extraction was observed.

Experiments showed that the usual fibrous papermaking materials have the property of raising the pH of an acidic solution containing CO_2 or aluminum sulfate, and that neutral papers gave essentially the same pH, whether extracted with water of pH = 6.7 or with some of the same water containing CO_2 and having a pH = 5.9. Therefore, the requirements of present standard methods, with respect to the pH of the distilled water used for extraction, appear to be unnecessarily severe.

Other factors studied were time and temperature of extraction, neither one of which appears to be critical in the cold extraction. Previous workers have found that these two factors are important in the method of hot extraction.

Grinding was found to be unnecessary for the papers studied, but the aqueous mixtures of unground, thick, "kraft" papers should be allowed to stand 20 hours before determination of the pH.

CONTENTS

	Page
I. Introduction	553
II. Method of measuring the pH	555
III. Comparison of the pH values obtained with hot and with cold extraction	556
1. Relationship between the pH values and the amounts of alum used	556
2. Relationship between the pH values and the stabilities of the papers	559
IV. Study of the factors involved in the method of cold extraction	560
1. Purity of the water required for the extraction and the effect of fibers upon the pH	560
2. Effect of temperature	561
3. Effect of time	561
4. Manner of preparing the paper for extraction	562
V. Recommended procedure	564

I. INTRODUCTION

The pH of a paper extract is now usually considered one of the most reliable indices of the permanence of a paper, although the first

applications of pH values for papers were reported scarcely a dozen years ago.[1] Prior to the use of pH values, paper acidity was identified with the "total acidity" or titratable acid in extracts of the paper, an unstable paper usually having a higher acidity than a stable one. In order to find a method more suited to modern control work for measuring acidity than the measurement of total acidity, Hoffman[2] sought to replace it with the measurement of pH, and found that both types of data could be correlated equally well with the stability of a wide variety of papers. His results are in agreement with the later work of Köhler,[3] who previously had developed the method for titratable acid. Hoffman measured the pH of extracts prepared in the same manner as those for total acidity, namely, by extraction near 100° C for 1 hour.

This method, with changes for eliminating the possible effect of CO_2, both in the filtration and cooling procedure and with the specification that the water used for extraction should have a pH value between 6.6 and 7.0, was adopted by the Technical Association of the Pulp and Paper Industry.[4] Grinding of the paper was further specified and the extraction temperature was fixed between 95° and 100° C. The method of measuring the pH was left to the choice of the analyst, and the values obtained were to be expressed to the nearest 0.05 pH unit for the electrometric and 0.1 pH unit for the colorimetric determination. The Federal specifications[5] are essentially the same, except that water of pH 6.9 to 7.1 is prescribed.

The accuracy implied in the TAPPI method is, however, much higher than is compatible with actual experience. Under the supervision of Wehmhoff,[6] three different Government laboratories conducted cooperative tests on given papers, using procedures essentially within the specifications of the TAPPI method. Variations between laboratories in pH values obtained were 0.34 pH unit, on the average, with a maximum variation of 1.0 pH unit, indicating that some modification of either the method or the precision requirements, or both, was necessary.

Investigators have studied the factors involved in the hot extraction. Browning and Ulm[7] found that hot extraction gave lower pH values than cold extraction for three commercial papers, and that the temperature at which the hot extraction is made should be controlled to 99° to 100° C instead of 95° to 100° C as permitted in the standard methods. They found, in agreement with Wehmhoff,[6] that the pH values, obtained using hot extraction, are not equilibrium values, since they tend to rise if the mixtures are allowed to stand in the cold. They also found that atmospheric CO_2 has no appreciable effect in the pH range up to 6.0, during either the hot extraction or the cooling process and, therefore, that the precautions prescribed by the TAPPI method in this respect are not necessary. Furthermore, they question the wisdom and feasibility of grinding the paper.

[1] W. Holweck, Papier-Fabr. 25, 659 (1927).
[2] W. F. Hoffman, Paper Trade J. 86, TS143 (March 1, 1928).
[3] Sigurd Köhler, Investigations into the determination of acidity and copper number in paper, Report No. 56 of the Statens Provningsanstalt, Stockholm (1932). See especially pages 7 and 11. (In Swedish.)
[4] TAPPI-T435m, Hydrogen ion concentration (pH of) paper extracts, Sept. 6, 1934. Copies may be obtained from the Association, 122 E. 42d Street, New York, N. Y.
[5] Federal Specification for Paper; General Specification UU-P-31a, page 10 (June 1937). Obtainable from the Superintendent of Documents, Government Printing Office, Washington, D. C., price 5 cents.
[6] B. L. Wehmhoff, Progress Report on the Determination of pH Values and Total Acidity in Paper. United States Government Printing Office (1930).
[7] B. L. Browning and R. W. K. Ulm, Paper Trade J. 102, 89 (Feb. 20, 1936). This contains an extensive bibliography and a historical survey.

The procedure of hot extraction has been adhered to in the past, doubtless because the data have been lacking which are necessary to show that extraction in the cold gives a pH value which is representative of the paper. Furthermore, the TAPPI method of preparing the paper extract involves filtration to allow application of a wide variety of methods of measuring the pH. Colorimetric methods, which are known to depend largely upon the psychological and physiological qualities of the analyst, usually require colorless, clear extracts, and necessitate filtering and excessive handling, which normally involve the danger of contamination. Again, the use of the hydrogen electrode demands filtration and a knowledge of the chemical composition of the solution to be tested to insure against poisoning of the electrode. Thus, in limiting the method of measuring the pH to glass electrodes, which do not require preliminary handling of the extracts, a simplicity of procedure can be achieved, which is especially important in pH work.

In previous investigations in which commercial papers were studied, the proportions of alum used in their manufacture were either not known or not given. In the present investigation a large number of experimental papers were available whose papermaking details were known and had been varied in such a manner as to permit a study of the relationships between the proportions of alum used in the manufacture of the papers, the pH values, and the chemical stability of the papers. Such data should show whether pH values obtained by cold extraction are as valid as those obtained by hot extraction. The experimental papers were produced under carefully controlled conditions in the semicommercial paper mill of the National Bureau of Standards. One commercial coated paper and eight samples of file-folder stock were also included in the study.

II. METHOD OF MEASURING THE pH

A commercial glass electrode, in conjunction with a saturated potassium chloride-calomel half cell, calibrated in the usual manner with 0.05 *M* potassium acid phthalate of pH=4.0, was used for all determinations of pH throughout the present work. The advantages of this electrode are well-known, but some care must be used in applications to paper-water mixtures. When determinations in neutral or nearly neutral systems were made, after the glass electrode had been used in solutions either distinctly acidic or alkaline, the values obtained were at first too low or too high, in the direction of the previously measured pH. This is shown in table 1 for paper 21. The glass electrode was carefully rinsed with distilled water after each treatment described in column 2 and then inserted in the unfiltered extract of the ground paper. For papers farther removed from neutrality, as for example paper 24, the effect was no longer noticeable. Another glass electrode gave similar results with a paper extract of pH=7.1, while a paper extract of pH=6.0 showed a smaller but nevertheless appreciable effect. Ordinarily 1 to 2 minutes appear to suffice for the attainment of equilibrium, but for measurements in the neutral range, especially if the preceding measurement was of an alkaline solution, approximately 15 minutes time should be allowed, or the electrode should be immersed for 1 minute in a solution having a lower pH than the one about to be measured. The phthalate

buffer, pH=4.0, was found convenient for this purpose. Thus, the large errors involved in approaching from the alkaline side are replaced by the smaller errors involved in approaching from the acidic region.

TABLE 1.—*Effect of previous treatment of glass electrode when used to measure* pH *of paper extracts*

PAPER SAMPLE 21

Previous treatment of glass electrode	Time interval after insertion of electrode (minutes)	pH measured after Time interval	Relative error (pH Units)
One hour in distilled water	10	6.6	.....
Ten minutes in paper extract of pH=9.4	1	7.8	1.2
	9	6.9	.3
	14	6.7	.1
Twenty minutes in solution of pH=4.0	1	6.4	−.2
	3	6.4	−.2
	11	6.5	−.1
One hour in distilled water	10	6.6	0

PAPER SAMPLE 24

Fifteen minutes in distilled water	10	5.6	.....
Ten minutes in solution of pH=4.0	1	5.6	0
	10	5.6	0
Ten minutes in paper extract of pH=9.4	1	5.6	0
	10	5.6	0

III. COMPARISON OF THE pH VALUES OBTAINED WITH HOT AND WITH COLD EXTRACTION

1. RELATIONSHIP BETWEEN THE pH VALUES AND THE AMOUNTS OF ALUM USED

The acidity of newly made paper is practically all derived from the salt, aluminum sulfate, termed in the trade "papermakers alum", which is used to aid the formation of the fibers into a sheet, to precipitate rosin from rosin size onto the fibers to make the paper water-repellent, and as a mordant for coloring materials. Therefore, the relationship between the amounts of alum used in the papermaking process and the pH values is an important criterion of the validity of the latter.

The pH values for cold extraction were obtained after mixing 1.00 g of ground paper with 70 ml of distilled water, pH=6.6 to 6.9, at 20° to 30° C, allowing the mixture to stand for 1 hour and then measuring with a glass electrode by direct insertion into the paper-water mixture. After this measurement, the same mixtures were used to obtain the pH values for hot extraction. They were heated in a Pyrex flask covered loosely with a watch glass and immersed to the neck in a steam bath (99° to 100° C) for 1 hour, after the temperature of the mixture had become constant. After cooling the mixture, the pH values were obtained, and were the same as those obtained from mixtures made up directly with hot distilled water and kept in the steam bath for 1 hour, and subsequently cooled.

The pH values are listed in table 2, along with the alum percentages. A comparison between these variables must be limited, however, to papers made with like amounts of rosin size,[8] inasmuch as the pH values are affected also by the rosin size. This is owing to the fact that rosin size, which is a suspension of free rosin in sodium resinate solution, reacts with strong acids to precipitate rosin, which is a weak insoluble acid or group of acids, and reacts with aluminum ion to form a more or less well-defined insoluble compound of aluminum and rosin, thus reducing the concentration of aluminum ion. The effect on the values for pH-cold and on the changes in (H^+) during heating, of varying the amount of rosin size, is easily seen in the pairs 12 and 13, 25 and 26, and, to a smaller extent 1 and 2, 3 and 4.

TABLE 2.—*Relation between the acidity values and chemical characteristics of the papers*

1	2	3	4	5	6	7	8	9
Sample number	Resin	Alum [a]	pH, using cold extraction	pH, using hot extraction	Δ pH	Δ (H^+)	(H^+) Corresponding to pH cold	Decrease in alpha-cellulose
NEW RAGS								
						Equiv/liter ($\times 10^{-7}$)	*Equiv/liter* ($\times 10^{-7}$)	*Percent*
1	0.9	4.0	4.9	4.3	0.6	380	130	8.0
2	1.7	4.0	5.1	4.4	.7	320	79	7.0
3	.9	2.0	5.2	4.5	.7	250	63	4.9
4	1.7	2.0	5.4	4.7	.7	160	40	5.3
5	.2	1.5	5.5	4.9	.6	94	32	3.2
6	1.8	1.2	5.6	5.0	.6	75	25	4.6
7	.9	1.1	5.6	5.0	.6	75	25	2.9
8	1.6	.9	6.4	5.9	.5	9	4	2.0
9	.3	.8	6.4	6.0	.4	6	4	.9
10	.8	.7	6.3	6.0	.3	5	5	1.4
11	.3	.5	7.2	7.3	-----	-------	.6	.3
SODA-SULFITE (1:1)								
12	1.2	2.4	5.2	4.6	0.6	190	63	6.3
13	.2	2.1	4.9	4.3	.6	380	130	7.6
14	.2	1.5	5.3	4.8	.5	110	50	3.3
15	1.6	1.4	5.5	4.9	.6	94	32	5.0
16	0.9	1.3	5.8	5.1	.7	63	16	2.0
17	1.0	1.3	5.9	5.1	.8	66	13	3.2
18	1.2	1.1	6.0	5.3	.7	40	10	4.0
19	.3	1.0	6.4	5.7	.7	16	4	1.2
20	.9	.8	6.2	5.5	.7	26	6	2.6
21	.3	.5	6.6	6.2	.4	4	2.5	1.0
22	.3	0	6.9	6.4	.5	3	1.3	0
SPECIAL SULFITE [b]								
23	1.9	2.3	5.2	4.9	0.3	63	63	4.6
24	1.7	1.1	5.6	5.3	.3	25	25	3.6
25	1.1	.8	5.6	5.0	.6	75	25	2.9
26	1.6	.8	6.1	5.7	.4	12	8	.8
27	1.1	.6	6.0	5.7	.3	10	10	1.8
28	.2	0	6.9	7.2	-----	-------	1	.4

See footnotes at end of table.

[a] Papers with resin contents, shown in table 2, from 0.8 to 1.2 percent, were made with a definite volume of rosin size calculated to contain a total amount of rosin, the weight of which was 1 percent of that of the dry fibers. Papers with resin contents from 1.6 to 1.9 percent were made with double this volume of rosin size. All other papers had no added rosin but contained natural resins or waxes in small amounts. Added rosin and natural resins are termed "resin" when determined analytically.

TABLE 2.—*Relation between the acidity values and chemical characteristics of the papers*—Continued

1	2	3	4	5	6	7	8	9
Sample number	Resin	Alum	pH, using cold extraction	pH, using hot extraction	Δ pH	Δ (H^+)	(H^+) Corresponding to pH cold	Decrease in alpha-cellulose
BLEACHED SULFATE [b]								
29	1.0	2.3	5.2	4.9	0.3	63	63	1.4
30	.9	1.0	5.8	5.0	.8	84	16	.8
31	.9	.7	6.4	6.0	.4	6	4	.7
32	.1	0	6.8	7.0	-----	-------	2	.2
OLD RAGS								
							Surface sizing	
33	1.1	1.6	5.0	4.7	0.3	100	Glue: pH=4.7	
34	1.1	1.6	5.8	4.9	.9	110	Starch: pH=7.2	
35	1.1	1.5	5.7	4.9	.8	110	None [c]	
36	1.1	1.5	5.2	4.8	.4	97	Glue: pH=4.7	
NEW RAGS								
37	1.1	1.5	5.7	5.1	0.6	59	Glue: pH=4.5	
COMMERCIAL COATED								
38	-----	-----	6.3	5.4	0.9	35	None.	

[a] Percentage of alum was based on dry weight of solid materials in the chest.
[b] Pulps subjected to special purifying process by the manufacturers.
[c] No surface sizing; starch added to beater.

In figure 1 the alum percentages are plotted against the pH values, for series of papers made with like amounts of rosin size and made from the same fibrous materials. The heavy lines connecting the points represent hot extractions, and the light lines of similar structure represent corresponding cold extractions. Figure 1 shows that the much simpler method of cold extraction gives pH values which are related to the amounts of alum used in making the papers, and that there is no advantage in this respect, in using the method of hot extraction.

Such an analysis for papers 33 to 38 was not possible, since the surface-sizing solutions also may be expected to affect the pH-alum relationship somewhat. It should be noted, however, that the pH changes upon heating the extracts, for these papers, are not greatly different from those of the other papers.

The decrease in pH during heating, for papers 1 to 32, table 2, is shown in column 6 as "ΔpH," and it appears to be similar, 0.6, expressed as pH units, for all papers made with more than 0.5 percent of alum. Such a comparison is misleading, however, since the pH is a logarithmic function. When these changes in pH are expressed as increases in the hydrogen-ion concentration, Δ(H^+), column 7, the changes are seen to vary greatly and depend generally upon the proportions of

alum originally added. It is of interest to note that the changes in acidity upon heating, $\Delta(H^+)$, are usually three to four times as

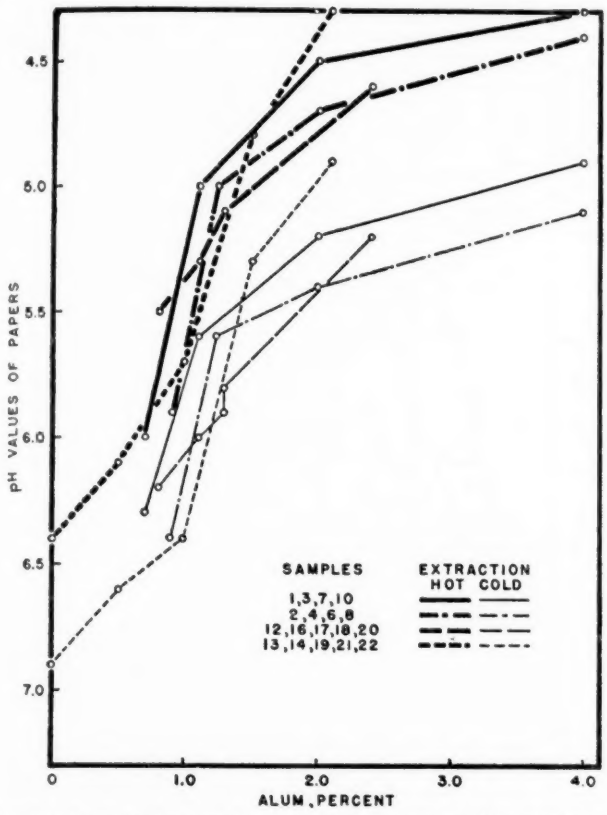

FIGURE 1.—*Relationship between the amounts of alum used in making the papers and the* pH *values for hot and cold extractions.*

large as the original acidity, (H^+), column 8, calculated from the values for pH-cold.

2. RELATIONSHIP BETWEEN THE pH VALUES AND THE STABILITIES OF THE PAPERS

Another important requirement of a method of extraction is that the acidity values thus obtained may be used as a basis for predicting relative stability of the papers. The change in alpha-cellulose content of a paper upon accelerated aging by heating is regarded as an index of relative stability. This criterion is especially applicable when comparisons are restricted to papers made from the same fiber.

The relative stability in terms of change in alpha-cellulose content upon accelerated aging, which consisted in heating the papers in air for 72 hours at 100° C, is given in table 2, column 9. When these are plotted against pH and the points connected as before with heavy and light lines, corresponding to hot and cold extractions, respectively,

it is seen from figure 2 that the method of cold extraction results in pH values which are as useful for predicting relative stability as are those of the method of hot extraction.

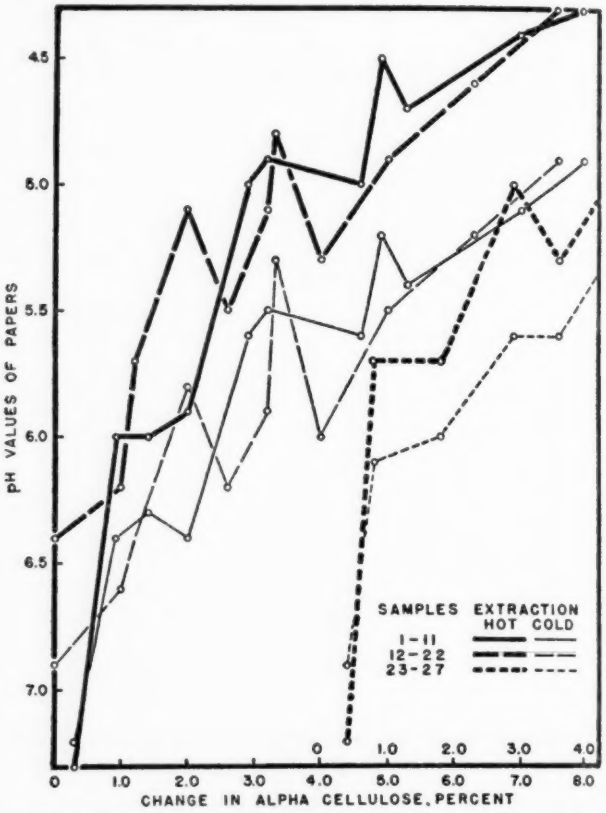

FIGURE 2.—*Relationship between the* pH *values for hot and cold extractions and the stabilities of the papers*

IV. STUDY OF THE FACTORS INVOLVED IN THE METHOD OF COLD EXTRACTION

1. PURITY OF THE WATER REQUIRED FOR THE EXTRACTION AND THE EFFECT OF FIBERS UPON THE pH

The use of water with a pH between 6.6 and 7.0 or 6.9 and 7.1, as prescribed by the TAPPI method and the Federal specification, requires redistillation of ordinary distilled water in a well-ventilated laboratory.

It is doubtful, however, if water of such purity is ever necessary in extractions of paper. Distilled water, which contains enough CO_2 to give a pH=6.1, but which is pure in other respects, contributes, according to calculation, only 0.1 pH unit in a paper-water mixture of which the measured pH=5.8. Actually, the effect of CO_2 is far less

than this, for the pH values of the practically neutral papers were not affected significantly by ordinary amounts of CO_2, as shown in table 3. Such papers gave practically the same pH, whether mixed with water of pH=6.7 or with a portion of the same water to which CO_2 had been added to give a pH=5.9. Water containing enough CO_2 to give a pH=5.0 underwent a rise in pH of approximately 1 unit when these papers were added. Acidity from other sources was similarly reduced by the fibers. For example, when these papers were mixed with water of pH=4.8, containing 0.013 g of alum per liter, the pH rose markedly in every case, as shown in column 5.

TABLE 3.—*Effect of fibers* [a] *upon* pH *values*

Sample number	pH values			
	pH of water =6.7	pH of water =5.9, CO_2 added	pH of water =5.0, CO_2 added	pH of water =4.8, alum added, 0.013 g per liter
11	7.1	7.0	6.0	5.9
20	6.2	6.2		
22	6.9	6.8	6.0	6.1
28	6.7	6.6	5.8	5.8
32	6.6	6.6	5.9	6.0
39 [b]	6.9	6.8		5.7
40 [b]	6.7	6.6		5.4

[a] Extractions were made on ground papers fo. 1 hour at room temperature.
[b] Papers 39 and 40, not listed in table 2, were made from old rags.

Since the samples listed in table 3 were representative of all of the usual papermaking materials, it appears that otherwise pure distilled water, containing small amounts of CO_2, of pH=5.9 or higher, is satisfactory for use in paper extractions, even at room temperature, and that the requirements of present standard methods employing hot water are unnecessarily severe in this respect.

2. EFFECT OF TEMPERATURE

No appreciable systematic difference in pH was found between extractions made at 20° and at 30° C over a wide range of pH. This is in agreement with the results obtained by Browning and Ulm, who found only small differences for the two temperatures, 20° and 50° C. They found, however, that the temperature of hot extraction should be rather closely controlled, between 99° and 100° C. It thus appears that the method of cold extraction has an important advantage in that extraction may be safely made over the rather wide range loosely designated as room temperature.

3. EFFECT OF TIME

Experiments in which the pH values of papers were determined at various intervals after mixing showed that time is not a critical factor for papers of ordinary weight and that the values obtained after 1 hour do not change significantly upon much longer standing. This applies to well-sized as well as poorly sized papers, and is especially significant for the surface-sized papers. The results are shown in table 4.

TABLE 4.—*Effect of time of extraction* [a] *upon the* pH *values of papers*

Sample number	Sizing value	pH values after various intervals			
		10 minutes	30 minutes	1 hour	20 hours
	Seconds				
1	5	5.0	----------	5.0	5.0
3	5	5.3	----------	5.2	5.2
9	0	----------	----------	6.4	6.2
10	2	6.3	----------	6.3	6.3
11	0	----------	----------	7.1	7.1
12	47	5.3	----------	5.2	5.0
13	0	4.9	4.9	4.9	4.9
14	0	5.4	5.3	5.3	----------
16	49	----------	----------	5.8	5.6
17	42	----------	----------	5.9	5.8
18	41	----------	----------	6.0	5.9
19	0	6.3	6.3	6.4	6.3
20	45	----------	----------	6.2	6.1
21	0	6.7	6.6	6.6	6.6
22	0	6.8	6.8	6.8	6.9
23	35	5.3	5.2	5.2	5.2
24	31	5.7	5.7	5.7	----------
27	13	----------	----------	6.0	5.9
28	1	7.0	6.9	6.9	6.8
31	14	----------	----------	6.6	6.6
32	4	7.0	6.9	6.8	6.7
33	31	4.9	----------	4.9	5.0
34	24	5.7	----------	5.7	5.7
35	9	----------	----------	5.9	5.8
36	19	----------	----------	5.2	5.3
37	21	----------	----------	5.7	5.7
38	------	6.3	----------	6.3	6.3

[a] Extractions were made of ground papers at room temperature.

4. MANNER OF PREPARING THE PAPER FOR EXTRACTION

Although required by the TAPPI method and given as an alternative to shredding in the Federal specification, advisability of grinding has been questioned by Browning and Ulm. Aside from the practical difficulty that many laboratories in which pH measurements of papers are made are not equipped with a grinder, it is of major importance, for this determination, that the paper be subjected to a minimum of treatment before testing. Contamination of the paper in the grinder by residues of previous papers is an ever-present possibility, despite careful cleaning.

During a period of 5 months, the papers described in this investigation were tested at intervals, both in the ground condition and in the form of cuttings, approximately 0.1 to 2 cm^2 in area. The results listed in table 5 show no important systematic difference between the values obtained from the unfiltered aqueous mixtures of the ground and cut materials. Each individual value is the average value of duplicate determinations. The maximum disagreement between the several values for each paper has an average value of 0.13 pH unit for the ground and 0.10 pH unit for the cut samples, showing reproducibility to be practically the same for both. Out of 28 comparisons, the average values for the ground material were higher in 11 cases and lower in 9 than those from the cuttings, and equal in 8 cases.

The specification of grinding, to the exclusion of cutting the sample, does not, therefore, appear justified in the testing of papers such as

those listed in table 5. When a paper is especially thick, however, proper extraction is not obtained with cut samples in 1 hour. Results with eight samples of commercial file-folder stock, with a thickness of approximately 0.01 inch, showed that very incomplete extraction is obtained unless such papers are ground, or unless the time is extended to 20 hours. The results are shown in table 6.

TABLE 5.—*Comparison of* pH *values* [a] *obtained from ground samples and from cuttings of papers*

Sample No.	Ground paper pH values at various intervals during 5 months	Maximum disagreement	Cut paper pH values at various intervals during 5 months	Maximum disagreement
1	4.9, 5.0	0.1	4.9, 4.9	0
2	5.1, 5.3	.2	4.9	
4	5.4, 5.4	0	5.4	
6	5.6, 5.7	.1	5.9, 5.9	0
7	5.6, 5.6	0	5.8, 5.8	0
8	6.4, 6.4	0		
9	6.3, 6.4	.1	6.0, 6.1	.1
10	6.0, 6.1, 6.0, 6.3	.3	6.2, 6.6	.4
11	7.2, 7.4, 7.1	.3	6.9, 6.7, 6.7	.2
12	5.2, 5.2, 5.2	0	5.0, 5.0, 5.0	0
13	5.0, 4.9, 4.9	.1	4.8, 4.9, 4.9	.1
14	5.4, 5.3, 5.5	.2	5.4, 5.6	.2
15	5.6, 5.5	.1	5.6, 5.8	.2
16	5.7, 5.8	.1	5.8, 5.9	.1
17	5.9, 5.9	0	5.8, 6.0	.2
18	6.0, 6.0	0	6.2, 6.1, 6.3	.2
19	6.4, 6.4, 6.3	.1		
20	6.2, 6.2	0	6.2, 6.3	.1
21	6.6, 6.6, 6.5	.1		
22	6.8, 6.9	.1	6.7, 6.6, 6.6	.1
23	5.1, 5.3, 5.2	.2	5.0	
24	5.6, 5.6, 5.7	.1	5.6, 5.6	0
25	5.6, 5.6	0	5.4, 5.4	0
27	6.0, 6.0, 6.1	.1		
28	6.7, 6.8, 6.7, 6.9, 6.7	.2	6.5, 6.5, 6.4, 6.5	.1
29	5.2, 5.1, 5.2, 5.3, 5.3, 5.4	.3	4.8, 4.8, 4.9, 4.9	.1
30	5.6, 5.8	.2	5.9, 5.8	.1
31	6.4, 6.7, 6.6	.3		
32	6.6, 6.8, 6.8	.2	6.6, 6.8	.2
33	5.0, 4.9, 5.0	.1	5.0, 4.9	.1
34	5.9, 5.8, 5.9, 5.7, 5.9	.2	5.9, 5.9	0
35	5.9, 5.7, 5.9, 5.9	.2	5.7, 5.8, 5.7	.1
36	5.1, 5.2, 5.2	.1	5.2, 5.1	.1
37	5.4, 5.7, 5.7	.3	5.5, 5.5, 5.5	0
38	6.3, 6.3	0	6.4, 6.4	0
	Average	0.13	Average	0.10

[a] Extractions were made for 1 hour at room temperature.

TABLE 6.—*Comparison of* pH *values* [a] *obtained from ground and cut samples of file-folder stock*

Samples	pH after 1 hour		pH after 20 hours	
	Ground	Cut	Ground	Cut
A	5.1	5.4	4.9	4.9
B	5.1	5.4	5.0	5.0
C	4.7	4.9	4.7	4.7
D	5.1	5.7	5.1	5.1
E	5.5	6.1	5.4	5.4
F	5.8	6.5	5.9	5.9
G	5.3	6.1	5.2	5.3
H	5.3	6.1	5.3	5.3

[a] Extractions were made at room temperature.

V. RECOMMENDED PROCEDURE

On the basis of the experimental results of this investigation, the following procedure is recommended for obtaining the pH value of paper. Weigh 1.0 g of ground, air-dry paper, and transfer to a 100-ml beaker. Instead of grinding the paper it may be cut into pieces of roughly 1 cm^2 if the paper is not especially thick. Add 20 ml of distilled water and macerate with a flattened stirring rod until the specimen is uniformly wet. Then add 50 ml more of the distilled water, stir well, cover with a watch glass, and allow to stand approximately 1 hour. If the paper is thick or dense, and if no grinder is available, the extraction time must be prolonged to 20 hours. The entire procedure is carried out at room temperature. After stirring the mixture once more, measure the pH of the unfiltered mixture with a glass electrode and report to the nearest 0.1 pH. Duplicate determinations should agree within 0.1 pH. The distilled water used in the extraction should not contain more CO_2 than corresponds to a pH=5.9, but it must be tested for alkaline impurities by boiling a small portion to expel the CO_2. If the pH of the water, after boiling, is definitely above 7.0, it should be redistilled, preferably from alkaline permanganate, to oxidize organic substances.

The author acknowledges the cooperation of M. B. Shaw and M. J. O'Leary in supplying the papermaking details and the assistance of W. K. Wilson in making some of the pH measurements.

WASHINGTON, February 10, 1939.

U. S. DEPARTMENT OF COMMERCE NATIONAL BUREAU OF STANDARDS

RESEARCH PAPER RP1206

Part of Journal of Research of the National Bureau of Standards, Volume 22, May 1939

FURTHER DATA ON GOLD-CHROMIUM RESISTANCE WIRE

By Theodore B. Godfrey

ABSTRACT

By heat treatment, the temperature coefficient of electrical resistance of gold-chromium coils containing 2.1 percent of chromium can be made extremely small within the interval 18° to 35° C, and the resistance of such coils is extremely stable. Consequently, a resistance bridge made with gold-chromium coils and without temperature control should be fully as good as the customary bridge with manganin coils and thermostatic control. Data obtained during the construction and testing of four 10-ohm coils are given.

CONTENTS

	Page
I. Introduction	565
II. Construction of coils	565
III. Heat treatment	566
IV. Temperature-resistance curves	569
V. Stability	570
VI. Pressure coefficient of resistance	571
VII. Conclusions	571

I. INTRODUCTION

The gold-chromium resistance alloys investigated by Linde [1] and by Thomas [2] seem to be ideally suited for the construction of very precise electrical-measuring instruments, such as the bridges used in resistance thermometry. It seems probable that a bridge made with gold-chromium alloy coils and without temperature control should be fully as good as the customary bridge with manganin coils and thermostatic temperature control. Since several manufacturers of electrical instruments are interested in the use of this alloy, and as the available information concerning its treatment and properties is limited, it is thought that the data obtained during the construction and testing of four 10-ohm gold-chromium coils and the data on the stability of Thomas' coils over a period of years are of sufficient interest to warrant their publication.

II. CONSTRUCTION OF COILS

Thomas found that in the interval 20° to 30° C the resistivity of gold-chromium alloys as a function of temperature could be represented by equations of the type

$$\rho_t = \rho_{25}[1+\alpha(t-25)+\beta(t-25)^2].$$

[1] J. O. Linde, Ann. Physik **402**, 52 (1931); **407**, 219 (1932).
[2] J. L. Thomas, J. Research NBS **13**, 681 (1934) RP737.

Since his data indicate that for an alloy containing 2.1 percent of chromium, the value of β is zero and the value of α can be lowered to zero by heat treatment, alloy of this composition was chosen for the construction of the four coils. Each coil was wound with bare, hard-drawn wire 0.2 mm in diameter. The wire for coils 1 and 2 was drawn from larger wire obtained from Thomas, and the wire for coils 3 and 4 was drawn from a new melt. The coils were similar in construction to the National Bureau of Standards strain-free type of platinum resistance thermometers,[3] this construction being more convenient, with the materials and equipment immediately available, than the more conventional construction of resistance standards. The two mica side pieces, however, were omitted in the construction of coils 3 and 4, so that each turn of these two coils was supported at only two points. Two gold wires were welded to each end of each coil, making it a four-terminal resistor, and to the gold wires were welded the copper wires for the bridge connections. Both electrowelding and oxy-hydrogen welding were found satisfactory for these operations. After the coils were washed and dried, they were placed within Pyrex tubes. The four terminal wires of coils 1 and 2 were wedged fast by a cork inserted in the end of the tube. The lead wires of coils 3 and 4 were completely insulated by glass. Later, after the heat treatment, the tubes were evacuated, filled with dry air at atmospheric pressure, and sealed with wax.

III. HEAT TREATMENT

Prior to heat treatment, the value of the temperature coefficient of resistance, α, of coils 1 and 2, at room temperature was about 125×10^{-6}/°C, and of coils 3 and 4 about 93×10^{-6}.

Coils 1 and 2 initially were heated at 200° C, the heating being interrupted at various times for the purpose of observing the changes in the values of the α's. The values of the α's were derived from resistance measurements at 20° and 30° C and plotted as a function of the time of heating, as shown in figure 1. At first the values of the α's decreased rapidly, falling to about 20×10^{-6} in the first hour. Thereafter, the rate of decrease diminished progressively and eventually became so small that an attempt was made to increase the rate by heating at 250° C. Contrary to expectation, there resulted an increase in the value of α for one coil and no change in the value for the other. After further heating the coils at 200° C, both were again heated at 250° C, and in each case the value of α became more positive. Eventually the value of α for both coils was reduced to less than 0.1×10^{-6}/°C.

Relying upon the data obtained with coils 1 and 2, coil 3 was heated initially for 5 hours at 200° C, and the value of α was then found to have been reduced to -3×10^{-6}. Heating the coil at 250° C, instead of reversing the direction of change, made the coefficient fall to still more negative values. After it was found that immersing the coil in liquid air had no effect on the value of α, cold-working was attempted. The wire was held by tweezers at two points about 1 mm apart and bent back and forth several times. This treatment was repeated over the whole length of the wire. In this manner the value of α was brought to 0.2×10^{-6}. This change in the value of the coefficient in

[3] T. S. Sligh, Jr., BS Sci. Pap. 17, 49 (1922) S407; Beattie, Jacobus, and Gaines, Proc. Am. Acad. Arts Sci. 66, 167 (1930).

the positive direction as a result of cold-working is unusual, since for other metals and alloys cold-working generally results in an increase in resistivity, and a negative change in the coefficient.

Before starting the regular heat treatment, coil 4 was kept for some time in boiling water to remove the borax flux which had been used in welding, and was dried at 150° C. The total time required for this was about 4 hours. The value of the coefficient was then found to

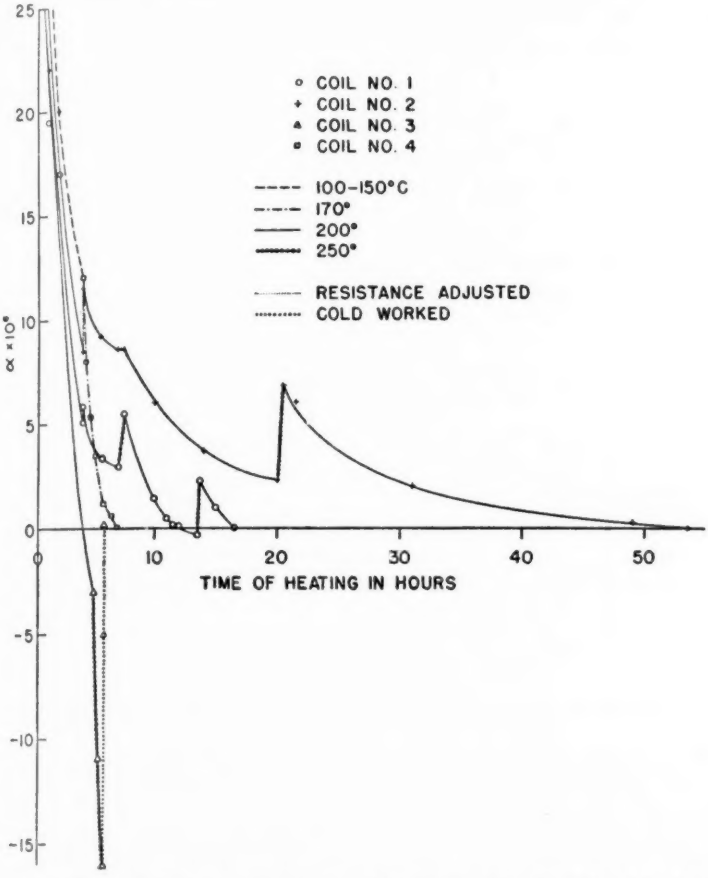

FIGURE 1.—*Changes in the temperature coefficient of resistance produced by heating.*

have dropped to 12×10^{-6}. Subsequent heating at 170° and 200° C quickly brought it to zero.

In the course of the heat treatment, resistance adjustments were made several times, either by shortening the coils at the lower end and welding the pieces together, or by scraping the wires at the upper ends of the coils. All such adjustments increased the value of α, although, except in two instances, the change was too small to be shown in figure 1.

As noted by Thomas, there is a linear relationship between the changes in the resistance of a gold-chromium coil at room temperature and the value of α during the heat treatment, the resistance increasing as the coefficient decreases, as shown for coils 1, 2, and 3 in figure 2. When coils 1 and 2 were heated at 250° C, the resulting unexpected increases in the value of α were accompanied by decreases in resistance consistent with this relationship, but when coil 3 was cold-worked, the relationship was not maintained, very probably because the dimensions of the wire were altered by this treatment. The average of the slopes of the curves in figure 2 corresponds to a decrease of 22×10^{-6}

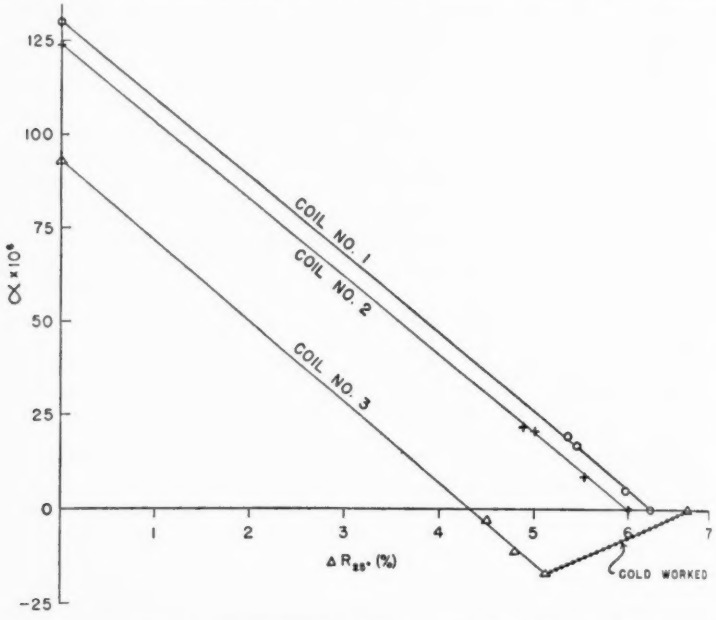

FIGURE 2.—*Linear relationship between α and resistance at 25° C.*

in the value of α for a 1-percent increase in resistance. The corresponding value found by Thomas, for an alloy containing 2.35 percent of chromium, was 26×10^{-6}.

It has been found difficult to account for the differences in the effects of heat treatment upon the coils, especially in the effects of heating at 250° C. At first it was thought that the increases in the value of α of coils 1 and 2 were caused in some way by strain in mounting, since when these coils were in place within their protecting tubes, the mica side pieces (omitted in the construction of coils 3 and 4) were forced toward the center by the glass, thus straining the wire. To test this possibility, the outer edges of the mica side pieces of coil 1 were sheared off so that they no longer pressed against the glass, and, in addition, were cut through radially every four or five turns. The coil was then replaced in its tube and heated at 250° C for 15 minutes. The value of α again increased as before (not shown in fig. 1), rising

from 0 to 2.2×10^{-6}. Another coil of wire of the same lot, wound on a quartz tube, after heating at 200° C, also showed the increase in the value of α when heated at 250° C. Consequently, it seems that the effect is a characteristic of the wire obtained from the first melt and not a result of the method of mounting.

In this last experiment with coil 1, the heating at 250° C was continued for some time, to see whether the value of α would continue

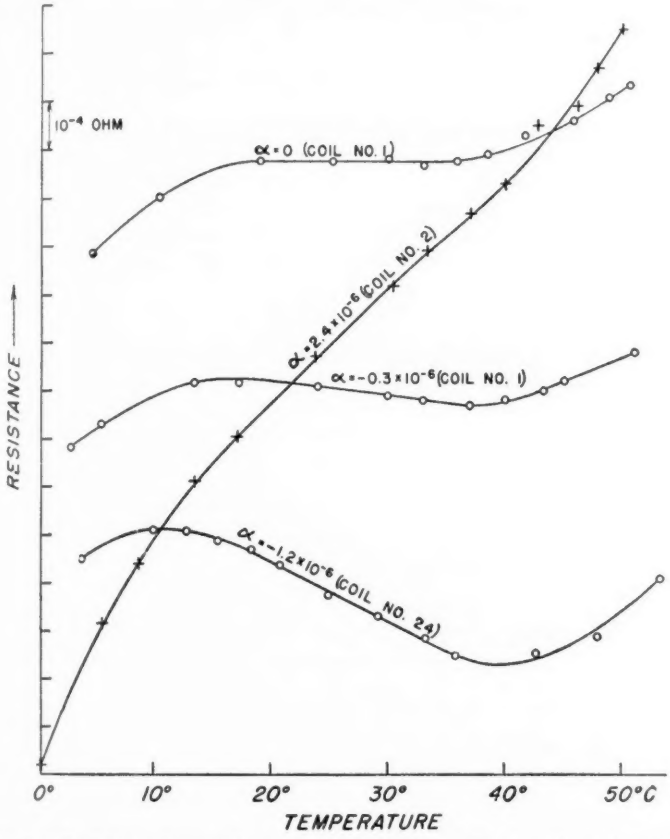

FIGURE 3.—*Resistance-temperature curves of 10-ohm coils at various stages of heat treatment.*

to increase. At the end of an hour, the value of α reached a maximum of 2.5×10^{-6} and then started to decrease at a rate which soon became comparable with the rate of decrease at 200° C.

IV. TEMPERATURE-RESISTANCE CURVES

At various times during the heat treatment and after its completion, measurements were made of the resistances of the four coils over a range of temperature extending from 0° to 50° C. Some of the results obtained are shown in figure 3, together with measurements on one of

Thomas' 10-ohm coils (coil 24). The curves all indicate that in this range of temperature an equation of the second degree is incapable of representing the resistance as a function of temperature, but that an equation of third or higher degree would be required. The values of α shown are the slopes of the straight parts of the curves. It will be noted that the range of temperature (18° to 35°C) in which the slope of the upper curve for coil 1 is not measurably different from zero includes the temperatures ordinarily prevailing in a laboratory, and that even outside of this range the slope of the curve as shown does not exceed 2×10^{-6}.

V. STABILITY

The early changes in resistance of three of the coils have been somewhat greater than those of the coils constructed by Thomas. The

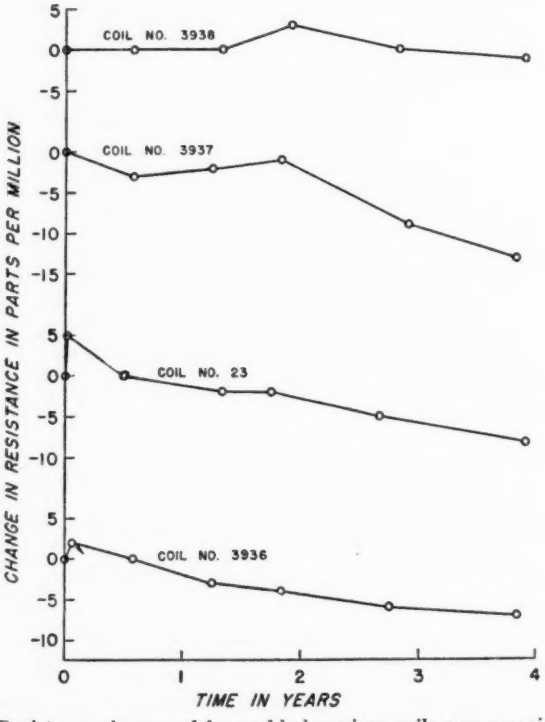

FIGURE 4.—*Resistance changes of four gold-chromium coils over a period of 4 years.*

resistance at room temperature of coil 1 has decreased 4 parts in a million in 2½ months; that of coil 2, after increasing 7 parts in a million in 45 days, has since remained constant for a month; that of coil 3 has increased 16 parts in a million in 3 months. Coil 4, however, in 3 months has shown no measurable change in resistance. This coil not only was mounted most nearly in a truly strain-free manner, but also was not subjected to cold working after mounting.

Thomas has kindly supplied later data on the changes in resistance of the gold-chromium coils for which resistance-time curves are shown

in his figure 4.[4] These curves, extended to cover a period of 4 years, are shown in figure. 4 Coil 3938, which was originally the most stable of the four, has remained practically constant in resistance. The resistances of the others have decreased 5 or 10 parts in a million below their original values. These coils were mounted in salvaged oil-filled containers, and it is probable that moisture has entered some of the containers. Even so, the coils compare favorably in stability with well-made manganin coils of usual construction. As might be expected, in view of the relation, discussed above, between changes in resistance and changes in the value of the coefficient, there has been no measurable change in the temperature coefficients of resistance of any of these gold-chromium coils.

VI. PRESSURE COEFFICIENT OF RESISTANCE

The resistance of coil 1 was measured at pressures from 0 to 3 atmospheres. The pressure coefficient of resistance of this coil determined from these measurements was positive, as in the case of manganin, and small—the value obtained being 1.1×10^{-6} per atmosphere.

VII. CONCLUSIONS

Further investigation has confirmed Thomas' data showing that gold-chromium alloy containing 2.1 percent of chromium is well suited for the construction of the coils of precise electrical-measuring instruments. Although coils made of wire taken from different melts, and even coils made of wire from the same melt, have shown large differences in their response to heat treatment, it has been possible to make the temperature coefficient of resistance of any coil as low as desired in the range of temperature 18° to 35° C. Whereas heating a coil usually lowers the value of the coefficient, mechanical working raises it, and may be resorted to if a negative value of the coefficient has resulted from carrying the heat treatment too far. However, for highest stability of resistance, the results indicate that mechanical working as well as strain in mounting should be avoided.

The pressure coefficient of resistance of a gold-chromium coil was measured and found to be equal to 1.1×10^{-6} per atmosphere.

I am indebted to J. L. Thomas, J. R. Coe, Jr., and D. C. Ginnings for data on coils which they have constructed, and to E. F. Mueller for helpful discussion.

WASHINGTON, March 21, 1939.

[4] J. L. Thomas, J. Research NBS **13**, 681 (1934) RP737.

U. S. DEPARTMENT OF COMMERCE NATIONAL BUREAU OF STANDARDS

RESEARCH PAPER RP1207

Part of Journal of Research of the National Bureau of Standards, Volume 22, May 1939

DISTRIBUTION OF OZONE IN THE STRATOSPHERE

By W. W. Coblentz and R. Stair

ABSTRACT

Measurements of the spectral quality and total intensity of ultraviolet solar radiation at a fixed ground station and at various elevations above the earth's surface are described.

For making measurements at a fixed ground station at a high elevation (Flagstaff, Ariz., elevation 2.2 km), a portable ultraviolet-intensity meter, consisting of a balanced amplifier, *Ti*-photoelectric cell, and microammeter was used, see RP647.

For measuring solar radiation in the stratosphere, an ultraviolet-intensity meter (consisting of a *Cd*-photoelectric cell and filter radiometer, connected with a balanced amplifier, relaxation oscillator, and radio transmitter) and a radio-operated barometer were transported aloft by means of unmanned balloons. The audio-frequency modulated radio wave, giving the intensity of the ultraviolet solar radiation and the altitude of the apparatus, was received and graphically recorded at a fixed ground station, see RP1075.

In the measurements at Flagstaff, Ariz., a close parallelism was observed in the variation in filter transmission with variation in barometric pressure. This is in agreement with the well-known variation in the amount of atmospheric ozone that accompanies changes in air pressure. No such systematic variation in filter transmission with variation in pressure of atmospheric aqueous vapor was observed.

A notable example is described in which the wave of low barometric pressure preceded, by 5 to 6 hours, an appreciable increase in atmospheric ozone; apparently indicating which was cause and which was effect, and suggesting a method of studying air circulation in the stratosphere.

In four balloon ascensions made in June 1938, the photoelectric ultraviolet-intensity meter and auxiliary radio-transmitting apparatus attained heights of 83,000 to 88,000 ft (25 to 27 km), penetrating about 65 percent of the ozone, the most of which was localized in a layer extending from an elevation of 18 to 27 km, with a wide maximum of concentration at a height of about 25 km. At the highest elevation attained by the instruments, the intensity of the ultraviolet of short wave lengths was about 10 times that of direct sunlight at sea level.

CONTENTS

	Page
I. Introduction	574
1. Relation between meteorological conditions and the amount of ozone in the atmosphere	575
II. Ultraviolet solar measurements at Flagstaff, Arizona	577
1. Measurements of sky radiation	578
2. Diurnal variation in ultraviolet solar radiation	580
3. Correlation of atmospheric transmission of ultraviolet solar radiation with barometric pressure	583
4. Variation in atmospheric transmission of ultraviolet solar radiation with turbulence in the ozone layer	588
5. Air-mass analysis of October 5, 1938	590
III. Exploration of the vertical distribution of ozone in the stratosphere	590
1. Description of the radio-operated ultraviolet-intensity meter	591
2. Description of improvements in the radio circuit of the photoelectric ultraviolet-intensity meter	591

III. Exploration of the vertical distribution of ozone in the stratosphere—Continued.
3. Description of a balloon-flight record 594
(a) Notes on the six flights 595
4. Evaluation of the ultraviolet-intensity measurements 596
(a) Variation in intensity of ultraviolet solar radiation with altitude above the earth's surface 601
(b) Calculation of the amount of ozone traversed 601
(c) Vertical distribution of ozone in the atmosphere 604
IV. References and notes 605

I. INTRODUCTION

An exploration of the vertical distribution of ozone in the stratosphere by measuring the intensity of ultraviolet solar radiation with a photoelectric cell and filter radiometer [1],[1] at different elevations above the earth's surface, was first considered in 1934 in connection with the flights of manned balloons [2].

The chief problem then was (and still is) the lack of a satisfactory photoelectric cell for measuring the ultraviolet intensity. Moreover, since nearly all the auxiliary equipment for such an undertaking remained undeveloped, but little progress was made in the design of suitable apparatus prior to the middle of the summer of 1935—too late to take part in the flight of the *Explorer II* which occurred on November 11, 1935 [2].

It was therefore decided to redesign the apparatus to make it transportable in small, inexpensive, unmanned balloons. This required a great reduction in the weight of all the essential parts that must be transported. Fortunately, through rapid developments then in progress in radio transmission as applied to meteorographs [3, 4], it became possible to leave a large part of the measuring and recording apparatus at a fixed ground station, and the weight of the apparatus to be transported aloft could be reduced to a few kilograms.

The part of the apparatus that must be sent aloft is relatively inexpensive. Hence, even if it is lost or broken in the descent, numerous flights are possible, and more data are obtainable at a less cost than in a single flight in a manned balloon.

The proposed method, and the first progress made in the development of a radiometric ultraviolet-intensity meter, consisting of a photoelectric cell and filter radiometer, and auxiliary radio-transmitting apparatus, to be transported aloft by sounding balloons, was described early in 1936 [4].

In the summer of 1937 quantitative measurements of ultraviolet solar intensities were obtained to a height of 64,000 ft (19 km) above sea level [5, 6]. The failure to obtain measurements at higher elevations was due to lack of power in that part of the radio-transmitting apparatus controlled by the photoelectric cell. The radio barograph indicated that the apparatus attained a height of 78,000 ft (24 km).

In the meantime, through improvements made in the radio-transmitting apparatus [7], during the summer of 1938 it was possible to secure quantitative measurements of ultraviolet solar intensities to the highest elevations (27 km) attained by the transporting balloons.

The object of the present communication is to describe the results of the ultraviolet solar-intensity measurements, obtained, in June 1938, by means of a radio-operated photoelectric cell and filter radiometer

[1] Figures in brackets indicate the literature references and notes at the end of this paper.

transported aloft by means of sounding balloons; also supplementary measurements made in September and October 1938, at the Lowell Observatory, Flagstaff, Ariz. (elevation 7,300 ft) for the purpose of determining the effect of humidity and of sky radiation upon ultraviolet intensities, which information is of interest in connection with the stratosphere measurements.

The sky radiation was measured with a *Cd*-photoelectric cell previously used in one of the stratosphere flights (flight 1). The effect of humidity and of clouds upon the spectral quality of the directly incident ultraviolet solar radiation was measured with one of the *Ti*-photoelectric cells and the glass filters used in similar measurements made in 1934 [8]. In the present measurements a higher precision was obtained than 4 years ago.

1. RELATION BETWEEN METEOROLOGICAL CONDITIONS AND THE AMOUNT OF OZONE IN THE ATMOSPHERE

Based upon researches of various observers, extending over the past 15 or more years, it appears to be definitely established that, in vertical distribution, ozone exists throughout the whole atmosphere, to a height of perhaps 40 km; with the most of it concentrated in a layer having a maximum density at a height of 20 to 25 km above sea level. It is the only atmospheric gas that has such a stratification.

In high latitudes (Tromsö, 69°40′) the ozone appears to be concentrated in a layer centered at a height of about 21 km above sea level, whereas at Arosa, Switzerland (46°45′ N) it is more uniformly distributed through the lower 30 km [17], as observed in the present investigation.

In geographic distribution, the total amount of ozone increases with latitude, being about 2 mm in thickness (ntp) at the equator and 3.5 mm or more in Northern latitudes (Spitzbergen, 78°55′ N).

There is a seasonal variation in the ozone content of the atmosphere, which is a maximum in the local spring (March, in the Northern Hemisphere) and a minimum in the local autumn [10, 14]. The seasonal variation is small at the equator and different in different latitudes. The difference between the average ozone content at the poles and at the equator is about four times as great in the spring as in the autumn [12].

The maximum ozone values are associated with air currents which (at least in the troposphere), in the Northern Hemisphere, have recently come from the Arctic. They are particularly high in the spring, after the long polar night. Similarly, the smallest ozone values are associated with tropical air currents in the troposphere [11, 14]. Nothing appears to be known regarding the circulation of air currents in the ozone layer. According to Dobson [11], it is necessary to assume their direction to be opposite to those in the troposphere in order to support the hypothesis that ozone is formed chiefly by sunshine.

Marked daily variations in the amount of atmospheric ozone occur with varying meteorological conditions; relatively large amounts being generally observed with low barometric pressures (cyclonic regions) and relatively much smaller amounts with high barometric pressures (anticyclonic regions) [10, 12, 13].

Although it is presumed [9] that the amount of ozone in the atmosphere is greater in the morning than in the evening, as is probably to be expected, observers differ in their findings—Goetz and Dobson [19] reporting no diurnal variation of ozone, whereas Coblentz and Stair [8] recorded occasional variations (less ozone in the afternoon than the forenoon). But whether this variation was due to decomposition of ozone, or accompanies a change in barometric pressure (as herein reported) was not determined.[2]

In addition to this diurnal variation in ozone, Coblentz and Stair [8] observed also a temporary departure from (above or below) the seasonal average. Whether these variations in ozone content (observed at Flagstaff, Ariz., elevation 2,210 m) were caused by cyclonic and anticyclonic conditions was not determined.[3]

Recently such variations in the amount of atmospheric ozone were observed by Kiepenheuer [15] while making spectral ultraviolet measurements on the Jungfraujoch (elevation 3,460 m). He ascribes these variations to passing "Ozone clouds" and "Ozone holes," which caused great fluctuations in intensity of ultraviolet spectral radiation, particularly at the wave length 2880 A. From his description it appears that his so-called "Ozone holes" were caused by the circulation of masses of air which contained a low concentration of ozone, thereby increasing, for a short time, the transparency of the air to ultraviolet radiation, as observed in the Arizona measurements of 1934 [8].

In a recent paper, Meetham [16] reported the results of a study of the connection between the amount of ozone in the upper atmosphere, at any place, and the type of pressure disturbance at sea level. For this purpose he made use of the statistical data available, showing that over a low-pressure area (a) the tropopause is abnormally low, (b) the actual shortage of air, which is responsible for the low pressure, occurs chiefly in the stratosphere, and (c) the ozone density is unusually large in the lower stratosphere.

To account for the known facts, he found it necessary to assume an appreciable amount of vertical circulation in the stratosphere and he added "Distasteful as this assumption is, it provides one more reason why turbulence in the stratosphere should be further investigated."

In the ensuing discussion of this paper, Dobson emphasizes that the difficulty in such an analysis lies in separating cause from effect, and he concludes with the remark that it is "still a matter of doubt whether the amount of ozone is affected by the weather conditions, or vice versa." As will be shown presently, with the arrival of the wave of low barometric pressure (on October 5 at Flagstaff, Ariz.) some 5 to 6 hours in advance of the high concentration of ozone, it would appear that, at least in this particular instance, weather conditions were the controlling factor (the "cause") in changing the concentration of ozone. Whether this was the result of an influx of polar

[2] The diurnal high air pressure at Flagstaff, Ariz., occurs at about 10 a. m. (and 10 p. m.). Hence, if it should be found to be generally true that the variation in the ozone content of the atmosphere lags some hours behind the variation in barometric pressure, then the relatively lower ozone content observed at 1:30 to 3:30 p. m. would be associated with the diurnal barometric high pressure that occurred at 10:00 to 10:30 a. m. Evidently a study should be made of this phenomenon, using ultraviolet solar radiation; also infrared solar radiation, especially the spectral range comprising the large absorption band of ozone at 9.6 μ which falls within the band of relatively high transparency to atmospheric water vapor and relatively high intensity of solar radiation [18, 27].

[3] Since writing this paper, C. O. Lampland, of the Lowell Observatory, has sent us photographic copies of barograph records which show that on July 24, 27, and 30, 1934, when the observed filter transmissions were lower (ozone lower) than the average, the air pressure was 2.5 to 3 mm higher than the average; in good agreement with the measurements described in Section II (see fig. 4) of the present paper. However, since the precision attained in these earlier measurements was not comparable with this year's measurements, less weight is to be attached to the earlier observations.

air containing a higher concentration of ozone, or merely fresh oxygen that was then ozonized (as some have speculated), adds another complication to the solution of the problem.

In view of all the work that has been done during the past 15 or more years, it is surprising to find practically no information on the time of arrival of the wave of high concentration of ozone relative to the time of arrival of the wave of low barometric pressure. This may be owing to the method of observation, which consisted in measuring (photographing) the solar ultraviolet spectrum, morning, noon, and evening. Hence, there was no continuous record. Kidson [12], working in New Zealand, in attempting a correlation of ozone with barometric pressure, finds the best agreement by comparing the amount of ozone on a given day with the barometric pressure of the preceding day—a lag of 20 hours or more, in perception of the change in the amount of ozone after a change in barometric pressure.

In concluding this part of the discussion, it is to be noted that all the researches show that the low barometer does not appear to be the cause, but to accompany the cause, of the influx of ozone. For example, the measurements made by Barbier, Chalonge, and Vassy [20] during the polar winter of 1935 at Abisko, Sweden (Lat. 68°20′ N), show that the thickness of the ozone layer changed from 1.87 mm on January 25 to 4.04 mm on January 26, coincident with a great influx of Arctic air that extended to Spain. Yet, according to the weather map (data supplied by E. W. Woolard of the Weather Bureau), the drop in barometric pressure was relatively small—about 2.5 mm (0.1 in.).

II. ULTRAVIOLET SOLAR MEASUREMENTS AT FLAGSTAFF, ARIZONA

Supplementing the ultraviolet solar-radiation measurements made with sounding balloons, described in the following section of this paper, it was of interest to obtain similar measurements of spectral quality and total intensity through a cloudless sky at a terrestrial station having a high elevation.

Through the courtesy of V. M. Slipher, Director of the Lowell Observatory, Flagstaff, Ariz., elevation 7,300 ft. (2,210 m), it was possible for one of us (W.W.C.) to make ultraviolet solar-intensity measurements, thus extending the investigation begun in 1934 [8].

Information on the variation of the amount of ozone in the atmosphere is obtained from measurements of the spectral quality and total intensity of ultraviolet solar radiation of wave lengths shorter than about 3200 A, which are greatly absorbed by this gas. The measurements are made by means of a portable ultraviolet-intensity meter [1] consisting of a *Ti*-photoelectric cell and filter radiometer, in which the photoelectric current, after amplification, is measured on a precision microammeter.

The *Ti*-photoelectric cell responds only to wave lengths shorter than about 3400 A. The filters used are opaque to wave lengths ranging from 2950 to 3100 A. The spectral band measured therefore comprises: (a) the component transmitted by the filter, consisting of wave lengths between about 3100 and 3300 A that are affected but little by ozone absorption, and (b) the component intercepted by the

filter, consisting of wave lengths shorter than about 3100 A that lie in the region of great absorption by ozone, and, hence, are easily affected by a change in concentration in (or the length of path through) the layer of ozone traversed by the solar rays. Moreover, the photoelectric cell is about 60 to 70 times more sensitive at 2900 A than in the region of 3300 A, which is practically the long-wave-length limit of photoelectric response of the *Ti*-cells used.

As a result of this high selective response of the photoelectric cell, a slight change in the amount of ozone in the path of the solar rays has an appreciable effect upon the atmospheric transmission of ultraviolet at 2900 to 3100 A and, hence, upon the percentage transmission of the filter, which increases with increase in the amount of ozone in the atmosphere.

Consequently, with the well-known increase in the amount of atmospheric ozone that occurs during a cyclonic (low pressure) disturbance, there should be (and is) observed an appreciable increase in the percentage transmission of the filter for a given air mass (say, $m=1.5$) relative to the value obtained on days of average barometric pressure. Similarly, as will be noted presently, with the relatively much smaller amount of ozone that is known to be present in an anticyclonic (high pressure) area there should be (and is) observed an appreciable decrease in the filter transmission relative to the value observed on days of average barometric pressure [30].

1. MEASUREMENTS OF SKY RADIATION

In the radiometric measurements of 1934 at Flagstaff, Ariz., it was found [8] that, in an angle of about 22° surrounding the sun, the sky contributed about 0.3 to 0.4 percent to the total ultraviolet solar radiation measured. In connection with the stratosphere ultraviolet solar radiation measurements it was of interest to determine the amount of cloudless sky radiation relative to the total (sun + sky) that could enter the photoelectric cell. In the balloon ascensions the sky was never cloudless. Hence, the herein-described measurements are minimum values for an altitude of 7,300 ft—clouds near the sun would increase the amount of sky radiation.

The measurements of sky radiation were made with *Cd*-photoelectric cell No. 38303, previously used in the stratosphere flight made on June 16, 1938 (see fig. 9). For this purpose the window of the photoelectric cell was covered with two diffusing screens (four fine-ground surfaces) of Corex-*A* glass, over which was mounted an opaque shield with an opening 17 mm in diameter, shown (at *Cx*) in figure 6, as used in the stratosphere flights.

For measuring sky radiation, the *Cd*-photoelectric cell was mounted in a container without the protruding vestibule shown in figure 1 of a previous publication [8]. In this manner the interior of the photoelectric cell was exposed to the sky comprised in an angle of about 128°, as used in the stratosphere flights, and in contrast with an aperture of 22°, as the instrument is ordinarily used [8]. By means of black cardboard disks, 17 to 40 mm in diameter, supported at various heights above the window, the direct solar rays and, in some measurements, additional parts of the sky could be excluded from the photoelectric cell. By turning the photoelectric cell through 90° (in the same azimuth), a measurement was obtained of the amount of

sky radiation in a solid angle of about 128°, with its central axis directed at the antisolar point.

Measurements of ultraviolet sky radiation of wave lengths less than about 3300 A are depicted in figure 1. The data in the upper part, *A*, of the illustration were obtained by shadowing the opening of the photoelectric cell with a disk 18 mm in diameter situated 17 cm above the surface of the window. The air mass represents the solar height or column of air passed through by the directly incident solar rays.

The upper part, *A*, of figure 1, depicts the percentage of ultraviolet sky radiation relative to the total (sun plus sky) radiation incident upon the window of the photoelectric cell, exposed normal to the sun. For any given solar height (column of air traversed; air mass, say, $m=1.4$), the ultraviolet sky radiation comprised in a solid angle of 128°

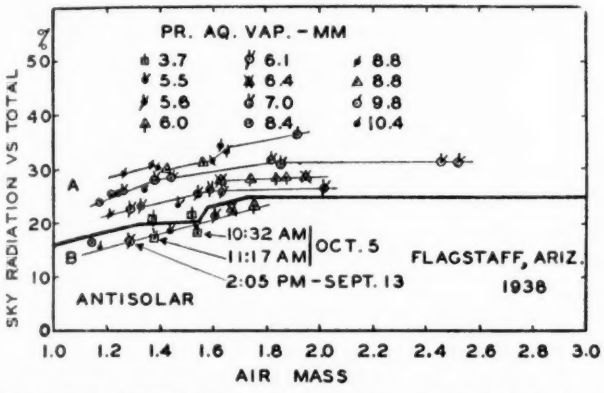

FIGURE 1.—*Part A, ultraviolet sky radiation relative to the total incident (sun plus sky) radiation for different solar heights, i. e., column of air traversed by the directly incident solar rays; part B, ultraviolet sky radiation from the antisolar point, i. e., 90° from the sun.*

varies from 20 to 30 percent, depending upon scattering by dust particles, as indicated by the width of the corona around the sun, and, to some extent, upon the pressure of aqueous vapor (i. e., the amount of precipitable water), indicated at the top of figure 1.

The lower part, *B*, of figure 1, gives the amount of ultraviolet sky radiation in a solid angle of 128°, centered on a point 90° from, and in the same azimuth with, the sun (the antisolar point) compared with the amount of directly incident solar radiation (i. e., sun minus sky radiation mentioned in the preceding paragraph).

The sky radiation from the antisolar point is more uniform from day to day and in that respect less dependent upon atmospheric water vapor. The measurements at 10:32 a. m. and 11:17 a. m. on October 5 are interesting, because they were made between sets of filter-transmission measurements (fig. 3), with a *Ti*-photoelectric cell having an opening of 22° to the sky.

From the fact that the sky radiation on October 5 was the lowest observed during the course of the whole series of measurements, it appears that the high values of the filter transmissions depicted in figure 3, and the total intensities in figure 2, are affected but little by

scattered ultraviolet radiation, as compared with the effect of variations of ozone in the stratosphere.

2. DIURNAL VARIATION IN ULTRAVIOLET SOLAR RADIATION

The present measurements of the total intensity and spectral quality (spectral-energy distribution) of ultraviolet solar radiation of short wave lengths were made with the photoelectric cell, *Ti–1*, and filters used in 1934 [8]. The so-called rainy season seemed to continue longer and there appeared to be more cloudiness this year than during the same season 4 years ago. Measurements were therefore made only on the clearest days.

In figure 2 are depicted various measurements of total (integrated) intensities of ultraviolet solar radiation of wave lengths shorter than

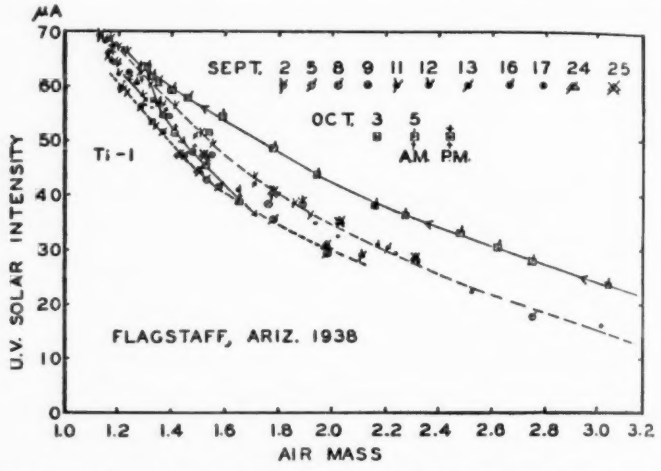

FIGURE 2.—*Ultraviolet solar intensities on different dates, and different solar altitudes—air masses traversed by the directly incident rays.*

about 3300 A. The intensities are relative values; that is, deflections of the microammeter needle.

The main point of interest in these curves is that there is a tendency for the intensities observed on days of high barometric pressure to be higher than on days of average air pressure (see fig. 4). A notable example is the series of intensity measurements made on October 5, which, even for a large air mass (m=3.05 at 8:23 a. m.) was about 65 percent higher than the best values previously observed. However, by afternoon the intensities decreased to the lowest values observed during the season, in spite of the fact that (judged by the smallness of the solar corona) the sky continued to be clear and relatively free from nuclei. The reason therefore is to be found in the increase in ozone content, as interpreted from the filter transmission depicted in figure 5.

In figure 3 are shown the transmissions of the four filters used (*Ba–3*, *Ba–1*, *Ni*, and *Cx–D*, previously described [8]) for various air masses traversed by the solar ultraviolet rays. The various symbols depict the transmissions on different days that may be identified by comparison with figure 4.

The accuracy attained in the measurements of the percentage transmissions of the filters is relatively high. That is to say, two sets of measurements, made in succession at intervals of 1 to 2 minutes,

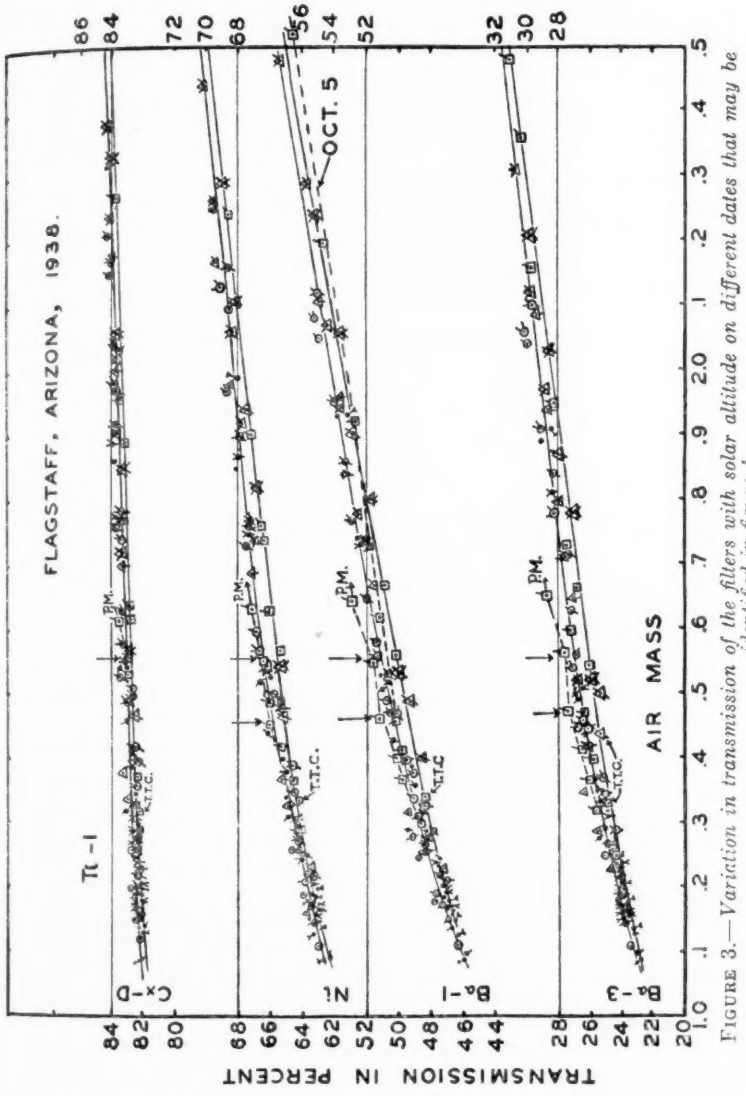

FIGURE 3.—*Variation in transmission of the filters with solar altitude on different dates that may be identified in figure 4.*

differed by only 1 to 3 parts in 500; and this difference was frequently ascribable to a change (of only $\Delta m = 0.01$) in the air mass traversed by the solar rays. The precision attained in the measurements is ascribable to improvements in the ultraviolet-intensity meter and to unusual

meteorological conditions (uniform barometric pressure and a clear sky), which makes it possible to correlate the change in percentage transmission of a given filter (e. g., *Ba–1*), from day to day, even though the numerical values differ by only a few percent.

It is to be noted that for any one filter the ultraviolet transmissions fall into two groups; the upper curve, as will be noticed in figure 4, belonging to average air pressures and the lower curve belonging to high barometric pressures. Variations in pressure of aqueous vapor, which ranged from 5 to 11 mm, show no systematic effect upon the filter transmissions—partly because water vapor has no selective absorption in this spectral region.

The points marked *T.T.C.* represent measurements through thin cirrus clouds that suddenly appeared. The measurements of October 3 are especially noteworthy because part of the sky, from the zenith southward, became overcast with a thin diaphanous sheet of cirrus clouds, in long rolls ("corrugation in cirrus") that were practically

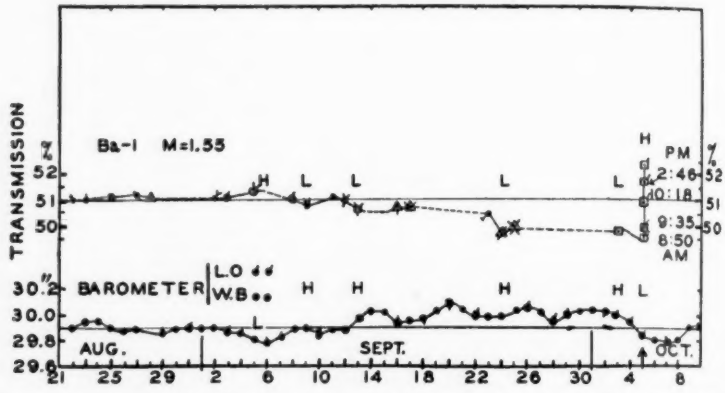

FIGURE 4.—*Graphs showing the percentage transmission of a certain filter (Ba–1), and the barometric pressure on different dates.*

stationary for some 8 to 10 minutes; permitting a complete series of filter measurements, which show that (water) ice spicules have practically no selective absorption in the ultraviolet, as previously observed through a thin fog [8].

Most important are the filter transmissions on October 5, which were conspicuously low early in the forenoon (table 1) and gradually increased to high values in the afternoon (see dotted curve in fig. 3). The arrows show two series of measurements, indicating turbulence that continued for more than half an hour.

Since it requires from 7 to 10 minutes to complete a series of measurements with a set of four filters, and since all values in each series depart consistently in the same direction from the average curve, it appears that this irregularity in the measurements of October 5 is not caused by errors in observation. Incidentally, it is relevant to state that, each time, before making a set of measurements the filter was wiped with a soft linen cloth, or with a fine-haired brush, and examined in reflected light to ascertain that no dust or lint adhered to the surfaces (attracted by electrostatic charges—a common occurrence in a dry climate), thus reducing the percentage transmission.

3. CORRELATION OF ATMOSPHERIC TRANSMISSION OF ULTRAVIOLET SOLAR RADIATION WITH BAROMETRIC PRESSURE

As noted on a preceding page, it is well established that a change in barometric pressure is accompanied by a change in the ozone content in the upper atmosphere; high ozone values accompanying low-pressure areas and vice versa. Hence, these variations in atmospheric ozone should affect the filter transmissions. That is to say, relatively higher filter transmissions should be observed when the barometric pressure is low, and vice versa.

In order to separate this effect from the variation in filter transmission with solar height (air mass traversed by the rays, depicted in fig. 3) it is necessary to compare the data for a particular air mass traversed by the rays. For the purpose of the present paper, an air mass of $m=1.55$ is used; or the solar height at 9:15 to 10:30 a. m. (MST), depending upon the time of the year.

In figure 4 the lower curve gives the barometer readings (in inches; reduced to sea level) on different dates. The atmospheric pressure data taken from the barograph record at the Lowell Observatory ("L. O."), which is at a somewhat higher elevation (80 m) than the U. S. Weather Bureau ("W. B."), are in good agreement with the mercurial barometer readings supplied by the Weather Bureau. The latter measurements are made at 5:30 a. m. (MST).

The upper curve in figure 4 gives the percentage transmission of the filter, *Ba–1*, [8] for air mass $m=1.55$ on different dates. The particular titanium photoelectric cell used was *Ti–1* [8, 21].

The point of interest in these two curves is that after September 1, when the so-called "rainy season" had practically terminated, there is a fairly systematic correlation of high barometer readings and low transmissions (marked "H" and "L" in fig. 4) and vice versa; particularly after September 13, when the barometer continued relatively "high" (about 30.0 in.) until after October 3, 1938. During this time the filter transmissions remained conspicuously lower than the values obtained prior to September 12 and higher than the average for that time of the year [21]. Unfortunately, cloudy weather prevented making measurements during the time of high barometric pressures between September 26 and October 2.

While observations were in progress it was noted that on September 5 the filter transmissions were irregular—"high in a clear sky," except for a short while when they were low for $m=1.3$; and they were "low for $m=1.15$ to 1.5—forenoon and afternoon" on September 9. Since completion of the measurements a study has been made of these results, and as shown in figures 4 and 5, the reason for these variations is apparent.

In his investigations of the variation in atmospheric ozone with meteorological conditions in the southwestern part of the United States, Kimball [12] has shown that, during the months of August and September, surface pressure conditions in Southern California are dominated almost continuously by a "Pacific high" and a "Yuma low" barometric-pressure area. Apparently, from the daily weather maps and from figure 4, this effect extends to Flagstaff, Ariz., where (during these measurements) the barometric pressure remained remarkably uniform, with only one small marked ("low") cyclonic disturbance, which arrived an hour or so in advance of the usual diurnal low on October 5.

TABLE 1.—*Filter transmissions of integrated ultraviolet solar radiation, using titanium photoelectric cell, Ti–1*

[Filters: *Ba–8*=barium flint, thickness 3 mm; *Ba–1*, same, thickness 1 mm; *Ni*=Nillite (trade name); *Cr*=Corex-*D* (trade name); *Tr*=percentage transmission; *m*=air mass; *μa*=microammeter reading for *Rg2* and amplifier sensitivity=12.0 *μa*; Mountain Standard Time (MST), which is 25 min 45 sec faster than local time; dagger (†) and asterisk (*) associate intensity with air mass; *p*=pressure of aqueous vapor in the atmosphere. Observations at Flagstaff, Ariz. (Lat. 35°12′ N; Alt. 7,300 ft) in 1938.]

1	2	3	4	5	6	7	8	9	10	11
Date, 1938, and time	Intensity	*Ba–8*		*Ba–1*		*Ni*		*Cr*		Remarks
		m	*Tr*	*m*	*Tr*	*m*	*Tr*	*m*	*Tr*	
August 25:	*μa*									
10:19 to 10:26 a. m.	†56.3	1.25	25.1	1.25	48.8	1.26	64.7	†1.26	82.8	*p*=8.38 mm at 12:15 p. m. Sky cloudless, small corona at 10:20 a. m. Fracto-cumulus near at 11:30 a. m.
10:46 to 10:54 a. m.	†59.7	1.18	24.2	1.18	47.7	1.19	63.8	†1.20	82.8	
11:40 to 11:46 a. m.	*65.3	*1.11	23.5	1.11	46.3	1.11	63.1	1.12	82.2	
August 27:										
9:17 to 9:25 a. m.	†37.5	1.50	27.1	1.51	51.1	1.52	66.7	†1.54	83.5	*p*=8.82 mm at 10:55 a. m. Large cumulus clouds on S horizon and fracto on S. F. Peaks at 9:30 a. m. Sky overcast at 10:35; rain at 11:15 a. m.
9:30 to 9:38 a. m.	†42.3	†1.42	27.2	1.43	50.4	1.44	66.2	1.46	83.2	
10:04 to 10:14 a. m.	*51.2	*1.28	25.5	1.29	49.5	1.31	65.0	1.32	83.2	
August 28:										
9:46 to 9:53 a. m.	†45.2	1.35	26.4	1.35	50.3	1.37	65.3	†1.38	83.3	*p*=8.82 mm at 11:45 a. m. Fracto-cumuli on S horizon, and cumuli on S. F. Peaks at 10 a. m. Large cumuli near sun at 10:27 a. m.
9:56 to 10:19 a. m.	†49.7	†1.28	25.4	1.32	49.5	1.33	65.1	1.34	83.0	
10:23 to 10:35 a. m.	*51.5	*1.23	24.7	1.25	48.5	1.26	64.3	1.26	82.3	
September 2:										
1:02 to 1:09 p. m.	†69.3	1.13	23.3	1.13	46.3	1.13	63.4	†1.13	82.0	*p*=10.4 mm at 3:07 p. m. Sky full of fracto-cumuli, except clear area around the sun, angle 40°.
1:20 to 1:27 p. m.	†68.7	1.16	23.9	1.15	46.5	1.15	63.3	†1.14	82.3	
1:42 to 1:46 p. m.	*64.8	*1.18	23.7	1.18	46.9	1.18	63.8	1.18	82.4	
September 5:										
8:22 to 8:32 a. m.	†25.8	2.06	30.1	2.08	55.3	2.13	69.2	†2.17	84.2	
8:38 to 8:44 a. m.	*29.7	1.91	29.1	1.95	54.1	1.97	68.9	*1.98	84.0	
8:57 to 9:04 a. m.	*35.5	*1.78	28.2	1.77	53.0	1.76	67.4	1.74	83.4	*p*=7.0 mm at 11:30 a. m. Sky cloudless; light W breeze at 8:15 a. m. Clouds on S. F. Peaks at 9:05 a. m.; extend E past The Elden at 10:20 a. m. Fracto-cumulus forming in S and SW at 10:50 a. m.; over sun at 11:20 a. m.
9:23 to 9:29 a. m.	†41.8	1.54	27.1	1.56	51.3	1.57	66.8	†1.58	83.3	
9:38 to 9:48 a. m.	*47.3	*1.45	26.7	1.47	50.5	1.49	66.1	1.50	82.7	
10:08 to 10:20 a. m.	†51.2	1.33	25.2	1.34	49.2	1.35	64.5	†1.36	82.4	
10:35 to 10:46 a. m.	*56.3	1.25	24.4	1.26	48.3	1.27	64.2	*1.28	82.3	
10:58 to 11:08 a. m.	†59.5	†1.21	24.1	1.22	47.4	1.22	63.7	1.23	82.3	
11:12 a. m.								1.20	82.5	

September 8:										
7:53 to 8:04 a. m.	†17.5	2.60	32.9	2.65	58.7	2.70	71.2	†2.75	85.3	
9:02 to 9:22 a. m.	*38.2	1.63	27.2	1.65	52.1	1.73	67.6	*1.76	83.7	
9:39 to 9:53 a. m.	†42.5	1.46	26.5	1.49	50.8	1.50	65.8	†1.53	83.4	
10:02 to 10:49 a. m.	*60.4	*1.27	24.8	1.28	49.2	1.29	64.3	1.42	82.6	p=8.0 mm at 12:12 p. m. Sky cloudless at 8 a. m.; numerous fracto at 9:30 to 10 a. m.; cloudless but faintly murky at 10:30; cirrus haze at 11:55 a. m.; faint murky haze, in waves, at 1 p. m.; sky covered with large fracto after 1:30 p. m.
11:14 to 11:32 a. m.	†64.1	†1.19	24.1	1.19	47.6	1.21	63.8	1.22	82.3	
11:33 to 11:49 a. m.	*65.8	*1.16	23.7	1.17	47.0	1.18	63.5	1.19	82.5	
11:53 to 11:59 a. m.	†68.2	†1.15	23.8	1.16	46.8	1.16	63.4	1.16	82.1	
12:55 to 1:06 p. m.	*62.5	*1.16	23.9	1.16	46.9	1.15	63.3	1.15	82.6	
1:14 to 1:23 p. m.	†64.3	†1.18	24.1	1.18	47.3	1.17	63.8	1.17	82.4	
September 9:										
9:34 to 9:44 a. m.	*47.3	1.51	26.5	1.52	50.7	1.54	66.2	*1.55	83.2	p=5.5 mm at 12:02 p. m. Sky faintly murky at 10 a. m.; large fracto clouds at 11:20 to 11:50 a. m.; fracto-cumulus clouds and smoke at 1:27 p. m. Filter transmission low for m=1.15 to 1.5, as on September 5.
10:08 to 10:20 a. m.	†54.3	1.35	25.4	1.36	49.1	1.38	65.2	†1.39	82.7	
10:56 to 11:04 a. m.	*62.2	*1.24	24.1	1.25	47.4	1.25	64.0	1.26	83.4	
11:24 to 11:35 a. m.	†56.3	1.19	24.0	1.19	47.2	1.20	63.0	†1.21	82.3	
11:39 to 11:52 a. m.	*58.4	*1.17	24.0	1.17	46.6	1.18	62.8	1.18	82.2	
1:18 to 1:27 p. m.	†54.0	†1.19	24.2	1.19	47.5	1.18	63.3	1.18	82.3	
September 11:										
8:20 to 8:54 a. m.	†28.8	1.89	29.3	1.93	53.9	2.25	69.8	†2.32	84.5	
8:56 to 9:05 a. m.	*38.4	1.79	28.0	1.84	53.6	1.85	68.3	*1.86	83.9	
9:07 to 9:36 a. m.	†49.7	†1.55	27.5	1.74	52.7	1.76	67.7	1.77	83.6	
9:39 to 9:45 a. m.	*51.3	1.51	27.0	1.52	51.3	1.53	66.0	1.55	83.1	
10:08 to 10:20 a. m.	†56.5	1.37	25.7	1.39	49.2	1.40	65.3	†1.41	82.7	p=7.2 mm at 12:25 p. m. Small corona. Sky cloudless until 10:30 a. m. Then fracto-cumulus on horizon. Murky cirrus haze at 11:55 a. m.; stopped at 12:08 p. m. by fracto- cumulus cloud extending from sun to SW horizon.
10:25 to 10:37 a. m.	*60.2	*1.32	24.9	1.33	48.8	1.34	65.1	1.35	82.5	
10:44 to 10:49 a. m.	†62.3	†1.28	24.5	1.29	48.3	1.30	64.4	1.30	82.4	
11:30 to 11:38 a. m.	*67.2	1.20	24.1	1.20	47.3	1.19	63.5	*1.21	82.0	
11:40 to 11:47 a. m.	†67.7	†1.18	23.8	1.19	46.8	1.18	63.4	1.19	82.1	
11:55 a. m. to 12:03 p. m.	*67.5	1.17	23.8	1.17	46.8	1.17	63.4	*1.16	82.0	
12:05 to 12:08 p. m.	†67.3	1.16	23.7	1.16	46.8	1.16	63.7	†1.16	82.2	

TABLE 1.—*Filter transmissions of integrated ultraviolet solar radiation, using titanium photoelectric cell, Ti–1*—Continued

1	2	3	4	5	6	7	8	9	10	11
Date, 1938, and time	Intensity	*Ba–8*		*Ba–1*		*Ni*		*Cz*		Remarks
		m	*Tr*	*m*	*Tr*	*m*	*Tr*	*m*	*Tr*	
September 12:	μa									
8:55 to 9:05 a. m.	†39.2	1.81	28.3	1.84	53.3	1.87	68.2	†1.89	84.1	
9:07 to 9:16 a. m.	*43.3	*1.71	27.8	1.73	52.5	1.75	67.5	1.78	83.8	
10:34 to 10:44 a. m.	†61.8	†1.31	24.9	1.32	48.5	1.33	64.8	1.30	82.6	
10:53 to 11:02 a. m.	*63.5	1.26	24.6	1.27	48.1	1.27	64.1	*1.28	82.4	
11:07 to 11:16 a. m.	†66.3	†1.23	24.2	1.24	47.7	1.25	63.7	1.25	82.3	
11:54 a. m. to 12:02 p. m.	*66.5	*1.17	23.6	1.17	46.8	1.18	62.8	1.18	82.1	
1:20 to 1:27 p. m.	†62.2	1.20	24.1	1.20	47.3	1.20	63.4	†1.20	82.3	
1:34 to 1:45 p. m.	*61.3	*1.24	24.6	1.23	47.8	1.22	63.9	1.21	82.5	
2:02 to 2:09 p. m.	†58.0	†1.29	25.2	1.28	48.7	1.28	64.2	1.27	82.7	
September 15:										
8:33 to 8:40 a. m.	*30.6	2.10	29.6	2.12	55.1	2.16	68.8	*2.21	84.4	
8:50 to 9:04 a. m.	†36.3	1.85	28.3	1.86	53.3	1.90	68.0	†1.92	83.9	
9:09 to 9:19 a. m.	*42.2	*1.71	27.4	1.74	52.1	1.76	67.4	1.78	83.4	
9:54 to 10:03 a. m.	†50.8	1.45	26.1	1.47	50.2	1.48	65.4	†1.49	83.1	
10:15 to 10:26 a. m.	*56.8	*1.37	25.3	1.38	49.2	1.39	64.7	1.40	82.4	
10:46 to 10:55 a. m.	†61.2	†1.29	24.4	1.29	47.8	1.30	64.4	1.31	82.6	
11:24 to 11:37 a. m.	*64.4	1.20	24.1	1.21	47.0	1.22	63.4	*1.23	82.2	
11:49 a. m. to 12:04 p. m.	†65.3	†1.16	23.7	1.17	46.7	1.18	63.0	1.18	82.3	
1:21 to 1:32 p. m.	*59.8	*1.22	24.0	1.21	47.1	1.21	63.1	1.20	82.3	
1:39 to 1:50 p. m.	†58.8	1.25	24.7	1.24	47.7	1.24	63.3	†1.23	82.2	
2:13 to 2:26 p. m.	*52.4	*1.34	25.2	1.33	48.4	1.31	64.2	1.30	82.4	
2:40 to 2:51 p. m.	†47.8	†1.42	26.0	1.40	49.6	1.39	64.8	1.38	82.3	
September 17:										
7:58 to 8:12 a. m.	*16.3	*3.02	34.4	2.84	57.7	2.70	71.3	2.60	85.1	
8:14 to 8:24 a. m.	†22.4	†2.52	32.4	2.48	57.3	2.44	70.2	2.38	84.3	
8:29 to 8:37 a. m.	*29.2	2.31	30.6	2.29	55.8	2.26	69.6	*2.24	84.2	
8:45 to 8:53 a. m.	†32.4	2.10	29.6	2.07	54.5	2.06	68.4	†2.02	83.8	
8:58 to 9:04 a. m.	*35.3	*1.97	28.8	1.95	53.6	1.92	67.8	1.90	83.7	
9:14 to 9:23 a. m.	†40.1	1.80	27.9	1.78	52.5	1.75	67.0	†1.72	83.3	
9:48 to 9:56 a. m.	*46.2	*1.52	26.7	1.53	50.7	1.54	66.2	1.55	82.9	
10:56 to 11:10 a. m.	†56.5	1.27	24.7	1.28	48.3	1.29	64.2	†1.30	82.3	
11:27 to 11:41 a. m.	*60.8	*1.22	24.2	1.23	47.3	1.23	63.5	1.24	82.2	

p=5.6 mm at 12:10 p. m. Sky cloudless; deep blue; small corona until 11:30 a. m. Hazy around sun at 11:55 a. m. Fine haze in zenith at 1:15 p. m. Thin cirrus haze SW of sun at 1:45 p. m.; formed into small fracto at 1:47 p. m. Sky murky around sun at 1:55 p. m.; clear at 2:05 p. m.

p=6.1 mm at 12:15 p. m. Sky cloudless; small corona; light breeze from ESE; fracto low on S horizon. In afternoon, corona wider; sky more hazy; long wisps of fracto SW and NW of sun at 2:50 p. m.

p=5.6 mm at 11:55 a. m. Sky cloudless, deep blue; small corona. Smoke from train at 9:56 a. m. Fracto-cumulus clouds begin forming on S. F. Peaks at 10 a. m.; spread E and W; cover 50 percent of sky at 11 a. m.

September 24:										
9:08 to 9:21 a. m.	†30.8	1.87	28.0	1.90	53.1	1.94	67.7	†1.98	83.8	p=5.2 mm at 10:50 a. m. Sky cloudless but murky; wide white corona at 9 a. m. Third series (10:28 to 38 a. m.) observed through thin clouds—showing nonselective absorption of ultraviolet.
10:14 to 10:20 a. m.	*44.5	*1.50	25.3	1.49	49.3	1.48	65.3	1.47	82.6	
10:28 to 10:38 a. m.	†47.5	†1.44	25.6	1.40	48.5					
September 25:										
8:40 to 8:50 a. m.	†28.3	2.21	29.8	2.24	55.3	2.29	69.0	†2.33	84.0	p=6.4 mm at 10:25 a. m. Sky cloudless, no smoke; small corona at 8:45 a. m. Sky murking rapidly in SW at 10:05 a. m. Thin fracto-cirrus around sun, and cumulus rising in SW at 10:15 a. m.
8:56 to 9:06 a. m.	*35.0	2.03	28.6	2.06	53.6	2.10	68.2	2.14	83.8	
9:23 to 9:30 a. m.	†40.6	†1.78	27.1	1.80	51.8	1.82	66.8	1.85	83.3	
10:03 to 10:12 a. m.	*47.5	*1.52	25.9	1.53	50.2	1.55	65.3	1.57	83.1	
October 3:	μa									
9:34 to 10:06 a. m.	†38.5	1.65	26.9	1.67	51.0	1.74	66.5	†1.89	83.3	p=5.1 mm at 12:50 p. m. Sky cloudless; small corona; SE breeze at start. Third series (11:30 a. m.) observed through thin, billowy cirrus clouds. Thin haze over sun at 1:09 p. m. (*Ba-3*). Cloudy p. m.
10:10 to 10:26 a. m.	*51.7	*1.54	26.1	1.56	50.3	1.57	65.4	1.62	82.8	
11:28 to 11:38 a. m.	†56.6	†1.33	25.1	1.34	48.5	1.34	64.3	1.35	82.6	
1:01 to 1:09 p. m.	*55.8	1.30	25.3	1.30	48.8	1.30	64.3	*1.30	82.2	
1:27 to 1:34 p. m.	†53.0	†1.33	25.7	1.33	48.8	1.32	64.4	1.32	82.3	
October 5:										
8:23 to 8:35 a.m.	†23.5	†3.05	34.3	2.90	58.3	2.85	70.4	2.80	84.5	
8:37 a.m.	*28.0	*2.75	32.0							
8:43 to 8:53 a.m.	†33.2	†2.48	31.0	2.52	56.6	2.58	69.8	2.62	84.2	
9:03 to 9:12 a.m.	*38.3	*2.16	29.7	2.20	54.8	2.24	68.7	2.27	83.8	
9:29 to 9:37 a.m.	†43.8	†1.94	28.3	1.92	52.8	1.90	67.3	1.96	83.7	
9:51 to 10:01 a.m.	*48.6	1.72	27.8	1.73	51.8	1.76	66.9	*1.78	83.4	p=3.7 mm at 12:30 p.m.
10:11 to 10:21 a.m.	†54.3	†1.59	27.2	1.62	51.3	1.63	66.2	1.64	82.8	p=3.9 mm at 3:25 p.m.
10:40 to 10:51 a.m.	*57.7	*1.46	26.5	1.47	50.3	1.49	65.6	1.50	82.7	Sky cloudless; deep blue; small corona. High, gusty wind from SW. Small fracto north of S. F. Peaks and The Elden at 11:45 a.m.
10:58 to 11:10 a.m.	†59.2	†1.40	25.8	1.41	49.8	1.42	65.4	1.43	82.6	
11:27 to 11:37 a.m.	*60.4	*1.35	25.6	1.35	49.3	1.36	64.5	1.37	82.6	
11:46 to 11:58 a.m.	†61.5	1.32	25.3	1.33	49.2	1.34	64.3	†1.34	82.4	In p.m. corona appears wider. A small fracto appears, then disappears near sun at 2:07 p.m. Clouds low on horizon NW. of S. F. Peaks after 1 p.m. Less wind; sky whiter in p.m.
12:05 to 12:14 p.m.	*63.8	*1.31	25.3	1.31	48.8	1.32	64.5	1.32	82.7	
1:05 to 1:14 p.m.	†61.8	1.32	25.4	1.32	48.8	1.32	64.3	†1.31	82.3	
1:21 to 1:32 p.m.	*57.2	*1.34	25.8	1.34	49.3	1.33	64.9	1.33	82.5	
1:37 to 1:47 p. m.	†54.7	†1.37	25.8	1.36	49.8	1.36	64.8	1.35	82.7	
1:54 to 2:06 p.m.	*51.5	*1.41	26.4	1.40	50.1	1.39	65.3	1.38	83.0	
2:17 to 2:26 p.m.	†47.8	†1.47	27.4	1.46	51.3	1.44	65.9	1.43	82.8	
2:40 to 2:49 p.m.	*45.3	1.56	27.6	1.55	51.6	1.54	66.2	*1.53	82.9	
2:57 to 3:09 p.m.	†38.8	†1.65	28.7	1.64	53.1	1.63	67.1	1.61	83.4	

4. VARIATION IN ATMOSPHERIC TRANSMISSION OF ULTRAVIOLET SOLAR RADIATION WITH TURBULENCE IN THE OZONE LAYER

As already noted in the review of previous observations on the variation of the amount of atmospheric ozone with weather conditions, it is uncertain which is cause and which is effect [16]. Presumably the variations in the filter-transmission measurements made on September 5, and in the measurements of 1934 [8], were caused by turbulence in atmospheric ozone.

In connection with the question of convection and turbulence in the ozone layer, the most important and far-reaching results were obtained on October 5, when a barographic "low" was registered at 4 a. m.[4] and continued (excepting the usual slight rise to a maximum, between 10 to 11 a. m.) throughout the next 3 days.

In view of the unusual measurements obtained on this date, it is relevant to include a brief description of meteorological conditions on October 5. During all the preceding measurements, there had been but little wind; only light breezes from the south or southwest. On October 5 there was a strong, at times gusty, wind from the southwest (or SSW) during the greater part of the day. At the start (8:20 a. m.) and continuing until noon, the corona of scattered light around the sun was exceedingly small. By 1:30 p. m. the coronal scattering seemed wider, and by 2 p. m. the sky near the sun was conspicuously whiter. Small fracto clouds appeared in the east by 3 p. m., and the measurements were then terminated.

Evidently conditions in the stratosphere had been changing imperceptibly all day. This is shown by the filter transmissions. If it had been simply a question of the condition of the sky, as it appeared to the eye, then the filter transmissions on the afternoon of October 5 should have been below, instead of above, the average of the season.

At the start (8:20 a. m.), the filter transmissions were, for the same air mass, about the same as observed on October 3. But by 10:50 a. m. the transmissions had increased to the average, and by 3 p. m. the concentration of ozone had increased to such an extent that the filter transmissions greatly exceeded all values previously observed through that air mass ($m=1.65$).

In figure 4 the filter transmissions of October 5 indicated at 8:50 and 9:35 a. m. (MST) represent the values that would have been observed through an air mass, $m=1.55$ (at 10:30 a. m.) if, in the meantime, in each case, the amount of ozone had remained the same as at the time when the measurement was made (i. e., through air masses $m=2.5$ and $m=1.9$, respectively—see fig. 3). The point depicted at 2:46 p. m. was observed through an air mass $m=1.55$ (table 1). It shows the rapid increase in ozone in the same air mass since 10:30 a. m. The highest point, 52.5 percent, was observed at 3:05 p. m. (actual value, 53.1 percent; $m=1.64$). Incidentally, it is relevant to note (table 1) that the pressure of aqueous vapor (amount of precipitable water) was low and changed but little during these measurements.

[4] The diurnal variation in air pressure is much smaller in magnitude and the "low" occurs regularly at about 5:30 a. m. It is a mere coincidence that the cyclonic low happened to arrive about the same time.

In figure 5 is shown the change in transmission of the filter, *Ba–1*, with increase in the amount of ozone during the day. For comparative purposes the observed transmissions are reduced to the values that would have been observed through an air mass, $m=1.55$, as described in the second preceding paragraph.

In this illustration the barometer readings, "29.18 in.," etc., are the uncorrected values read from the barograph record. For comparative purposes the barograph record of September 24 is set to the same scale (29.18 in.) to show the somewhat larger increase in pressure that usually occurs during midday. The corrected pressures (29.85 and 30.0 in., respectively) for these dates may be read from figure 4. A significant part of this illustration is the observation that the change in barometric pressure preceded by some 5 to 6 hours the advection (or formation) of an appreciable amount of ozone above

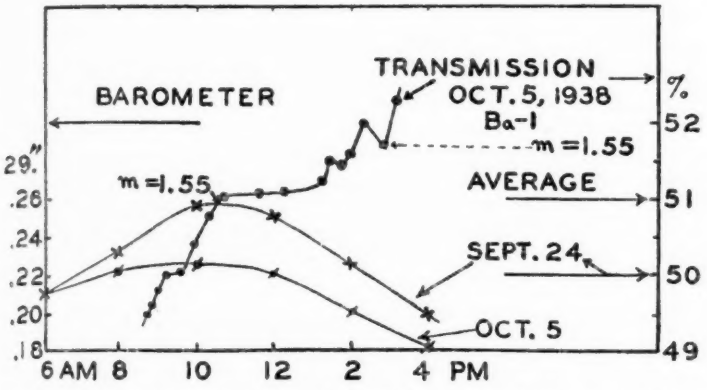

FIGURE 5.—*Change in transmission of ultraviolet solar radiation through the filter, Ba–1, caused by a change in atmospheric ozone, on October 5, 1938.*

the average that obtained during the preceding days of relatively high atmospheric pressure.

Another significant point in this illustration is the irregularity in the increase in the transmission of ultraviolet through the filter, showing that this influx (or formation) of ozone is irregular, turbulent; a phenomenon that should, no doubt, be expected. Whether the small increase in barometric pressure had a stabilizing effect in keeping the filter transmission uniform at the noon hour (see fig. 5) is an interesting question.

In conclusion, it may be noted that the observed change in filter transmission represents an increase of 8 to 10 percent in the amount of atmospheric ozone during the barometric low pressure of October 5, 1938.

Supplementing the above cited references [10 to 14], showing variations in the amount and distribution of ozone in the upper atmosphere, the foregoing measurements on the variation in transparency of the atmosphere with meteorological conditions supply additional evidence showing that such variations from day to day are to be expected.

5. AIR-MASS ANALYSIS OF OCTOBER 5, 1938

Since writing this paper, Edgar W. Woolard, Chief of the Division of Meteorological Research (U. S. Weather Bureau), has sent us an analysis of the weather maps for October 3 to 7, inclusive, prepared by the personnel of his Air Mass Section. His report dated January 19, 1939, is as follows:

Frontogenesis appears in Utah and Arizona on the 7:30 a. m., EST, map of October 5 due to cooler air flowing in from the northwest as indicated by the San Diego meteorograph ascent.

As this cool air passed over the warm surface of Arizona, Southern Utah, and New Mexico, it was heated rapidly at low levels wiping out the discontinuity between air masses over the great basin. However, this cooler air is still observed aloft on October 6, causing the steepened lapse rates at Cheyenne, Wyo.; Salt Lake City, Utah; and El Paso, Tex.

Another influx of colder air from the northwest (note temperature drop at San Diego, Calif.) created a new cold front on the morning of October 7 through Southern Utah and Arizona.

The weather map of October 5 accompanying Dr. Woolard's report is interesting in showing that the position of the cold front (*cP*+*mTk*; polar continental+tropical maritime—steep lapse rate, air cooler than surface) was over Flagstaff and Phoenix, Ariz., at 11:30 a. m. (MST), which, as shown in figure 5, is about the time that the influx of ozone began to stabilize, and maintain a fairly uniform concentration for the next 2 to 3 hours. Whether this has any significance can only be determined by repeated observations. The foregoing report is included for completeness of record of various phenomena involved in this investigation.

III. EXPLORATION OF THE VERTICAL DISTRIBUTION OF OZONE IN THE STRATOSPHERE

Under the present heading is given a description of the results obtained during June 1938 in measuring ultraviolet solar intensities and thereby in determining the vertical distribution of atmospheric ozone at various elevations above the earth's surface. The apparatus and methods used are essentially the same as previously employed [5, 6] but embody improvements that naturally develop as the result of the discovery of weak points that are found in the course of development of any new project. The chief improvements were in the radio-transmitting system [7], whereby it was possible to measure ultraviolet intensities to the height (25 to 27 km) attained by the transporting balloons; in contrast with last year's ascensions, when, as already stated, the ultraviolet-intensity measurements ceased at 19 km (64,000 ft.)

Briefly summarized, an ultraviolet-intensity meter, consisting of a photo-electric cell and filter radiometer, connected with an audio-frequency generator and radio transmitter, is transported aloft by means of unmanned balloons. The height attained by the balloons is indicated by a radio barograph. The radio signals giving the altitude of the apparatus and the ultraviolet intensities are received and recorded graphically at a ground station. In this paper only the improvements in apparatus and methods, with brief references to the previous paper, will be given.

1. DESCRIPTION OF THE RADIO-OPERATED ULTRAVIOLET-INTENSITY METER

An earlier model of the ultraviolet-intensity meter, consisting of a spherical-shaped photoelectric cell and filters which controlled a radio-wave transmitting device, was described in previous papers [5, 6]. Unfortunately, the interior coating, which constitutes the photo-sensitive surface of the cell, was not so uniform in response as in the cells used a year ago. Hence, to minimize this defect the window of the photoelectric cell was covered with two superposed fine-ground diffusing plates of Corex *A* glass (*Cx*, with a black paper window 17 mm in diameter; fig. 6) instead of one diffusing plate, as used a year ago. This produced a fairly uniform response curve for different angles of incidence, somewhat similar to the response curve shown in fig. 6 of the previous paper [6].

In figure 6 is shown a photograph of the assembled apparatus, housed in a balsa-wood box, open at the top and front to show the most important parts of the apparatus. The relaxation oscillator and radio transmitter occupy the rear half of this box.

The present ultraviolet filter apparatus differs from that used a year ago in that all four of the elliptical openings in the cardboard disk were covered; two of the openings being covered with glass filters (*F* in fig. 6), and the other two openings with thin perforated metal screens, *S*, the holes of which were drilled of a size to transmit approximately 30 and 50 (actually 27 and 48) percent, respectively, of the total incident solar radiation. These perforated metal screens (thickness 0.06 mm) served two important purposes: (a) being non-selective in transmission, the ratio of the intensities (scale readings on the electronic frequency meter) observed through these screens served as a check on the measurements with the glass filters; and (b) all the scale readings on the frequency meter and recorder being reduced to about the same size (fig. 8), it was possible to use a larger amplification of the scale readings at the ground level, and yet keep the recorder arm from going off the scale at the highest elevations (highest ultraviolet intensities), which occurred on one of the ascents in 1937, when the amplification of the scale reading was too high.

From the numerous details described in the previous report [6] it is relevant to note that the electric motors used in rotating the filters over the window of the photoelectric cell were of the same type as used in 1937.

Before making the ascents, each photoelectric cell outfit was calibrated against a standard of ultraviolet radiation [22]. As will be noticed later in this paper, with the much greater stability in this year's radio-transmitting device, the ultraviolet intensities, measured on different flights, are in much better agreement than obtained last year.

2. DESCRIPTION OF IMPROVEMENTS IN THE RADIO CIRCUIT OF THE PHOTOELECTRIC ULTRAVIOLET-INTENSITY METER

In a previous paper [6] brief mention was made of improvements in the photoelectric ultraviolet-intensity meter which, combined with the radio-operated barometer, is transported in unmanned balloons. As there stated, in the new instrument a stable electric circuit is obtained by amplifying the photoelectric current before it reaches the

relaxation oscillator. Furthermore, the sensitivity of the entire unit is automatically tested each time the barograph interrupts the ultraviolet signal to give an indication of the altitude.

The instrument shown diagrammatically in figure 7 and briefly described in detail elsewhere [7] virtually combines the balanced direct-current amplifier [1] (previously designed for precision work in the laboratory) with a relaxation oscillator and short-wave transmitter, similar to that developed by Diamond and his collaborators [3]. Wired in this manner, sufficient power and sensitivity are available for the relaxation oscillator to operate under normal circuit constants (voltages, resistances, capacitances) and, hence, in a condition of stable equilibrium.

For a given photoelectric cell the sensitivity of the instrument depends upon the circuit constants of both the relaxation oscillator and the direct-current amplifier. Referring to figure 7, in the relaxation oscillator, keeping the other constants of the circuit fixed, the sensitivity is inversely proportional to the capacitance of C_1. The value of R_1 determines the base frequency of the oscillator with no light on the photoelectric cell.

In the balanced amplifier, with the plate voltages and resistances adjusted for proper operation, the sensitivity is increased or decreased by a change in R_2.

In operation, as a small motor rotates the disk, *D* (fig. 7; see also fig. 6) carrying various filters over the photoelectric cell, the direct-current amplifier becomes unbalanced in a degree proportional to the intensity of the light incident on the cell. This unbalance in the plate circuit of the amplifier (also a part of the grid circuit of the relaxation oscillator *1A6*) causes an increase in the charging rate of the condenser, C_1, and, hence, the audio frequency of oscillation. Tests of the several instruments built and used in the 1938 flights gave frequency changes which were linear with variations in light intensity to within about 1 percent throughout the range of 50 to 200 c/s.

The potentiometer arrangement, *K*, (fig. 7) consisting of two type-*Z* Penlite cells, shunted by approximately 120,000 ohms, is connected with the barograph, *B*, which impresses fixed potentials on the grid of tube *T–1* each time the contact arm reaches one of the segments of the pressure switch (see also *PS* in fig. 6). This in turn causes an increase in audio-frequency oscillation indicative of the absolute sensitivity of the complete instrument (see *B*, *C*, or *D* in fig. 8). In practice, the contacts, *b* and *f*, (see fig. 7) are used as reference points of altitude only while the more numerous contacts, *c*, are used for both sensitivity calibration and altitude determination.

The aim has been to make the various units in this instrument small and light in weight and yet retain materials of sufficiently good quality to insure precision operation. Most of the resistor units are of the standard 0.5-watt type. The batteries are of minimum size sufficient to give about 3 to 4 hours of dependable operation. To give more reliable and stable operation of the direct-current amplifier, S. S. White or wire-wound resistors are used in the grid and plate circuits of this part of the instrument. This precaution is very important since a small change in these resistances may shift the audio-frequency base level (*G* in fig. 8) off the scale in either the positive or negative direction. A slight drift (usually downward) generally occurs during a flight. This is not a serious matter, however, so long as the drift is

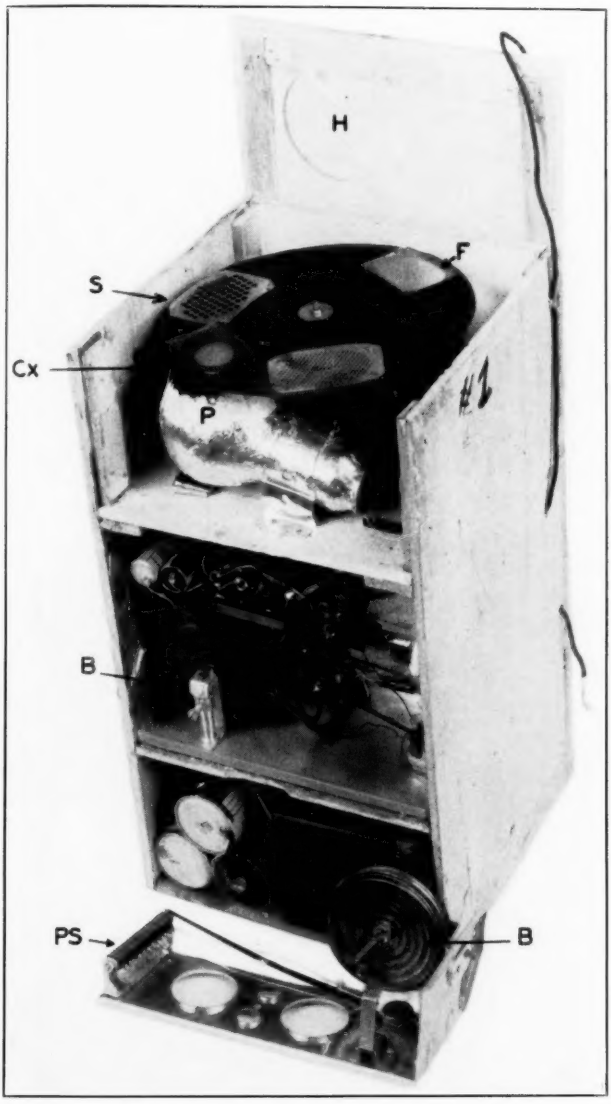

FIGURE 6.—*Assembled stratosphere ultraviolet-intensity meter, housed in balsa-wood box, open at the top and front, showing the photoelectric cell, P, covered with a diffusing window Cx; the two glass filters, F; the two perforated metal screens, S; the radio-barograph, B, and pressure switching device, PS; the cover with hole, H, that exposes the photoelectric cell to the sun; and part of the radio accessories.*

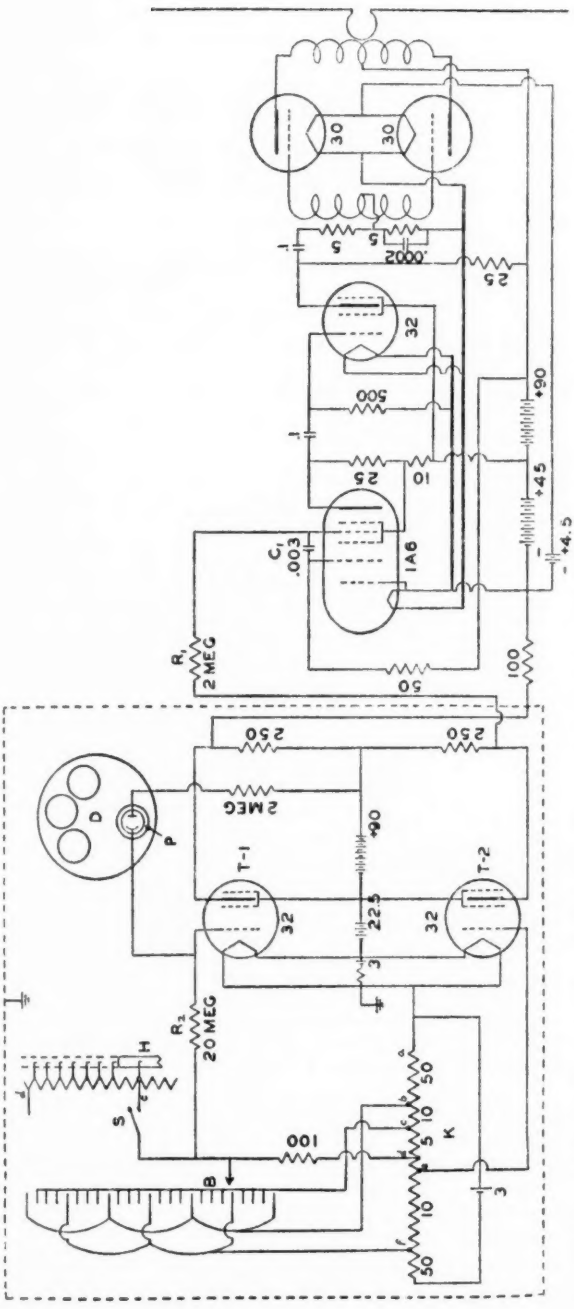

FIGURE 7.—*Electric circuit of the photoelectrically controlled, P, audio-frequency generator, the amplifier circuit, and the radio-barograph circuit, B.*

not sufficient to reach the nonlinear portion of the scale (toward the lower frequencies) because the absolute sensitivity of the complete instrument (amplifier and relaxation oscillator) is checked each time a barograph contact is made.

3. DESCRIPTION OF A BALLOON-FLIGHT RECORD

In a previous paper [5, 6] a description was given of the ground-station receiving and graphically recording apparatus, consisting of a

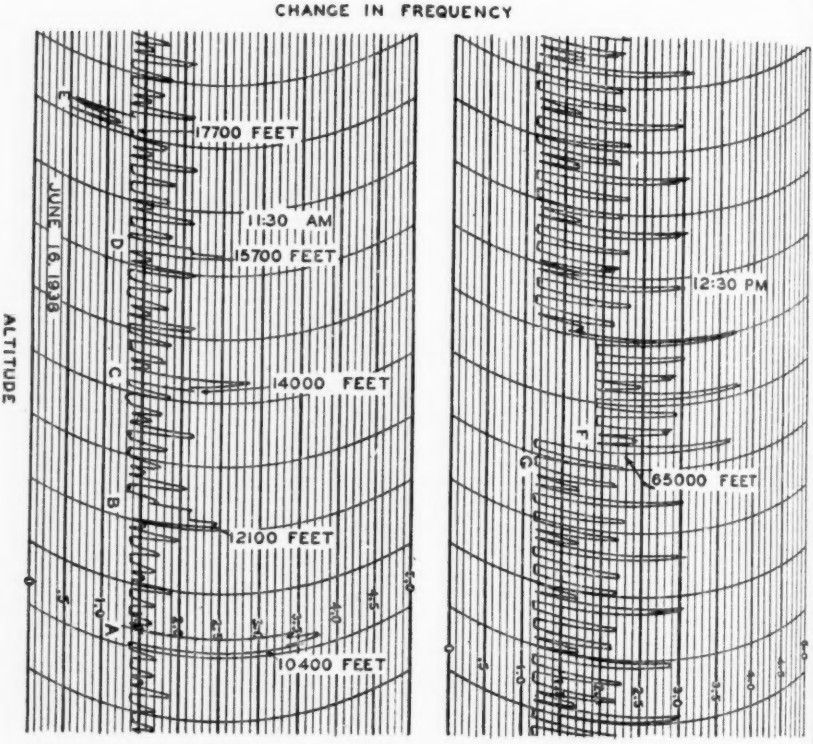

FIGURE 8.—*Reproduction of two parts of a graphic record of the ascension of a stratosphere ultraviolet-intensity meter, showing the change in frequency (ordinates) with change in intensity of ultraviolet radiation transmitted through the glass filters; also the audio-frequency signals, A, B, C, D, E, F, of the radio-barograph showing the method of identification of the different altitudes attained.*

super-regenerative receiving set, an electronic-frequency meter, an amplifier and electrical filter, and a recorder. To save time in the subsequent calculations, the values of the audio frequencies, emitted from aloft by the radio transmitter, were read directly on the dial of the electronic-frequency meter and written on the corresponding part of the graphic record shown in figure 8.

Referring to figure 6, it may be noted that, as the disk rotates, the large opaque spaces between the filter, *F*, and the two perforated metal screens, *S*, act as a shutter to exclude solar radiation from the photo-

electric cell; and the lowest audio frequencies recorded (between the lower horizontal lines marked 1.0 and 1.5, fig. 8) are reference frequencies, analogous to a graphic record of the scale reading of a galvanometer.

In one complete rotation of the disk there are recorded four deflections of the recorder arm, representing four ultraviolet intensities; two through the glass filters, *F*, and two through the perforated metal screens, *S*, shown in figure 6.

As noted in the previous paper [5, 6], with change in elevation, the arm of the radio-operated barometric-pressure apparatus crosses the metal contacts on the pressure switching element (*PS* in fig. 6) and an entirely different audio-frequency note is emitted, as indicated at the points *A*, *B*, *C*, etc., figure 8. As already noted, the direction and the magnitude of the audio-frequency indication on the recorder serve to identify the altitude attained in the flight [28].

(e) NOTES ON THE SIX FLIGHTS

The weight of the complete apparatus including the rubber shock cord was close to 5 lb (2.3 kg). In all the flights latex balloons model 750 (the average weight in grams), made by the Dewey & Almy Chemical Co., were used.

The apparatus was transported by three, four, or five balloons which were inflated with hydrogen to exert a total pull of about 10 lb, as determined with a small spring balance. When three balloons were used (each lifting 3 lb) the rubber was already under strong tension before ascension. When five balloons were used (each one inflated to lift about 2 lb; total pull, in quiet air, 11 lb) the rubber bags were not fully distended. Nevertheless, in each flight one or more of the balloons burst before reaching an elevation of 90,000 ft, showing that the heat and photochemical action of the (ultraviolet) solar rays, and presumably atmospheric ozone (and not the degree of distension of the rubber) were the cause of the failure of the balloons.

As regards the rate of ascent, it is relevant to record that this appears to depend on the total lifting force exerted, with little or no dependence upon the number of (i. e., interference by the) balloons. For example, in flights 1 and 2, using three and four balloons, respectively, and a lifting force to 9 to 10 lb, the rates of ascent were, respectively, 950 and 940 fpm. In flights 4 and 5, each using four balloons, and a total lifting force of 10 and 11 lb, respectively, the rate of ascent was 1,000 fpm. In flight 6, using five balloons and a total pull of 11 lb, the rate of ascent was 1,020 fpm. In this connection, it is of interest to note that in all of these ascents, when the balloons (tethered at different heights from a common meeting point [5, 6]) were released they moved outward, as the result of air streaming, and remained in that position in their flight. All the ascents were made at Beltsville, Md. Out of six flights there were four recoveries of apparatus, as compared with five recoveries out of six flights made in 1937.

Flight 1.—Unit No. 5. Transported aloft by means of three balloons. Ascent started at 11:12 a. m., EST, on June 16, 1938. Balloons drifted NNE, through thick clouds—no sun. Descent started at 1:05 p. m., last signal at 2:10 p. m. Apparatus was recovered at about 3:30 p. m., at Cambridge, Md., about 50 miles

southeast of the starting point. Finder reported that two balloons had burst. Maximum height attained was 82,700 ft.

Flight 2.—Unit No. 6. Transported by four balloons. Quiet ascent, drifting ESE. Sky covered with thin fracto-cirrus; a little sunlight through the clouds at the start. Ascent started at 10:29 a. m. on June 18. Descent started at 12:05 p. m.; last signal at 12:40 p. m.; no recovery of apparatus. Maximum height attained was 88,200 ft (26.5 km).

Flight 3.—Unit No. 4. Transported by four balloons. Sky lightly overcast at start; thick overcast a short while later. Quiet ascent SSW. Ascent started at 10:53 a. m., June 20. Apparatus visible to W. at 11:03 a. m. Noise after 11:18 a. m., altitude 26,000 ft. Radio silent after 11:27 a. m. No recovery.

Flight 4.—Unit No. 2. At the start there was sunshine through thick hazy sky; later fracto-cumulus clouds. Quiet, four-balloon ascent, drifting SSE. Ascent started at 10:47 a. m., June 23; good record to 50,000 ft. Radio off at 11:35 a. m., balloons still rising. Apparatus recovered at 3 p. m., two balloons still inflated, at Union Mills, Md., about 43 miles north of starting point.

Flight 5.—Unit No. 1. Sky turbid. Quiet, four-balloon ascent, drifting N, then NNE. Ascent started at 10:42 a. m., June 25; good record to top—close to 88,000 ft. Descent started at 12:30 p. m.; signals received until 2:05 p. m. Instruments recovered at 2:30 p. m. by a forest-fire lookout (stationed about 7 miles northeast of Manassas, Va.) who witnessed the two-balloon descent and recovered the instruments from the top of a tall tree. Maximum altitude attained was 87,300 ft.

Flight 6.—Unit No. 2. This was the second flight of this set of instruments, this time with five balloons. The ascent started at 10:51 a. m., June 30; and the descent, which began at 12:20 p. m., was followed till 2:05 p. m., when the signals became weak, although subsequently the sky was reported to have been "very clear" at that hour. The apparatus, with two balloons still inflated, landed at 3:30 p. m. in an orchard near Adelina, Md., about 40 miles southeast of the starting point. Maximum altitude attained was 86,000 ft.

In all these flights it is interesting to note that the place of landing of the apparatus was at relatively short distances from the starting point and in a region that usually was situated in an entirely different direction from that noted when the ascent was begun. In view of the interest in these flights, relative to radio fadeouts, the Radio Section of the National Bureau of Standards reported that no fadeouts occurred in the radio signals; except on June 30 when there was a fadeout at 10:04 a. m., lasting until 10:30 a. m. On this same day, between 12:44 p. m. and 12:58 p. m., a slight fadeout was noted at the Toronto, Canada, receiving station.

Aside from the decrease in intensity of our ultraviolet-intensity radio signals at 2 p. m., which was ascribed to clouds (although later inquiry elicited the information that the sky had been "very clear") there is nothing in our ultraviolet-intensity measurements that indicates a connection between the radio fadeout and the ozone distribution in the atmosphere.

4. EVALUATION OF THE ULTRAVIOLET-INTENSITY MEASUREMENTS

The evaluation of solar ultraviolet intensities in the stratosphere involves no assumptions. The calculations require a knowledge of (a) the spectral-response curves of the photoelectric cells (shown in fig. 3 of ref. [6]); (b) the spectral ultraviolet transmissions of the filters (practically the same as *LS* and *Ba–1* in fig. 3, ref. [6]), as employed in calculating data secured with our standard photoelectric-intensity meter at a ground station [21]; and (c) the spectral-absorption coefficient of ozone. Numerous determinations of the spectral-absorption

coefficients of ozone in the atmosphere (required in the hereindescribed measurements) are in close agreement with similar measurements on ozone prepared in the laboratory [23].

Another important factor that enters into our calculations is the shape of the solar spectral-energy curve, of wave lengths shorter than

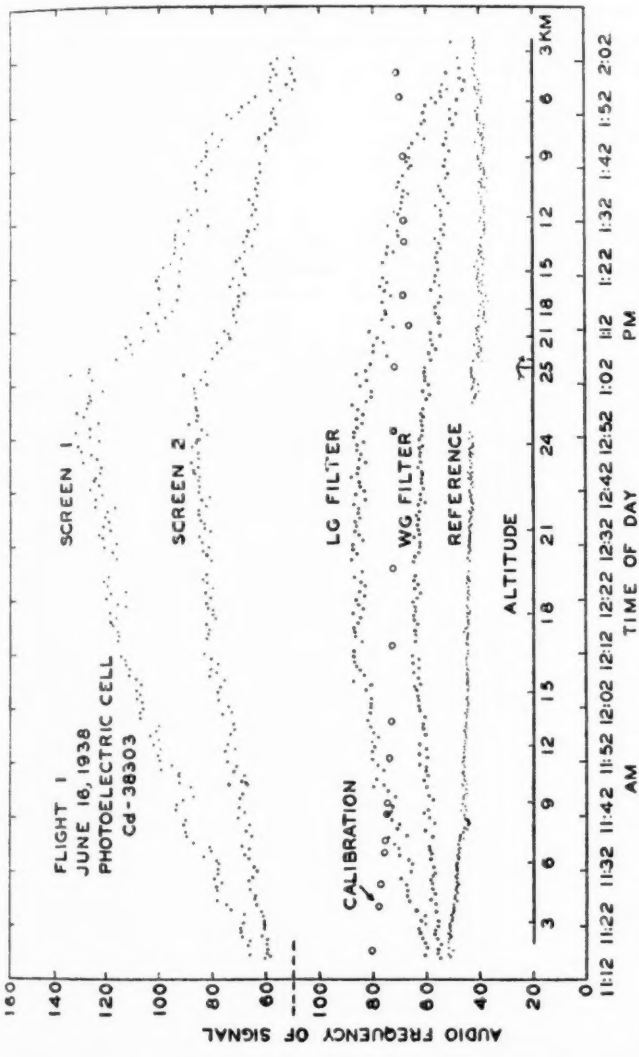

FIGURE 9.—*Variation in ultraviolet intensity (audio-frequency signal) with altitude above the earth's surface, measured through the two glass filters and the two perforated metal screens.*

Data taken from the complete graph, part of which is shown in figure 8.

about 3200 A, outside the earth's atmosphere. As shown in a previous paper [4], experimental data indicate that a calculation of the solar spectral-energy curve, using a black-body temperature of 6,000° K, is inadmissible. Our curve of the solar spectral-energy distribution outside the earth's atmosphere [4] obtained with filters at sea level is in qualitative agreement with Pettit's spectral-energy measurements

[24] obtained at an elevation of about 2,300 ft (760 m). We have, therefore, used Pettit's extra-terrestrial solar spectral-energy distribution in calculating the distribution of ozone in the stratosphere.

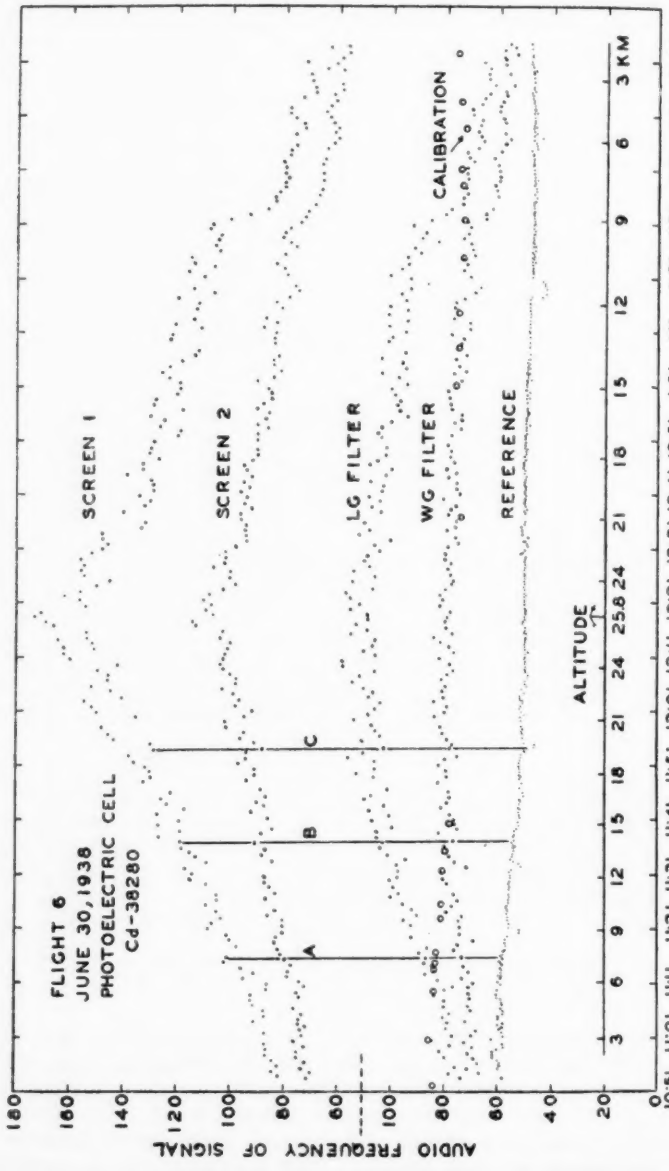

FIGURE 10.—*Variation in ultraviolet intensity (audio-frequency signal) with altitude above the earth's surface, observed in flight 6 (see fig. 9).*

In figures 9 and 10 the series of points represent the audio-frequency signals (the ultraviolet intensities) observed during the flights of June 16 and 30, 1938, respectively. These points are the maxima of the graphic record of the audio frequencies emitted by the photo-

electrically controlled radio transmitter, during ascent and descent, parts of which record are shown in figure 8.

The designations *LG* and *WG* (figs. 9 and 10) represent the trade names of the glass filters used. The vertical lines *A*, *B*, and *C* in figure 10 show the frequencies recorded in sequence of a single rotation of the disk. Some of the irregularities are caused by lack of uniformity in sensitivity of different parts of the photoelectric cell, which becomes apparent as the apparatus vibrates as a pendulum and rotates around the suspending cord. Another irregularity, which is eliminated in the calculations, is caused by a temporary drop in the reference frequency as depicted in line *C*, of figure 10, showing the importance of having a record of this part of the radio broadcast as well as the ultraviolet intensities through the filters and screens. For a further discussion of this question, reference is made to the preceding paper [6].

The data depicted in figures 9 and 10, and similar charts for the other flights were reduced by two methods: (a) By drawing a smooth curve through the observed points, and (b) by taking the arithmetical averages over intervals of 5 minutes (approximately 5,000-ft. changes in altitude). In spite of the apparently great irregularities in the observations, partly accounted for in the variation in the reference frequencies (see figs. 9 and 10) the calculated percentage transmissions of the glass filters (*WG* and *LG*) depicted in figure 11 do not depart from the smooth curves by a greater amount than is to be expected taking into consideration the various disturbing factors that enter into an ascent, and especially in the descent of the apparatus. In fact, the observations of flight 1, depicted in figure 11, compare favorably with measurements made in the laboratory, and demonstrate very clearly what may be expected when a better grade of photoelectric cell can be produced—the *Cd*-cell used in flight 1 was the best of the lot used in this year's flights.

In figure 11 the percentage transmission of the filter, *WG* (and *LG*) is the height of the ordinate of a point on the line *A*, in figure 10 above the reference frequency, divided by the height of the ordinate I_0 similarly deduced from the frequency scale for either screen 1 or screen 2. In figure 11 the transmission of each filter (*WG* and *LG*) at a given elevation is the average of two calculations, using the readings of the two screens, 1 and 2.

Although all the steel plates had been assembled in two piles and each hole drilled through all, the transmissions of the finished screens differed from the average by about 1 percent, which was about 27 and 48 percent for screen 2 and screen 1, respectively. In the calculations for each flight, the actual transmission values of the screens (e. g., in flight 6; tr=26.4 and 48.4, respectively) were used in deducing the transmissions.

Since the photoelectric cell is selective in response, in the evaluation of ultraviolet data it is necessary to incorporate two important factors, designated *P* and *G* [6].

The factor *P* depends upon the kind (the spectral response) of photoelectric cell and the constants of the relaxation oscillator. In practice it is equivalent to a standardization of the scale reading of the frequency meter in terms of radiation in microwatts per square centimeter, by exposure of each stratosphere ultraviolet solar-intensity meter to a standard of ultraviolet radiation [22].

The factor G is used in evaluating the ultraviolet in solar radiation of wavelengths shorter than 3132 A, relative to the total range of wavelengths intercepted by the photoelectric cell, and, hence, must be determined for each cell [21].

The observations must be corrected for solar height (angle of incidence on the photoelectric cell). The data in solar ultraviolet in-

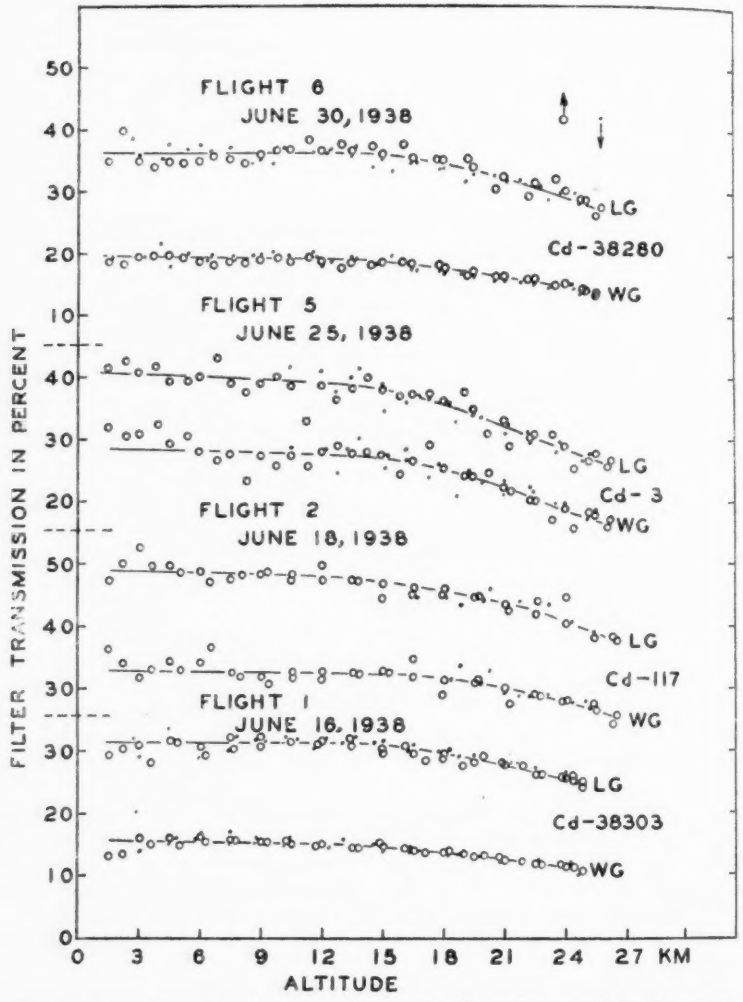

FIGURE 11.—*Percentage transmission of the glass filters used in the various stratosphere flights.*

The data were calculated by two methods as described in the text, based upon direct measurements, some of which are depicted in figures 9 and 10.

tensities are therefore reduced to an air mass, $m=1.04$. This correction is small, because only at the beginning of the flights was the solar height lower than the equivalent of $m=1.06$. For a more

complete discussion of the various operations in reducing the data, the reader is referred to the preceding paper [6].

(a) VARIATION IN INTENSITY OF ULTRAVIOLET SOLAR RADIATION WITH ALTITUDE ABOVE THE EARTH'S SURFACE

Owing to clouds and possible disturbances from air currents in the lower atmosphere no attempt is made to accurately coordinate the data for elevations below about 9 km.

By means of the measurements obtained with screens 1 and 2, as depicted in figure 10, corrected for transmission, total ultraviolet solar intensities are obtained. To these values must be applied a factor G to obtain the proportional part of wave lengths shorter than 3132 A. The factor G was determined for every 5,000-ft. (1.5 km) elevation; requiring a spectral-energy curve representing the filter transmissions at that particular altitude [21].

In figure 12 is given the intensity of ultraviolet solar radiation of wave lengths shorter than 3132 A, at various elevations above sea level, observed on the four flights that attained high elevations. Each point is the average of 5 readings for each screen, or a total of 10 readings.

It is to be noted that beginning at an elevation of about 15 km there is a change in the trend of the ultraviolet intensities, indicating the region (tropopause) where the apparatus is entering into the region of rapidly increasing concentration of ozone. Above this point there is a marked change in trend to higher intensities as the apparatus penetrates, more and more, through the ozone layer. The high values in the region of 3 to 9 km are partly owing to scattered ultraviolet radiation from the sky and clouds, which, as already noted on a preceding page, amounts to some 25 percent of the total, in the clearest sky, at an elevation of 2.2 km (Flagstaff, Ariz.). The low values at 3 to 6 km for flight 2 are owing to clouds, as described on a preceding page.

In figures 11 and 12, the arrows above the symbols associated with the flights on different days indicate the direction of movement (ascent or descent) of the apparatus.

At the highest altitudes attained, 27 km, the intensity of ultraviolet solar radiation of wave lengths shorter than 3132 A is about 900 $\mu w/cm^2$. But even at this elevation, as will be shown presently, some 35 percent of the ozone remained above the apparatus. Extrapolated to a point outside the ozone layer this would indicate an intensity of about 1,500 $\mu w/cm^2$, or more than 2½ times the value previously deduced [21] by extrapolation of measurements made at the earth's surface. One reason for this discrepancy is the fact that in the earlier extrapolation (as in the present one) the calculations do not take account of (do not include) wave lengths shorter than 2900 A which are observed at high altitudes, but do not occur in the measurements at low elevations, which form the basis for the extrapolation.

(b) CALCULATION OF THE AMOUNT OF OZONE TRAVERSED

In order to obtain an estimate of the amount of ozone traversed at a given height above the earth's surface it is necessary to correct the observed filter transmissions (fig. 11) for molecular (Rayleigh) scattering [6]. Then by means of the spectral-absorption coefficients of ozone [23] the effect of change in ozone thickness upon the

filter transmission is calculated in the manner outlined on p. 210–212 of the previous paper [6]; the only difference being in the use of an ultraviolet solar spectral-energy curve for each height, instead of the average spectral-energy curve given in column 2 of table 2 of the previous paper [6]. Based upon the above outlined method of calculating the amount of ozone traversed, with elevation of the radiometric apparatus, the curves depicted in figure 13 are obtained. It is to be noted that each point is the average calculated from the transmission measurements of two filters, instead of one filter used in calculating the observations of 1937.

An inspection of the curves in figure 13 shows that at a height of 18 km (60,000 ft) the amount of ozone traversed ranged from 0.024

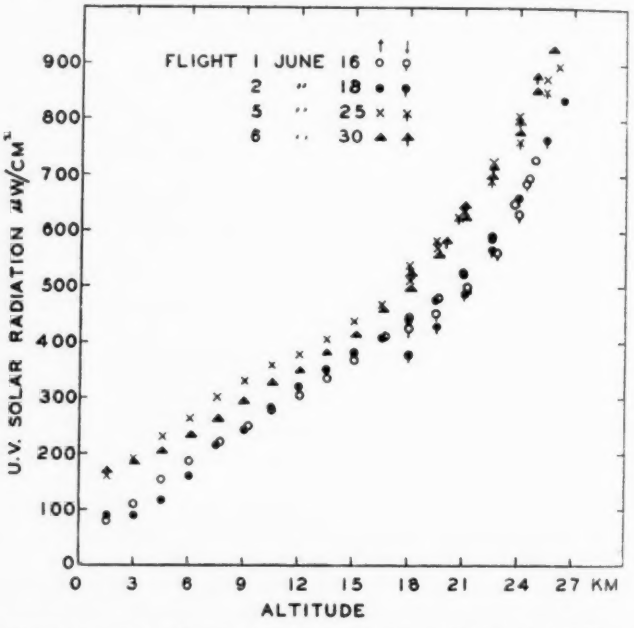

FIGURE 12.—*Integrated ultraviolet solar and sky radiation intensities, of wave lengths shorter than 3132 A at various altitudes above the earth's surface.*

to 0.035 cm, or an average of 0.03 cm for the four flights that attained that altitude. Roughly, this amounts to 15 percent of the superposed ozone.

In the two flights of 1937, the amounts of ozone penetrated at 18 km were 0.04 and 0.08 cm, respectively, as deduced by one method of calculation and 0.025 and 0.05 cm by another method of calculation. Considering the crudeness of the instruments and methods employed in 1937, as compared with the much higher precision attained in the flights of 1938, the data are in good agreement in showing that below the 18-km level there is a substantial amount of ozone relative to the total in the stratosphere.

In figure 13 the heavy black curve shows the average of all the flights of 1938. Flight 4 attained a height of only 15 km (50,000 ft), and in

this range the amount of ozone traversed happens to coincide with the average of all the flights.

It is to be noted in figure 13 that the total amount of atmospheric ozone above the instrument, at sea level, on different dates ranges from about 0.19 to 0.25 cm (flights 6 and 1) with an average of 0.22 cm. This is in good agreement with the average seasonal value for this latitude [12]. Such variations from day to day are to be expected, but in this series of measurements the precision attained is not sufficient to show a definite correlation of the amount of ozone with surface air pressure, such as described in section II of this paper. Calculations (and fig. 13) show that at an elevation of 27 km (90,000 ft) the radiometric apparatus had traversed about 65 percent of the ozone layer.

In figure 13 the dotted curve NGS shows the part of the ozone layer traversed by the manned balloon (*Explorer II*) in November 1935 [2] also Regener's [25] curve of the flight with unmanned balloons in July 1934. In both cases, the data were obtained photographically with a quartz spectograph. Regener's calculations are based upon a hypothetical solar spectral-energy curve at a black-body temperature of 6,000° K and an assumed ozone content of 0.28 cm (ntp), which is the average value for that season in the latitude where the ascents were made.

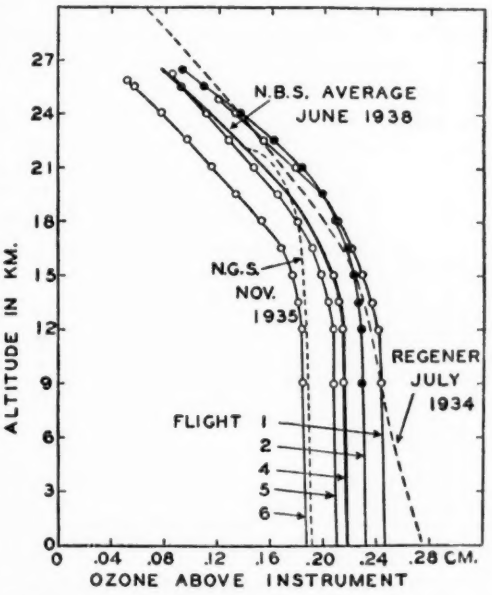

FIGURE 13.—*Graphs showing the amount of ozone above the ultraviolet-intensity meter, at various heights above the earth's surface, observed in the flights of 1938.*

Dotted curves show Regener's observations in 1934, and the National Geographic Society (NGS) measurements of November 1935.

In Regener's flights of June 26, July 7, and 31, 1934, respectively, heights of 20, 30, and 31 km were attained. At a height of 30 km, exposures of 10 minutes registered wave lengths slightly longer than 2863 A, and 70 percent of the ozone layer was below the apparatus. This is in substantial agreement with our measurements, taking into consideration the total amount of ozone present on a particular date and assuming no turbulence of the type recorded in section II of this paper.

In concluding this part of the presentation of data on the calculation of the amount of ozone in the stratosphere, it is relevant to compare the method of attack by different observers, particularly in the use of the solar spectral-energy curve, of short wave lengths, outside the earth's atmosphere.

As noted elsewhere [4], for wave lengths shorter than about 3200 A, calculations using a black-body temperature of 6,000° K are entirely in disagreement with the experimentally determined spectral-energy curve [29]. However, in the spectral region of 3200 to 3500 A the observed solar spectral-energy distribution [24] has approximately the same slope as that of a black body at 6,000° K. Since the ultraviolet intensities in this part of the spectrum greatly exceed those in the region of 2900 to 3200 A, rough calculations indicate that the use of a black-body energy curve at 6,000° K would have no marked effect upon the curves depicted in figure 13.

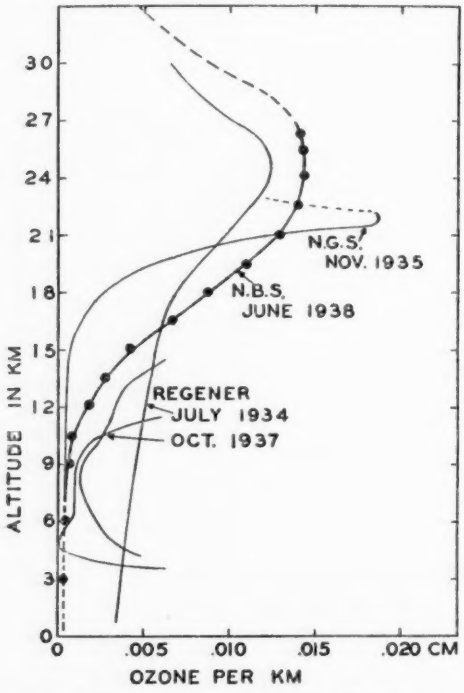

FIGURE 14.—*Graphs showing the distribution of ozone at various elevations above the earth's surface.*

(c) VERTICAL DISTRIBUTION OF OZONE IN THE ATMOSPHERE

Differentiation of the curve (fig. 13) of average values of ozone at different heights above the ultraviolet meter gives the amount of ozone per kilometer (O_3/km) at different elevations above the earth's surface. This is shown in the heavy curve, NBS June 1938, in figure 14. The upper, dotted part of this curve shows the distribution required to account for the 35 percent of the ozone above the apparatus, at an elevation of 27 km above sea level.

Owing to clouds and presumably other effects upon the filter transmissions, at low elevations, no accuracy can be claimed for values below 6 km; but, as shown in figures 11 and 13, beginning at about 9 to 12 km (30,000 to 40,000 ft) there is a definite change in the slope of the observed curves, indicating an appreciable penetration into the ozone layer.

As shown in the heavy curve in figure 14, and as noted in the flights of 1937, at a height of 12 km the change in ozone concentration is rapidly increasing—about 0.002 cm/km.

At an elevation of 15 km the concentration amounted to about 0.005 cm/km, and in the region of maximum concentration (at about 25 km) the amount of ozone was about 0.015 cm/km.

The main portion of the ozone appears to be situated between 20 and 30 km, with a region of maximum concentration between 23 and 27 km, as previously observed by Götz at Arosa, Switzerland [18].

The sharply defined maximum concentration of ozone observed by O'Brien and his collaborators [2] (see fig. 14, curve NGS, November 1935) is entirely different from the results of other observers [18].

The earlier observations of Regener [25] (July 1934, in fig. 14) are in substantial agreement with the present explorations indicating a maximum concentration at a height of about 25 km. His recent measurements [26] (October and December 1937, in fig. 14) are in general agreement with others between 5 and 10 km elevation.

In view of the effect of convection and turbulence during great changes in atmospheric pressure, as described in Section II of this paper, it is a question whether anything more than a general agreement in the form of the vertical distribution of ozone in the atmosphere is to be expected.

Acknowledgment is made to the National Academy of Sciences for a grant from the Joseph Henry Fund, which was used in defraying part of the expense of this investigation.

IV. REFERENCES AND NOTES

[1] W. W. Coblentz and R. Stair, *A portable ultraviolet intensity meter, consisting of a balanced amplifier, photoelectric cell, and microammeter*, BS J. Research **12**, 231 (1934) RP647.

[2] The National Geographic Society-U. S. Army Air Corps Stratosphere Flight of 1935, in the Balloon *Explorer II*, Nat. Geographic Soc. Contrib. Tech. Papers, Stratosphere Series No. 2, Washington (1936).

[3] H. Diamond, W. S. Hinman, Jr., and F. W. Dunmore, Bul. Am. Meteorolog. Soc. **18**, 73 (1937); J. Aeronaut. Sci. **4**, 241 (1937); J. Research NBS **20**, 369 (1938) RP1082.
Development of a radio-meteorograph for measuring humidity, temperature, etc., at high elevations.

[4] W. W. Coblentz and R. Stair, *Distribution of energy in the extreme ultraviolet of the solar spectrum*, J. Research NBS **17**, 1 (1936) RP899.

[5] W. W. Coblentz and R. Stair, *A radiometric method of measuring ultraviolet solar-radiation intensities in the stratosphere*, Bul. Am. Meteorolog. Soc. **18**, 345 (1937); Radiologica **1**, 12 (1937).
A brief description of the methods used and a preliminary report of the results obtained in the stratosphere flights of 1937.

[6] R. Stair and W. W. Coblentz, *Radiometric measurements of ultraviolet solar intensities in the stratosphere*, J. Research NBS **20**, 185 (1938) RP1075.
Complete report of the results of the stratosphere flights of 1937.

[7] R. Stair, *A precision radio instrument for transmitting measurements of ultraviolet intensities from unmanned balloons to a ground station*, J. Research NBS **22**, 295 (1939) RP1181.

[8] W. W. Coblentz and R. Stair, *Factors affecting ultraviolet solar-radiation intensities*, J. Research NBS **15**, 123 (1935) RP816.
A study of the effect of fog, snow, sky, altitude, and geographic latitude upon ultraviolet solar radiation. See page 140 for a discussion of a low concentration of ozone.

[9] P. Harteck, *Schwankungen des Ozongehaltes der Atmosphere*, Naturwissenschaften **19**, 858 (1931).

[10] G. M. B. Dobson and A. R. Meetham, *Atmospheric ozone and meteorology*, Quart. J. Roy. Meteorolog. Soc. (London) **60**, 265 (1934).

[11] G. M. B. Dobson, D. N. Harrison, and J. Lawrence, *Measurements of the amount of ozone in the earth's atmosphere and its relation to other geophysical conditions, Part II*, Proc. Roy. Soc. London [A] **114**, 521 (1927); part III, **122**, 456 (1929).
A study of the distribution of ozone in cyclonic and anticyclonic areas.

[12] G. M. B. Dobson, *Measurements of th amount of ozone in the earth's atmosphere and its relation to other geophysical conditions*, part IV, Proc. Roy. Soc. London [A] **129**, 411 (1930). Appendix I, by H. H. Kimball, p. 418; appendix II, by E. Kidson, p. 421.
Data and graphs are given of the amount of ozone in the earth's atmosphere as a function of the latitude and the season of the year.

[13] R. Ladenburg, *Light absorption and distribution of ozone*, J. Opt. Soc. Am. **25**, 259 (1935).
A review of the subject.
[14] F. W. P. Goetz, *Seasonal variation in the amount of ozone at different latitudes*, Gerlands Beitr. Geophys. **31**, 119 (1931).
[15] K. O. Kiepenheuer, *Über sonnenstrahlung zwischen 2,000 und 3,000 A*, Z. Astrophys. **14**, 348 (1937).
[16] A. R. Meetham, *Correlation of the amount of ozone with other characteristics of the atmosphere*. Quart. J. Roy. Meteorolog. Soc. (London) **63**, 289 (1937).
[17] A. R. Meetham and G. M. B. Dobson, *The vertical distribution of atmospheric ozone in high latitudes*, Proc. Roy. Soc. London [A] **148**, 598 (1935).
[18] F. W. P. Goetz, *Die vertikale verteilung des atmosphärischen ozons*. Ergebn. Kosmischen Physik, **III**, 253–326, Leipzig, 1938.
An up-to-date summary of the researches on atmospheric ozone including 21 references to his own work, published since 1931. His survey of previous investigations on atmospheric ozone is published in the "Ergebnisse," **I**, 180–235 (Leipzig, 1931).
[19] F. W. P. Goetz and G. M. B. Dobson, *Observations of the height of the ozone in the upper atmosphere*, Proc. Roy. Soc. London [A] **120**, 251 (1928).
[20] D. Barbier, D. Chalonge, et E. Vassy, *Mesure de l'épaisseur réduite de l'ozone atmosphérique pendant l'hiver polaire*, Compt. rend. **201**, 787 (1935).
[21] W. W. Coblentz and R. Stair, *Evaluation of ultraviolet solar radiation of short wave lengths*. J. Research NBS **16**, 315 (1936) RP877.
[22] W. W. Coblentz and R. Stair. *A standard source of ultraviolet radiation for calibrating photoelectric dosage-intensity meters*, J. Research NBS **16**, 83 (1936) RP858.
[23] C. Fabry and H. Buisson, *Data on ozone absorption*, Compt. rend. **192**, 457 (1931).
Ny Tsi-Ze et Choong Shin-Piaw, Compt. rend. **195**, 309 (1932); **196**, 916 (1933).
F. W. Paul Goetz, Ergebn. Kosmischen Physik **3**, 253 (1938).
[24] E. Pettit, *Measurement of ultraviolet solar radiation*. Astrophys. J. **75**, 185 (1932); Pub. Astronom. Soc. Pacific **47**, No. 280 (December 1935).
[25] E. Regener and V. H. Regener, *Aufnahmen des ultravioletten sonnenspektrums in der stratosphere und vertikale ozonverteilung*. Physik. Z. **35**, 788 (1934).
[26] V. H. Regener, *Neue messungen der vertikalen verteilung des ozons in der atmosphäre*. Z. Physik **109**, 642 (1938).
[27] Arthur Adel, V. M. Slipher, and E. F. Baker. *The absorption of sunlight by the earth's atmosphere in the remote infrared region of the spectrum*, Phys. Rev. **47**, 580 (1935).
[28] Nat. Advisory Comm. for Aeronaut., Tech. Report 538 (1935). Altitude-pressure table based upon U. S. standard atmosphere.
[29] D. H. Menzel, J. G. Baker, and L. Goldberg, *Equivalent widths and temperature of the solar reversing layer*. Astrophys. J. **87**, 81 (1938).
They find that 4400° K best represents the mean effective excitation temperature of the reversing layer. The higher value (5700 to 6000° K) is a kinetic temperature. The two need not necessarily be the same.
[30] Preliminary studies of filter-transmission data, obtained at Washington, D. C., indicate that, instead of barometric pressure, more attention should be given to the movement of masses of polar air.

WASHINGTON, January 15, 1939.

U. S. DEPARTMENT OF COMMERCE NATIONAL BUREAU OF STANDARDS

RESEARCH PAPER RP1208

Part of Journal of Research of the National Bureau of Standards, Volume 22, May 1939

TORQUE BETWEEN CONCENTRIC SINGLE-LAYER COILS

By Chester Snow

ABSTRACT

This paper is concerned with several types of small correction terms which must be taken into account when computing the torque or the mutual inductance between two concentric single-layer helices. These are to be added to the formula previously developed for two current sheets. The seven types of corrections are those which may be foreseen from experience with other absolute electrical measurements. Many others will arise which cannot be anticipated at this time. The corrections (a) to (g) are given in section I.

CONTENTS

		Page
I.	Introduction	607
II.	Mutual inductance between two circular filaments, f_1 and f_2, whose axes intersect at an angle, θ	609
III.	Mutual inductance between a sheet and a filament	610
IV.	Mutual inductance between two turns of wire	611
V.	Mutual inductance of the coils	612
VI.	Torque including the first four corrections	614
VII.	Effect of errors in centering the coils	618
VIII.	Effect of axial components of current	618
IX.	Effect of lead-in wires	623
X.	Summary	625

I. INTRODUCTION

The mutual inductance, M, from which the torque is derived by differentiation with respect to the angle, θ, between their axis, consists principally of that between two equivalent current sheets. A formula for the latter is derived in Bureau Research Paper RP24, eq 32.[1] In applying it to the case of actual single-layer coils, formula 35, a factor $\cos \alpha_2$ was written in front of the series, which should have been $1/\cos \alpha_2$. With this correction, the formula may be put in the following form, where N_1 and N_2 are the total number of turns, l_1 and l_2 the lengths, a_1 and a_2 the radii, r_1 and r_2 the semidiagonals, and μ_1 and μ_2 are $\cos \alpha_1$, $\cos \alpha_2$, where α_1 and α_2 are the angles between the diagonals of the coils and their respective axes and $\mu = \cos \theta$.

$$M_{1,2}(l_1, a_1; l_2 a_2; \mu) = 4\pi \frac{N_1}{l_1} \pi a_2^2 N_2 \cdot \mu_1 \cdot \left\{ \mu - \left(\frac{1-\mu_1^2}{2} \right) \sum_{n=1}^{\infty} \left(\frac{r_2}{r_1} \right)^{2n} \cdot C_n(\mu_1) C_{n+1}(\mu_2) P_{2n+1}(\mu) \right\}, \quad (1)$$

[1] Chester Snow, *Mutual inductance and torque between two concentric solenoids*, BS J. Research **1**, 685 (1928) RP24.

where

$$C_n(\mu)=\frac{2P'_{2n}(\mu)}{2n(2n+1)\mu}=F\left(1-n,\ n+\frac{3}{2},\ 2;\ 1-\mu^2\right)$$

$$=\frac{-2(-1)^n\Gamma\left(n+\frac{1}{2}\right)}{\sqrt{\pi}}\frac{}{\Gamma(n+1)}F\left(1-n,\ n+\frac{3}{2},\ \frac{3}{2};\ \mu^2\right)$$

and

$P_n(\mu)$ is Legendre's polynomial and $P'_n(\mu)$ is $\frac{dP_n(\mu)}{d\mu}$. The subscript 1 refers to the outer current sheet, s_1, and subscript 2 to the inner sheet, s_2.

The small corrections to be found are:

(a) That which replaces the current sheet by a system of parallel, equally spaced turns of wire (instead of the tape windings with no

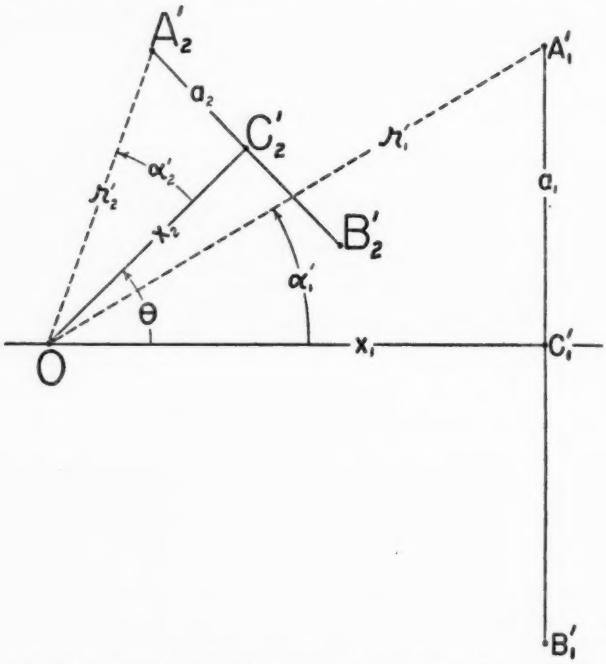

FIGURE 1.—*Section containing the intersecting axes of two circular filaments* $A'_1C'_1B'_1$ *and* $A'_2C'_2B'_2$.

radial thickness or insulating space between them which constitute a current sheet).

(b) The effect of the nature of the current distribution over the sections of the wire. Two cases are considered: Uniform distribution and the "natural" one which is inversely proportional to the distance from the axis of the solenoid.

(c) The effect of small variations, $u_{a_1}(x_1)$ [and $u_{a_2}(x_2)$], in the radii of the turns, which are observed functions of the distance, x_1 (and x_2), respectively, of the turn from the origin at the center of the coils.

(d) The effect of small variations in pitch, that is, of the small observed axial displacement, $u_x(x_1)$, (and $u_x(x_2)$) of the turn from the position corresponding to uniform spacing.

(e) The effect of errors in centering the coils.

(f) That due to the fact that the coils are helical and not a system of parallel turns of wire. This is the effect of the axial component of current.

(g) The contribution of lead-in wires.

II. MUTUAL INDUCTANCE BETWEEN TWO CIRCULAR FILAMENTS, f_1 AND f_2, WHOSE AXES INTERSECT AT AN ANGLE, θ

A section by a plane containing the intersecting axes is shown in figure 1. The trace of f_1 is $A_1'C_1'B_1'$ of f_2 is $A_2'C_2'B_2'$. Let

$$\left.\begin{aligned} &\overline{OA}_1'=r_1';\ \overline{OC}_1'=x_1=r_1'\cos\alpha_1';\ \overline{C_1'A}_1'=a_1=r_1'\sin\alpha_1' \\ &\overline{OA}_2'=r_2';\ \overline{OC}_2'=x_2=r_2'\cos\alpha_2';\ \overline{C_2'A}_2'=a_2=r_2'\sin\alpha_2' \\ &\mu_1'=\cos\alpha_1';\ \mu_2'=\cos\alpha_2'\ \mu=\cos\theta. \end{aligned}\right\} \tag{2}$$

If filament f_1 is any section of the larger current sheet, s_1, and filament f_2 of the inner sheet, s_2, which lies entirely within s_1 for any value of θ, then $r_2'<r_1'$. In this case the following series [2] has been shown to converge and to represent the mutual inductance, $M_{f_1f_2}$, of the two filaments when the angles α_1', α_2', and θ each lie in the range from zero to π, inclusive.

$$M_{f_1f_2}(x_1, a_1; x_2, a_2; \mu)$$

$$=4\pi^2\sum_{n=1}^{\infty}\left[\frac{(1-\mu_1'^2)P_n'(\mu_1')}{(r_1')^n}\right]\left[(r_2')^{n+1}(1-\mu_2'^2)P_n'(\mu_2')\right]\frac{P_n(\mu)}{n(n+1)} \tag{3}$$

It is readily found that the functions $V=(1-\mu^2)r^{-n}P_n'(\mu)$ and $V=r^{n+1}(1-\mu^2)P_n'(\mu)$ are solutions of the partial differential equation

$$\left(D_r^2+\frac{1-\mu^2}{r^2}D_\mu^2\right)V=0$$

that is,

$$\left(D_x^2+D_a^2-\frac{1}{a}D_a\right)V=0.$$

Hence, $M_{f_1f_2}$ satisfies the equation

$$\left(D_{x_1}^2+D_{a_1}^2-\frac{1}{a_1}D_{a_1}\right)M_{f_1f_2}=0 \tag{4a}$$

in the variables x_1 and a_1, and the similar equation

$$\left(D_{x_2}^2+D_{a_2}^2-\frac{1}{a_2}D_{a_2}\right)M_{f_1f_2}=0 \tag{4b}$$

in the variables x_2 and a_2, which are placed here for later reference.

[1] Chester Snow, *Mutual inductance of any two circles*, BS J. Research **1**, 531 (1928) RP18. (See eq 23, p. 539.)

III. MUTUAL INDUCTANCE BETWEEN A SHEET AND A FILAMENT

The mutual inductance of the two current sheets, $M_{s_1s_2}$, given in eq 1 was found by multiplying $M_{f_1f_2}$ by $\frac{N_1}{l_1}dx_1 \cdot \frac{N_2}{l_2}dx_2$ and integrating x_1 from $-l_1/2$ to $l_1/2$ and x_2 from $-l_2/2$ to $l_2/2$.

For the purpose of finding the corrections mentioned above, it is necessary to write down the results of each of these two integrations. The integration with respect to x_1 gives the mutual inductance between sheet s_1 and filament f_2, which may be called $M_{s_1f_2}(l_1, a_1; x_2, a_2; \mu)$, where

$$M_{s_1f_2}(l_1, a_1; x_2, a_2; \mu)=\frac{N_1}{l_1}\int_{-l_1/2}^{l_1/2} dx_1 M_{f_1f_2}(x_1, a_1; x_2, a_2; \mu),$$

or since by eq 2

$$dx_1=-a_1\frac{d\alpha_1'}{\sin^2\alpha_1'}=a_1\,[1-(\mu_1')^2]^{-\frac{1}{2}}\,d\mu_1'$$

$$M_{s_1f_2}=\frac{4\pi^2N_1a_1}{l_1}\sum_{n=1}^{\infty}\frac{P_n(\mu)}{n(n+1)}\left[\frac{(r_2')^{n+1}(1-\mu_2'^2)P_n'(\mu_2')}{a_1^n}\right]\cdot\int_{-\mu_1}^{\mu_1}(1-\mu^2)^{\frac{n-1}{2}}P_n'(\mu)d\mu.$$

Now

$$(1-\mu^2)^{\frac{n-1}{2}}P_n'(\mu)=-\frac{1}{(n-1)}\frac{d}{d\mu}\left[(1-\mu^2)^{\frac{n+1}{2}}P_{n-1}'(\mu)\right]$$

hence

$$\int_{-\mu_1}^{\mu_1}(1-\mu^2)^{\frac{n-1}{2}}P_n'(\mu)d\mu=0, \text{ if } n \text{ is even}$$

$$=2\mu_1, \text{ if } n=1$$

$$=\frac{-2(1-\mu_1^2)^{s+1}P_{2s}'(\mu_1)}{2s}, \text{ if } n=2s+1,$$

where s is a positive integer.

This gives

$$M_{s_1f_2}(l_1, a_1; x_2, a_2; \mu)=4\pi\frac{N_1}{l_1}\pi a_2^2\cdot$$

$$\cdot\left\{\mu\mu_1-2(1-\mu_1^2)\sum_{n=1}^{\infty}\frac{P_{2n}'(\mu_1)P_{2n+1}'(\mu_2')P_{2n+1}(\mu)}{2n(2n+1)(2n+2)}\left(\frac{r_2'}{r_1}\right)^{2n}\right\} \quad (5a)$$

The integration with respect to x_2 gives the mutual inductance between filament f_1 and current sheet s_2

$$dx_2=a_2\frac{d\mu_2'}{(1-\mu_2'^2)^{\frac{1}{2}}}$$

$$M_{f_1s_2}(x_1a_1; l_2a_2; \mu)=\frac{N_2}{l_2}\int_{-l_2/2}^{l_2/2}M_{f_1f_2}(x_1, a_1; x_2a_2; \mu)dx_2$$

$$=\frac{4\pi^2N_2a_2^2}{l_2}\sum_{n=1}^{\infty}\left[\frac{(1-\mu_1'^2)P_n'(\mu_1')}{(r_1')^n}\right]\frac{P_n(\mu)a_2^n}{n(n+1)}\int_{-\mu_2}^{\mu_2}(1-\mu^2)^{-\frac{n+2}{2}}P_n'(\mu)d\mu$$

Using the relation

$$(1-\mu^2)^{-\frac{n+2}{2}}P'_n(\mu)=\frac{1}{n+2}\frac{d}{d\mu}[(1-\mu^2)^{-\frac{n}{2}}P'_{n+1}(\mu)]$$

gives

$$\int_{-\mu}^{\mu}(1-\mu^2)^{-\frac{n+2}{2}}P'_n(\mu)d\mu=0, \text{ if } n \text{ is}$$

$$=\frac{2}{2s+3}(1-\mu_2^2)^{-s-\frac{1}{2}}P'_{2s+2}(\mu_2), \text{ if } n=2s+1,$$

where $s=0, 1, 2, 3 \ldots$

This gives

$$M_{f_1f_2}(x_1, a_1; l_2, a_2; \mu)=\frac{8\pi^2N_2a_2^2(1-\mu_1'^2)}{l_2}\cdot$$

$$\cdot\sum_{n=1}^{\infty}\frac{P'_{2n-1}(\mu_1')P'_{2n}(\mu_2)P_{2n-1}(\mu)}{(2n-1)2n(2n+1)}\left(\frac{r_2}{r_1'}\right)^{2n-1} \qquad (5b)$$

IV. MUTUAL INDUCTANCE BETWEEN TWO TURNS OF WIRE

Let $M_{f_2w_1}$ denote the mutual inductance between the filament, f_2 and a wire, w_1, whose section is symmetrical with respect to its center of gravity, $(x_1, \bar{a}_1)$, so that if $dS_1=dx_1'da_1'$ the integrals over the section of $(x_1'-x_1)$, $(x_1'-x_1)^3$, $(a_1'-\bar{a}_1)$, and $(a_1'-\bar{a}_1)^3$ are zero, as would be the case for squares or circles. If $\frac{\rho_1}{2}$ denotes the radius of gyration of this section, so that

$$\frac{\rho_1^2}{4}=\frac{1}{S_1}\int\int(x_1'-x_1)^2dS_1=\frac{1}{S_1}\int\int(a_1'-\bar{a}_1)^2dS_1$$

then, in the case of round wire, ρ_1 is just the radius of the wire.

The current density, i_1, with unit current in the turn, is such that

$$\int\int i_1dx_1'da_1'=\int\int i_1dS_1=1$$

and

$$M_{f_2w_1}(x_1, \bar{a}_1; x_2a_2; \mu)=\int\int M_{f_1f_2}(x_1', a_1'; x_2a_2; \mu)i_1dx_1'da_1'=\int\int M_{f_1f_2}i_1dS_1$$

If the ratio of any linear dimension of the wire section, S_1, to the mean radius, $\bar{a}_1$, of the turn is so small that terms of higher order than the third in this ratio are negligible compared to unity, then the "natural" distribution of current density (proportional to $1/a_1'$) may be written

$$i_1=\frac{1}{S_1}\left\{1-C_1\left(\frac{a_1'-\bar{a}_1}{\bar{a}_1}\right)+\frac{C_2}{\bar{a}_1^2}\left[(a_1'-\bar{a}_1)^2-\frac{\rho_1^2}{4}\right]-C_3\left(\frac{\bar{a}_1-a_1}{\bar{a}_1}\right)^3\right\},$$

where $C_1=C_2=C_3=1$. For the uniform distribution we place $C_1=C_2=C_3=0$. To the same precision, the expansion may be used

$$M_{f_1f_2}(x_1', a_1'; x_2, a_2; \mu)=\left[1+\phi+\frac{\phi^2}{2}+\frac{\phi^3}{6}\right]M_{f_1f_2}(x_1, \bar{a}_1; x_2, a_2; \mu),$$

where ϕ is the operator $(x'-x_1)D_{x_1}+(a_1'-\bar{a}_1)D_{\bar{a}_1}$.

Multiplying this by $i_1 dS_1$ and integrating gives

$$M_{f_1 w_1}=\left\{1+\frac{\rho_1^2}{8}\left(D_{x_1}^2+D_{\bar{a}_1}^2-\frac{2C_1}{\bar{a}_1}D_{\bar{a}_1}\right)\right\}M_{f_1 f_1}(x_1, \bar{a}_1; x_2, a_2; \mu)$$

or by eq 4a

$$M_{f_1 w_1}=\left\{1+\frac{\rho_1^2}{8\bar{a}_1}\cdot(1-2C_1)D_{\bar{a}_1}\right\}M_{f_1 f_1},$$

which may be written (since $C_1=0$ for uniform current and $C_1=1$ for the "natural" distribution) $M_{f_2 w_1}=\left(1\pm\frac{\rho_2^1}{8\bar{a}_1}D_{\bar{a}_1}\right)M_{f_1 f_2}$, the upper sign being used when the current distribution is uniform, the lower when it is the "natural" one. Hence the mutual inductance, $M_{w_1 w_2}$, between two wires is

$$M_{w_1 w_2}=M_{f_1 f_2}\pm\frac{1}{8}\left[\frac{\rho_1^2}{\bar{a}}D_{\bar{a}_1}+\frac{\rho_2^2}{\bar{a}_2}D_{\bar{a}_2}\right]M_{f_1 f_2} \tag{6a}$$

It is similarly found that the mutual inductance, $M_{t_1 t_2}$, between two tapes of radii $\bar{a}_1$ and $\bar{a}_2$, one extending from $x_1-\frac{l_1}{2N_1}$ to $x_1+\frac{l_1}{2N_1}$, the other from $x_2-\frac{l_2}{2N_2}$ to $x_2+\frac{l_2}{2N_2}$, is

$$M_{t_1 t_2}=M_{f_1 f_2}+\frac{1}{24}\left[\left(\frac{l_1}{N_1}\right)^2 D_{x_1}^2+\left(\frac{l_2}{N_2}\right)^2 D_{x_2}^2\right]M_{f_1 f_2}, \tag{6b}$$

so that eq 6a may be written

$$M_{w_1 w_2}=M_{t_1 t_2}\pm\frac{1}{8}\left(\frac{\rho_1^2}{\bar{a}_1}D_{\bar{a}_1}+\frac{\rho_2^2}{\bar{a}_2}D_{\bar{a}_2}\right)M_{f_1 f_2}-\frac{1}{24}\left[\frac{l_1^2}{N_1^2}D_{x_1}^2+\frac{l_2^2}{N_2^2}D_{x_2}^2\right]M_{f_1 f_2} \tag{6c}$$

If the wires are now given a small translation, $u_x(x)$, in the direction of their axis, and if their mean radius, $\bar{a}_t$, is given a small increase, $u_a(x_1)$, then if u_x^2 and u_a^2 are negligible, eq 6c becomes

$$M_{w_1 w_2}(x_1, \bar{a}_1; x_2, \bar{a}_2; \mu)=M_{t_1 t_2}(x_1, \bar{a}_1; x_2, \bar{a}_2; \mu)+$$

$$+\left\{\pm\frac{1}{8}\left(\frac{\rho_1^2}{\bar{a}_1}D_{\bar{a}_1}+\frac{\rho_2^2}{\bar{a}_2}D_{\bar{a}_2}\right)+u_x(x_1)D_{x_1}+u_a(x_1)D_{\bar{a}_1}+u_x(x_2)D_{x_2}+u_a(x_2)D_{\bar{a}_2}\right.$$

$$\left.-\frac{1}{24}\left(\frac{l_1^2}{N_1^2}D_{x_1}^2+\frac{l_2^2}{N_2^2}D_{x_2}^2\right)\right\}M_{f_1 f_2}(x_1, \bar{a}_1; x_2, \bar{a}_2; \mu) \tag{7}$$

V. MUTUAL INDUCTANCE OF THE COILS

This is obtained by multiplying eq. 7 by $\frac{N_1}{l_1}dx_1\cdot\frac{N_2}{l_2}dx_2$ and integrating x_1 from $-\frac{l_1}{2}$ to $\frac{l_1}{2}$ and x_2 from $-\frac{l_2}{2}$ to $\frac{l_2}{2}$. This integration, as

far as the principal term of eq. 7 is concerned, is exactly equivalent to a summation of all possible pairs of filaments, one of which is always in the first sheet, the other in the second. As to all other terms, it is permissible to replace the double summation by integrations, because they are small, the result holding in a macroscopic sense. It is thus found that

$$M=\left[1\pm\frac{1}{8}\left(\frac{\rho_1^2}{\bar{a}_1}D_{\bar{a}_1}+\frac{\rho_2^2}{\bar{a}_2}D_{\bar{a}_2}\right)\right]M_{s_1s_2}(l_1,\ \bar{a}_1;\ l_2,\ \bar{a}_2;\ \mu)$$

$$+\frac{N_1}{l_1}\int_{-l_1/2}^{l_1/2}[u_x(x_1)D_{x_1}+u_a(x_1)D_{\bar{a}_1}]\cdot M_{f_1s_2}(x_1\bar{a}_1;\ l_2,\ \bar{a}_2;\ \mu)dx_1$$

$$-\frac{l_1}{12N_1}[D_{x_1}M_{f_1s_2}]_{x_1=l_1/2}$$

$$+\frac{N_2}{l_2}\int_{-l_2/2}^{l_2/2}[u_x(x_2)D_{x_2}+u_a(x_2)D_{\bar{a}_2}]M_{f_2s_1}(l_1,\ \bar{a}_1;\ x_2,\ \bar{a}_2;\ \mu)dx_2$$

$$-\frac{l_2}{12N_2}[D_{x_2}M_{f_2s_1}]_{x_2=l_2/2} \quad (8)$$

Up to this point, terms of the order of magnitude of $\left(\frac{\rho_2}{\bar{a}_2}\right)^4$ have been neglected in comparison with unity. Thus if $\rho_2=0.05$ cm and $\bar{a}_2=5$ cm $\left(\frac{\rho_2}{\bar{a}_2}\right)^4=(10)^{-8}$. If we let $\Delta\bar{a}_2\equiv\frac{\rho_2^2}{8a_2}$, then $\frac{(\Delta\bar{a}_2)^2}{2}=3(10)^{-9}$, which is also negligible. Hence if the *effective radii*, a_1 and a_2, be defined by

$$a_i\equiv\bar{a}_i\left[1\pm\frac{1}{8}\left(\frac{\rho_i}{\bar{a}_i}\right)^2\right]\text{ for }i=1,\ 2, \quad (9)$$

then, since $f(a_i)=f(\bar{a}_i)+f'(\bar{a}_i)\cdot\Delta\bar{a}_i+f''(\bar{a}_i)\left(\frac{\Delta\bar{a}_i}{2}\right)^2$ it is evident that eq 8 may be written

$$M=M_{s_1s_2}(l_1,\ a_1;\ l_2,\ a_2;\ \mu)+\frac{N_1}{l_1}\int_{-l_1/2}^{l_1/2}[u_x(x_1)D_{x_1}+u_a(x_1)D_{a_1}]M_{f_1s_2}(x_1,\ a_1;\ l_2,$$

$$a_2;\ \mu)dx_1+\frac{N_2}{l_2}\int_{-l_2/2}^{l_2/2}[u_x(x_2)D_{x_2}+u_a(x_2)D_{a_2}]M_{s_1f_2}(l_1,\ a_1;\ x_2,\ a_2;\ \mu)dx_2-\frac{l_1}{12N_1}$$

$$[D_{x_1}M_{f_1s_2}]_{x_1=l_1/2}-\frac{l_2}{12N_2}[D_{x_2}M_{f_2s_1}]_{x_2=l_2/2} \quad (10)$$

Where by eq 5b one finds

$$-\frac{l_1}{12N_1}[D_{x_1}M_{f_1s_2}]_{x_1=l_1/2}=\left[\frac{4\pi N_1}{l_1}\pi a_2^2N_2\mu_1\right]\frac{(1-\mu_1^2)(1-\mu_2^2)l_1^2}{12a_2^2N_1^2}\cdot$$

$$\cdot\sum_{n=1}C_n(\mu_1)C_n(\mu_2)P_{2n-1}(\mu)n\left(n+\frac{1}{2}\right)\left(\frac{r_2}{r_1}\right)^{2n} \quad (10')$$

and by eq 5a

$$-\frac{l_2}{12N_2}[D_{x_2}M_{f_2s_1}]_{x_2=l_2/2}=\left[4\pi\frac{N_1}{l_1}\pi a_2^2N_2\mu_1\right]\frac{(1-\mu_1^2)(1-\mu_2^2)l_2^2}{12a_2^2N_2^2}\cdot$$

$$\cdot\sum_{n=1}^{\infty}C_n(\mu_1)C_n(\mu_2)P_{2n+1}(\mu)n\left(n+\frac{1}{2}\right)\left(\frac{r_2}{r_1}\right)^{2n}. \quad (10'')$$

VI. TORQUE INCLUDING THE FIRST FOUR CORRECTIONS

When the coils are at right angles to each other, $\mu=0$ and the torque is $T=(D_\mu M)_{\mu=0}$, so that

$$T=T_{s_1s_2}+\frac{N_1}{l_1}\int_{-l_1/2}^{l_1/2}[u_x(x_1)D_{x_1}+u_a(x_1)D_{a_1}]T_{f_1s_2}(x_1,\ a_1)dx_1$$

$$+\frac{N_2}{l_2}\int_{-l_2/2}^{l_2/2}[u_x(x_2)D_{x_2}+u_a(x_2)D_{a_2}]T_{s_1f_2}(x_2,\ a_2)dx_2, \quad (11)$$

where, by eq 1

$$T_{s_1s_2}=\left(4\pi\frac{N_1}{l_1}\right)\pi a_2^2N_2\mu_1(1+S+S_1) \quad (12)$$

$$S=(1-\mu_1^2)\sum_{n=1}^{\infty}(-1)^{n+1}\left(\frac{r_2}{r_1}\right)^{2n}C_n(\mu_1)C_{n+1}(\mu_2)\left(n+\frac{1}{2}\right)A_n, \quad (12')$$

where

$$A_n=\frac{\Gamma\left(n+\frac{1}{2}\right)}{\sqrt{\pi}\Gamma n+1}=\frac{1\cdot3\cdot5\cdot\ \ldots\ (2n-1)}{2\cdot4\cdot6\cdot\ \ldots\ 2n}$$

$$S_1=\frac{(1-\mu_1^2)(1-\mu_2^2)}{6a_2^2}\sum_{n=1}^{\infty}(-1)^{n+1}\left(\frac{r_2}{r_1}\right)^{2n}C_n(\mu_1)C_n(\mu_2)n\left(n+\frac{1}{2}\right)A_n\cdot$$

$$\left[n\frac{l_1^2}{N_1^2}-\left(n+\frac{1}{2}\right)\frac{l_2^2}{N_2^2}\right] \quad (12'')$$

Also, $T_{f_1s_2}(x_1,\ a_1)=(D_\mu M_{f_1s_2})_{\mu=0}$ is the torque exerted by filament f_1 at x_1 (with unit current) upon the current sheet s_2 (also carrying unit current).

$$\frac{N_1}{l_1}T_{f_1s_2}(x_1,\ a_1)=\left(4\pi\frac{N_1}{l_1}\pi a_2^2N_2\right)\cdot\frac{2(1-\mu_1'^2)}{l_2}\sum_{1}^{\infty}(-1)^{n+1}\left(\frac{r_2}{r_1'}\right)^{2n-1}$$

$$\cdot\frac{P'_{2n-1}(\mu_1')P'_{2n}(\mu_2)}{(2n-1)(2n+1)}\cdot A_n \quad (13)$$

Or, since $\mu_1'=\frac{x_1}{r_1'}$ and $r_1'=\sqrt{x_1^2+a_1^2}$ and

$$D_x\left[\frac{(1-\mu^2)P'_{2n-1}(\mu)}{r^{2n-1}(2n-1)}\right]=-\frac{(1-\mu^2)P'_{2n}(\mu)}{r^{2n}},$$

we find the following expressions by which $D_{x_1}T_{f_1s_2}$ and $D_{a_1}T_{f_1s_2}$ may be computed for use in the graphical or numerical evaluation of the integrals, in eq 11 when the variations u_x, and u_a are known.

$$\frac{N_1}{l_1}D_{x_1}T_{f_1s_2}=-\left(4\pi\frac{N_1}{l_1}\pi a_2^2N_2\right)\cdot\frac{2(1-\mu_1'^2)}{l_2r_2}\sum_1^\infty(-1)^{n+1}\left(\frac{r_2}{r_1'}\right)^{2n}$$

$$P'_{2n}(\mu_1')P'_{2n}(\mu_2)\frac{A_n}{2n+1}, \quad (13')$$

and since

$$D_a\left[\frac{(1-\mu^2)P'_{2n}(\mu)}{r^{2n-1}(2n-1)}\right]=\frac{\sqrt{1-\mu^2}2nP_{2n}(\mu)}{r^{2n}}=-D_x\left[\frac{\sqrt{1-\mu^2}P_{2n-1}(\mu)}{r^{2n-1}}\right]$$

$$\frac{N_1}{l_1}D_{a_1}T_{f_1s_2}=\left(4\pi\frac{N_1}{l_1}\pi a_2^2N_2\right)\cdot\frac{2\sqrt{1-\mu_1'^2}}{l_2r_2}\sum_1^\infty(-1)^{n+1}\left(\frac{r_2}{r_1}\right)^{2n}\cdot$$

$$P_{2n}(\mu_1')P'_{2n}(\mu_2)\cdot\frac{2n}{2n+1}A_n, \quad (13'')$$

which may also be written

$$\frac{N_1}{l_1}D_{a_1}T_{f_1s_2}=-\left(4\pi\frac{N_1}{l_1}\pi a_2^2N_2\right)\frac{2}{l_2}D_{x_1}\left\{\sqrt{1-\mu_1'^2}\sum_1^\infty(-1)^{n+1}\left(\frac{r_2}{r_1'}\right)^{2n-1}\cdot\right.$$

$$\left.P_{2n-1}(\mu_1')P'_{2n}(\mu_2)\frac{A_n}{2n+1}\right\} \quad (13''')$$

The torque exerted upon filament f_2 at x_2 by current sheet s_1 is $T_{s_1f_2}=(D_\mu M_{s_1f_2})_{\mu=0}$, so that

$$\frac{N_2}{l_2}T_{s_1f_2}(x_2,\,a_2)=\left(4\pi\frac{N_1}{l_1}\pi a_2^2N_2\right)\left\{\frac{\mu_1}{l_2}+\frac{2(1-\mu_1^2)}{l_2}\sum_1^\infty(-1)^{n+1}\left(\frac{r_2'}{r_1}\right)^{2n}\cdot\right.$$

$$\left.\frac{P'_{2n}(\mu_1)P'_{2n+1}(\mu_2')}{2n(2n+2)}\cdot A_n\right\}$$

$$=\left(4\pi\frac{N_1}{l_1}\pi N_2\right)\left\{\frac{\mu_1a_2^2}{l_2}+\frac{2(1-\mu_1^2)}{l_2}\sum_1^\infty(-1)^{n+1}\left[\frac{(r_2')^{2n+2}(1-\mu_2'^2)P'_{2n+1}(\mu_2')}{(2n+2)}\right]\cdot\right.$$

$$\left.\frac{P'_{2n}(\mu_1)A_n}{2nr_1^{2n}}\right\}, \quad (14)$$

where

$$\mu_2'=\frac{x_2}{r_2'} \text{ and } r_2'=\sqrt{x_2^2+a_2^2}$$

Since

$$D_r\left[\frac{r^{2n+2}(1-\mu^2)P'_{2n+1}(\mu)}{2n+2}\right]=(1-\mu^2)r^{2n+1}P'_{2n}(\mu),$$

it is found that

$$\frac{N_2}{l_2}D_{z_1}T_{z_1 f_2}=\left(\frac{4\pi N_1}{l_1}\pi a_2^2 N_2\right)\frac{2(1-\mu_1^2)}{l_2 r_1}\sum_1^\infty(-1)^{n+1}\left(\frac{r_2'}{r_1}\right)^{2n-1} P'_{2n}(\mu_1)P'_{2n}(\mu_2')\frac{A_n}{2n} \quad (14')$$

Also since

$$D_a\left[\frac{r^{2n+2}(1-\mu^2)P'_{2n+1}(\mu)}{2n+2}\right]=\sqrt{1-\mu^2}(2n+1)r^{2n+1}P_{2n}(\mu)$$

one finds

$$\frac{N_2}{l_2}D_{a_1}T_{z_1 f_2}=\left(\frac{4\pi N_1}{l_1}\pi a_2^2 N_2\right)\left\{\frac{2\mu_1}{l_2 a_2}+\frac{2(1-\mu_1^2)}{l_2 a_2}\sum_1^\infty(-1)^{n+1}\left(\frac{r_2'}{r_1}\right)^{2n}\cdot P'_{2n}(\mu_1)P'_{2n}(\mu_2')\frac{(2n+1)}{2n}A_n\right\} \quad (14'')$$

When the outer coil is relatively long, the inner lies in a region where the axial field of the outer has the practically uniform value $4\pi\frac{N_1}{l_1}$. The series S, eq 12′, is then very small and μ_1 is nearly 1 and the term S_1, eq 12″, still smaller. This will be the case if $l_1=100$ cm and $a_1=15$ cm, so that $\mu_1=0.9578$ and $1-\mu_1^2=0.0826$ and $r_1=52.44$ cm. If the inner coil has the radius $a_2=5$ cm and length $l_2=10$ cm, then $\mu_2=\frac{1}{\sqrt{2}}$ and $1-\mu_2^2=\frac{1}{2}$, while $r_2=7.07$ cm.

Since $r_1'\geqq a_1$ so that $\left(\frac{r_2}{r_1'}\right)^2<\left(\frac{r_2}{a_1}\right)^2=\frac{1}{4}$, it is seen that the series 13 will differ from the sum of the first two terms by less than 4 percent. The first two terms of eq 14 give a still better approximation.

To this approximation eq 13 and 14 become

$$\frac{N_1}{l_1}T_{f_1 z_2}=4\pi\frac{N_1}{l_1}\pi a_2^2 N_2\cdot\frac{a_1^2}{2(x_1^2+a_1^2)^{\frac{3}{2}}}\left\{1+\frac{3(l_2^2-3a_2^2)}{16a_1^2}\left[\frac{5}{\left(1+\frac{x_1^2}{a_1^2}\right)^2}-\frac{4}{1+\frac{x_1^2}{a_1^2}}\right]\right\} \quad (15)$$

and

$$\frac{N_2}{l_2}T_{z_1 f_2}=4\pi\frac{N_1}{l_1}\pi a_2^2 N_2\frac{\mu_1}{l_2}\left\{1+\frac{9(4x_2^2-a_2^2)a_1^2}{(l_1^2+4a_1^2)^2}\right\} \quad (16)$$

Since the small observed displacements, u_x, u_{a_1}, cannot be measured with a precision of more than 3 or 4 percent it is evident that the terms within the braces of eq 15 and 16 may be placed equal to unity so that a good approximation for eq 11 is

$$T=4\pi\frac{N_1}{l_1}\pi a_2^2 N_2\mu_1\left\{1+S+S_1+\frac{2}{l_2 a_2}\int_{-l_2/2}^{l_2/2}u_a(x_2)dx_2+\frac{a_1}{2\mu_1}\int_{-l_1/2}^{l_1/2}\left[u_x(x_1)D_{x_1}\frac{a_1}{(x_1^2+a_1^2)^{\frac{1}{2}}}-u_a(x_1)D_{x_1}\frac{x_1}{(x_1^2+a_1^2)^{\frac{1}{2}}}\right]dx_1\right\} \quad (17)$$

If $u_{a_1}(x_2)=\delta a_2=$ constant, $u_a(x_1)=\delta a_1=$ constant and $u_x(x_1)=\frac{\delta l_1}{l_1}\cdot x_1$, the

evaluation of these integrals gives

$$T=4\pi\frac{N_1}{l_1}\pi a_2^2N_2\mu_1\left\{1+S-\frac{l_1^2}{l_1^2+4a_1^2}\frac{\delta l_1}{l_1}-\frac{4a_1^2}{l_1^2+4a_1^2}\frac{\delta a_1}{a_1}+\frac{2\delta a_2}{a_2}\right\} \tag{18}$$

The displacement $u_x(x_1)=\frac{\delta l_1}{l_1}x_1$ corresponds to an increase in the length, l_1, without changing the total number, N_1, of turns, which amounts to increasing the pitch of the windings a constant amount. A similar displacement, $u_x(x_2)=\frac{\delta l_2}{l_2}x_2$, in the second coil would by eq 17 have contributed nothing to the second member of eq 18. The latter may be written

$$\frac{\delta T}{T}=-\frac{l_1^2}{l_1^2+4a_1^2}\frac{\delta l_1}{l_1}-\frac{4a_1^2}{l_1^2+4a_1^2}\frac{\delta a_1}{a_1}+0\frac{\delta l_2}{l_2}+2\frac{\delta a_2}{a_2} \tag{18'}$$

These variations would give by eq 12

$$\frac{\delta T_{s_1s_2}}{T_{s_1s_2}}=-\left[\frac{l_1^2}{l_1^2+4a_1^2}-\frac{l_1}{1+S}\frac{\partial S}{\partial l_1}\right]\frac{\delta l_1}{l_1}-\left[\frac{4a_1^2}{l_1^2+4a_1^2}-\frac{a_1}{1+S}\frac{\partial S}{\partial a_1}\right]\frac{\delta a_1}{a_1}$$
$$+\frac{l_2}{1+S}\frac{\partial S}{\partial l_2}\cdot\frac{\delta l_2}{l_2}+\left[2+\frac{a_2}{1+S}\frac{\partial S}{\partial a_2}\right]\frac{\delta a_2}{a_2} \tag{19}$$

A comparison of eq 18′ and 19 shows (since $\frac{\delta T_{s_1s_2}}{T_{s_1s_2}}$ is practically the same as $\frac{\delta T}{T}$) that the first approximation eq 17, which was derived by neglect of all but the first term in the brackets of eq 15 and 16, is compatible with the statement that S is so small that its variations may be neglected in computing the variations of δT caused by varying l_1, a_1, a_2, and l_2. If the more precise variation formula eq 19 were desired it could be found by retaining all the terms in eq 15 and 16. The cylindrical shell upon which the outer solenoid is wound may be slightly compressed by the tension of the wires so that the effective radius, $a_1(x)$, of the current sheet may be represented by the parabolic equation

$$a_1(x_1)=a_1(0)+\left[a_1\left(\pm\frac{l_1}{2}\right)-a_1(0)\right]\left(\frac{2x_1}{l_1}\right)^2. \tag{20}$$

The effective mean radius, a_1, of the equivalent sheet is then

$$a_1=\frac{2}{l_1}\int_0^{l_1/2}a_1(x_1)dx_1=\frac{2}{3}a_1(0)+\frac{1}{3}a_1\left(\pm\frac{l_1}{2}\right), \tag{21}$$

so that

$$u_a(x_1)=a_1(x_1)-a_1=-\left[a_1\left(\pm\frac{l_1}{2}\right)-a_1(0)\right]\left[\frac{1}{3}-\left(\frac{2x_1}{l_1}\right)^2\right]$$

and

$$\int_0^{l_1/2}u_a(x_1)dx_1=0.$$

Equation 17, then, gives the correction for this deformation in the form

$$\frac{\delta T}{T}=-\frac{4a_1\left[a_1\left(\pm\frac{l_1}{2}\right)-a_1(0)\right]}{l_1^2}\left\{1+\frac{1}{3\left[1+\left(\frac{2a_1}{l_1}\right)^2\right]}-\sqrt{1+\left(\frac{2a_1}{l_1}\right)^2}\cdot\log\left(\frac{l_1+\sqrt{l_1^2+4a^2}}{2a_1}\right)\right\} \quad (22)$$

In computing this small correction term, a_1 may be taken as the mean radius defined by eq 21, where $2a_1$ (x) is the over-all diameter of the coil at x_1 diminished by the diameter $2\rho_1$ of the wire. This was denoted previously (in section V) by $\bar{a}_1$, but there is no need to distinguish between a_1 and $\bar{a}_1$ in computing the small correction, eq 22. However, this correction is applicable only provided that the term μ_1 $(1+S)$ of eq 17 is computed using the "effective" or "electrical" mean radius, a_1, defined in eq 9 by $a_1=\bar{a}_1\left(1\pm\frac{\rho_1^2}{8a_1^2}\right)$ the upper sign being taken if we believe the current distribution is uniform over the section of the wires, the lower sign if it is the natural distribution.

The corrections (a) and (b) mentioned in the section I are represented by this choice of effective radii of the current sheets (eq 9). The corrections (c) and (d) are made by the integrals in eq 17.

VII. EFFECT OF ERRORS IN CENTERING THE COILS

The effect upon the torque of an error in centering the outer coil may be found by giving it a constant displacement in the direction of its axis. But if u_x (x_1)=constant the corresponding integral in eq 17 vanishes. Similarly, there is a negligible effect in giving the inner coil a constant displacement in its axial direction. Both of these results are aspects of the fact that the inner coil lies in a region where the field of the outer is practically uniform, so that for the same reason it is evident that the only other independent displacement of the inner coil would also be negligible. This is a displacment perpendicular to the plane of the two axes.

VIII. EFFECT OF AXIAL COMPONENTS OF CURRENT

Up to this point the current sheets have been assumed to have only the angular components of current whose surface density per unit length is N_t/l_t. Each coil is, however, a helix, so that there is an axial component of current whose surface density is $\pm 1/2\pi a$ per unit length, the positive sign being taken when the axial current is in the direction of increasing x_t (fig. 1). To see what modification this makes in the torque, we first see what modification must be made in the mutual inductance between the two sheets when their axes are inclined at an angle $\theta=\cos^{-1}\mu$. To do this we first modify the expression for the mutual inductance between filament No. 2 whose trace is $A_2'C_2'B_2'$ in figure 1 and filament No. 1 trace $A_1'C_1'B_1'$, remembering that these now have the additional axial components of current.

Let A° (xyz) be the *vector* potential at any point (xyz) which is due

to the angular component of current $\frac{N_1}{l_1}\,dx_1$ in No. 1 and let $A\,(xyz)$ be that due to the axial current $\pm\frac{dx_1}{2\pi a_1}$ in No. 1.

The angular component of current in filament No. 2 is $\frac{N_2}{l_2}\,dx_2$, its axial component is $\pm\frac{dx_2}{2\pi a_2}$. Hence the mutual electrokinetic energy between these filaments is

$$M.\ E.=\frac{N_2 dx_2}{l_2}\int ds_2[A^0_{s_2}+A_{s_2}]+\frac{dx_2}{2\pi a_2}\int[A^0_{n_2}+A_{n_2}]ds_2,$$

where the line integrals are taken around circle No. 2 (right handedly), A_{s_2} is the tangential component of the vector A and A_{n_2} its component normal to the plane of the circle. Only the last three terms need be considered here, since the first, $\int A^0_{s_2}ds_2$, leads to the mutual inductance, $M_{s_1s_2}$, already found. The second is a line integral of the tangential component of the vector A and by Stokes' theorem may be written $\frac{N_2dx_2}{l_2}\int\int H_{n_2}dS_2$, the integral being taken over the area of the circle No. 2, where H=curl A=magnetic vector due to the axial component of current in filament No. 1.

Since the vector A at any point is in the direction of the axis of circle No. 1 it is evident that $A_{n_2}=A_{x_1}\cos\theta=\mu A_{x_1}$, so that the fourth integral is $\pm\frac{dx_2}{2\pi a_2}\mu\int A_{x_1}ds_2$.

Hence the mutual energy is (omitting the first term)

$$M.\ E.=\frac{N_2}{l_2}dx_2\int\int H_{n_2}dS_2\pm\frac{dx_2}{2\pi a_2}\int A^0_{n_2}ds_2\pm\frac{dx_2}{2\pi a_2}\mu\int A_{x_1}ds_2 \qquad (23)$$

Now, if x, r, ϕ are cylindrical coordinates of any point, the axis being that of the circle 1, then A_{x_1} is a function of x and r only, r being the distance of the point from the axis. Since $H=$curl A, the cylindrical components of H are $H_x\equiv H_r\equiv 0$, $H_\phi=-D_rA_{x_1}(x,\,r)$.

Hence $\int\int H_n dS_2=0$, since the value of H_n has equal and opposite values at the two points in the area S_2, whose coordinates are x, r, ϕ, and x, r, $-\phi$. Similarly, the second integral of equation 23 vanishes, since the only nonvanishing cylindrical component of A^0 is A^0_ϕ, which is a function of x and r only. At two elements of arc of the circle No. 2, whose coordinates are x, r, ϕ, and x, r, $-\phi$, the values of $A^0_{s_2}$ cancel.

The expression 23 for the mutual energy then reduces to that between the two axial currents in the filament and may be written

$$m_{f_1f_2}dx_1dx_2=\pm\frac{\mu dx_2}{2\pi a_2}\int A_{x_1}ds_2 \qquad (24)$$

Since A_{x_1} at any point xyz is given by

$$A_{x_1}=\pm\frac{dx_1}{2\pi a_1}\int\frac{ds_1}{R}, \qquad (25)$$

where R is the distance from xyz to the line element ds_1 of circle 1, it is evident that the mutual inductance of the two unit axial currents in the filaments is

$$m_{f_1 f_2} = \pm \frac{\mu}{2\pi a_1 2\pi a_2} \int ds_2 \int \frac{ds_1}{R}, \tag{26}$$

where R is the distance from ds_1 to ds_2, the $+$ sign applying to the case where the axial currents have the same sign, the $-$ where their algebraic signs are different, positive axial current being in the direction of increasing x_1 or x_2, as shown in figure 1.

The double line integral in equation 26 without the factor $\pm\mu$ represents the mutual electrostatic energy of the two circular filaments when they are regarded as unit line charges of electricity.

The contribution of the axial components in the current sheets to their mutual inductance is therefore

$$m_{s_1 s_2}(\mu) = \int_{-l_2/2}^{l_2/2} dx_2 \int_{-l_1/2}^{l_1/2} dx_1 m_{f_1 f_2} \tag{27}$$

and the contribution to the torque is

$$t_{s_1 s_2} = [D_\mu m_{s_1 s_2}(\mu)]_{\mu=0} \tag{28}$$

To evaluate the integral $\frac{1}{2\pi a_2}\int A_{x_1} ds_2$, we note that A_{x_1} is a solution of Laplace's equation, which, in rectangular coordinates, is

$$(D_x^2 + D_y^2 + D_z^2) A_{x_1} = 0.$$

Expand A_{x_1} by Taylor's theorem in the symbolic form

$$\begin{aligned} A_{x_1}(x,y,z) &= A_{x_1}(x_0 + x - x_0, y_0 + y - y_0, z_0 + z - z_0) \\ &= e^{(x' D_{x_0} + y' D_{y_0} + z' D_{z_0})} A_{x_1}(x_0, y_0, z_0), \end{aligned}$$

where $x' = x - x_0$, $y' = y - y_0$ and $z' = z - z_0$.

It is then found by integration that, if $J_0(z)$ is Bessel's function $\frac{1}{2\pi a_2}\int A_{x_1}(x,y,z) ds_2 = J_0(a_2 D_{n_2}) A_{x_1}(x_0, y_0, z_0)$, where x_0, y_0, z_0 are rectangular coordinates of the center of the circle No. 2 and D_{n_2} represents the directional derivative in the direction normal to the plane of the circle No. 2. Since we have used x_2 as the distance $\overline{OC_2}$ in figure 1 (not a rectangular coordinate) this becomes

$$\frac{1}{2\pi a_2}\int A_{x_1} ds_2 = J_0(a_2 D_{x_2}) A_{x_1}(x_0, y_0, z_0), \tag{29}$$

which holds when A_{x_1} is any harmonic scalar point function.

Now

$$A_{x_1}(x_0, y_0, z_0) = \pm \frac{dx_1}{2\pi a_1} \int \frac{ds_1}{R},$$

where R is the distance from x_0, y_0, z_0 to the element ds_1 of the circular arc of No. 1, so that A_{x_1} at any point is $\pm dx_1$ times the electrostatic potential at that point due to a unit circular line charge (the circle No. 1). It may be put in the form

$$A_{x_1}(x_0, y_0, z_0) = \pm dx_1 \int_0^\infty e^{-s|x_0 - x_1|} J_0(a_1 s) J_0(rs) ds,$$

where r is the distance of x_0, y_0, z_0 from the axis of the circle No. 1. This may also be written, symbolically, $A_{x_1}(x_0, y_0, z_0) = \pm dx_1 J_0(a_1 D_{x_1}) \frac{1}{R_{12}}$, where R_{12} is the distance between the centers of the two circles.

Now

$$\frac{1}{R_{12}} = \frac{1}{\sqrt{x_1^2 - 2x_1x_2\cos\theta + x_2^2}} = \sum_{n=0}^{\infty} \frac{x_2^n}{x_1^{n+1}} P_n(\mu), \text{ if } x_1 > |x_2|$$

Hence

$A_{x_1}(x_0, y_0, z_0)$

$$= \pm dx_1 \sum_{s=0}^{\infty} \frac{(-1)^s \left(\frac{a_1}{2}\right)^{2s}}{\Gamma(s+1)\Gamma(s+1)} D_{x_1}^{2s} \sum_{n=0}^{\infty} \frac{x_2^n}{x_1^{n+1}} P_n(\mu)$$

$$= \pm \frac{dx_1}{x_1} \sum_{s=0}^{\infty} \frac{(-1)^s \left(\frac{a_1}{2x1}\right)^{2s}}{\Gamma(s+1)\Gamma(s+1)} \cdot \sum_{n=0}^{\infty} \left(\frac{x_2}{x_1}\right)^n \frac{\Gamma(n+2s+1)}{\Gamma(n+1)} P_n(\mu)$$

$$= \pm \frac{dx_1}{x_1} \sum_{n=0}^{\infty} \left(\frac{x_2}{x_1}\right)^n \frac{P_n(\mu)}{\Gamma(n+1)} \sum_{s=0}^{\infty} (-1)^s \left(\frac{a_1}{2x_1}\right)^{2s} \frac{\Gamma(2s+n+1)}{\Gamma(s+1)\Gamma(s+1)}$$

$$= \pm \frac{dx_1}{x_1\sqrt{\pi}} \sum_{n=0}^{\infty} \left(\frac{2x_2}{x_1}\right)^n \frac{P_n(\mu)}{\Gamma(n+1)} \sum_{s=0}^{\infty} (-1)^s \left(\frac{a_1}{x_1}\right)^{2s} \frac{\Gamma\left(s+\frac{n+1}{2}\right)\Gamma\left(s+\frac{n+2}{2}\right)}{\Gamma(s+1)\Gamma(s+1)}$$

$$= \pm \frac{dx_1}{x_1} \sum_{0}^{\infty} \left(\frac{x_2}{x_1}\right)^n P_n(\mu) F\left(\frac{n}{2}+1, \frac{n}{2}+\frac{1}{2}, 1; -\frac{a_1^2}{x_1^2}\right),$$

so that

$$A_{x_1}(x_0, y_0, z_0) = \pm dx_1 \sum_{0}^{\infty} \frac{x_2^n P_n(\mu_1') P_n(\mu)}{(r_1')^{n+1}} \text{ since } r_1' > |x_2| \qquad (30)$$

The derivation assumes x_1 positive, but by repeating the above argument, when $x_1 < 0$ but $|x_1| > |x_2|$, it is found that eq 30 remains valid for all real values of x_1 and x_2 for which $r_1' > |x_2|$

Now

$$J_0(a_2 D_{x_1}) \sum_0^\infty \frac{x_2^n P_n(\mu_1') P_n(\mu)}{(r_1')^{n+1}} = \sum_{s=0}^\infty \frac{(-1)^s \left(\frac{a_2}{2}\right)^{2s}}{\Gamma(s+1)\Gamma(s+1)} D_{x_2}^{2s} \sum_{n=0}^\infty \frac{x_2^n P_n(\mu_1') P_n(\mu)}{(r_1')^{n+1}}$$

$$= \sqrt{\pi} \sum_{s=0}^\infty \frac{(-1)^s \left(\frac{a_2}{2}\right)^{2s}}{\Gamma(s+1)\Gamma(s+1)} \sum_{n=0}^\infty \left(\frac{x_2}{2}\right)^{n-2s} \frac{\Gamma(n+1) P_n(\mu_1') P_n(\mu)}{\Gamma\left(\frac{n+1}{2}-s\right)\Gamma\left(\frac{n+2}{2}-s\right)(r_1')^{n+1}}$$

$$= \sqrt{\pi} \sum_{n=0}^\infty \left(\frac{x_2}{2}\right)^n \frac{P_n(\mu_1') P_n(\mu) \Gamma(n+1)}{(r_1')^{n+1}} \sum_{s=0}^\infty (-1)^s \left(\frac{a_2}{x_2}\right)^{2s}$$

$$\cdot \frac{1}{\Gamma(s+1)\Gamma(s+1)\Gamma\left(\frac{n+1}{2}-s\right)\Gamma\left(\frac{n+2}{2}-s\right)}$$

$$= \sum_{n=0}^\infty \frac{x_2^n}{(r_1')^{n+1}} P_n(\mu_1') P_n(\mu) F\left(\frac{-n}{2}, \frac{1}{2}-\frac{n}{2}, 1; -\frac{a_2^2}{x_2^2}\right)$$

$$= \sum_{n=0}^\infty \frac{r_2'^n}{(r_1')^{n+1}} P_n(\mu_1') P_n(\mu_2') P_n(\mu)$$

The mutual inductance of the two current filaments with unit axial currents is therefore, by eq 26, 29, 30, and the preceding equation

$$m_{f_1 f_2} = \pm\mu \sum_{n=0}^\infty \frac{r_2'^n}{(r_1')^{n+1}} P_n(\mu_1') P_n(\mu_2') P_n(\mu) = \frac{\pm\mu}{2\pi a_1 2\pi a_2} \int ds_2 \int \frac{ds_1}{R} \quad (31)$$

which converges for $r_2' < r_1'$, which is always the case if f_1 is in sheet No. 1 and f_2 in sheet No. 2.

Hence

$$m_{s_1 f_2} = \int_{-\frac{l_1}{2}}^{\frac{l_1}{2}} m_{f_1 f_2} dx_1 = \pm\mu \sum_{n=0}^\infty r_2'^n P_n(\mu_2') P_n(\mu) \int_{-\frac{l_1}{2}}^{\frac{l_1}{2}} \frac{P_n(\mu_1')}{(r_1')^{n+1}} dx_1.$$

Since $\frac{P_n(\mu)}{r^{n+1}} = -D_x \frac{P_{n-1}(\mu)}{n r^n}$ if $n > 0$

$$= D_x \log (x + \sqrt{x^2+a_2}) \text{ if } n=0,$$

the integration gives

$$m_{s_1 f_2} = \pm 2\mu \left\{ \log\left(\frac{l_1 + \sqrt{l_1^2 + 4a_1^2}}{2a_1}\right) - \sum_{n=1}^{\infty} \left(\frac{r_2'}{r_1}\right)^{2n} \frac{P_{2n-1}(\mu_1) P_{2n}(\mu_2') P_{2n}(\mu)}{2n} \right\}. \quad (32)$$

Then

$$m_{s_1 s_2} = \int_{-\frac{l_2}{2}}^{\frac{l_2}{2}} m_{s_1 f_2} dx_2 \text{ and since } r^{2n} P_{2n}(\mu) = D_x \left[\frac{r^{2n+1} P_{2n+1}(\mu)}{2n+1} \right]$$

$$m_{s_1 s_2}(\mu) = \pm 2\mu \left\{ l_2 \log\left(\frac{l_1 + \sqrt{l_1^2 + 4a_1^2}}{2a_1}\right) - 2r_2 \sum_{n=1}^{\infty} \left(\frac{r_2}{r_1}\right)^{2n} \cdot \frac{P_{2n-1}(\mu_1) P_{2n+1}(\mu_2) P_{2n}(\mu)}{2n(2n+1)} \right\}, \quad (33)$$

so that the torque is

$$t_{s_1 s_2} = \pm 2 l_2 \left\{ \log\left(\frac{l_1 + \sqrt{l_1^2 + 4a_1^2}}{2a_1}\right) + \frac{1}{\mu_2} \sum_{n=1}^{\infty} (-1)^{n+1} \left(\frac{r_2}{r_1}\right)^{2n} \cdot \frac{P_{2n-1}(\mu_1) P_{2n+1}(\mu_2)}{2n(2n+1)} \cdot A_n \right\} \quad (34)$$

For the case here considered the series is negligible so that we may take

$$t_{s_1 s_2} = \pm 2 l_2 \log\left(\frac{l_1 + \sqrt{l_1^2 + 4a_1^2}}{2a_1}\right), \quad (34')$$

(+ if axial components of current have the same algebraic sign)

which must be added to the expression 17 for the torque. For the case noted, $l_1 = 100$ cm, $a_1 = 15$ cm, and $l_2 = 2a_2 = 10$ cm, so that $t_{s_1 s_2} = \pm 27.2$.

The principal part of the torque is $T_{s_1 s_2} = 4\pi \frac{N_1}{l_1} \pi a_2^2 N_2$, so that if $N_1 = 1{,}000$ and $N_2 = 100$, $T_{s_1 s_2} = \pi^2 10^5 = 10^6$, so that the correction $t_{s_1 s_2}$ amounts to 27 parts in a million.

IX. EFFECT OF LEAD-IN WIRES

Consider the inner coil with its axis vertical, the coil being balanced on a knife-edge which is perpendicular to the plane of figure 1. If the lead-in wires to the inner coil lie in the vertical plane containing the knife-edge, the electromagnetic forces upon them would contribute nothing to the torque about that knife-edge. The force on any element of these wires would lie in the vertical plane containing the knife-edge, since the magnetic field of the outer coil is practically

uniform. It remains to compute the effect of the return current in the lead wire of the outer coil. This will be done for the case where the return wire is just outside the solenoid and in the plane of the paper of figure 1, either above the solenoid or below it. The unit current in this wire will have an opposite algebraic sign to that of the axial unit current in coil No. 1. Its vector potential at any point will reduce to the single x_1-component, A_{x_1} parallel to the axis of coil 1. Let $m_{l_1 f_2}$ and $m_{l_1 s_2}$ denote the mutual inductance between this lead wire and filament No. 2, sheet No. 2, respectively. The mutual energy between filament No. 2 and this wire will be of the same form as eq 23 without the term A^0, and the surface integral of H_{n_2} will also vanish because the lead-in wire lies in the plane of the common axes of the coils, so that the mutual energy is

$$m_{l_1 f_2} dx_2 = \pm \mu dx_2 \frac{1}{2\pi a_2} \int A_{x_1} ds_2 = \pm \mu dx_2 J_0(a_2 D_{x_2}) A_{x_1}(x_0, y_0, z_0), \quad (35)$$

where the choice of signs is the same as in eq 23, positive if the axial current in f_2 is upward.

In this expression, $A_{x_1}(x_0, y_0, z_0)$ instead of being given by eq 30 is now given by

$$A_{x_1}(x_0, y_0, z_0) = \mp \int_{-\frac{l_1}{2}}^{\frac{l_1}{2}} \frac{dx_1}{R}, \quad (36)$$

where R is the distance from x_0, y_0, z_0 to dx_1, and the upper sign is taken when the axial current in sheet No. 1 is positive (to the right).

If the lead wire is above the solenoid $R^2 = (x_1 - x_0)^2 + (a_1 - y_0)^2$, where $x_0 = x_2 \cos\theta$ and $y_0 = x_2 \sin\theta$. If the lead wire is below the solenoid $R^2 = (x_1 - x_0)^2 + (a_1 + y_0)^2$.

In the first case, it is found that

$$A_{x_1}(x_0, y_0, z_0) = \mp \log \frac{\sqrt{r_1^2 - 2r_1 x_2 \cos(\theta - \alpha_1) + x_2^2} + r_1 \cos\alpha_1 - x_2 \cos\theta}{\sqrt{r_1^2 + 2r_1 x_2 \cos(\theta + \alpha_1) + x_2^2} - r_1 \cos\alpha_1 - x_2 \cos\theta} \quad (37)$$

By changing the sign of α_1 in this, it applies for the second case where the lead wire is below the solenoid. Since $\left(\frac{x_2}{r_1}\right)^2$ is negligible, this reduces to

$$A_{x_1}(x_0, y_0, z_0) = \mp 2 \left\{ \log \left(\frac{l_1 + \sqrt{l_1^2 + 4a_1^2}}{2a_1} \right) + \frac{x_2 \sin\theta \cos\alpha_1}{a_1} \right\} \quad (37')$$

If the wire is below the solenoid the last term has the negative sign. However, this term disappears in the integration with respect to x_2, so that both positions of the lead-in wire have the same effect. On substituting this value of $A_x(x_0, y_0, z_0)$ in eq 35, it must be remembered

that the ambiguities in sign do not represent the same alternative. Hence

$$m_{l_1 l_1} = \mp 2\mu \left\{ \log\left(\frac{l_1 + \sqrt{l_1^2 + 4a_1^2}}{2a_1} \right) + \frac{x_2 \sin\theta \cos\alpha_1}{a_1} \right\} \tag{38}$$

and

$$m_{l_1 s_1}(\mu) = \int_{-\frac{l_2}{2}}^{+\frac{l_2}{2}} m_{l_1 l_1} dx_2 = \mp 2\mu l_2 \cdot \log\left(\frac{l_1 + \sqrt{l_1^2 + 4a_1^2}}{2a_1} \right) \tag{39}$$

The contribution of this lead wire to the torque is $t_{l_1 s_2} = (D_\mu m_{l_1 s_2})_{\mu=0}$ or

$$t_{l_1 s_2} = \pm 2 l_2 \log \left[\frac{l_1 + \sqrt{l_1^2 + 4a_1^2}}{2a_1} \right] \tag{40}$$

In this equation the upper sign applies when the axial currents on the solenoids are both positive or both negative (i. e., in the direction of increasing x_1 or x_2 of fig. 1). In this case the upper sign applies to eq 34′. A comparison of eq 40 and 34′ shows that the correction for axial components of current is compensated for by this arrangement of lead-in wires.

X. SUMMARY

The torque between concentric solenoids with axes at right angles is given by eq 17, in which the integrations enable one to correct for small observed variations in diameter and spacing of the turns of wire in the two coils. The remainder of eq 17 is the torque between two current sheets, the term S being computed by eq 12′. The fact that the coils consist of discrete turns of wire of radii ρ_1 and ρ_2 (and not of tape windings with no insulation space between them as in current sheets) is taken into account by using the "effective" or "electrical" radii a_1 and a_2 of the coils in computing the torque between the sheets. The mean diameter, $2\bar{a}_i$, of a coil is the over-all diameter diminished by the diameter $2\rho_i$ of the wire, and its effective diameter is $2a_i$ where, by eq 9, $a_i = \bar{a}_i \left[1 \pm \frac{1}{8}\left(\frac{\rho_i}{\bar{a}_i} \right)^2 \right]$ the positive sign applying if the current is uniformly distributed over the section of the wires; the minus sign, if it is the natural distribution (inversely proportional to the distance from the axis). The same results hold if the section of the wire is not round but symmetrical with respect to its center of gravity (such as a square), provided that $\rho_i/2$ then denotes the radius of gyration of the section.

The correction terms are derived on the assumption that the outer coil is relatively long, and that its magnetic field is nearly uniform over the region occupied by the inner coil. Application is made to the case where the coil is compressed more at its middle than at its ends because of the tension in the windings. This gives the correction term in eq 22. The effect of errors in centering the coils is shown to be generally negligible, although formula 17 enables one to compute these errors if necessary.

Since a single-layer coil is necessarily helical, the axial components of current in both coils contribute a small term to the torque whose value is found by eq 34′. It amounts to about 3 parts in one hundred thousand. It is shown by eq 40 that this torque is practically compensated for, when the lead-in wire of the outer coil is very near to it (either above or below) and lies in the plane containing the axes of the coils.

The derivation of these formulas was undertaken, having in mind their application to a proposed absolute measurement of current in the Pellat type of current balance to be made at the National Bureau of Standards.

The formulas have also (unexpectedly) been found useful by E. A. Johnson of the Department of Terrestial Magnetism, who devised a method of absolute measurement of the earth's magnetic field, by uniform rotation of the secondary. Instead of measuring torque, he observed the induced electromotive force, both of which however, require the differentiation of the mutual inductance with respect to the angle, θ.

WASHINGTON, January 31, 1939.

○